The Use of Urea Condensates as Novel Flame Retardant Materials

Maryam Sharzehee

Submitted in accordance with the requirements for the degree of Doctor of Philosophy

The University of Leeds
Department of Colour Science

Dec 2009

Acknowledgement

I would like to express my sincere thanks to Professor Lewis for his invaluable supervision, interest, thoughtful suggestions and help during my work.

I wish to express my profound gratitude to Dr. Clark for his help during my Ph.D, particularly for reading my reports.

I also should appreciate my Iranian supervisors, Dr. Mirjalili and Dr. Dadfarnia for their helpful guidance and supports.

I would like to express my cordial thanks to the Department of Textile Eng. and Chemistry of Yazd University for their cooperation and for providing the required facilities for my research work.

Many thanks must also be expressed to all of those who have been my friends throughout the courses of this work. I would especially like to mention my gratitude to Celine, Loan, Will, Gillya, Murial and also Mansour.

It is a great pleasure to express my appreciation to Dr. Kazlauclunas and Mr. Asaf for their assistance in using laboratory instruments.

Finally I would like to express my thanks to my husband "Abbas" and my children who gave me all their supports and encouragement throughout this work. I love them more than words can say, and thank them from the depth of my heart.

Abstract

The aim of this work was to produce environmentally safe flame-proofing compositions to give a wash-durable finish on textile and other substrates. Thus this work describes the preparation and application of new urea condensates formed from the reaction of urea with a variety of chemicals including phosphoric acid, phosphorous acid and sulphamic acid; the condensates gave different degrees of flame retardancy (FR) on a variety of substrates. Studies of urea thermal decomposition showed the production of isocyanic acid and ammonia, above the urea melting point (138°C). Using an open reaction vessel, urea, sulphamic acid and phosphorous acid gave an exothermic reaction over the temperature range 120 -140°C with gas liberation. The condensates thus formed contained aliphatic polyamide chains, containing urea groups and sulphur and phosphorus residues. According to the type and amount of initial materials, various urea condensates, capable of imparting different degrees of flame retardancy, were synthesized. The sulphamic acid/urea (S/U), phosphoric acid /urea (PA/U), sulphamic acid/phosphoric acid/urea (S/PA/U) and also sulphamic acid/phosphorous acid/urea (S/PH/U) condensates were produced. When these urea condensates were cooled down, water-soluble products were produced, and these materials could be applied to the textile substrate using a pad-bake technique.

Cotton fabrics were treated with these condensates: typically a pad-liquor contained 500 g/l of urea condensate, 10 g/l of wetting agent; fabric was padded to 80% wet pick-up, dried (80°C) and cured for two minutes (165°C). These urea condensates, when cured on cotton at high temperature (165°C), change to water-insoluble products; as a result of reactions between cellulose hydroxyl group and the urea condensate a complicated polymer structure network can be produced on the surface of a fabric and a flame retardant effect imparted. The S/U condensate only produced partial FR properties, while the rest of the compounds produced completely flame retardant fabrics. FT-IR analysis and NMR analysis was carried out on the urea condensates and also on the flame retardant fabrics. DSC thermal analysis was performed on the initial materials, urea condensates and also the treated fabrics. The characterization of urea condensate treated fabrics were studied further using SEM and energy dispersion X-ray micro analysis.

In the case of the urea condensates a small amount of sulphamic acid has a significant influence on the reaction between phosphating agents and urea; in fact the presence of SA reduces the exothermic reaction. However, at high concentrations of urea, the exothermic reaction occurred at a higher temperature and a hard crystalline product was produced, thus application required dissolution in warm water (50°C). A urea condensate of 1 mole sulphamic acid, 1 mole phosphorus acid and up to 18 moles of urea could produce a durable flame retardant finish on cotton fabric. A higher amount of phosphorous acid in the urea condensate products (1S/2PH/10U) reduced the exotherm temperature and a high quality flame retardant effect was produced on cotton fabric.

The evenness of phosphorus and sulphur elemental distribution on the surface and cross section of treated fibre was confirmed using SEM. Desirable flame retardancy effects from the urea condensate treated fabrics were obtained with comparatively low levels of sulphur and phosphorus (in comparison with the current commercially available Proban and Pyrovatex treated fabrics). However, in the washing process of the condensate-treated fabrics, no significant reduction in P or S concentration/level was found. The excellent flame retardancy of the new system can be explained due to the N/P/S-containing polymer formed on the surface of the fabric. DSC results from the treated fabrics confirmed these observations. Fabrics treated with Proban and Pyrovatex showed a very sharp exotherm after 300°C, but for fabrics treated with the urea condensates only a small exotherm effect appeared.

In FT-IR analysis and NMR analysis, the production of aliphatic polymer chains of different length was verified, however, for the insoluble product formed in situ by heating at 160°C, and also for the condensates formed on the fabric at high temperature, a complicated polymer structure was shown to contain a possible combination of cyanuric acid, cyclic urea, triazine and melamine. All these materials have been identified in the FT-IR spectra of a water- insoluble urea product formed at 160°C.

To make a model reaction with other hydroxyl group-containing substrates, starch and polyvinyl alcohol were treated with the 1S/2PH/10U condensate. The flame retardancy effect on both these treated substrates was confirmed by DSC thermal analysis.

Advantages of this new wash-durable FR system over the currently available Proban/Pyrovatex systems include: no formaldehyde, low cost, ready availability of materials, simplicity of the treatment (no specific equipment required), and maintenance of all the desirable physical properties of the fabric, such as soft handle, acceptable tensile strength, no effect on dyed grounds and also no yellowing of the fabric.

Table of Contents

List of Figures

Chapter 1

Chapter 2

Chapter 3

Chapter 4

Chapter 5

List of Tables

Chapter 1

Chapter 3

Chapter 4

List of Schemes

Chapter 1

Chapter 3

Chapter 4

Abbreviations:

APO	Aziridinyl Phosphine Oxide
APP	Ammonium PolyPhosphate
Asym	Asymmetric
ATR	Attenuated Total Reflection
Br	broad
BSE	Back Scattered Electron
CRT	Cathod Ray Tube
CW	Continuous wave spectroscopy
CYA	Cyanuric Acid
def	Deformation
DP	Degree of Polymerization
DSC	Differential Scanning Calorimetry
DTA	Differential Thermal Analysis
DTG	Differential Thermo-gravimetry
EGA	Evolved Gas Analysis
EM	Electro Magnetic
EDX	Energy Dispersive X-ray
FT-IR	Fourier Transform Infrared
GC.MS	Gas Chromatography Mass Spectrometry
HDPP N.	Hydroxymethyl 3- dimethyl Phosphonopionamide
HNCO	Isocyanic Acid
HPLC	High Performance Liquid Chromatography
LOAEL	The Lowest Observed Adverse Effect Level
LOI	Limited Oxygen Index
ISE	Ion Selective Electrode
m	medium
m.p.	Melting point
NOAEL	No Observed – Advanced Effect Level
NMMO	N-Methylmorpholine –N-Oxide
NMR	Nuclear Magnetic Resonance
Owf	On Weight of fabric
PA	Phosphoric Acid
PH	Phosphorous Acid
PMT	Photo Multiplier Tube
ppm	Part per million
PVC	Polyvinyl Chloride
RfD	Reference Dose
s	Strong
S	Sulphamic acid
SA	Sulphamic Acid
SEM	Scanning Electron Microscope
Sh	Sharp
Str	Stretching
S/PH/U	Sulphamic acid/Phosphorous acid/Urea

S/PA/U	Sulphamic acid/Phoshoric acid/Urea
Sym	Symmetric
TAP	Triallyl Phosphate
TGA	Therom-Gravimetric Analysis
THP	Tris (Hydroxy methyl) Phosphine
THPC	Tetrakis Hydroxy methyl Phosphonium Chloride
THPOH	Tetrakis (hydroxyl methyl) phosphonium hydroxide
TOI	Temperature Oxygen Index
TMM	Trimethylol Melamine
UFs	Uncertainty Factors
Vib	Vibration
vs	Very strong
w	Weak
%w/w	Percentage by Weight

Chapter 1

Introduction

Most conventional textile fibres are flammable; they also have a high specific surface area. When exposing this material to an ignition source, the material decomposes and subsequently produces some flammable gases, leading to ignition with flame propagation and heat products. Most flame retardant textiles are designed to reduce the ease of ignition, by a small source (e.g. a lighted match) and reduce flame propagation rate.

Cotton is the most commonly used of all textile fibres and with regenerated cellulosic fibres, such as viscose, provides 60% of the world annual fibre consumption. Flame-proofed cotton and viscose currently holds about 90% of the total textile flame retardant market [1].

Chemical modification of cotton fabric has been researched for many centuries. As early as 1640, clay and plaster of Paris paints were applied to theatre curtains as flame retardants. By 1740, the flame retardant properties of alum had been discovered and put to use. Since the end of the 18^{th} century the majority of flame retardant studies on cellulosic fabrics and other materials have centred round the use of phosphorus-containing compounds [2].

Various forms of organo-phosphorus based flame retardants have been developed such as phosphates, phosphonamides and phosphonium salts, however only a few of them have been commercially successful. The majority of the above phosphorus compounds were water soluble inorganic salts. They were applied to the textile materials from aqueous solution, but the durability of the fabric flame retardant (FR) properties, following washing, was the main problem. In order to solve these undesirable problems, considerable effort has been expended to develop wash-durable flame retardant finishes. This work has been quite successful, and a number of permanent flame retardant finishes are now available, but, unfortunately, no complete satisfactory finish has been achieved until now. The treating agents are quite expensive and effective treatment requires the application of a large amount of these materials. The high add-ons often give poor physical properties and harsh handle on the finished fabric which is not acceptable.

Since the last decade, increasing concerns over the toxicological and environmental consequences of using such chemicals on textile substrates have been raised.

The high specific surface area, and close contact with the skin, of textile material have created a barrier to the development and application of new chemistry.
The objective of this chapter is to act as a literature review which covers cellulose properties, its thermal pyrolysis behaviour, the nature of the burning process and the action of flame retardants on cellulose. Processes involving the production and application of urea condensates as flame retardants are also reviewed, along with thermal analysis of urea and its thermolysis products to allow us to understand the mechanisms involved in urea condensate reactions. Isocyanic acid, as the main initial product of urea thermal decomposition, plays a significant role in urea condensate reactions; it is therefore important to discuss isocyanate reactive ions in this section.

1.1 Cellulose fibres

Cellulose (Latin word cellula, "little cell") is a complex carbohydrate and forms the structural component of the primary cell wall of green plants, many forms of algae and comycetes. Cellulose is the most common important natural polymer on earth, about 33% of all plant matter is cellulose [3]. The cellulose content of cotton fibres is 90%, of wood 50% and of non-wood agricultural materials 40% [4].

For industrial application, cellulose is mainly obtained from wood pulp and cotton. It is used in the textile industries and also to produce cardboard and paper; to a smaller extent it is converted into a wide variety of derivatives such as rayon fibre and cellophane. Recently, the conversion of cellulose into bio-fuels has been carried out as an alternative, environmental friendly fuel source [5].

1.1.1 History of the cotton fibre

In the 5th century BC, the Greek historian Herodotus was the first man who discovered, in India, from a wild plant that bears cotton as its seed-head. In the next century, Alexander the Great brought this plant from India to Greece. Although the early Greeks and Romans used cotton for awnings and sails as well as for clothing; it was not adopted for wide-spread use in Europe until later centuries.

Cotton textiles were found in the West Indies and in South America by explorers in the 15th and 16th centuries. Cotton was cultivated by the early American colonists and when Eli Whit, introduced the cotton gin in 1793 it became the most important staple fibre in the world [6].

1.1.2 Cellulose chemical structure

Cellulose was isolated from plant sources in 1838 by the French chemist Anselme Payen, who also determined its chemical formula [7]. Hyatt Manufacturing Company introduced the first thermoplastic polymer, celluloid, derived from cellulose in 1870. The polymer structure of cellulose was determined by Hermann Staudinger in 1920. Cellulose was first chemically synthesized (without the use of any biologically derived enzymes) in 1992, by Kobayashi and Shoda [8].

Cellulose is an organic compound with the formula $(C_6H_{10}O_5)$; it is a polysaccharide consisting of a linear chain of many repeating units of β(1- 4) linked D – glucose unit, as shown in Figure1.1.

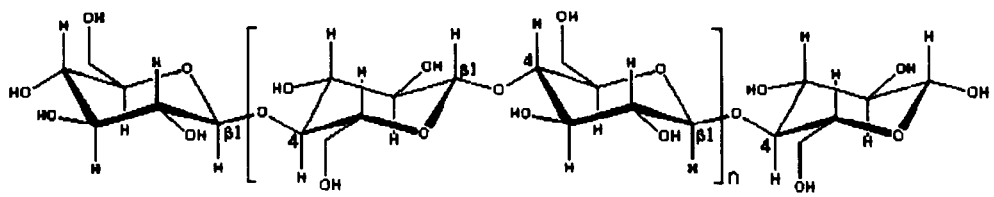

Figure1.1. The structure of cellulose, showing the cellobiose repeating unit [3].

This linkage motif contrasts with that of the α(1-4) glucosidic bonds present in starch, glycogen and the carbohydrates. Cellulose is a straight chain polymer, unlike starch, and no coiling or branching occurs. It has been suggested that, the molecule adopts an extended and rather stiff rod–like conformation [7].

In plants, cellulose is normally combined with hemicelluloses, lignin, pectin and other substances, while microbial cellulose[1] is quite pure, has much higher water content, and consists of a long chain [3].

In Figure 1.2 the plant cell walls all around the plasmalemma is shown. In the course of cell growth, according to the type of macromolecule composed, the dimensions of the cell wall differ. The middle lamella is the first wall deposited after cell division, and is made up of pectic material. The primary cell wall is a glycoprotein hydrated layer which is composed of pectin, cellulose, hemi-cellulose and proteins.

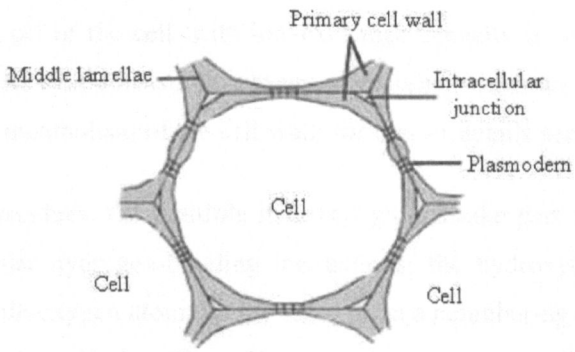

Figure1.2. Structure of the plant cell wall [3].

Cellulose chains in the micro fibril form, represent about 20 -30% by dry weight of cell wall material and takes up about 15% of the cell wall volume. The orientation and disposition of micro fibril in the cell wall is very important, in fact the subsequent extent of any deformation is controlled by this factor. The other wall polymer includes lignin which is incorporated into the spaces around the polysaccharide fibrillar elements to form lignin–polysaccharides. Lignin is a highly cross–linked aromatic polymeric material with three dimensional architectures. Lignin has no regular repeat unit, because it is formed by free radical condensation. Between 10 -30% by dry weight of wood is made up of lignin; it contributes to the mechanical strength of the plant cell wall [8].

1. Microbial cellulose is a form of pure cellulose that is produced by bacteria, from the green Aerobacter, Acetobacter and Achromobacter.

Hemi-cellulose is a polysaccharide related to cellulose, which comprises 20% by weight biomass of most plants. It consists of shorter chains around 200 sugar units, and is branched. In the course of differentiation, hemicelluloses and lignins can provide a type of liquid crystalline matrix in which micro-fibrils of cellulose are arranged in order and also disorder stabilized by molecular interactions such as hydrogen bonds and van der Waal's forces [9].

Pectins constitute about 35% dry weight of the cell wall, and are a major component of dicotyledonous higher plants. Pectins represent a complex range of carbohydrate molecules whose backbone is composed chiefly of chains of α-D-(1-4) galacturonan interrupted by units of β-L-(1-2) rhamnose. In fact, control of the ionic environment and pH of the cell, with ion–exchange capacity is enforced by pectins [9]. The plant cell wall consists of a range of proteins which are implicated in the organization and metabolism of the cell wall; for further details see reference [8].

On the glucose residues, the multiple hydroxyl groups take part in inter-molecular and intra-molecular hydrogen-bonding interactions; the hydroxyl group from one chain interacts with oxygen atoms on the same or on a neighboring chain, holding the chain firmly together side by side. This extended hydrogen-bonding imparts high tensile strength to the cell wall which is important in rigidity of the plant cells. In fact a net-work of self–bonding cellulose fibres within network structure affects the chemical and physical characteristics of the products [3], Figure1.3.

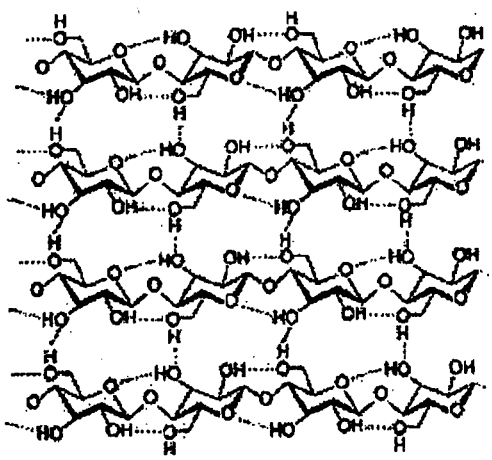

Figure1.3. Net work structure of cellulose with inter-molecular hydrogen-bonding [3].

The chain length or degree of polymerization has an effect on cellulose properties. The degree of polymerization, DP, of cellulose variously depends on its source, and is usually expressed as an average number of anhydroglucose units per chain molecule. However a wide distribution of molecular chain lengths is always found in any particular sample. Cellulose from wood pulp typically has DP between 300 – 1700. Native cellulose such as cotton and other plant fibre as well as bacterial cellulose contains cellulose I with chain length ranging from 800 to 10000 units. However alkaline treatments usually reduce the DP to a maximum of 2000. Regenerated cellulose has a DP in the range 250 – 300 and may contain small numbers of aldehyde, ketone and carboxylic acid groups, introduced during manufacturing. Regenerated cellulose is nearly identical to native cellulose; the difference between the two types arises mainly from their supramolecular structure and physical structure. Polynosic fibres have higher DP in the range 500 – 700 [10]. In the production of Lyocell a cellulose sheet with DP 1000 is dissolved in aqueous NMMO (N-methylmorpholine-N-oxide) solution the concentration of the obtained solution is about 11% w/w cellulose and does not contain any un-dissolved cellulose particles. The DP of the Lyocell cellulose is reported to be about 980 [11].

Cellulose is soluble in cupri-ethylenediamine (CED), cadmium-ethylenediamine (Cadoxan), N-methylmorpholine-N-oxide (NMMO) and in a lithium chloride/ dimethylformamide mix. In recent years, NMMO has been used in Lyocell fibre manufacturing [6].

The hydroxyl groups of cellulose can be partially or fully reacted with various reagents to afford derivatives with useful properties, such as cellulose ethers and cellulose esters. Among the esters, cellulose acetate and cellulose triacetate were introduced as fibre- and film-forming materials that find a variety of uses. The inorganic ester, nitro–cellulose, was initially used as an explosive and was an early film-forming material. Some other cellulose ether derivatives such as ethyl-cellulose, methyl-cellulose, carboxymethyl-cellulose and hydroxyl-propyl-methyl-cellulose and hydroxymethyl-cellulose are in this category, together with ethyl-cellulose which is a commercial thermoplastic, used in coating, inks, binders, and controlled release drug tablets [3,12].

1.1.3 Physical structure of cellulose

Cellulose is a semi–crystalline natural polymer, with crystalline regions (regular arrangement of chain molecule), and non-crystalline, amorphous, regions (a non–regular arrangement), in a highly ordered fibrous morphology.

In the study of the physical structure of cellulose, the poly-morphology of cellulose crystalline and the supermolecular morphology are two interesting points for scientists. From the studies of X-ray diffraction and electron diffraction, it has been suggested that long chain cellulose molecule are arranged with their long axes parallel to the length of the elementary fibrils, which are ~ 3.5 nm in width and of finite length. Thicker fibres can be formed by aggregation of the cellulose chain molecules with high packing density and strong hydrogen bonding.

It is known that cellulose exists in several crystalline forms, cellulose I, II, III, IV, III(1), III (2), IV(1) and IV(2). The pure cotton fibre and microbial cellulose has the structure of cellulose I and by treating with 12 – 18% of NaOH solution, cellulose II is formed. The regenerated cellulose fibre such as rayon, viscose and also mercerized fibre have this structure.

When cellulose I is treated with liquid ammonia at low temperatures -30°C, cellulose III and IV will be produced. The most stable states of cellulose are cellulose I and II. Depending on the conditions of transformation, other conversion steps, including some chemical modification may or may not be reversible. In Figure 1.4 the transition of cellulose structure is illustrated [13].

According to the results from X-ray diffraction [10], electron diffraction, configuration analysis and finally vibration spectroscopy, based on inter- and intra-molecular hydrogen-bonding of cellulose chains, the unit cell structure of cellulose has been proposed. In cellulose I and II, the two helix chain conformation with a 1.3 nm fibre repeat distance as reported.

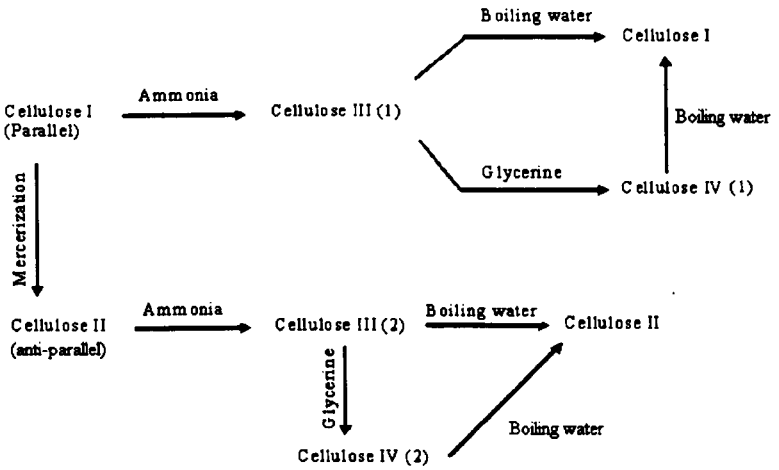

Figure1.4. Transition of physical structure of cellulose fibre at various conditions.

The unit cell of cellulose I is monoclinic, with lattice dimensions of:

a= 0.935nm, b= 1.03nm (fibre axis), C=0.79nm and $\beta = 96°$

The lattice cell of cellulose II is also monoclinic with dimensions of: a= 0.8nm, b= 1.3nm (fibre axis), c= 0.9nm and $\gamma=117°$

Both structures consist of two chains per unit, one cellobiose unit (repeated unit of cellulose) residue belonging to the chain molecule passing through the centre of the cell the other is one corner of each cell. The polarity of the two chains is parallel in cellulose I and anti parallel in cellulose II.

As shown in Figure 1.5 the orientation of the chains packed into the cell is provided by hydrogen bonding between the hydroxyl groups on the cellulose chain. Therefore the three dimensional packing of the sheets is different between the parallel (cellulose Iα) and anti parallel chains (cellulose Iβ). A combination of Iα and Iβ in variable proportion, depends on the source of cellulose has been suggested for native cellulose. In cellulose I, most parallel chain orientation has been suggested, however in cellulose II with different conformation and unit cell size, anti parallel packing in a regular alternating, up–down arrangement with high proportion is indicated [9].

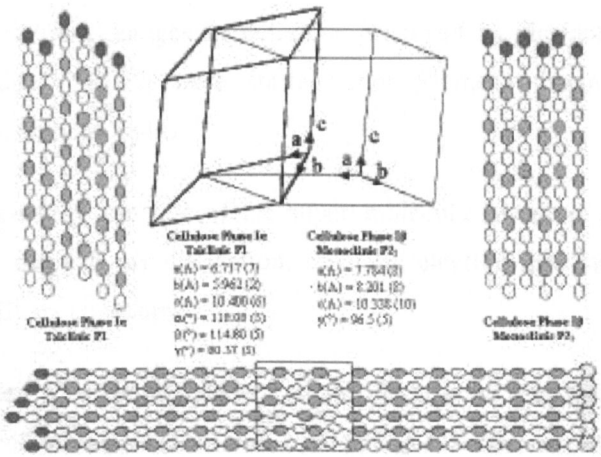

Figure1.5. Structure of cellulose unit cell, cellulose I with parallel chain orientation and cellulose II with anti-parallel chain packing alternating up-down arrangement [3].

[9]. http://www.cermav.cnrs.fr/glyco3d/lessons/cellulose/index.html

The crystalline forms of cellulose III (III (1) and III (2)) are reversible and the chain orientation is the same as in the starting material. The unit cell dimensions have been measured using X-ray diffraction, a = 1.02nm, b = 0.77 nm, c = 1.03 nm and γ = 122.4° [14].

In cellulose IV (1) and IV (2), the conversions are never totally completed, because of it is not possible to produce a good quality X-ray diffraction patterns. The unit cell dimensions have been measured for the two allomorphs. In IV (1) structure, a=0.803 nm, b= 0.813 nm, c= 0.103 nm which are very close to those found for form IV (2), a=0.799nm, b=0.81 nm, c=1.03 nm. In both these cases, poor quality of the diffraction X-ray patterns, does not allow the determination of the space group [15].

1.1.4 Cellulose degradation

Cellulose fibres are chemically stable which is very important from the industrial point of view. Six different degradative agents have been identified; acids, alkalis, oxidizing agents, enzymes, heat and radiation.

Cellulose chemists know that cellulose is strongly swollen by aqueous alkaline solution, resulting in partial dissolution of the cellulose. Extensive studies of the swelling and structural changes in cellulose produced by the action of aqueous solution hydroxide (NaOH) were started after Mercer's discovery (so called mercerization) as early as 1844.

In recent research [16], the role of the super–molecular structure of cellulose has been studied by using X-ray diffraction, scanning electron microscopy, C^{13} NMR analysis and FTIR spectroscopy.

Cellulose samples with the cellulose I crystal form were prepared by applying a "steam explosion" treatment and acid hydrolysis, to soft wood pulp and cotton linters. Their solubility toward aqueous alkaline solution has been described in detail. In conclusion, the researchers confirmed that, the cellulose solubility in alkaline solution is governed by X_{am} (C3)[1], expressing the degree of break down in O3 – H...O'5 intra-molecular hydrogen bond, as confirmed for cellulose with crystal form cellulose II. This property can be elucidated more precisely by X_{am} (C3+C6) expressing the degree of breakdown in both O3 – H...O'5 and O2 – H...O'6 intramolecular hydrogen bonds Figure 1.6.

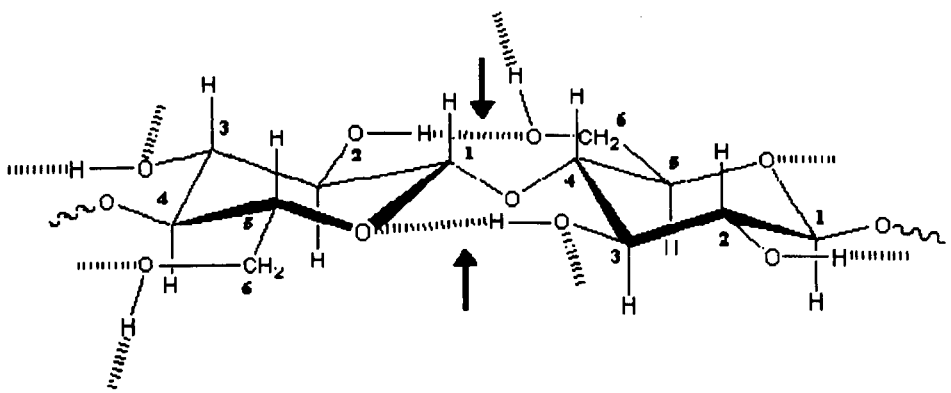

Figure1.6. Scheme showing the type of intra-molecular hydrogen bonds in the dimer fragments of the cellulose macromolecule [16].

1. The amorphous fraction X_{am} (C), of the sample was calculated from the crystallinity C_c (C), which was estimated by Segal's method. X_c (C) = 100 ($I_{002} - I_{am}$)/I_{002} (%)
X_{am} (C) = 100 – X_c(X) (%)
Here, I_{002} and I_{am} are the mean peak intensities, corresponding to (002) plane (2θ = 22.6°) and amorphous region (2θ = 19°).

FTIR analysis can estimate the degree of disruption of intermolecular hydrogen bond.

Other researchers [17] found that alkaline solution used at higher temperatures increase the initial rate of cellulose degradation - however the extent of degradation is independent of air temperature. They suggest three distinct stages in the alkaline degradation procedure.

- At first de-crystallization due to breaking of the hydrogen bonds and separation of the fibres.
- Recrystalization, due to preferential degradation and digestion of the more easily affected amorphous region.
- De-crystallization within the crystalline region.

Furthermore, the chemical reactivity of the resulting oxycellulose may be related to imperfections in the crystal lattice and does not depend on the crystalline/amorphous ratio [18].

The researchers also indicated that, repeated drying and wetting of the cellulose decreases liquid water absorption and the tensile strength of cellulose paper. The property can be explained by elimination of hydrogen-bonding sites when the cellulose paper is immersed in the liquid which is confirmed in the fibre polymer structure. However, liquid water absorption was significantly improved, by alkaline addition to both methyl-alcohol and ethyl-alcohol solvent systems [18].

1.2 Burning process

A clear definition of the burning process can lead us to understand the influence of flame retardant processing on the combustion process. The burning of a solid material essentially proceeds in three stages: the heating phase, a thermal pyrolysis or decomposition and finally ignition. In this section to simplify the process, a brief explanation of each stage is provided.

1.2.1 Primary heating

The application of an external heat source, such as a flame, or a spark normally raises the temperature, and following that ignition will occur. If the temperature is high enough, ignition occurs spontaneously.

In the case of a solid polymer, due to the external heat source, such as radiation, flame or by thermal heat back, the first stage of burning process would be explained by raising the temperature.

In the case of a thermoplastic material with linear chain structure, during initial heat exposure, they become soft or melt and start to flow. On the other hand, thermosetting plastics with three dimensional cross-linked molecular structures remain essentially unchanged. In this stage, if the temperature of melting is reached, it can have a pronounced effect on subsequent processes. In the case of thermoplastic materials, they lose rigidity and following that there is a decrease in the melt viscosity, raising the temperature, allows these liquids to recede from the ignition source, which prevents the next stage of pyrolysis and ignition occurring. However the thermosetting materials require more heat at the first stage for this to occur [19].

1.2.2 Pyrolysis and decomposition

At this stage the chemical composition of the original samples play the main role. The temperature and rate of heat propagation depends on the thermal stability of the materials and the chemical decomposition reactions which occurred. By increasing the amount of heat at this stage, the polymer starts to pyrolyse and evolve small volatile molecular species. The decomposition temperature is much higher, for thermosetting polymers compared to thermoplastic materials. Thermal pyrolysis generally proceeds in three closely related phases:

■Temperature between 100 – 250°C

In this temperature range, only specific chemical bonds requiring low energy reactions will decompose and with the elimination of significant amounts of functional groups, chain ends and small molecules such as water and hydrogen halides might be seen.

■Temperature between 250 – 500°C

In this temperature range, sufficient energy becomes available for decomposition of high energy bonds, which usually maintain the solid structure of the material. In fact, thermal decomposition at this stage leads to unzipping of some polymer chains. Alternatively natural, organic polymers will produce organic flammable materials. Both types of products can sustain gas phase flame reactions. In some cases, recombination of these polymer fragments can lead to the formation of aromatic, condensed ring systems which are stable under the pyrolytic conditions. In this case, the third stage of pyrolysis will occur.

■Temperature of 500°C or higher

At these temperatures any aromatic, condensed ring structure formed in the second stage, are condensed with elimination of most elements with the exception of carbon. Char formation at this stage is highly insulative and such chars are difficult to flame at normal oxygen concentrations. If the intermediate products of the char can be maintained in a viscous elastic state, the flammable evolved gases will be trapped in the viscous liquid and cause the char to expand into carbon forms.

In one simple way, the mechanism of combustion at this stage contains a condensed phase and a vapour phase together. The char formation is also introduced at this stage. It has to be stated that, the decomposition of polymer, requires a high level of energy, therefore, the endothermic process for pyrolysis can be defined. As individual polymers differ in structure, their decomposition temperature also varies within certain limits. In fact this limiting temperature will change following any variation in the chemical composition of the polymer [20].

1.2.3 The ignition and burning

At this stage, at high temperature, the rate of production of gaseous degradation products increases until a mixture is reach with enough oxygen in the air, to be able to ignite.

The rate of volatile flammable gas production and availability of surrounding oxygen, can lead to an increase in the rate of the combustion processes. During the

ignition, the burning process is exothermic with a lot of energy evolved, and this will overcome the endothermic requirement for polymer pyrloysis. The combustion gas phase reaction of hydrocarbons in a flame has been studied. In Scheme 1-1 some of the chain reactions involved in the oxidation of methane are indicated. In a simple way, at this stage, the complicated series of free radical reactions can be explained. The chain branching step is one of the important steps which is propagated by the highly reactive $H^{\bullet}$ and $OH^{\bullet}$ radicals. In the presence of O_2, the chain branching reactions 8 and 9, lead to an exponential increase in radical concentration. The hydroxyl radicals attack the saturated hydrocarbon and the rest of the radical reactions, follows. The overall reaction products are water and carbon dioxide. Therefore to inhibit the propagation of a hydroxyl radical, control of the two reactions 8 and 9 is necessary. The use of hydrogen halides as flame retardants controls the burning process by inhibiting this chain branching reaction [20].

Propagation

$CH_4 + H^{\bullet} \longrightarrow CH_3 + H_2$ (1)

$CH_4 + HO^{\bullet} \longrightarrow H_2O + CH_3^{\bullet}$ (2)

$CH_3^{\bullet} + O_2 \longrightarrow HCHO + OH^{\bullet}$ (3)

$HCOH + O^{\bullet} \longrightarrow HC(=O)^{\bullet} + HO^{\bullet}$ (4)

$HC(=O)^{\bullet} \longrightarrow CO + H^{\bullet}$ (5)

$CO + HO^{\bullet} \longrightarrow CO_2 + H^{\bullet}$ (6)

$2HO^{\bullet} \longrightarrow H_2O + O^{\bullet}$ (7)

Chain Branching

$H^{\bullet} + O_2 \longrightarrow OH^{\bullet} + O^{\bullet}$ (8)

$O^{\bullet} + H_2 \longrightarrow HO^{\bullet} + H^{\bullet}$ (9)

Overal reaction

$CH_4 + 2O_2 \longrightarrow 2H_2O + CO_2$ (10)

Three body reaction

$2O^{\bullet} \xrightarrow[\text{Catalyst}]{\text{Solid}} O_2$ (11)

Scheme 1.1. The combustion gas phase reactions of hydrocarbon in a flame [20].

The theory of combustion in the gas phase through free radicals would be acceptable for simple hydrocarbons such as propane but the generality of these reactions to

higher hydrocarbons has not been demonstrated [20]. By measuring the actual amount of gas produced during the combustion, of polyethylene, and n-eicosane [$C_{20}H_{42}$], using mass spectrographic analysis, Burge and Tipper found that, the oxygen in the air was shown to be almost completely consumed at the surface of the polymer [21]. Calculation of the heat fluxes supplied to the burning process indicated that 90% was from an oxidative reaction which occurred at the surface of the molten polymer and only 10% was estimated to be supplied by radiation [22].
In fact, the condensed–phase oxidation is the primary important part of the combustion.
Studies on the burning of polymethyl-methacrylate also confirmed that the pyrolysis reaction produced a high concentration of monomer at the beginning of the melting process. At a small distance from the polymer surface, the high level of carbon oxides increases while the monomer concentration is reduced [21].
Ionic flame reaction is another suggested process which might be seen during the combustion process. McWilliam has suggested that trace amounts of ethanol or benzene, in polymers, are present in a flame zone, where the oxidation of carbon monoxide was occurring; the ionic reactions are also important. However, this mechanism has yet to be established for flame-retardant finishes on polymers [20].

1.3 Combustion-inhibition mechanism of flame-retardant finishes

If the combustion process and the mechanism of flame retardant can be elucidated to determine the mode of action of a flame retardant, it is necessary to understand the fundamental fire-retardant finishes, currently available. There are four general methods of modifying the flammability of polymeric materials [20].

- **Coating:** By applying non-flammable materials to the surface of samples. It would be possible to prevent the normal pyrolytic and also combustion processes on the solid materials. This coating mechanism acts by insulating the substrate from the heat source and also exclusion of the fuel from the gas phase, together with air from the surface of the condensed phase.
- **Condensate phase:** The presence of some chemicals or elements in the composition of the substrate can influence the rate of pyrolysis and inhibit the exothermic gas phase reactions.

- **Vapour phase:** some components on a solid substrate can prevent the flammable gas reaction by producing sufficient quantitative of non-flammable gas to dilute the generated fuel gas stream to below the level of flammability.

- **Endothermicity:** During the burning process, some components of the solid substrate are consumed leading to pyrolytic decomposition reaction to be cooled. Therefore, the surface of substrate falls to below the ignition point.

In flame-retardant finishing it is possible to apply any of these methods. In fact, a meaningful analysis of the fire-retardant mechanism is very complicated.
Therefore the first action is to apply the flame retardant to the surface of the polymer, in order to lower the decomposition temperature. The feed back heat and radiation can be controlled in the other the stages of the burning process. At the second stage of combustion which involves pyrolysis and decomposition, volatile and non-volatile products are produced, some of which are flammable, Figure 1.7.
In order to interrupt the burning process, five action modes (a) – (e) are proposed and flame retardants may function in one or more of these. Each mode of action with a relevant flame retardant step is explained [23].

(a) Removal of heat

Some materials can reduce the heat of combustion and therefore prevent the burning cycle proceeding. Some are in solid form and can be applied as fillers in a coating of a polymer substrate; products in this category include aluminium hydrate, organic and inorganic phosphorus compounds and are used as flame retardants on textile materials.

(b) Increase of the decomposition temperature

As elucidated previously, the chemical modification of a polymer substrate with specific chemical elements can inhibit the exothermic reaction and the decomposition proceeding at a higher temperature. This system has the best laundering durability effect.

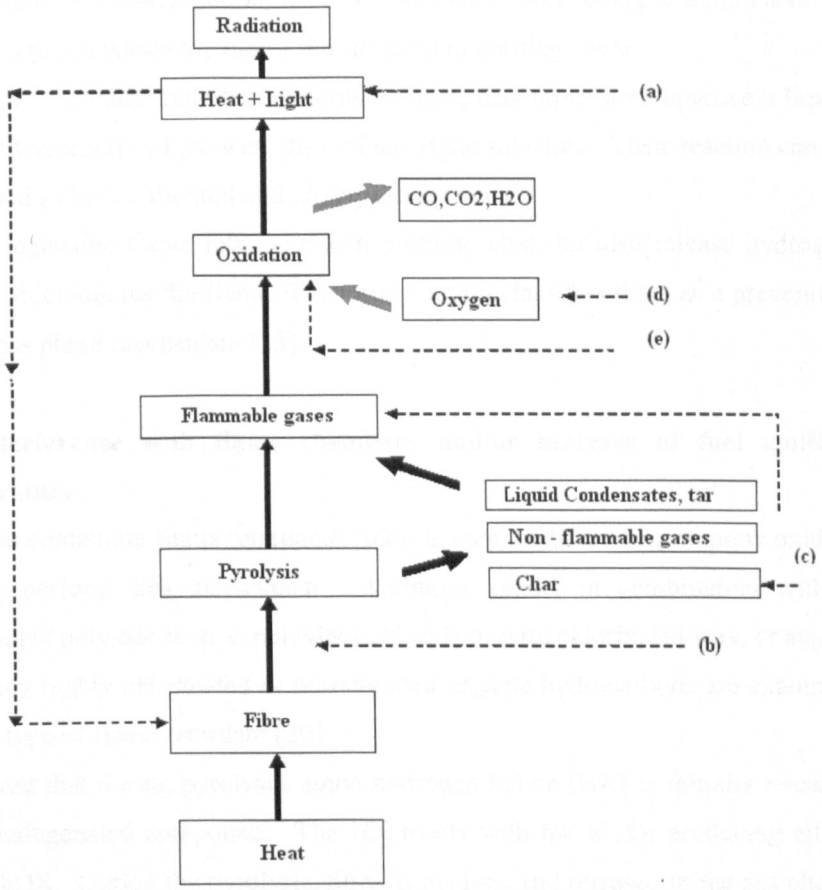

Figure 1.7 Combustion process as a feedback mechanism with flame retardant actions [23].

(c) Char formation acting to reduce the evolution of flammable gases

During the second stage of burning, the high temperatures bring about the decomposition process, producing volatile and non-volatile materials. In the case of polymer materials, the flammability of some of the volatile products can increase the rate of the burning process. Flame retardants which initiate desirable char formation include metal complex dyes on wool and also compounds containing phosphorus and nitrogen elements used as flame retardants on cellulose and wool fibres.

(d) Reduced access to oxygen or flame dilution

After polymer decomposition some flammable gases are produced along with high levels of free radicals, all in the presence of air oxygen. The chemical

exothermic oxidation reaction, leads to combustion proceeding to a high level of heat generation which facilitates the subsequent burning cycle.

Some generic flame retardant materials, during decomposition, produce a liquid phase intermediate which wets the surface of the substrate. Their reaction can be explained as both a thermal and an oxygen barrier.

The halogenated flame retardants can promote char but also release hydrogen halide which dilutes the flame. Their main action classifies them as a preventing in the gas phase mechanism [23].

(e) Interference with flame chemistry and/or increase of fuel ignition temperature

Halogen containing flame retardants, often in combination with antimony oxides, usually perform this mechanism. Antimony oxide, in combination with a chlorinated polymer such as polyvinyl chloride or with chlorinated wax, or any of the many highly chlorinated or boronimated organic hydrocarbons are examples of this type of flame retardant [20].

It is believed that during pyrolysis, some hydrogen halide (HX) is initially released from the halogenated compound. The HX reacts with the Sb_2O_3 producing either SbX_3 or SbOX. During the pyrolysis, SbX_3 is evolved and released to the gas phase, whereas SbOX which is a strong Lewis acid may operate in the condensed phase by facilitating the char formation by dissociation of the C-X bonds [24].

The activity of Sb_2O_3 to produce more char formation in combination with halogenated compound has also been confirmed [25].

The antimony oxides can also react in the condensation phase. Cellulosic fabric treated with chlorine compound in the presence of antimony oxides show a reduction in the char temperature [26].

During the burning process, the antimony halides reaching the gas phase react with atomic hydrogen producing HX, SbX, SbX_2 and Sb. Antimony reacts with atomic oxygen, water and hydroxyl radicals, producing SbOH and SbO. It is believed that the antimony halides delay the escape of halogen from the flame and increase its concentration, and at the same time dilute the flame. An alternative way to interfere with the flame chemistry can be the blanketing action of antimony halide which prevents the penetration of oxygen into the pyrolysing polymer [27].

1.3.1 Gas phase mechanism

The action of flame retardant in the gas phase can be explained according to a series of chemical reactions which interfere with the burning reactions and result in reducing the heat of combustion. The chain reaction, leading to the oxidation of hydrocarbons in common flames, has been illustrated in section 1.2.3.

Initial attack on substrate hydrocarbons by hydroxyl radicals which are generally produced in a reaction between oxygen and hydrogen radicals. Therefore, only reactions 8, 9 (section 1.2.3) lead to an exponential increase in radical concentration and preventing these reactions can disrupt the entire combustion chain.

The required energy for maintaining the flame is provided by the main exothermic reaction 6. The gas phase inhibiting effect of halogen derivatives, such as chlorine and bromine is considered to operate by releasing a halogen radical especially, if the flame retardant molecule does not contain hydrogen, and or release of hydrogen halides [27].

$$MX \longrightarrow M^{\bullet} + X^{\bullet} \quad (12)$$

$$MX \longrightarrow HX + M^{\bullet} \quad (13)$$

Where $M^{\bullet}$ is the residue of the flame retardant molecule, the hydrogen halides interact with and inhibit the activity of the free radicals $H^{\bullet}$, $OH^{\bullet}$ according to the following reactions:

$$H^{\bullet} + HX \longrightarrow H_2 + X^{\bullet} \quad (14)$$

$$OH^{\bullet} + HX \longrightarrow H_2O + X^{\bullet} \quad (15)$$

These inhibition reactions are pro-longed by the regeneration of hydrogen halides from the reaction of halides with appropriate hydrocarbon gases which are produced during the degradation.

$$RH + X^{\bullet} \longrightarrow HX + R^{\bullet} \quad (16)$$

It has been indicated that, the rate of reaction (14) is twice as fast as reaction (15) [27].

As explained previously, to slow down or stop the combustion process, it is imperative to prevent the chain branching reactions. Reaction (14) is the main inhibiting reaction. The high value of the ratio H_2:$OH^{\bullet}$ confirmed this statement. It is believed that competition between reaction (14) and (8) in chain branching,

determines the inhibiting effect observed in the gas phase mechanism. In reaction (8), two free radicals are produced for each H atom consumed, and in reaction (14), two halogen radicals recombine to form the relatively stable halogen molecule [27]. Despite the considerable amount of data supporting the hydrogen halides as primary inhibiting agents, some scientists do not believe this theory completely. The direct injection of halogen halide as a flame retardant did not show any inhibiting effect in the combustion procedure [27].

There should be some other mechanism which operates in the halogen inhibition however the consumption of hydrogen halide during the pyrolysis has been confirmed [28]. Until now the importance of these inhibition reactions to the flammability of the polymer has not been conclusively confirmed.

The removal of hydrogen atoms from the combustion chain by the following series of reactions is generally the most accepted mechanism for halogen inhibition.

$$X^{\bullet} + H^{\bullet} + M \longrightarrow HX + M^{*} \qquad (17)$$

The halogen atoms act as a catalyst in all the reactions.

Another theory in this mechanism has involved the catalytic recombination of oxygen atoms, as indicated in the following possible reactions [29].

$$O^{\bullet} + X^{\bullet} + M \longrightarrow XO^{\bullet} + M^{*} \qquad (18)$$

$$O^{\bullet} + X2 \longrightarrow XO^{\bullet} + X^{\bullet} \qquad (19)$$

$$O^{\bullet} + XO^{\bullet} \longrightarrow O2 + X^{\bullet} \qquad (20)$$

A physical mechanism theory has also been published [30]. These researchers believe that, their radical trap activity is not the only action of the halogenated flame retardants. The physical factors such as the density and mass of the halogen and its heat capacity have a profound influence on the flame retardancy activity. The halogenated flame retardant materials can work by reducing the heat evolved in the combustion of the gases given off, during the decomposition process.

1.3.2 The condensed phase mechanism

This process actually occurs at temperatures lower than those of the pyrolytic decomposition and leads to char formation. This mechanism can be explained in two modes; dehydration and cross-linking.

■Dehydration

This mode of action can be illustrated by the effect of many phosphorus-containing flame retardants on cellulosic materials. The interaction of the phosphorus compound with the polymer without a hydroxyl group is very slow and has to be preceded by an oxidation process. During the pyrolysis of many phosphorus flame retardant, approximately 50 – 90% of weight loss is observed due to the possible production of P_2O_5 or other oxides which are able to evaporate from the substrate surface [31]. A primary condensed phase mechanism is the most generally acceptable mechanism for phosphorus-containing flame retardants on cellulose. In fact, phosphorus oxyacids are generated from the fire retardant during pyrolytic decomposition which esterifies the cellulose subsequent thermal decomposition of the resulting ester gives rise to double bond formation with dehydration and finally char formation. Alternatively simple acids can catalyse the elimination of water from alcohols and further dehydration can result from this reaction. The Scheme below illustrates this mechanism [20]:

(21)

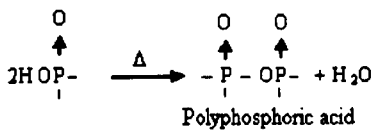

(22)

Esterification and dehydration

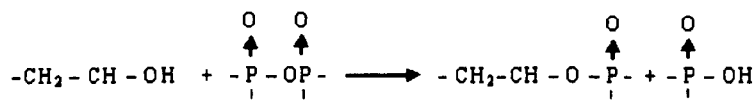

(23)

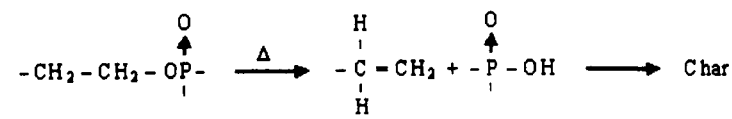

(24)

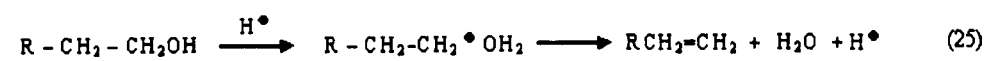

(25)

Scheme1.2. The dehydration and char formation mechanism for phosphorus containing flame retardants on cellulose [20].

Additionally, many other esters of strong mineral acids, such as sulphuric acid are also very effective as flame retardants for cellulose fibres. Sulphated cellulose is obtained by sulphation with ammonium sulphamate. The dehydration process can be explained via carbonium ion formation in scheme (26) [24].

The application of phosphorus compounds as flame retardants largely depends upon the chemical composition of the polymer substrate. These phosphorus compounds are generally important in hydrocarbon polymers with highly oxygenated contents.

■Cross linking and char formation

In the case of cellulose fibres, providing additional covalent bonds between the chains by using cross-linking agents, will improve cellulose stability. The cross-linking structure is much stronger than hydrogen-bonding, therefore in the initial degradation procedure more energy is required to break this linkage. The degree of polymerization and also the length of molecular chain structure have an effect on the pyrolysis of the cross-linked cellulose fibre. In rayon fibres, with low degrees of polymerization, this cross-linking can provide more space between the polymer chains and therefore create more access for oxygen in the structure leading to rapid depolymerization. The LOI value for viscose rayon is higher than formaldehyde cross-linked fibre [32].

Char formation is the most important condensed phase mechanism which can modify the combustion process. Char functions as a barrier to heat from the mass flow, and also prevents the combustion gases reaching the surface of the material. The ability to form char depends on the chemical and physical structure of the substrate, and also the rate of char formation is related to the other degradation mechanisms. The char formation in cellulose is initiated by rapid autocross-linking due to the formation of ether-oxygen-bridges formed from the hydroxyl groups on adjacent chains. In fact, studies of rapid initial weight loss, due to water evaporation, confirmed autocross-linking to be linearly related to the amount of char produced [32].

It was suggested that in the combustion process this auto cross-linking may increase the viscosity of the molten polymer thereby reducing the rate of transport of the combustion pyrolysis products to the flame [24].

In conclusion polymers with a high susceptibility to β-elimination reactions produce low levels of non-flammable volatile degradation products (e.g. water or hydrogen halide), a high yield of non-combustible char and a relatively low flammability performance [20].

A review of char formation has been recently published [33]. In Figure 1.8, ideal and non-ideal chars are illustrated schematically.

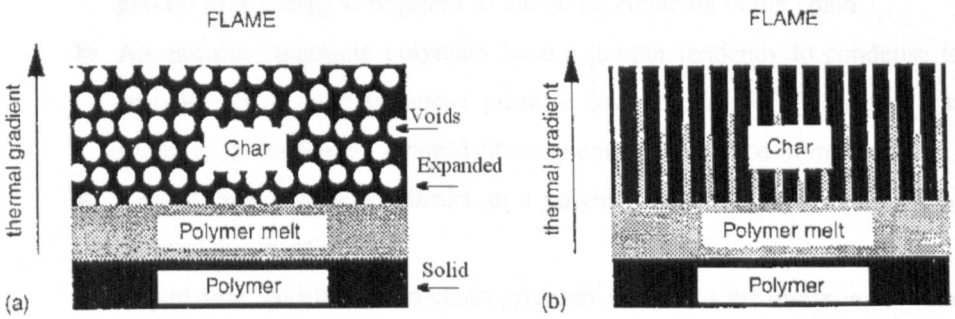

Figure1.8. (a) ideal char structure, (b) poor char structure [33].

The effect of physical structure of the produced char plays an important role on the fire retardant properties. For an ideal char formation, the gas bubble must become frozen into the expanding and thickening polymer, which produces a solid "honey-comb" or voided structure.

This "honey-comb" structure prevents the flow of volatile liquid or vapour into the flame, and also with sufficiently increased thermal gradient, can protect the remaining polymer, or polymer melt below from reaching its decomposition temperature. In non-ideal or poor char structures, when there are no closed cells, channels are produced in the pathway for the gas evolved on the surface of the melted polymer, volatile flammable gases can escape and produced further decomposition.

The types of char formation are still not probably understood but some factors have influence, such as, polymer melt viscosity, surface tension of the melt-gas interface, the kinetics of gasification and polymer cross-linking [34].

The structure of a polymer influences both its flammability and the amount of smoke formation. Polymers containing oxygenated aliphatic backbone structures have a tendency towards low-smoke generation, while polymers with pendent aromatic groups produce more smoke [35].

In addition to chemical structure and bond strength, there are still several parameters that have a reasonable influence on polymer pyrolysis such as, chain rigidity, resonance stability, aromaticity, crystallinity, orientation and degree of polymerization. The rate of thermal decomposition depends on the chemical and physical structure of the polymer.

- High chain rigidity increases the rate of decomposition and therefore greater heat energy is required to move the elements in the chain.
- Aromaticity: aromatic polymers have a greater tendency to condense to aromatic chars, and therefore produce low amounts of flammable gas products in the flame. Aramid fibres exemplify this type of material.
- Crystallinity: high crystallinity in a polymer leads to greater stability to thermal decomposition.
- Orientation: an increase in chain orientation reduces the distance between the polymer chains and therefore results in a more compact polymer. The low rate of oxygen diffusion into the polymer results in a decreased rate of pyrolysis [24]

1.4 Studies of cellulose thermal pyrolysis

The thermal degradation of cellulose has been studied for a long time and several theories have been proposed in this regard, but even with modern analytical techniques, there is still some unknown chemistry involved in this pyrolysis.

The mechanism of cellulose pyrolysis starts by depolymerization of macromolecules to lower molecular weight species. Further decomposition proceeds with some of these species while the rest undergo dehydration and polymerization, increasing the heat release and producing highly polymeric materials. These new products decompose again to aromatized materials and the evolve carbon monoxide, carbon dioxide, methane and hydrogen.

The proposed mechanism of the thermal pyrolysis of cellulose is summarized in Figure 1.9. Two different path-ways, regarding short length polymer chain degradation are indicated in this theory. Of these degraded polymer chains 40% lead to formation of non-flammable gases and production of char as final products. Of the remaining short chain polymers, approximately 60% are epoxides, and produce levoglucosan.

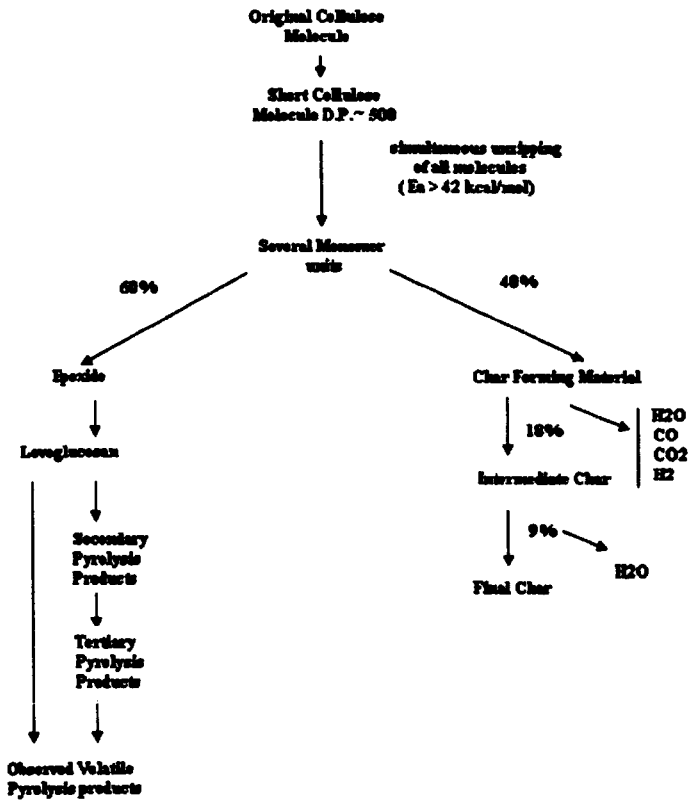

Figure1.9. Summary of cellulose decomposition pathways [20].

In the chemical structure of cellulose, the C-O bonds are thermally less stable than C-C bonds, therefore thermal scission of these linkages between glucose rings followed by transferring a hydrogen from the primary hydroxyl group to the oxygen of the broken glycoside linkage and an oxygen linkage between C1, C6 would occur forming levoglucosan, Figure 1.10 [36].

Following the three step levoglucosan production, secondary and tertiary pyrolysis products, volatile materials and tar would be formed. Reactions involving the production of tar are exothermic, with a high level of heat generation, which leads to further combustion. Some of these are outlined below:

- In the thermal pyrolysis of cellulose, if de-polymerization to levoglucosan was the first step, then it is possible to modify the cellulose at the carbon 6 position to minimize the formation of levoglucosan and decrease flammability [37].

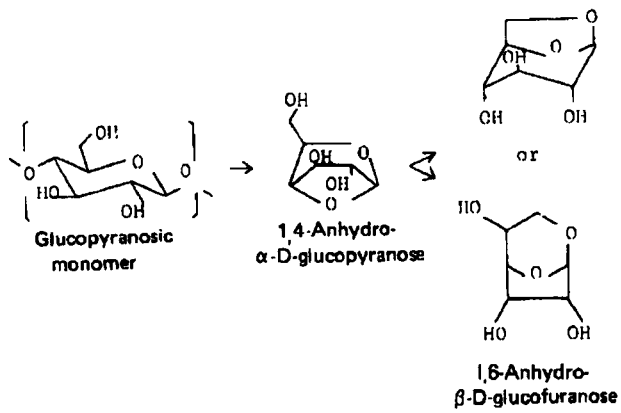

Figure1.10. Depolymerization of cellulose through 1, 4 anhydroglucose unit [36].

- The rate of thermal decomposition of viscose rayon is faster than cotton; this can be explained by the lower DP of the rayon [38]. The effect of DP and physical structure of cellulose fibre on its pyrolytic decomposition in a vacuum have been investigated. It was found that, cotton cellulose gave approximately 60% levoglucosan, whilst mercerized cotton cellulose yields 38%, hydrocellulose. The physical structure has an effect on the pyrolytic decomposition route a decrease in packing density was believed to cause a decrease in levoglucosan formation [39].
- The mechanism of pyrolysis involves the initial break-down to a DP of 200 follow by complete depolymerization of the chain end yielding levoglucosan. During the first step of pyrolysis, levoglucosan production was low and a large amount of volatile materials was produced. During later stages of pyrolysis, the yield of levoglucosan increased and remained constant as degradation continued [39].
- It was also found that [40] oxygen gas catalyses the decomposition process. In fact the accessibility of oxygen to the cellulose determines the rate of pyrolysis. The actual weight losses were two to eight times greater in air than in vacuum. Apparently under these conditions, it was found that, the reduction of DP in air pyrolysis was much greater than in vacuum pyrolysis.

Further research showed the effect of cellulose conformation on the pyrolysis reaction [41]. In order to form levoglucosan, from the anhydroglucose unit of the cellulose chain, the conformation change from the all equatorial C1 to the higher energy, all axial 1C state, must occur, Figure 1.11.

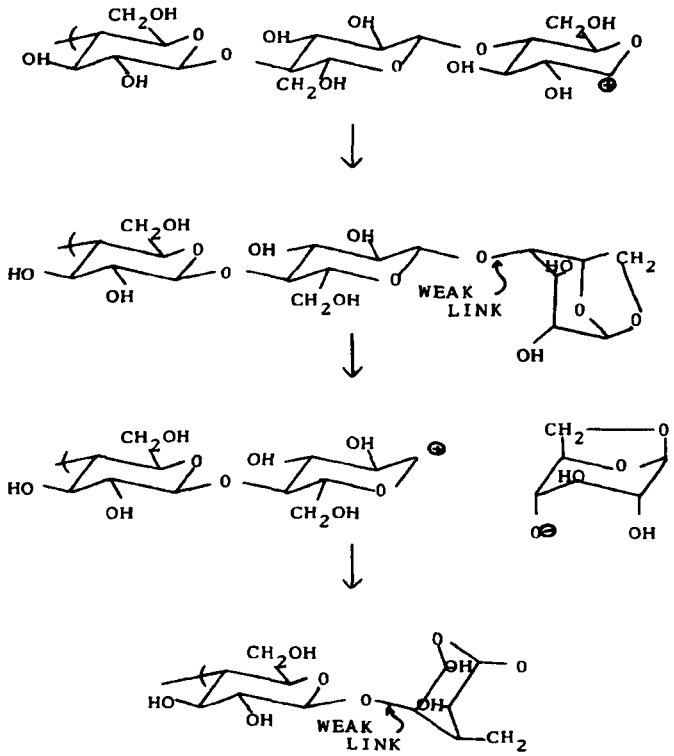

Figure1.11. Competitive de-polymerization of cellulose involving C1 and B1 conformations [41].

It was found that only at higher temperature, there would be sufficient thermal energy to produce a significant rate of unzipping and levoglucosan formation relative to degradation, cross-linking and aromatization. This could cause considerable strain to the glucosidic bond at the end of chain, and therefore facilitates the cleavage of terminal unit from the chain.

- Mack and Donaldson have also studied the effect of added inorganic bases on cellulose decomposition [42]. They found that, the presence of inorganic bases can reduce the levoglucosan formation during cellulose pyrolysis. In fact by catalyzing the decomposition process it is possible to change the thermal behaviour of the cellulose and increase the percentage of char obtained.

- The free radical transformation mechanism for cellulose thermal degradation was proposed by Shafizadeh [43]. The free radicals produced by the dehydration and degradation of the anahydroglucopyranose unit, lead to the

formation of oligomers. He pointed out that, the cleavage of glucosidic groups occurs with the participation of one of the free hydroxyl groups. A summary of these processes is shown in Figure 1.12.

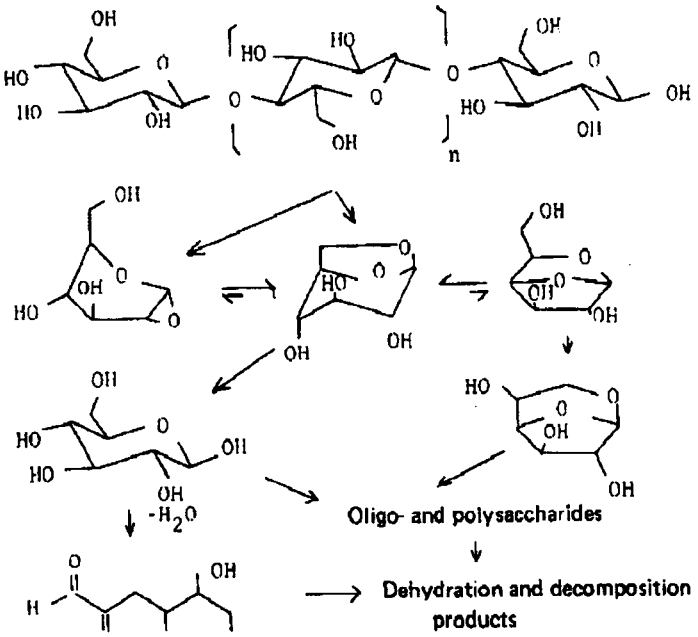

Figure1.12. Pyrolysis of cellulose and transformation of products [43].

■Shafizadeh also indicated that, the thermolysis as a heterolytic process must be sensitive to the effect of acid and alkaline reagents. Therefore this sensitivity was studied in detail. It was found that under acidic conditions, the thermal degradation products formed by elimination of various bonds and hydroxyl groups result in substantial amounts of water and char. However under alkaline conditions, cleavage of the anhydro ring and breakdown of the sugar, gives a variety of carbonyl compounds [43].

■The mechanism of cellulose pyrolysis after the formation of levoglucosan has been studied by several researchers [44]. It has been proposed that, through a free radical mechanism, some gases, aldehydes, ketones and also unsaturated products would be produced.

■FTIR analysis of the gases evolved from thermal degradation of pure cotton fabric in air has been reported [45]. The optical densities (OD) of identified pyrolysis products as a function of temperature are shown in Figure 1.13.

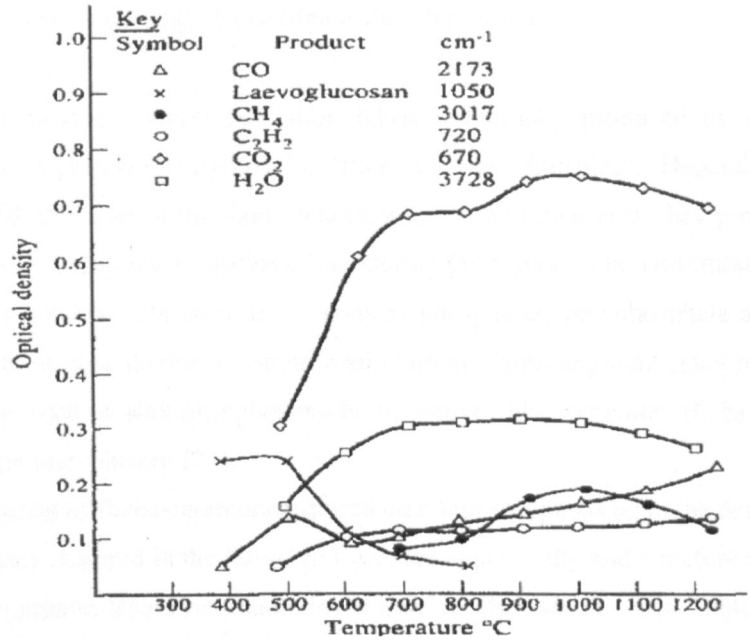

Figure1.13. The main gaseous pyrolysis products from pure cotton fabric evolved at different temperature [45].

These results indicate that, the concentration of levoglucosan formed at 400°C reaches a maximum at 500°C. At higher temperature, gases are evolved; CO and CO_2 concentrations increased while the levoglucosan concentration decreased gradually. Measurable quantities of methane, CH_4, are indicated in the range 700-1200°C. The acetylene, C_2H_2 concentration shows a similar temperature dependence of optical densities to that of H_2O vapour but with a lower OD value. The evolution of CO gas increased at high temperature up to 1200°C.

1.5 Flame-retardant cotton fibre

Previous research work in the field of cellulose thermal decomposition has served as a background for numerous investigations of flame-retardant systems. During thermal degradation, the fire retardant agents for cellulose serve two basic functions [20]:

- At the primary step of pyrolysis, the agents change fuel production processes, by reducing the 60/40 ratio between epoxide and char-formation materials, or alter the secondary decomposition of epoxide, levoglucosan to promote char formation products.

■To retard glowing combustion of the char products.

Flame-retardancy effects on cotton fabric are usually produced by after-treating fabric with chemical materials, i.e. 'flame retardant finishing'. Depending upon the chemical character of the flame-retardant agents and their cost, they provide various degrees of durability to different laundering processes. The non-durable category, includes soluble salts such as ammonium phosphates, polyphosphate and bromide; borate-boric acid mixtures. Some wash-durable flame-retardants may be chemically reactive, such as alkylphosphonamide derivatives like Pyrovatex (Ciba) and Proban (Albright and Wilson) [23].

The amount of flame-retardant required on a fabric depends upon the degree of flame retardancy required in the fabric end-use, the area density and structure of the fabric. Some common flame retardants for cellulosic fibre are listed in Table 1.1. In the treatment with phosphorus flame retardants compounds, the level of phosphorus is approximately 1.5 – 4 % (w/w) P on the fabric with the finishing add-ons in the range of 5 – 20% (w/w). To obtain the so-called synergistic anti-flame mobility properties of phosphorus / nitrogen containing agents, P: N molar ratios of between 1:1 and 1:2 are recommended [46]. In back-coating using the Sb–Br system, the total application level is typically between 20 - 30 % (w/w) (present in a 1:3, Sb: Br molar ratio) which is equivalent to an effective bromine add-on between 5 – 8 % (w/w) [25].

The effect of phosphorus flame retardants on cellulosic materials has been studied for a long time. A summary of their activity is indicated as follows:

Decomposition of the retardant generally yields phosphoric acid and polyphosphoric acid. At this stage, the production of the cellulose phosphorylate by reaction of intermediate phosphorus species would take place with the gradual release of water. This reaction can eliminate the heat generation and therefore reduces fuel release, and forms the protective barrier char [47].

Table1.1. Flame retardant materials for cellulosic fibres [46].

Type	Durability	Structure /formula
Salts:		
(1) Ammonium polyphosphate	Non – or semi durable	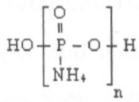
(2) Diammonium phosphate	Non – durable	$(NH_4)_2HPO_4$
Organophosphorus:		
(1)Cellulose reactive methylolated phosphonamides	Durable to more than 50 launderings	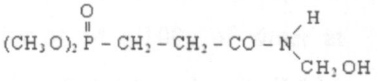 e.g. Pyrovatex CP (Ciba) TFR 1 (Albright & Wilson) Afflamit (Thor)
(2) Polymeric tetrakis (hydroxyl methylol) phosphonium salt condensates	Durable to more than 50 launderings	THPC – Urea – NH_3 Condensate e.g. Proban CC (Albright and Wilson)
(Back coatings):		
(1) Chlorinated paraffin waxes	Semi – durable	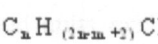
(2) Antimony / halogen (aliphatic or aromatic bromine – containing species)	Semi – to fully durable	Sb_2O_3(or Sb_2O_5) + Decarboromodiphenyl oxide or Hexabomocyclododecane + Acrylic resin e.g. Mylfam (Mydrin) Flacavon (Schill + Seliacher)

Further flame inhibition by phosphorus flame retardants is brought about by inhibiting the complete conversion of char to carbon dioxide; the main oxidation product would be carbon monoxide which means that less heat is evolved in the combustion process. Mono, di, tri pentaerythritol are commonly used as char yielding polyols [48].

Some phosphorus containing compounds, in combination with certain nitrogen compounds, typically melamine, urea or dicyanidiamide will enhance the phosphorus action as a flame retardant. This often synergism action depends upon the specific nitrogen compound available. The formation of the strong phosphorylating agents

with P-N groups has been reported. This product may also prevent loss of the phosphorus from the condensed phase [49].

Soluble ammonium phosphate

This compound is well known as a non-durable flame retardant for use on cellulosic materials, such as disposable textiles, non-wovens, paper and wood. The history of these compounds is thought to go back to 1821, when they were used on theatre curtains in France. They can inhibit smoldering combustion as well as flaming combustion [50].

Akzo's FYREX is a commercial blend, consisting of 60% diammonium phosphate and 40% mono-ammonium phosphate with a solubility of 54 g/100g of water at 25°C. In this category a formulation of ammonium phosphates are also available, with admixed ammonium bromide and wetting agents. This combination produces an improved soft handle on the treated fabric [50].

Insoluble ammonium polyphosphate

Thermal dehydration of ammonium phosphates in the presence of urea or under pressure with ammonia can lead to produce a high molecular weight ammonium polyphosphate with a chain length of over 50 repeated units exhibiting low water solubility. Actually various crystal morphologies have been reported from different manufacturers. This insoluble product can be applied as a flame retardant alone or in combination with other nitrogenous resins to textile materials and also to specific polymers [51].

It has been mentioned that, to obtain a successful treatment, the relative efficiency of the ammonium polyphosphate-nitrogen resin formulation has to be studied carefully. Depending upon the end-use, thermal decomposition, the type of the polymer, and also the required amount of each compound in formulation should be optimized [51].

Organic phosphorus, containing reactive methylol compounds

Pyrovatex is a finish developed by Ciba-Geigy (now Huntsman), and is a typical reactive, phosphorus-based flame retardant compound: N-methylol-dialkyl-phosphonopropionamide. A formulation consists of 40% Pyrovatex, 5% methylol-melamine resin, 1% urea, 1% softener, 0.1% wetting agent, and approximately 0.5% of an acid catalyst such as phosphoric acid. This water soluble formulation is applied

to the fabric by the conventional pad-dry heat cure method. The treated fabric is given an after-wash to remove unreacted chemicals. The toxicity of this treatment is low, and a soft handle is produced. This treatment is durable to home laundering and has been primarily used in the production of children's flame retardant cotton sleepwear as well as curtains and other soft furnishings.

This class of flame retardant in textile finishing is well known as a successful material particularly for cotton and cotton-rich blends [52].

Tetrakis-hydroxymethyl phosphonium chloride/sulphate/acetate is produced by the reaction of phosphine with formaldehyde in the presence of the chosen acid:

$$4\,HCHO + PH_3 + HCl \longrightarrow \underset{THPC}{(HOCH_2)_4\,P^+\,Cl^-} \qquad (26)$$

These salts are produced commercially as stable aqueous solutions and can therefore be easily padded onto the fabric. Using a high temperature curing process, they can be converted to stable, durable finishes on cellulosic substrates by pre-condensation with reactive nitrogen containing species. Many reactions with amino resins, urea and ammonia have been described and reviewed [54]. In Table 1.2., the procedure of each reported treatment has been briefly indicated [53], [54].

The most significant methods consist of three steps:

1 - Neutralization of THPC to form THPOH

$$\underset{THPC}{(HOCH_2)_4\,P^+\,Cl^-} + NaOH \longrightarrow \underset{THPOH}{(OHCH_2)_4\,P^+\,OH^-} + NaCl \qquad (27)$$

2 - The THPOH solution is applied to the fabric by padding, followed by drying and exposure to ammonia vapour in a special chamber for curing the THPOH. At this stage, the structure of the finish is probably mainly a network of N-CH_2-P linkage, where the phosphorus is still in the lower state (organophosphine) of oxidation.

3 - Air oxidation or exposure to dilute hydrogen peroxide or perborate on the cured finished fabric is necessary to produce stable P(O)–CH_2-NH–CH_2-P(O) linkages. Thus a highly cross-linked P-N polymer is encapsulated within the fibre. This treatment can withstand 50 or more multiple home laundering processes, and is resistant to the highly alkaline conditions of industrial laundering [52].

The pre-reaction of THPC with urea has been studied and specific improvements in fabric quality are indicated [55]. This avoids formaldehyde emission and facilitates

the rapid curing of the finish product. Durable press finishing can be produced by this method of treatment.

A study on the thermal decomposition of ammonium polyphosphate in the presence of selected metal ions, and their potential for improving cotton fabric flame retardancy has been reported recently [56]. Fabric was coated with prepared emulsions containing resin-based PVC-acrylic latex and ammonium polyphosphate (APP) as a flame retardant and 2% metal salt by weight of APP. The fabric was coated using the K-bar technique giving approximately 30% dry formulation add-on by weight of fabric. The fabric was dried at 100°C and cured at 150°C for 3 minutes. It was shown that certain metal ions, particularly Mn^{2+} and Zn^{2+} promote thermal degradation of APP at lower temperature. This achievement with metal ions is significant especially in the case of back coating of textile materials where the flame retardant formulations are required to become active at temperature below normal substrate ignition temperature.

The flame retardant properties and also thermal analysis of fabric treated with THPC-amide, THPOH-amide, THPOH-NH_3 and THPC-cyanamide were investigated before and after five washes [57]. It was found that the THPC-amid, THPOH-amide and THPC-cyanamide finishes appear to react in a similar manner to provide fabric flame retardancy properties. In thermal analysis three steps of decomposition were indicated, at first, chain break-down and dehydration by an acid catalyzed, was reported; During the second step carried out in the range 345-350°C, phosphorylation of the C6 hydroxyl in the cellulose glucose unit was indicated giving char formation. Thermal analysis of the THPOH-NH_3 finished fabric, under nitrogen gas, revealed a strong exothermic reaction. The fabric treated with THPC-cyanamide did not show good flammability properties after the laundering process. There was a linear relationship between ΔH and N:P ratios.

Phosphorus compounds increase char formation. Ammonium phosphate has a greater dehydration power, imparting the tendency to form aromatic chars, more so than those finishes based on organic phosphorus. Most of the original phosphorus remains in the char for all these condensed phase flame retardants [58].

Clearly char formation is not a simple process, the presence of functional groups with the ability to dehydrate and cross-link is required. Therefore at first, an aliphatic carbonaceous product is generated and finally the aromatic char structure is

formed. It has been indicated that, the present of elements such as nitrogen and sulphur are well known to enhance synergistically the performance of phosphorus flame retardants, and lead to further char-forming tendencies. It is also very interesting to study the char structure thermal stability which can be achieved by formation of P-N and C-N bonds [59].

The permanency of the flame retardant properties of cellulose-treated fabric with various phosphorus and nitrogen compounds has been investigated [60]. It has been indicated that, compounds containing P-N bonds, despite their desirable flame retardancy properties, have poor durability to alkaline laundering conditions. While the compounds containing P-C bonds were much more promise as permanent flame retardants. The polar nature of the phosphorus-nitrogen bond encourages nucleophilic attack at the phosphorus atom. Therefore in alkaline washing processes, this bond is hydrolysed and is removed from the fabric. This effect can be controlled by the presence of strongly electron–donating groups substituted on the nitrogen atom.

In additional research, by treating the cellulose fabric with N-methylolacetamides, workers found that, by increasing the nitrogen to phosphorus ratio in the compound with constant phosphorus add-on, the flame retardancy was improved [61].

Several phosphorus nitrogen combinations, in order to investigate P-N synergism have been applied to the cotton fabric. For example the LOI[1] value of the samples increased continuously as the amount of either the phosphorus or the nitrogen concentration was increased and the best results were obtained with a substituted melamine while the lowest effectiveness was obtained when using the urea derivatives [62].

Cotton fabric pretreated to contain quantities of nitrogen in the form of amines, amides or nitrile functional groups, was treated with THPOH [63]. It was found that the best flame retardancy occurred with the most basic and most nucleophilic nitrogen aminated cellulose; the cyanoethylated materials with the least basic and least nucleophilic nitrogen exhibited the worst performance. The amount of phosphorus lost from the fabric during the pyrolysis, was much higher.

1. LOI, "limited oxygen index", is the maximum concentration of oxygen in an oxygen-nitrogen mixture, required to just support down ward burning of a vertically mounted test specimen. Therefore, higher value represents better flame retardency.

Table1.2. Summary of Tetrakis-(hydroxymethyl)- phosphonium derivatives applied successfully to cotton fabric [53].

THP Derivatives	Curing method	Comments
(i) THPC		
THPC – urea	Catalyst, Heat 150 - 160°C	HCHO release, fabric stiffening with some degree of crease recovery, fabric tendering
THPC – trimethylol melamine (TMM)		
THPC – cyanamide		
THPC – dimethylolcyanoguanidine		
THPC – thiourea		
THPC – urea – ammonia	NH_3 Catalyst, heat 160°C	All above factors reduced Improved crease resistance
THPC – tris (1- aziridinyl phosphine oxide or sulphide (APO or APS)		
(ii) THPOH (from THPC + NaOH at 7-7.5)		
THPOH – TMM – urea	Heat 150°C or NH_3	Reduced fabric tendering and stiffness
THPOH – ammonia	NH_3	No fabric tendering or increase in stiffness
(iii) THPS		
THPS – urea	Catalyst, heat	Comparable with respective THPC and THPOH analogues
THPS – ammonia	NH_3	
(iv) THP carboxylates		
THP acetate (+ phosphate)	NH_3	Reduced free formaldehyde formation
THP oxalate	NH_3	

It was also shown that following pyrolysis of cellulose, when the nitrogen was present as the nitrile, the amount of phosphorus lost from the fabric is much higher in comparison with the nitrogen (N) being present in the amine or amide form.

It is obvious therefore, that the chemical structure of the nitrogen compound used synergistically with the phosphorus compound has a significant effect on flame retardancy effectiveness.

During the thermal decomposition of the phosphorus-nitrogen compounds, an intermediate product containing numerous P-N bonds was formed by the nuclophilic attack upon the phosphate. These P-N bonds are more polar than the corresponding P-O bonds, therefore giving high electrophilicity on the phosphorus atom, resulting in phosphorylation of the cellulose hydroxyl groups. The more electron deficient phosphorus would also have higher Lewis acidity and therefore the rate of acid-catalysed degradation would be increased [64].

Studies of the thermal degradation of cellulose ammonium phosphate and its metal complexes have been reported [65]. Cotton cellulose and carbamide were treated with phosphorus oxychloride in pyridine for 24 hours at 388°k. This product was filtered, washed and dried. Some selected metal complexes were applied to each sample 5% copper sulphate, zinc sulphate, cobalt sulphate, iron sulphate and cerium nitrate, respectively. Each reaction mixture was stirred at ambient temperature for 72 hours. DTA and TGA thermo-gravimetric analyses were carried out on each sample. In fact in this treatment, a decrease in the activation energy for decomposition was reported while an increase in char yield compared with untreated cellulose gave reasonable results.

The Pyrovatex CP was recently applied to the cotton fabric with two different cross-linking agents to see their effect on thermal degradation of cellulosic fabric [66]. In this way a new flame retardant finishing system based on hydroxyl-functional organophosphorus oligomer (HFPO) in combination of Pyrovatex with bonding agent such as trimethylol-melamine (TMM) and dimethyloldihydroxy-ethyleneurea (DMDHEU) was developed. The network cross-linking structure facilitates the fixation of phosphorus on treated fabric, after 50 home laundering processes.

1.6 Thermal analysis of flame-retardant cellulose

Thermal analyses of untreated cotton fabric, fabrics treated with the commercial condensed phase active flame retardant, namely ammonium polyphosphate (Amgard TR, Albright and Wilson Ltd) a phosphonopropionamide (Pyrovatex CP, formerly Ciba – Geigy Ltd now Huntsman) and a phosphonium salt – urea – polycondensate (Proban CC formerly, Albright and Wilson Ltd now Rhodia) and also the commercial vapour phase active, such as ammonium polyphosphate – ammonium bromide (Amgard CD, Albright and Wilson Ltd) and antimony (III) oxide – aliphatic bromide (Flacavon, Schill and Seilacher) have been investigated [67]. Thermo- gravimetric studies were carried out using the TG – 750 instruments. All samples were pyrolysed at various heating rates, over the range 2 – 15 °C min^{-1}, in a dry nitrogen atmosphere Figure1.14.

Each sample was found to show a characteristic TG curve with three distinct regions, which can be explained as three stages of the decomposition process: dehydration, volatiles evolution and finally char formation.

All the information provided in the TG and DTG curves, the temperature location, slope, shape and peak area, is characteristic for a particular physical or chemical transformation. Therefore with thermal spectra, the identification as well as the quantitative and qualitative analysis of the polymeric materials are possible.

As has been indicated, pyrolysis occurs in three stages. In the first stage, the rate of weight loss is relatively slow, and is probably due to the dehydration of the cellulose. In the second stage, a rapid weight loss can be interpreted as the evolution of the most volatile gases produced by the decomposition of levoglucosan, and the cellulose molecule.

At this stage 75% of the weight loss has occurred. In the final stage, the rate of weight loss slows down again and a tailing off of the TG curve is observed. The char formation in the solid state might be happening at this stage with evolution of mostly water, carbon dioxide and carbon monoxide.

At low temperature, between 200-280°C de-polymerization and dehydration occurred. Rapid volatilisation from the expected levoglucosan; finally levoglucosan breaks down to give smaller molecules, aldehydes, ketenes, aromatic hydrocarbons etc. Finally repolymerization of these volatiles leads to the char formation. However with other flame retardants which are vapour phase active, and also with antimony

oxide/aliphatic bromide finishes, the TG curve was too complex to be interpreted in the above simple way.

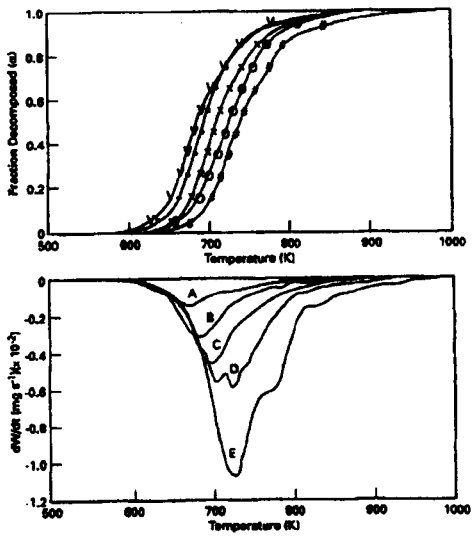

Untreated cotton fabric

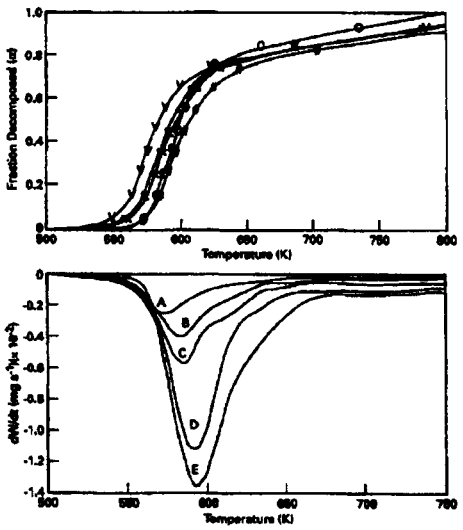

Proban CC treated cotton fabric

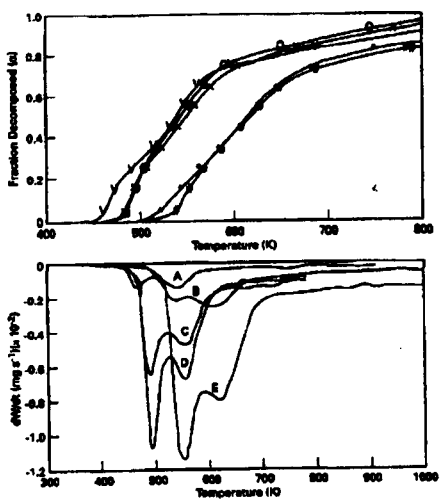

Amgard CD treated cotton fabric

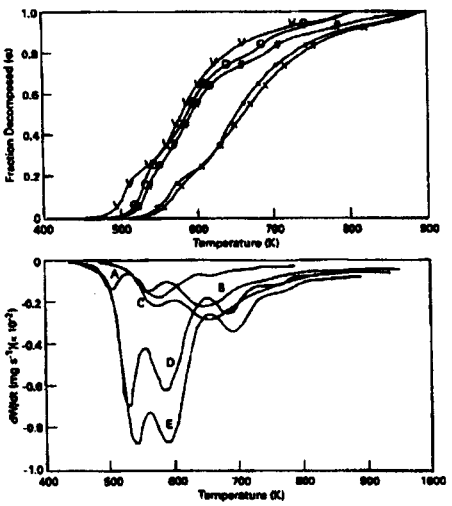

Flacavon (Sb/Br) treated cotton fabric

Figur1.14. TGA and the corresponding DTG curves for thermal decomposition of cotton fabrics treated with different flame retardant agents, under nitrogen using various heating rates. Heating rate in kmin^{-1}: A=2, B= 3, C=5, D=10 and E=15 [67].

Throughout this research it was indicated that, those fabric samples which produced more char after pyrolysis also gave higher activation energy values in the order:

Proban CC > Amgard TR > Pyrovatex CP > untreated cotton

The highest activation energy for Proban was related to its ability to produce char via the P- N bonds [68].

The influence of flame retardants on the mechanism of pyrolysis of cotton fabric in air has been discussed in detail [69]. The same flame retardant treatments have been carried out in this research, plus FTIR analysis which can monitor and identify the gaseous products produced during pyrolysis. GC-MS was used to identify the volatiles products; 30 model compounds were chosen as being representative of the pyrolysis, and then by routine quantitative analysis by GC, the presence of each product was determined. In fact, combining the information achieved via GC and FTIR analysis, led to a proposal for a simple reaction Scheme which explained the processes occurring within the three various temperature stages. At each stage, the temperature and products were indicated as in Figure 1.15.

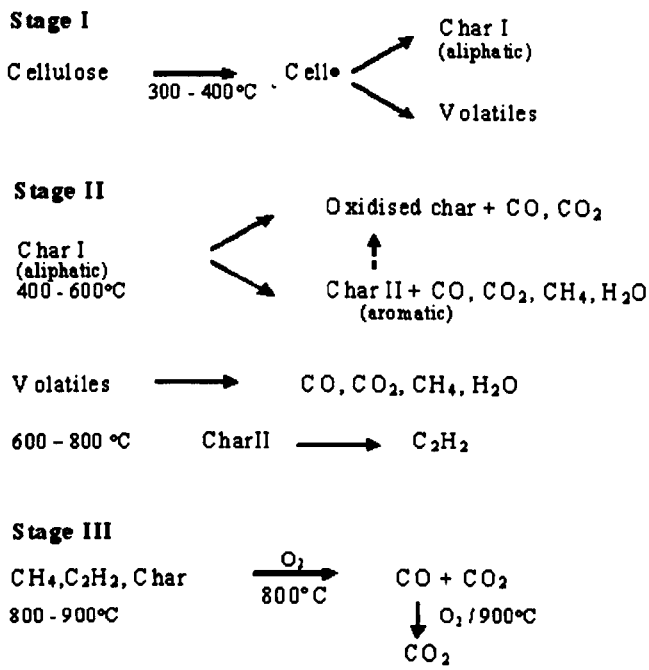

Figure1.15. Three stages of cellulose pyrolysis proposed on the basis of thermal analysis using FT-IR, TOI (temperature oxygen index) and EGA (evolved gas analysis) techniques [69].

In the first stage, 300- 400°C, two competing pathways are involved, which produce aliphatic char and volatiles materials. Char forming is increased by using P-N containing flame retardants. Stage II, 400-800°C, the aliphatic char changed to an aromatic char, by chemical reaction and evolution of CO and CO_2 gases, as a consequence of simultaneous, carbonisation and char oxidation. In the final stage III, above 800°C, further oxidation takes place, char and any remaining hydrocarbon species, convert to CO_2 and some CO.

The effect of each applied flame retardant on the thermal decomposition of cellulosic fabrics was indicated here. The organo-phosphorus and nitrogen containing condensed phase retardants, act in stage II, over the temperature range 400 – 600°C. Proban and Pyrovatex gave more furans[1]. Subsequently the production of aliphatic chars from them has been confirmed; in the presence of oxygen gas, oxidised char formation proceeds. On the other hand, the inorganic P/N retardants, antimony and bromide retardant produce an aromatic char, which can oxidise later. The volatile materials are oxidised to CO, CO_2, H_2O and various organo compounds. In the high temperature range, 600 – 800°C, the aromatic char decomposes to low molecular weight species such as acetylene.

The FTIR analysis of gases evolved from cotton and flame retardant cotton fabrics with various commercial flame retardant was also carried out [45]. Infrared absorption band assignments for all samples are shown in Table 1.3.

Table1.3. Infrared absorption band assignment for samples tested [45].

Band assignment	Frequency (cm^{-1})	Samples in which peaks appeared
Water, H_2O	3728 3625	All samples tested
Methane, CH_4	3017 1305	All samples tested
Carbon dioxide, CO_2	2359 2342	All samples tested
Carbon monoxide, CO	2173 2118	All samples tested
Aldehydes: Formaldehyde, HCHO; Acetaldehyde and acrolein	1700 1724	All samples tested
Propylene, C_3H_6	1410	Only sample H_{CD} and, H_F
Levoglucosan	1050	H_P, H_{PV} and H_F
Ethane, C_2H_4	950	All samples tested
Acetylene, C_2H_2	720	All samples tested
Carbon dioxide, CO_2	670	All samples tested

Amgard CD: H_{CD}, Proban CC: H_P, Pyrovatex CP: H_{PV}, Flacavon H14/587: H_F

All the fabric samples were pyrolysed in air over the extended temperature range 300 to1200°C. The results indicate that, at 400°C, for untreated cotton fabric, a considerable concentration of levoglucosan is formed which reaches a maximum at 500°C. At higher temperature, due to the production of CO, CO_2, the levoglucosan

1. Furan, C_4H_4O, is a cyclic flammable liquid compound which is obtained from wood oil of pines or made synthetically.

concentration decreases to a low level. Measurable quantities of CH_4, C_2H_2 are observed at 3017 cm^{-1} and 720 cm^{-1}, between "700 to 1200°C". Products from all the fabrics studied start to emit measurable CO around 400°C and CO_2 evolution were determined at 670cm^{-1}, from 400 to 900°C.

The flame retardant containing P-N compounds, such as Proban CC, ammonium diphosphate and Pyrovatex CP show similar product evolution behaviour following pyrolysis. However for Br- containing flame retardant fabrics, Amgard CD and Flacavon treated cotton, the decomposition to volatiles occurred at lower temperature around 300°C.

A second pyrolysis stage is identified in the region 450 – 800°C. For untreated cotton CO evolution increased at higher temperatures up to 1200°C. Finally the most appropriate model showing all the details for cotton pyrolysis in air has been revised, Figure 1.16.

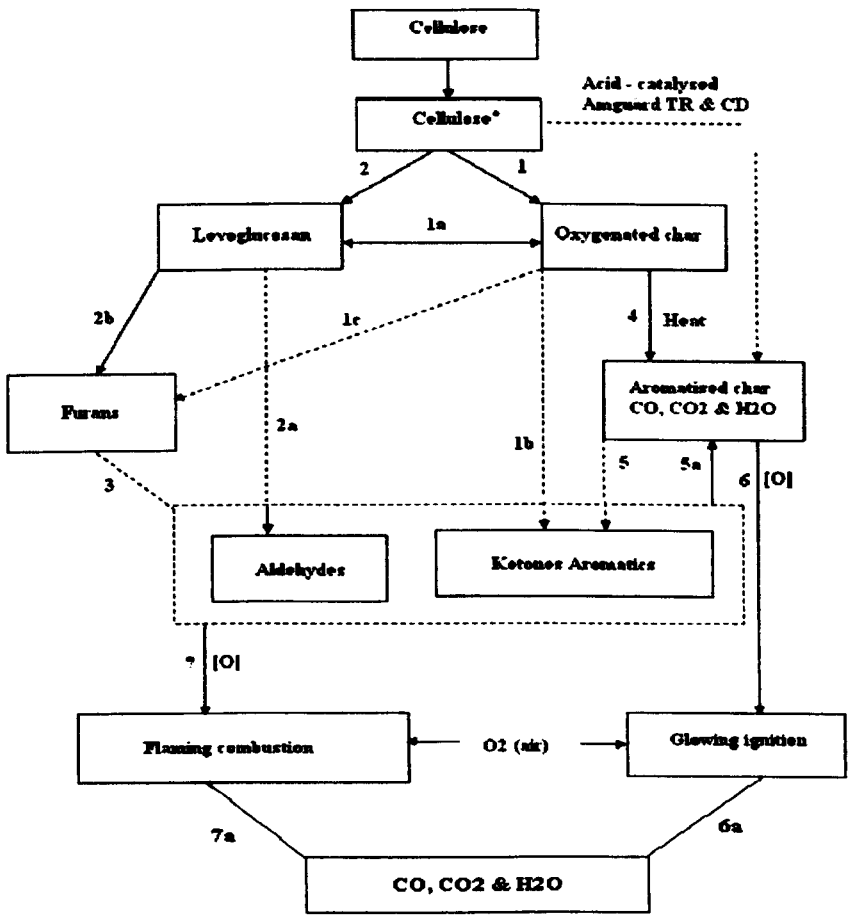

Figure1.16. A revised proposed model for cellulose pyrolysis in air [69].

A most recent proposal on the thermal decomposition behaviour of organo phosphorus compounds as flame retardant finishes on cotton fabric has been published recently [70]. In this work, three organphosphorus compounds, N-hydroxymethyl-3-dimethylphosphonopropionamide (HDPP), triallyl phosphate (TAP) and triallylphosphoramide were selected as flame retardants. The flame retardancy of the treated fabrics was characterized by using limiting oxygen index (LOI). Further investigations were carried on by using thermal analysis methods such as DSC, TGA and also chemical analysis of the products from pyrolysis, using FTIR spectroscopy. A new mechanism of the flame retardant was proposed based on the results.

The FTIR studies indicated that, during the decomposition process of flame retarded fabric treated with HDPP, some intermediate materials would be formed at 300°C. They can phosphorylate the cellulose at C6 position or catalyse the dehydration of cellulose at lower temperature and prevent the formation of volatile materials. Based on the FTIR studies, a proposed reaction mechanism is shown in Figure 1.17.

The FTIR spectra of the HDPP-treated fabric indicated that the decomposition of P-CH_2-R bonds and also the presence of a new product with unsaturated C=C bonds at 300°C. The newly formed double bond also exists in acrylamide, which is one of the initial synthesis materials for HDPP. The formation of an intermediate phosphorus compound without the P-CH bond and with the P-OH bond was indicated. The formation of a trivalent phosphorus compound without the P-CH_2 and P=O group has also been suggested.

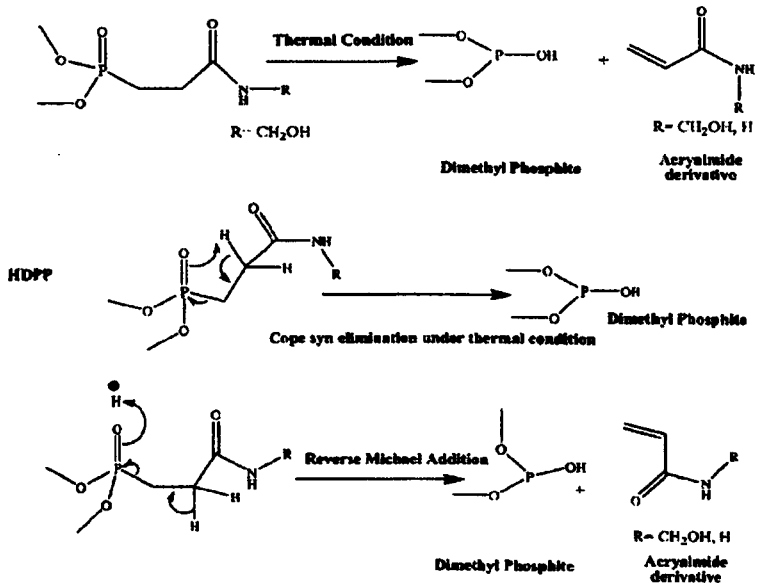

Figure1.17. Proposed mechanism of thermal decomposition of HDPP [70].

In fact, during pyrolysis, the intermediate materials have limited stability thus making it more complicated to identify the actual products. The production of dimethyl-phosphate as an intermediate product was confirmed in this study. The intermediate itself as well as dimethylphosphate are both acidic and thus cause cellulose phosphorylation, which could start around 250°C as shown in the DSC data. The dehydration process leads to char formation, as shown in Figure 1.18.

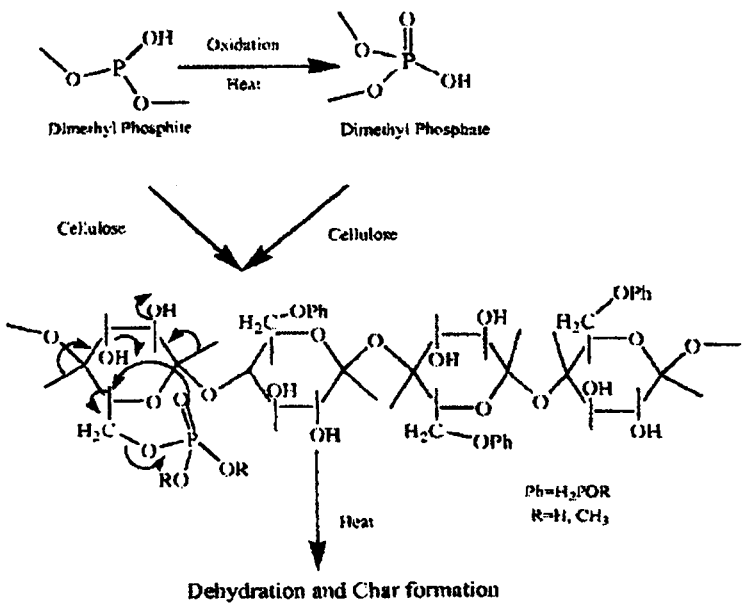

Figure1.18. Phosphorylation and pyrolysis mechanism of cellulose [70].

The pyrolysis results for fabric treated with TAP indicated that, most of the TAP was lost as vapour without converting to an intermediate. Therefore in conclusion it is possible to say that, the difference between the phosphorus flame retardants may be related to their ability to phosphorylate cellulose under initial thermal decomposition. This step would effectively inhibit the formation of levoglucosan and accelerate the rate of char formation.

1.7 Smoke

Smoke definition is generally, considered as a cloud of particles, individually invisible, but as a result of light-scattering and/or light-absorption these particles appear opaque. Visible smoke is produced during the burning of polymer materials, especially as a result of incomplete combustion. In recent research using pyrolysis/ gas chromatography/ mass spectroscopy and special kinetic methods, it was shown that within a flame produced during thermal degradation procedure of polymer materials, the unsaturated hydrocarbon molecule formed as an intermediate product, will polymerise and dehydrogenate to form carbon or soot [33].

Intermediate molecules can form unsaturated species or they can cyclise to form polybenzenoid structures, both of which produce soot. The procedure of soot formation has been summarized in Figure1.19.

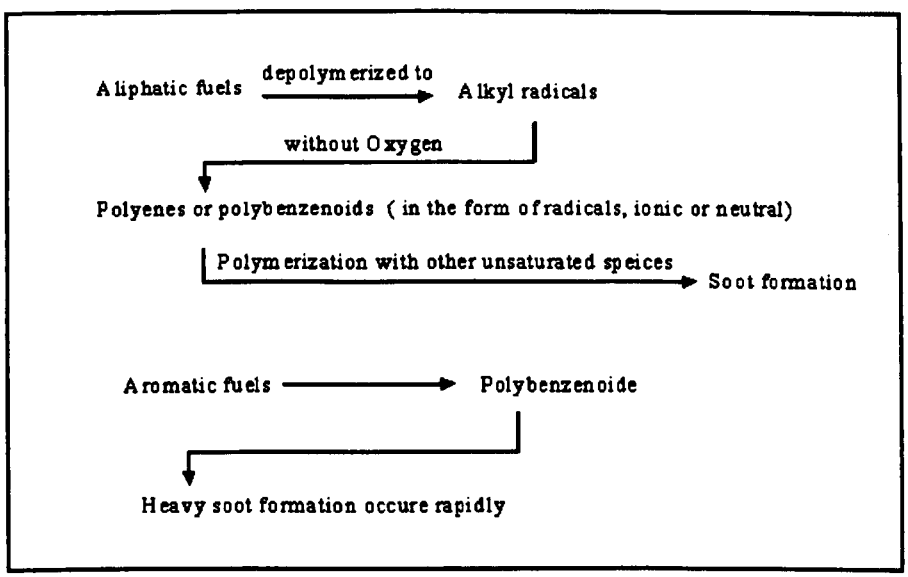

Figure1.19. A summary of the procedure of soot formation [33].

In the presence of oxygen the tendency for soot formation generally decreased. Hydrogen halide may promote soot formation through dehydrohalogenation, assisting ring closure and finally producing olefins and polyenes [71]. It should be indicated that from an individual polymer the relative distribution of pyrolysis products depends on the pyrolysis temperature, rate of heating and also the condition and atmosphere of pyrolysis.

1.8 Regenerated cellulosic fibres

The process of making viscose, which is the oldest commercial man-made fibre, was discovered by C.F.Cross and E.J.Bevan in 1891. The preparation of the viscose solution is complicated as is the manufacturing of this type of regenerated cellulose fibre.

The process of manufacturing viscose rayon from wood pulp cellulose consists of the following steps:

(1) Steeping, (2) Pressing, (3) Shredding, (4) Aging, (5) Xanthation, (6) Dissolving, (7) Ripening, (8) Filtering, (9) Degassing, (10) Spinning, (11) Drawing, (12) Washing and (13) Cutting.

After delignification and also some other purification processes, the wood pulp is sent to the viscose production plant.

(1) Steeping: Alkali cellulose is produced by immersing the wood pulp cellulose in 17–20% (w/w) NaOH solution at 18 -25°C.

(2) Pressing: To obtain an accurate ratio of alkali to cellulose, the swollen alkali cellulose wood pulp is pressed to a wet weight equivalent of 2.5 to 3.0 times of the original wood pulp weight.

(3) Shredding: The pressed alkali cellulose is shredded mechanically into fluffy particles called "crumbs".

(4) Ageing: Leaving the alkali cellulose for at least 24 hours at 18° to 30°C brings about some cellulose depolymerization

(5) Xanthation: The reaction of the aged alkali cellulose with carbon disulphide is carried out at 20°C to 30°C in vats to produce an orange coloured solution of cellulose xanthate. This solution is then diluted with sodium hydroxide solution, at 15°C to 20°C under high-shear mixing conditions, then filtered to remove insoluble fibre materials and deaerated.

$$(C_6H_9O_4ONa)_n + nCS_2 \longrightarrow (C_6H_9O_4\text{-}SC\text{-}SNa)_n \quad (28)$$

(6) Dissolving: The alkaline solution reduces the inter-chain hydrogen bonds and allows water molecules to solvate and separate the chains, to produce a useable viscose solution.

(7) Ripening: The viscose solution is allowed to stand for a period of time to "ripen". At this stage, the reversible xanthation reaction allows, some of the xanthate groups revert to cellulosic hydroxyls by losing CS_2; this reduction in the cellulose xanthate solubility is important since it facilities the regeneration of the cellulose filaments.

$$(C_6H_9O_4O\text{-}SC\text{-}SNa)_n + nH_2O \longrightarrow (C_6H_{10}O_5)_n + nCS_2 + n\,NaOH \quad (29)$$

(8) Filtering: The viscose is filtered to remove undissolved materials.
(9) Degassing: Prior to spinning, the bubbles of air entrapped in the viscose must be removed.

(10) Spinning: The viscose solution is metered through a spinneret into a spin bath (wet spinning) containing sulphuric acid, sodium sulphate and zinc sulphate. In the spinning bath coagulation occurs to form the regenerated cellulose from cellulose xanthate. The chemical reaction in spinning bath is indicated in Scheme 30.

$$(C_6H_9O_4O\text{-}SC\text{-}SNa)_n + (n/2)\,H_2SO_4 \longrightarrow (C_6H_{10}O_5)_n + nCS_2 + (n/2)Na_2SO_4 \quad (30)$$

(11) Drawing: The rayon filaments are stretched; chain orientation and inter-chain hydrogen bonding occurs at the drawing stage and gives the required physical properties to the fibres.

(12) Washing: Several different washing techniques may be used to remove salts and water soluble impurities.

(13) Cutting: To produce a staple fibre, the group of filaments (termed "tow") is passed through a rotary cutter to provide a fiber of required length [72].

In high tenacity rayon fibres, including those termed polynosic, by shortening the time of ageing and ripening processes, viscose solutions with a high level of DP are produced. In the drawing stage, slow regeneration of cellulose and stretching of rayon will lead to greater areas of crystallinity within the fibre.

Cuprammonium rayon with similar properties to the viscose fibre is produced via a different method. In fact the cellulose is reacted with copper and ammonium hydroxide (Schweizer's reagent). Due to the environmental effects of this production method, cuprammonium rayon is no longer produced in the United States.

Lyocell is the generic name for solvent spun cellulose fibres which has been defined in 1989 by BISFA, Bureua International Pour La Standardization de Ia Rayonne et des Fibre synthetics. Today this fibre is produced by many companies around the world, originally by Courtaulds Plc (UK) with brand name "Tencel", and subsequently Lenzing AG (Austria) with the production of the "Lenzing Lyocell" fibre; the Courtaulds Tencel business are now part of Lenzing. There is also continued investigation in Lyocell filament yarns, and in the production of their variations, by Akzo Faser AG (Holland) who uses the trade name "Akzo Newcell". In Germany, TITK (Thuringisches Institute fur, Textile and Kunststoff Forschung), have developed their own Lyocell fibre known as Alceru. Lyocell fibre as a regenerated cellulosic fibre is more crystalline with a high degree of polymerization compared to viscose rayon fibre [73].

In Lyocell production, hot NMMO dissolves the wood pulp via a continuous dissolving unit under intensive shearing and water evaporation. At room temperature NMMO is a crystalline solid substance which is able to exist in various hydrated forms. The structure of NMMO can be seen in figure 1.20.

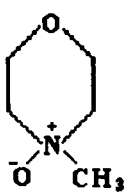

N-methyl morpholine oxide

Figure1.20. A solvent for cellulose [73].

NMMO monohydrate, which contains 13.3% water by weight, is a very stable form which dissolves cellulose. When the water content of the water/NMMO mix is reduced its dissolving power is increased, however, its melting point is also raised [74].

The spinning solution is an activated mixture consisting of 10 – 30% by weight of powdery cellulose and 70 – 90% NMMO plus 1% of a heat stabilizer (butyl gallate). The solution is filtered and extruded into a non-solvent bath to coagulate the cellulose. Any suitable aprotic organic liquid, non-solvent for cellulose, which is miscible with water and will not react with amine oxide, may be used; such as alcohol and dilute acid, methyl alcohol, butanol, toluene or xylene [74].

The solvent is removed from the spinning and washing processes then purified, re-concentrated and finally fed again into the process.

1.8.1 Flame Retardant Viscose Fibre

In the case of viscose fibre, as a regenerated cellulosic fibre, with the similarity of the chemical structure to cotton fibre, finishing with cotton flame retardants may be recommended.

Flame retardant viscose fibres may also be produced by incorporation of the flame retardant agents into the spinning dope, before fibre spinning. Flame retardant viscose fibres have been produced in numerous countries; some of the available commercial products are [75]:

Organophosphorus and nitrogen/sulphur-containing species, e.g. Sandoflam 5060 (Clariant), Lenzing FR.

Polysilicic acid and complexes, e.g. Visil AP (Sateri)

This approach presents many problems because of the particular chemistry of the viscose process. The flame retardants are required to be stable, inert to the alkaline viscose and also to the acidic coagulation bath in which the viscose is extruded. During spinning subsequent processing, such as stretching, the chemicals imparting flame retardance must neither be extracted nor chemically changed [73].

These materials must not interfere with the spinning process, by blocking of the spinneret orifices or changing the rheological behaviour of the spinning dope.

In the field of viscose flame retardancy, a large number of additives have been suggested [75]. They include alkyl-and aryl phosphates and phosphonates, halogen-substituted phosphates and phosphonates and phosphorus polymers such as emulsions from triallylphosphate and tetrabromethane, dibromopropyle phosphate – acrylamide condensates, THPC derivatives and others. Phosphazenes are liquid, flame retardants produced in organic solvent medium [76].

$$n PCl_5 + n NH_4Cl \longrightarrow (PNCl_2)_n + 4\,n\,HCl \qquad (31)$$

The chlorine atoms of the phosphazene can be reacted with a large number of compounds. The hexa-propoxy-cyclotriphosphazene in a mixture with the tetramer and higher cyclic polymers as well as with one or several additional substituted groups can be applied in the viscose solution [77].
Some disadvantages of this process are indicated below.

- In the spinning bath some of these materials migrate to the surface of the fibre and enter the coagulation bath. Therefore the flame retardant effectiveness can be reduced. However, an increase in corrosiveness, unpleasant smell and similar phenomena also has to be considered.
- The above mentioned materials are hydrolysable in alkaline media, therefore partial decomposition is expected, which has an effect on the flame retardancy properties.
- These materials can react with carbon disulphide which is present in the viscose as strongly coloured by-products on the surface of the fibre can not be removed by a bleaching process [75].

Phosphonitrile chloride derivatives and phosphonitrilate polymers have also been suggested in the field of viscose flame retardancy additives [78]. The considerable concentration of this compound which will enter in the coagulation bath means there is no commercial application of this process.
It is possible for red phosphorous to be spun into the viscose fibre, generally without any adverse effects on fibre production. However a dark violet colour is produced which limits its textile application [75].

Sandoflam 5060, from Clariant utilizes 2, 2'-oxybis-(5,5-dimethyl-1,2,3-dioxaphosphorinane-2,2'-disulfide) [79].

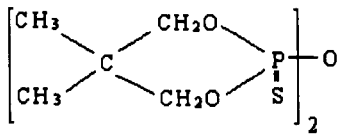

To achieve the desirable flame retardancy effect, approximately 20- 25% of this material is added to the fibre solution. In a research [80], it has been confirmed that there are no toxic gases emitted during the burning process.

An alternative method of producing flame retardant viscose is to use a mixture of finely divided deca-bromodiphenyl oxide with colloidal antimony pentoxide in a solid form applied to the viscose solution [79]. The reaction between the viscose fibre and the above compounds makes the viscose solution and the viscose fibre dark orange in colour, which is not acceptable. Polyvinyl bromide latex is another example which can produce a highly durable flame retardant effect, but due to discoloration of viscose dope, its application was rejected [75].

A proposed patent described the production of a flame retardant viscose fibre [81]:

- At first the viscose spinning solution is prepared in the usual manner.
- Adding "water glass" (sodium silicate) to the solution, approximately 12-16% by weight of viscose solution.
- Spinning the solution into the coagulation bath containing, 65g/l H_2SO_4, 20% w/w Na_2SO_4 and 45g/l $ZnSO_4$ at 50°C.
- The filament tow in the spin-bath was stretched in a stretching bath of water at 100°C to a length 90% greater then its original length.
- Cutting the filament into 40 mm staples
- Immerse the fibre in a sodium aluminate solution.
- Wash with water and surfactants.

The amount of aluminium used should be between 0.5 to 2% by weight of the fibre. During fibre manufacturing in the coagulation bath, where the viscose is regenerated into cellulose, the sodium silicate contained in it precipitated as polysilicic and distributed throughout the cellulose fibre.

The flame retardant fibre produced showed improved wash-fastness withstanding alkaline washing; it required a high level of polysilicic acid, but for techniqual reasons

this concentration must not be higher than 40% owf. It has been observed that using ordinary washing agents, the content of polysilicic acid falls to about half of the original concentration after 20 washing cycles. The high solubility of polysilicic acid in alkaline mediums has also led to problems in dyeing [81].

The Visil.RTM flame retardant fibre contains approximately 30-33% of aluminosilicate modified silica, $SiO_2Al_2O_3$ [82].

In recent years, a flame-retardant viscose rayon containing alkoxycyclotriphosphazene has been reported [83]. This compound can be added to the viscose solution which is then filtered, de-bubbled and matured. The viscose solution was then spun through a spinneret into a coagulation bath. The rest of the fibre manufacturing processes are the same as for conventional viscose fibre. The LOI value for the modified viscose can be LOI> 28. Some information regarding the thermal analysis of this fibre has been indicated in this research. The durability of this fibre in alkaline washing process is not indicated.

1.8.2 Flame Retardant Lyocell Fibre

Flame-retardancy incorporated by surface modification treatment on fresh, solvent spun cellulose fibre (Lyocell) has been studied in detail [84].

The Lyocell substrate, produced by Coutaulds Plc in the form of 2000 tex tencel tow was selected for this treatment, using Pyrovatex CP from Ciba Geigy. The successful recipe, to produce a flame-retardant Lyocell fibre, according to the standard formulation, consisted of 15% w/w Pyrovatex CP, 1% w/w Lyofix MLF as a cross-linking agent which is based on methylolated melamine, and 0.5% w/w phosphoric acid as a catalyst. This formulation was applied by padding to the tow at room temperature for 5 seconds and cured at 160°C for 3 minutes. A flame-retardant fibre with a limiting oxygen index (LOI) value of more than 29% was achieved. In comparison to cotton fibre, in Lyocell treatment only half of the amount of Pyrovatex CP flame retardant required to produce an equivalent degree of flame resistance.

In fact, the physical structure of the Lyocell fibre with a high degree of crystallinity has a more effective role in this successful achievement. This flame-retardant fibre can withstand industrial washing equivalent to 50 wash and tumble dry cycles, and maintains its flame retardancy with an LOI value higher than 26% while containing only 1% of phosphorus. The physical properties of the treated fibre have been

reported. The FR Lyocell fibre resulted in acceptable strength properties but with an increase in brittleness. High brittleness is one of the main disadvantages of this process and causes problems in industrial production.

1.9 Challenges in the production of flame retardant fibres

In the field of cellulose flame retardancy, there are still some unsolved problems and challenges for scientists [85]; such as:

1- Flame retardant textile materials are required to withstand 50 hot alkaline launderings in hard and as well as soft water.
2- Some physical properties of the treated substrate, such as tensile, tear and burst strength as well as abrasion resistance of the treated materials should remain unchanged.
3- By applying high deposits of chemical materials on the surface of the substrate, the effect of air permeability should remain acceptable.
4- Soft handle is required.
5- No change in the physical appearance of the substrate.
6- No change of the hue of the dye and or dye-ability of the material.
7- Health concerns are a big issue, the flame retardant substrate should pose no medical problems such as toxicity or skin irritation.
8- The process should not contain chemical materials suspected of being mutagenic or carcinogenic.
9- Low cost, simple production.
10 Process should not require new equipment and should be applicable in existing machinery.

In conclusion, a satisfactory durable flame-retardant treatment for cellulosic textile materials is still a significant challenge.

1.10 Toxicological risks of flame retardant chemicals

According to, the UK regulations (SI 1324,1988) for flame retardant chemicals, all elements of upholstered furniture are required to resist ignition by cigarette and also by a simulated lighted match according to British Standard 5852. The structure of upholstered furniture is composed of three parts, cover fabric from natural and synthetic fibre, upholstered filling materials such as polyester, polyurethane, feathers

and latex, interlining which acts as a fire barrier which must be of flame-retardant material such as aramide fibre and/or polyester wadding glass fibre.

National regulations and standards in some countries of Europe and the USA have specific regulations towards the ignitability of the upholstered furniture which are indicated in table 1.4 [86].

Assessment of risks and benefits in the use of flame-retardants in upholstered furniture has been carried out recently [86].

In health issue concerns, the possible risks to be involved in this issue are:

- Health risk assessment concerns the acute chemical toxicity of long term exposure, due to repeated exposure to a flame-retardant substance; an example being the chemical exposure of workers and release of chemicals in the environment.
- In domestic use under normal conditions, the risk of exposure of the flame-retardants species in the air, and also migration of these materials to the surface of fabric/ materials being in contact with skin.
- In the case of small ignition source, the risks of toxic gas emission due to the burning of the upholstered furniture which may or may not be flame-retardant.
- In recycling of the flame-retardant treated materials, the risk of toxic gas emission is also important.

In 2000, the US National Research Council (NRC) made a report regarding the toxicological risks of selected chemical materials identified as a flame- retardant in upholstered furniture [87]. The selected materials consist of 16 chemicals, (1) hexabromocylododecane,(2) decabromodipenyl oxide, (3) alumina trihydrate, (4) magnesium hydroxide, (5) zinc borate, (6) calcium and zinc molybdated, (7) antimony trioxide, (8) antimony pentoxide and sodium antimonate, (9) ammonium polyphosphates, (10) phosphonic acid, (3-([hydroxymethyl] amino)-3-oxopropyl)-dimethyl ester, (11) organic phosphonates, (12) tris (monochloropropyl) phosphate, (13) tris (1,3-dicholoropropyl-2)phosphate, (14) aromatic phosphate plasticisers, (15) tetrakis (hydroxymethyl) hydronium salts, and (16) chlorinated paraffins.

Table1.4. National regulation and standards in Europe and USA towards the ignitability of upholstered furniture [86].

Country	Type of building	Reference regulations	Type of furniture	Requirement	Test methods	Classification
France	Domestic Public	No. 200-164	Bedding	No ignition by cigarette	EN ISO 12952-1 and 2	Pass/fail
		U23 (health)	Bedding	No ignition by cigarette	EN ISO 12952-1 and 2	Pass/fail
			Mattress	No ignition by cigarette	EN 597-1	
		AM 18 (SpecTable)	Seat	No ignition by 20 g paper Cushion	NF D 60013	Pass/fail
				No ignition of the frame	NF P92501 and NF P92507	M3
		GPEMD1-90 (Prisons)	Mattress	No ignition by cigarette	EN 597-1	E
				No ignition by match	EN 597-2	D
				No ignition by higher ignition sources	GPEM DI 90 procedure	C,B,A (A the best)
UK/Ireland	Domestic	Furniture and funihing regulation n°1324, 1988	Seat / mattress	No ignition by cigarette	EN 1021-1	Pass/fail
				No ignition by match	EN 1021-2	
	Public	BS 7176	Filling	No ignition by cribe five	BS 5852	
			Seat	No ignition by cigarette	EN 1021-1	
				No ignition by match	EN 1021-2	Pass/fail
				No ignition by higher ignition sources in function of the level of hazard	BS 5852	
		BS 7177	Mattress	No ignition by cigarette		
				No ignition by match	EN 1021-1	
				No ignition by higher ignition sources in function of the level of hazard	EN 1021-2 EN 6807	Pass/fail
Italy	Public	DM26/06/1984	Seat/mattress	No ignition by a 40 mm high flame during s20, 80, 140	CSE RF 4/83	31M
			Filling			
US	Domestic	Federal mattress flammability Standard	Upholstered furniture	No ignition by cigarette	16 CFR Code of federal Regulation – Part 1632 (FF4-72, as amended)	Pass/fail

The aim of this research was to assess the potential health risks of these materials to the consumer and also the general population. This project was carried out by the Committee on Toxicology of the Board on Environmental, under the activation of a subcommittee member expertise in toxicology, epidemiology, pharmacology, chemistry, exposure assessment, risk assessment and biostatistics. In hazard identification, the relationship between the dose of an FR chemical and an adverse health effect are discussed. To identify the adverse health effect, associated with each flame retardant chemical a review on human (epidemiological studies, clinical observations and case reports) and also laboratory animal data on neurotoxicity, immunotoxicity, reproductive and developmental toxicity, organ toxicity, dermal and pulmonary toxicity, carcinogenicity, and other local and systemic effects were collected. In vitro data, the potential for genotoxicity as well as other toxic action are released. In the dose-response-assessment two relevant terms were indicated, NOAEL (no observed-advanced-effect-level) means, estimating the highest dose which no adverse effect were observed, and also LOAEL (the lowest-observed adverse effect level) which evaluates the lowest dose at which a statistically or biologically significant increase in an adverse effect were reported. The NOAEL or LOAEL were divided by two various explanations, uncertainty factors (UFs) and a reference dose (RfD). The RfD data gives a scale on which to calculate an estimate of lifetime daily dose that is believed to have a reasonable certainty of no harm. For the inhalation risk of exposure, reference concentrations were calculated from the RfDs.

In the Table 1.5 the toxicological risks of selected flame retardants applied to the cotton fabric have been indicated. The hazard index is calculated by dividing the exposure levels by respective RfDs or RfCs. Any chemical with a hazard index <1, indicates a non-cancer effect. For chemicals with in the limit <1 for lifetime exposure, excess cancer risk is estimated by multiplying the cancer potency factor by the lifetime-average exposure estimate.

In the case of higher levels of exposure, these are calculated based on the vapour pressure measurement for un-reacted starting materials which are still present on the upholstery substrate.

Table1.5. Summary of health risk assessment of flame retardant chemicals [87].

		Critical Toxicity End				Estimated worst-case Human Exposure levels			Hazard Index[a] for Non-Cancer Effects			Upper Limits on Lifetime Excess Cancer-Risk Estimate[b]		
Flame Retardant chemical	Point for Derivaton of RfD or RfC	Dermal (mg/kg-d)	Inhalation $\mu g/m^3$	Oral (mg/kg-d)	Cancer Potency Factor	Dermal (mg/kg-d)	Inhalation[c] $\mu g/m^3$	Oral (mg/kg-d)	Dermal (mg/kg-d)	Inhalation[c] $\mu g/m^3$	Oral (mg/kg-d)	Dermal (mg/kg-d)	Inhalation[c] $\mu g/m^3$	Oral (mg/kg-d)
Phosphonic acid	Inadequate data for any route	N/C	N/C	N/C	N/A	28×10^{-2}	0.35 (particles) UE (vapors)	7.5×10^{-4}	—[h]	—[h]	—[h]	N/A	N/A	N/A
Organic phosphonates (dimethyl hydrogen phosphate)	Oral: lung hyperplasia and alveolar/bronchiolar adenomas or carcinomas observed	N/C	N/C	0.12	5.4×10^{-3} per (mg/kg-d) (oral) 1.5×10^{-6} Per $\mu g/m^3$ (Inhalation[f])	2.2	0.72 (particles) UE (vapors)	5.9×10^{-2}	18.3	1.7×10^{-3} (particles)	0.49	6.1×10^{-2}	1.1×10^{-6} (particles) 6.6×10^{-4} (vapour)	9.1×10^{-6}
Tris(monochloropropyl) phosphate	Inadequate data for any route	N/C	N/C	N/C	N/A	1.5	0.48 particles) UE (vapors)	4.0×10^{-2}	—[g]	—[g]	—[g]	N/A	N/A	N/A
Tris (1,3-dichloropropyl-2) phosphate	Oral: testicularatrophy and seminal vesicle effects	N/C	N/C	5.0×10^{-3}	6.0×10^{-2} per (mg/kg-d) (oral) 1.73×10^{-5} per $\mu g/m^3$ (Inhalation[f])	2.6×10^{-3}	0.48 particles) UE (vapors)	4.0×10^{-2}	0.52	2.7×10^{-2} (particles)	8.0	1.6×10^{-4}	8.2×10^{-6} (particles) UE(vapors)	6.6×10^{-5}
Aromatic phosphate Plasticizers (tricresyl phosphate)	Oral: liver lesions and adrenal gland toxicity	N/C	N/C	7.0×10^{-2}	N/A	3.0×10^{-3}	0.48 (particles) 417(vapors)	4.0×10^{-2}	4.3×10^{-2}	1.9×10^{-3} (particles) 1.7 (vapors)	0.57	N/A	N/A	N/A
Tetrakis hydroxymethyl Phosphonium chloride (THPC)	Oral: liver toxicity	N/C	N/C	3.0×10^{-3}	N/A	—[i]	0.43 (particles) 417(vapors)	9.4×10^{-4}	N/C	4.1×10^{-2} (particles)	0.31	N/A	N/A	N/A

		Critical Toxicity End				Estimated worst-case Human Exposure levels			Hazard Index[a] for Non-Cancer Effects			Upper Limits on Lifetime Excess Cancer-Risk Estimate[b]		
Flame Retardant chemical	Point for Derivaton of RfD or RfC	Dermal (mg/kg-d)	Inhalation $\mu g/m^3$	Oral (mg/kg-d)	Cancer Potency Factor	Dermal (mg/kg-d)	Inhalation[c] $\mu g/m^3$	Oral (mg/kg-d)	Dermal (mg/kg-d)	Inhalation[c] $\mu g/m^3$	Oral (mg/kg-d)	Dermal (mg/kg-d)	Inhalation[c] $\mu g/m^3$	Oral (mg/kg-d)
Ammonium polyphosphates	Oral: calcification of the kidney	N/C	N/C	300	N/A	2.2	0.71 (particles) N/C (vapors)	5.9×10^{-2}	7.3×10^{-3}	6.8×10^{-7} (particles)	2.0×10^{-4}	N/A	N/A	N/A
Antimony trioxide	Ora;: liver toxicity; Inhalation: noncancer pulmonary toxicity;lung tumors	N/C	2.0×10^{-4}	0.2	7.1×10^{-4} Per $\mu g/m^3$ (Inhalation[f])	2.0×10^{-2}	0.24 (particles) N/C (vapors)	5.2×10^{-4}	0.1	1.2	2.6×10^{-3}	N/A	1.7×10^{-4} (particles)	N/A
Antimony pentoxide and sodium antimonite	Inadequate data for any route	N/C	N/C	N/C	N/A	2.0×10^{-2}	0.24 (particles) N/C (vapors)	5.2×10^{-4}	—[g]	—[g]	—[g]	N/A	N/A	N/A
Chlorinated paraffins Tris(monochloropropyl) phosphate	Oral: liver and kidney toxicity	N/C	N/C	0.3	N/A	0.59	0.28 particles) N/C (vapors)	1.6×10^{-2}	1.9	2.7×10^{-4}	5.3×10^{-2}	N/A	N/A	N/A

a- The hazard index is calculated by dividing exposure levels by RfDs or RfDs.
b- Lifetime excess cancer risk was calculated by multiplying the cancer potency factor by the exposure estimate.
c- Vapour exposure levels were calculated based on the vapour pressure measurement for un-reacted starting material.
d- In dermal RfD, the toxicity information was not available. They used oral RfDs as best estimate for internal dose.
e- In inhalation RfC, the toxicity information was not provided, therefore this value was estimated from oral RfD data.
f- In exposure to particles and vapour, following inhalation, cancer potency factor has been indicated.
g- There are inadequate toxicity data from any roué of exposure, therefore there is no value for RfDs, or RfCs for these compounds.
h- In the case of phosphonic acid, from any route of exposure there are no adequate toxicity data available. In fact this compound is likely to have a cross-linking with fabric componentsat.
i- The application of THPC to cotton fabric is provided by polymerizing of this compound on substrate, because of that, it is not possible to calculate any toxicity data for this compound.
Abbreviation N/A means, is not applicable because the chemical is not carcinogenic by the relevant route. N/C means is not calculated because of inadequate data. UE, means for this type of compound modelling produces unrealistic short-term exposure estimates, and because of that the maximum level of exposure is unknown.

In conclusion the NRC report found that for most of the 16 candidate flame retardants materials, in all three routes of exposure (dermal, inhalation and oral) the hazard indices for possible carcinogenic effects are less than 1. This means, even with the worse case exposure levels, there is no risk of cancer reported. However materials having a hazard index greater than 1, pose a cancer health risk as indicated in the Table 1.5. For some materials, the estimated excess cancer risks may be greater than 1×10^{-6}, but actual carcinogenic risk is likely to be much lower than this value [87]. The lists of flame retardants with minimal risk, even under worse case exposure, for use on residential furniture are:

- Hexabromocyclodecane
- Decabromodiphenyl oxide
- Alumina trihydrate
- Magnesium hydroxide
- Zinc borate
- Ammonium polyphosphates
- Phosphonic acid (3-([hydroxymethyl]amino)-3-oxopropyl)-dimethyl ester
- Tetrakis hydroxymethyl phosphonium salts (chloride salt)

The list of flame-retardants with the possible risk of cancer effects and/or the potential for cancer, are as follows:

- Antimony trioxide,
- Antimony pentoxide and sodium antimonates,
- Calcium and zinc molybdates,
- Organic phosphonates (dimethyl hydrogen phosphite),
- Tris(monochloropropyl) phosphates,
- Tris(1,3-dichloropropyl-2)phosphate,
- Aromatic phosphate plasticizers (tricresyl phosphate), and
- Chlorinated paraffins.

The toxicity of combustion products is highly dependent on the test conditions and does not seen to be mainly a material characteristic. A study of thermal oxidative degradation of some materials, such as triaryl, trialkyl and tris(haloalkyl) phosphates showed that tricresyl phosphate has the minimal degradation while the other compounds decomposed extensively [88]. In the case of tributhyl phosphate, butane

is the main pyrolysis products; hydrogen halides and a halogenated C2 and C3 species, are the main products from the halogenated phosphates.

Following application of tris(1,3-dichloro-2-propyl phosphate, acrolein and some other decomposition products formed from wood and cellulose have been indicated as the main toxic hazards.

During the decomposition of rigid urethane foam based on trimethylolpropane polyols, containing a number of diverse phosphorus flame retardants, both organic and inorganic, a particular neurotoxic bicyclic phosphate was formed as a product; thus the foam manufactures in USA, have refrained from using low molecular weight trimethylolpropane polyols and phosphorous flame retardants in combination.

In combustion processes, no considerable report of toxic hazard gases from phosphorus flame-retardants has been indicated [86].

1.11 The history of urea

Urea was first discovered in urine in 1773 by French chemist Hilaire Rouelle. In an experiment by evaporating urine and extracting with alcohol, the residue left was a "substance savoneuse", which gave, by analysis, much more than half of its weight of a volatile alkali. He claimed that the impure product obtained was rich in nitrogen, and gave upon fermentation, carbonic acid and ammonia.

For the first time from 1798 to 1799, Fourcrcoy and Vauqueline produced crystalline urea, from fresh concentrated urine by adding strong nitric acid.

Today, a specific component of urine, which gives rise to the carbonate of ammonium, is called urée. The study on urine decomposition by heat and by acids and alkalis has been carried out for many years respectively which their observation gave beneficial information to the chemical scientist.

In 1820, Proust removed nearly all of the coloured matter from urine by decomposing urea nitrate with carbonate and preparing almost colourless crystals. Later, he analysed the urea and determined its correct empirical formula. In 1828, Friedrich Wöhler in a failed attempt to prepare ammonium cyanate, by treating silver isocyanate with ammonium chloride, produced synthetic urea.

$$AgNCO + NH_4Cl \longrightarrow (NH_2)_2CO + AgCl \qquad (32)$$

He wrote triumphantly to Berzeliuis," I must tell you that I can make urea without the use of kidneys, either man or dog. Ammonium cyanate is urea". His discovery was one of great magnitude in the history of chemistry and he is considered by many to be the father of organic chemistry. In 1830, the first acid amide, namely ox-amide was prepared. Dumas obtained this compound by the action of heat on ammonium oxalate. His discovery showed that the relation between urea and ammonium cyanate, is the same as that between ox-amide to produce ammonium oxalate. By studying the decomposition of urea in strong sulphuric acid and potassium hydroxide, he has found that urea is to carbonate of ammonia as oxamide is to oxalate of ammonia. In 1830, Liebig and Wöhler prepared cyanic acid and cyanate of ammonia which had different properties than urea. Therefore they changed their false impression and confirmed that urea and cyanate of ammonia were possibly one and the same substance. Later Berzelius published the results of his investigation and introduced the isomerism of urea and ammonium cyanate. In 1856 Natanson proved that urea was formed from the interaction of phosgene and ammonia, and also in the present of ammonia solution by heating ethyl carbonate at 180°C. Therefore with the suggestion of direct synthesis of urea from two derivatives of carbonic acid, the names of urea and carbamide became synonymous terms. In 1868, the synthesis of urea by the action of heat on ammonium carbamate under pressure was announced by Basarov.

$$CO(NH_2).ONH_4 \longrightarrow CO.(NH_2)_2 + H_2O \qquad (33)$$

At that time, the symmetrical diamide formula for urea was accepted however several properties and decomposition pathways of urea were found not to follow with this hypothosis.

Since then different formulas have been suggested for urea such as $H_2N.C(NH).OH$ and $CO : NH_2.NH_3$ (the central nitrogen atom is represented as being pentavalent) but because of the evidence, and investigations relating to the chemistry of urea, there was still uncertainty in accepting the carbamide formula. Finally in 1913, the cyclic formula was announced by Werner. This formula represents the constitution of urea in its static condition or when present in a neutral solvent. This structure has confirmed all the chemical reaction behavior of urea in syntheses and decomposition procedure, Figure 1.21 [89].

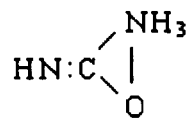

Figure1.21. Werner's urea structure.

In the field of flame retardancy, the application of urea in the form of urea condensate with phosphoric and sulphamic acid has been explained in section 1.14. However the urea alone is also applied in combination with the flame retardant products, such as Pyrovatex and also in Proban process, explained in section 1.5.

1.11.1 Urea chemical structure

Urea is an organic compound with the chemical formula $(NH_2)_2CO$, the molecule has two amine ($-NH_2$) residues joined by a carbonyl (-CO-) functional group. Each carbonyl oxygen atom accepts four N, H, O hydrogen bonds. This colourless compound is also named carbamide by the International Nanproprietary Name (INN) as established by the World Health Organization. It is highly soluble in water due to extensive hydrogen bonding with water and has a pKa close to zero. In fact up to eight hydrogen bonds may form, two from the oxygen atom, one from each hydrogen atom and one from each nitrogen atom [89].

Urea carbamides RR'N-CO-NRR' are based on a carbonyl group flanked by two organic amine residues. They can be accessed in the laboratory by reaction of phosgene with primary or secondary amines, proceeding through an isocyanate intermediate. Non-symmetric ureas can be obtained by reaction of primary or secondary amines with isocyanate. Examples of these compounds are carbamide peroxide, allantoin and hydantoin. Ureas are closely related to biurets and related in structure to amides, carbamates diimides, carbodiimides and triocarbamides [89].

1.11.2 Thermal analysis of urea

The thermal analysis of urea was the first analytical method used to study the constitution of urea. The generation of cyanuric acid from urea was recognized by scientists 30 years before the first compound of urea pyrolysis was announced. In fact in 1830, by the action of heat on pure urea, a considerable amount of cyanuric acid (CYA: 2, 4, 6-trihydroxy–1, 3, 5-triazine), as a urea product, was produced by

Wöhler. Later in the same year, the production of the sublimate contained ammonium cyanate during preliminary heating has been confirmed by Liebing. In 1845, by a prolonged thermal decomposition of urea, melanurenic acid was formed which has been reported by Liebing and Wöhler.

A few years later that, biuret $C_2H_5N_3O_2$ was produced by heating urea at 150°C – 170°C by Wiedemann. Finally the confirmation of urea decomposition by heat was announced which verified all previous results [89].

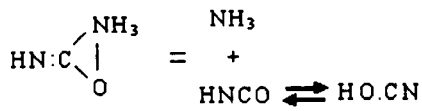

(34)

The instability and reactivity of cyanic acid is responsible for the products which were subsequently formed.

In terms of the outcome of this decomposition, the reaction conditions have a powerful role on the total product distribution, and also intermediate formation. The time and temperature of heating, the type of reaction vessel (closed or open), pressure and atmosphere all have an influence on the products obtained.

In recent published work by Stradella and Argentero [90], the thermal decomposition of urea has been studied using TGA and DSC together with evolved gas analysis (EGA) using an FTIR spectrometer. In the TGA curve for urea three steps were shown; the first at 135°C – 220°C, with 69% weight loss, corresponds to the formation of biuret; the second step from 220°C - 260°C, with 13.3 % weight loss represents the formation of cyanuric acid which can be produced as a product of initial decomposition materials, of urea, ammonia and cyanuric acid, plus a small amount of ammelide; the third step at 300-370°C, involves the decomposition of cyanuric acid with a 17.5% weight loss occurs. The IR analytical spectra of the volatiles evolved between 160°C - 360°C were identified the measurable absorption bands appear from the decomposition of urea at 160°C. Some suggestion of side products have also been published in this work.

Chen and Isa [91], they also indicated their studies using simultaneous TGA, DTA and mass spectroscopy on decomposition of urea under purge gas Ar, He or air conditions. In their research, they did not mention any details about the

accompanying materials and also some other by-products such as ammeline and ammelide.

A few years later in another work by Schaber and Colson, more details of urea decomposition in an open reaction vessel were reported [92]. In this study an analysis details of TGA, high performance liquid chromatography (HPLC), FTIR and an ammonium ion-selective electrode (ISE) information were indicated. Here both the urea residue and evolved gases were analysed and profiles of these materials at various temperature were reported. Major confirmed intermediate reactions and some possible reaction Schemes relevant to analysis temperature with observable intermediates are elucidated in this next section.

In this study, 30 g samples of urea in a 10 ml Pyrex ^{TM} beaker on a sand bath were heated until reaching the desired temperature and after that by removing from the heat and cooling, the residue were collected for analysis. Evolved gases were subsequently swept into an IR gas cell fitted with NaCl windows. The analytical analysis of the decomposition products of urea were reported between 133°C (melting point) to 450°C. Chromatographic analysis of the urea residue was conducted using HPLC to detect urea, biuret, CYA, ammelide, ammeline and melamine. These HPLC results are shown in Table 1.6 and the HPLC mass plot in Figure 1.22. The TGA data were collected, measured with a heating rate of 10 min^{-1} and N_2 gas purge between 50°C and 600°C, Figure 1.23.

Table 1.6. HPLC Mass Table urea pyrolysis in an open reaction vessel.[92]

Temperature (C)	Mass (g)	Urea (g)	Biuret (g)	CYA (g)	Ammelide (g)	Ammeline (g)	Melamine (g)	Total % recovery
133	100.0	98.7	1.0	-	-	-	-	99.7
190	80.0	60.5	20.0	0.6	0.5	-	-	102.0
225	33.0	6.0	4.6	15.6	6.1	0.9	-	100.5
250	29.0	0.3	0.2	19.9	7.7	1.3	0.058	101.4
275	28.0	0.5	0.3	18.9	7.5	1.3	0.056	102.3
320	20.0	-	-	12.1	4.9	1.1	0.044	90.7
350	5.0	-	-	3.1	1.0	0.5	0.100	94.0

The pyrolysis of urea in an open vessel reaction can be divided into four major reaction regions, with three major mass losses approximately 72%, 24% and 4% at each stage. It has been signified that in each specific temperature region, different chemical processes associated with various products occurred. All the details and possible reactions according to evidence from the analytical data are indicated here.

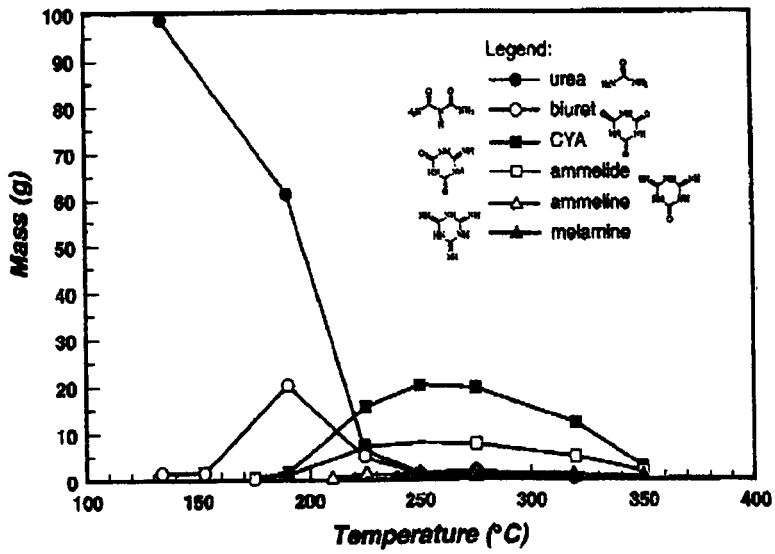

Figure1.22. HPLC Mass plot urea pyrolysis reaction (assume 100 g of urea initially) [92].

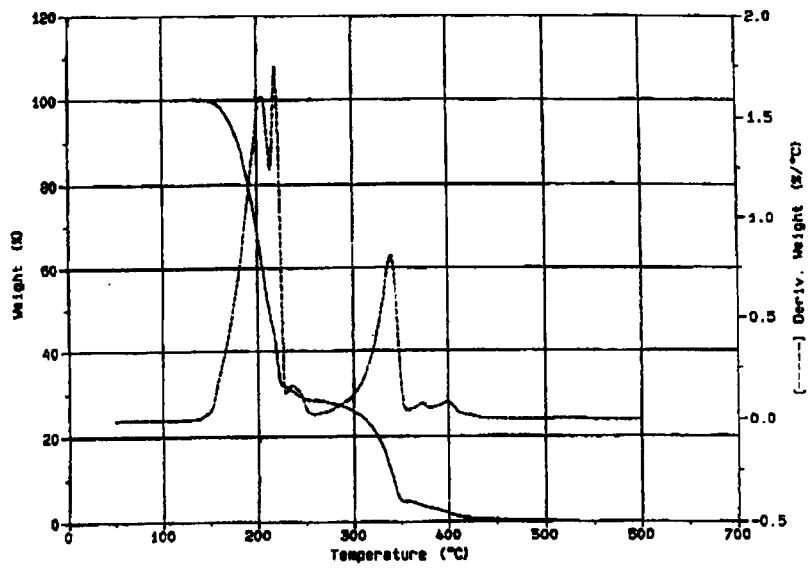

Figure1.23. TGA: urea thermal decomposition [92].

The FTIR spectra of urea pyrolysis reaction are shown in Figure 1.24.

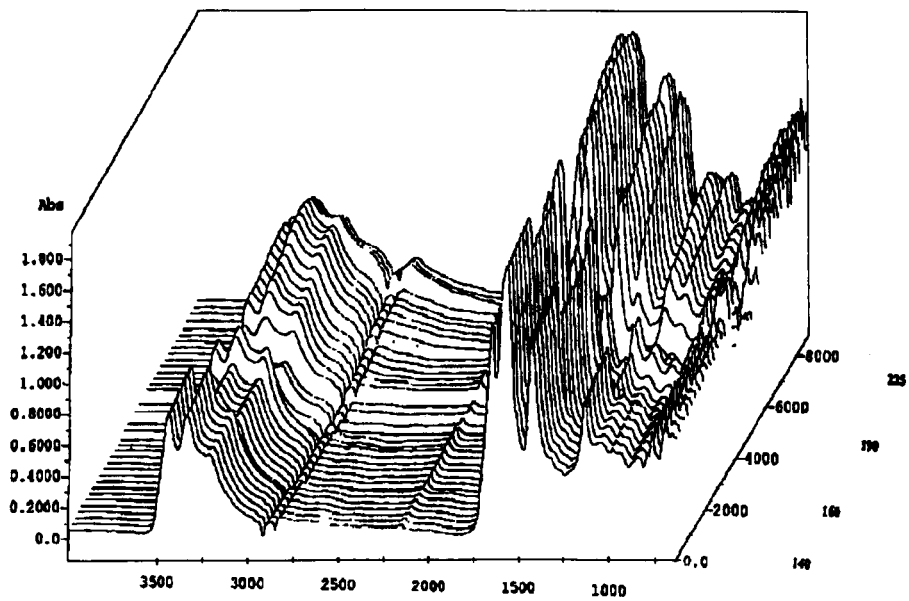

Figure1.24. FTIR Si-probe spectra: urea pyrolysis reaction [92].

Reaction region from room temperature to 190°C

TGA and HPLC analysis shows little significant urea mass loss even at the urea melting point of 138°C; 98.7% of urea and 1% of biuret being present. Urea decomposition is observed from 140°C, accompanied by urea vaporization - most of the weight loss indicated from 152°C to 160°C is due to two processes, continued urea vaporization and decomposition.

Urea decomposition:

$$\underset{\text{Urea}}{H_2N\text{-}CO\text{-}NH_2\ (m)} + \text{heat} \longrightarrow \underset{\text{ammonium cyanate}}{NH_4^+NCO^-\ (m)} \longrightarrow \underset{\text{ammonia}}{NH_3\ (g)} + \underset{\text{cyanic acid}}{NHCO\ (g)} \qquad (35)$$

At 160°C,the FTIR spectra of the melted urea, showed an increase in intensity of the [NCO^-] peak and strong presence of NH_3(g) (peaks at 3333cm^{-1}, 965 cm^{-1} and 930 cm^{-1}). Research by Chen and Isa [91] identified the production of HNCO (g). However the ammonium cyanate salt [NH_4 NCO^-] is formed as an intermediate product according to Eq.35 at this stage.

This result is consistent with urea initial decomposition to NH_3 (g) and HNCO (g). The possible production of biuret by the reaction of HNCO as an initial pyrolysis products and intact urea can be confirmed by the present of the intensity of the unique peak representing biuret at 1324 cm^{-1}.

Biuret production:

$$\underset{\text{Urea}}{H_2N\text{-}CO\text{-}NH_2}\ (m) + \underset{\text{cyanic acid}}{HNCO}\ (g) \longrightarrow \underset{\text{biuret}}{H_2N\text{-}CO\text{-}NH\text{-}CO\text{-}NH_2}\ (m) \qquad (36)$$

Between 10°C and 190°C, the decomposition of urea to HNCO and its reaction with intact urea continues to produce more biuret. Now a small amount of HNCO can begin to react with biuret itself (Eq.36, or Eq.37) to produce cyanuric acid (CYA), or with urea (Eq.39) to produce ammelide.

CYA production:

$$\underset{\text{biuret}}{H_2N\text{-}CO\text{-}NH\text{-}CO\text{-}NH_2}\ (m) + \underset{\text{cyanic acid}}{HNCO}\ (g) \longrightarrow \underset{\text{cyanuric acid}}{CYA}\ (s) + \underset{\text{ammonia}}{NH_3}\ (g) \qquad (37)$$

$$\underset{\text{Cyanic acid}}{3\ HNCO}\ (g) \longrightarrow \underset{\text{cyanuric acid}}{CYA}\ (s) \qquad (38)$$

Ammelide production:

$$\underset{\text{Cyanic acid}}{2HNCO}\ (g) + \underset{\text{urea}}{H_2N\text{-}CO\text{-}NH_2}\ (m) \longrightarrow \text{ammelide}\ (s) + 2\ H_2O\ (g) \qquad (39)$$

The presence of these materials at 175°C is supported by an increase in the intensity of respective unique peaks at 1058 cm^{-1} for CYA and ammelide at 977 cm^{-1}.

The potential route to CYA production has been explained by the crystallization of triuret ($H_2N\text{-}CO\text{-}NH\text{-}CO\text{-}NH\text{-}CO\text{-}NH_2$) followed by evolution of NH_3. In the work of Chen and Isa [91] TGA indicated the presence of urea trimer; however if this work, was carried out in an open reaction vessel no triuret was observed. The other possibility to produce ammelide in solid form was reported but it would occur under conditions of high pressure or temperatures above 300°C.

Direct reaction of biuret with HNCO (Eq.40) leading to the production of ammelide has also been suggested.

$$\underset{\text{biuret}}{H_2N\text{-}CO\text{-}NH\text{-}CO\text{-}NH_2}(s) + \underset{\text{cyanic acid}}{HNCO}\ (g) \longrightarrow \text{ammelide}(s) + H_2O\ (g) \qquad (40)$$

From the analysis, only small amounts of CYA and ammelide were formed in the residue Table 1.6.

Second region from 190°C – 250°C

In this region the beginning of biuret decomposition has been reported. Urea produced at this temperature is unsTable and will decompose further to HNCO (g) and NH_3 (g). The production of CYA and ammelide also occurred at this temperature.

Biuret decomposition:

$$\underset{\text{biuret}}{H_2N\text{-}CO\text{-}NH\text{-}CO\text{-}NH_2}\,(m) \longrightarrow \underset{\text{urea}}{H_2N\text{-}CO\text{-}NH_2}\,(m) + \underset{\text{cyanic acid}}{HNCO}\,(g) \qquad (41)$$

CYA production:

$$\underset{\text{biuret}}{2H_2N\text{-}CO\text{-}NH\text{-}CO\text{-}NH_2}\,(m) \longrightarrow \underset{\text{cyanuric acid}}{CYA}\,(s) + \underset{\text{cyanic acid}}{HNCO}\,(g) + \underset{\text{ammonia}}{2NH_3}\,(g) \qquad (42)$$

Ammelide production:

$$\underset{\text{biuret}}{2H_2N\text{-}CO\text{-}NH\text{-}CO\text{-}NH_2}\,(m) \longrightarrow \text{ammelide}\,(s) + \underset{\text{cyanic acid}}{HNCO}\,(g) + \underset{\text{ammonia}}{NH_3}\,(g) + H_2O\,(g) \qquad (43)$$

Stradella and Argentero [90] estimated that about 50% of biuret is converted to CYA. At temperature exceeding the melting point of biuret, 193°C, the large amounts of gaseous material produced is explained in Eq.42 and Eq.43.

At 250°C, the production of ammeline is also observed. This reaction can be summarised by the reaction of ammelide and ammonia gas (Eq.44), or another possible with an indirect reaction between HNCO and the remaining urea Eq.45.

Ammeline production:

$$\text{ammelide}\,(s) + NH_3(g) \longrightarrow \text{ammeline}\,(s) + H_2O\,(g) \qquad (44)$$

Or

$$\underset{\text{cyanic acid}}{2HNCO}\,(g) + \underset{\text{urea}}{H_2N\text{-}CO\text{-}NH_2}\,(m) \longrightarrow \text{ammeline}\,(s) + 2H_2O\,(g) \qquad (45)$$

At temperatures exceeding 210°C, the evolution of gases begins to visibly slow as a white precipitation was formed. The conversion of the melted products into a sticky solid matrix was complete at 225°C; CYA was the major compound in the residue. The $[NH_4^+]$ ion gives a maximum value at 225°C. The relevant reactions at this temperature are proposed inEq.46, Eq.47 and Eq.48.

Ammonium cyanate production:

NH_3 (g) + HNCO (g) $\longrightarrow$ $NH_4^+NCO^-$ (s) (46)
ammonia cyanic acid ammonium cyanate

Urea cyanurate production:

$H_2N\text{-}CO\text{-}NH_2$ (m) + CYA (s) $\longrightarrow$ $H_2N\text{-}CO\text{-}NH_3^+CYA^-$ (s) (47)
urea urea cyanurate

Biuret cyanurate production:

$H_2N\text{-}CO\text{-}NH\text{-}CO\text{-}NH_2$ (m) + CYA(s) $\longrightarrow$ $H_2N\text{-}CO\text{-}NH\text{-}CO\text{-}NH_3^+CYA^-$ (s)
biuret biuret cyanurate

(48)

At 250°C, for the first time, the present of melamine as urea decomposition by-products was indicated. The direct ammination of ammeline (Eq.49) is one possible route to melamine however the termerization of cyanamide is also reported.

ammeline (s) + NH_3 (g) $\longrightarrow$ melamine (s) + H_2O (g) (49)

$3H_2NC \equiv N$ (g) $\longrightarrow$ melamine (s) (50)
Cyanamide

Cyanamide production:

$H_2N\text{-}CO\text{-}NH_2$ (m) $\longrightarrow$ H_2O (g) + $H_2NC \equiv N$ (g) (51)
urea cyanamide

The production of cyanamide from urea decomposition under normal pressure has not been confirmed but it could be produced via an alternate decomposition route associated with urea dehydration (Eq.51), or by ammination of cyanic acid, (Eq.52a) and (Eq.52b).

HNCO (g) + NH_3 (g) $\longrightarrow$ H_2O (g) + $H2NC \equiv N$ (g) (52a)
cyanic acid cyanamide

$NH_4^+NCO^-$(s) $\longrightarrow$ H_2O (g) + $H_2NC \equiv N$ (g) (52b)
ammonium cyanate cyanamide

In fact it was suggested that the mixed trimerization of cyanamide and cyanic acid are responsible for the production of CYA, ammelide, ammeline and melamine at relatively low temperature. The chemical structures of these materials are shown in Figure 1.25.

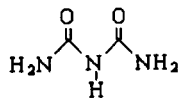

biuret

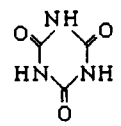

CYA

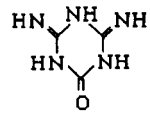

ammeline

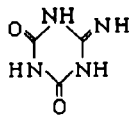

ammelide

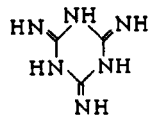

melamine

Figure1.25. The chemical structures of some products during thermal decomposition of urea.

However in FTIR analysis, there is no peak representing cyanamide; therefore the explanation for the production of relatively large amount of CYA, ammelide and ammeline products presents difficulties. The production of melamine is slow and only small amount of this product has been reported. In TGA analysis, only a small mass loss in the temperature region, between 225°C and 250°C occurred while the production of CYA ammelide and ammeline increased.

Analysis of trapped gases indicated a smaller amount of NH_3 (g) escape in this temperature range (225°C – 255°C). Ammonium salts are significantly lost from the matrix as confirmed by the difference in concentration of $[NH_4^+]$ residue.

In FTIR, a small peak corresponding to HNCO appears at approximately 2276 cm^{-1}, and also two other peaks at 2200 cm^{-1} and 2162 cm^{-1} associated with $[NH_4^+ NCO^-]$ and $[H_2O^+NCO^-]$, supports this idea. At 250°C, with only small amount of urea and biuret left, the solidification of the matrix has been completed.

Third reaction region between 250°C – 360°C

At 250°C only CYA, ammelide and ammeline are detected, but as temperature raise, CYA begins to loss mass via sublimation with a small amount of decomposition Eq. 53.

CYA decomposition:

$$\underset{\text{cyanic acid}}{\text{CYA (s)}} \longrightarrow 3\ \text{HNCO (g)} \qquad (53)$$

At this temperature small mass losses are confirmed for melamine and ammelide. The FTIR analysis of gaseous material collected at 275°C is also much different from that observed at 250°C. A substantial amount of water (peak at 3747 cm^{-1}),

[$NH_4^+NCO^-$], [$H_3O^+NCO^-$] and HNCO with an increase in intensity were reported at this stage. The presence of an ammonium peak at this temperature and a large CO_2 peak at 2361cm^{-1} are also observed. However analysis for [NH_4^+] ion in the residue showed it has decreased to a lower level (150 ppm). These results indicate the possibility of the ammonium cyanate decomposition reactions indicated in Eq.54 and 55.

Ammonium cyanate decomposition:

$$\underset{\text{ammonium cyanate}}{NH_4^+NCO^-(g)} \longrightarrow NH_3\,(g) + \underset{\text{cyanic acid}}{HNCO\,(g)} \qquad (54)$$

Decomposition of hydronium cyanate:

$$\underset{\text{hydronium cyanate}}{H_3O^+NCO^-(s)} \longrightarrow H_2O\,(g) + \underset{\text{cyanic acid}}{HNCO\,(g)} \qquad (55)$$

The reaction between water and available HNCO, can lead to the production of CO_2, Eq. 56.

CO_2 production:

$$\underset{\text{cyanic acid}}{HNCO\,(g)} + H_2O\,(g) \longrightarrow CO_2\,(g) + NH_3\,(g) \qquad (56)$$

At temperatures greater than 275°C, the production of CYA and ammelide will continue and ammeline begins to slow a mass loss. However, at 320°C, there is no sign of urea, biuret and melamine, and between 320°C–330°C, the CYA decomposition starts to show. While at the same time, ammeline and ammelide begin to sublime. In fact a substantial amount of NH_3 (g) is emitted from the system, indicated in FTIR spectra of the residue off-gaseous at 325°C. The FTIR analysis of the residue off-gases at 325°C, show the presence of water, CO_2 and HNCO, with a substantial amount of NH_3 (g) emitted from the system. Analysis of off-gases collected between 255 – 350°C, indicates a substantial amount of NH_3 (g). Also FTIR analysis still indicated the presence of water, CO_2 and HNCO, with a small amount of NH_3. At 350°C, the decomposition of CYA, and sublimation of ammelide and ammeline was confirmed from the HPLC data.

Fourth reaction region above 360°C

The decomposition of residual CYA is complete at 380°C while ammelide melts with decomposition prior to 410°C and ammeline melts with decomposition at 435°C. The

melting and decomposition of ammelide occurs prior to 410°C and it can be removed completely from the system at 600°C. Ammeline melts with decomposition at 435°C and requires temperatures in excess of 700°C to eliminate completely.

1.12 Isocyanic acid and its reaction

Isocyanic acid has the formula HNCO, discovered in1830 by Leibig and Wohler during thermal decomposition of urea above its melting point of 138°C.

This colourless substance is volatile and poisonous with a boiling point at 23.5°C.

Isocyanic acid can be made by protonation of the cyanate salts, such as potassium cyanate in the present of gases such as hydrogen chloride, or acids such as oxalic acid.

$$H^+ + NCO^- \longrightarrow HNCO \qquad (57)$$

HNCO also can be produced by thermal decomposition of cyanuric acid at high temperature.

The hydrolysis reaction of isocyanic acid is shown in Eq.58.

$$HNCO + H_2O \longrightarrow H_2N\text{-}COOH \longrightarrow CO_2 + NH_3 \qquad (58)$$

At sufficiently high concentrations of isocyanic acid, the oligomerization of this compound leads to various products such as cyanuric acid (trimer of HNCO) cyamelide [92], which have been elucidated in section 1.11.

In recent work [93], the polymerization path-ways of isocyanic acid have been studied using the semi-empirical PM3/VSTO-3G (d) method and by ab initio HF and MP2 calculations employing the 6-31G (d,p) basic set.

In fact that isocyanic acid can be formed with very strong hydrogen bonds, into the various possible formation of dimers or other polymers with the formula $(HNCO)_n$.

In this research, the isocyanic acid geometrical structure and its polymerization paths to form various chain polymer have been discussed in detail. In the isocyanic acid dimer structure five possible isomers have been offered by the writer but the most thermodynamically favourable at all levels of theory is $(O{=}C\text{-}NH)_2$ structure, Figure 1.26.

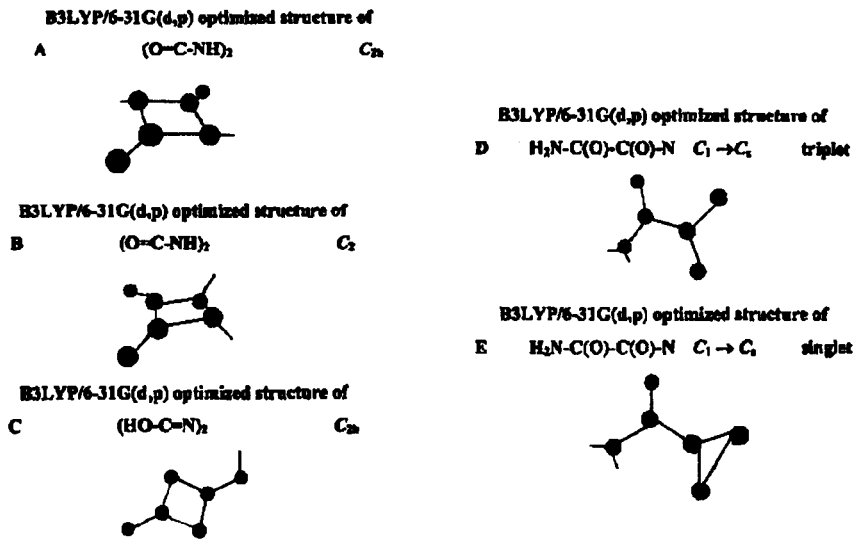

Figure 1.26.Optimized structures of isocyanic acid dimer[93].

The isocyanic acid trimer is cyanuric acid; its structure in the crystalline state and in solution, leads to two isomers, oxo (keto) structure and hydroxyl (enol) structure, Figure 1.27.

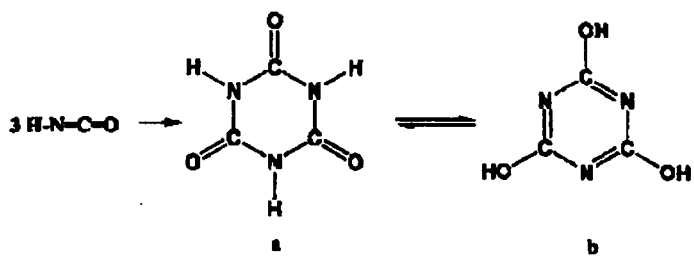

Figure1.27. The tautomeric forms of cyanuric acid: oxo (keto) structure (a) and hydroxyl (enol) structure (b) [93].

The equilibrium between the two isomers is affected by pH – under acidic conditions form (a) predominates and under alkaline conditions form (b) predominates, Figure 1.27.

In conclusion, various chain polymers containing up to 15 HNCO molecules have been investigated, Figure 1.28.

All the higher oligomers and polymers of HNCO of the type $(HNCO)_n$, with n= 4,5,..., 15 are of comparable stability which is just slightly lower that of the trimer $(HNCO)_3$.

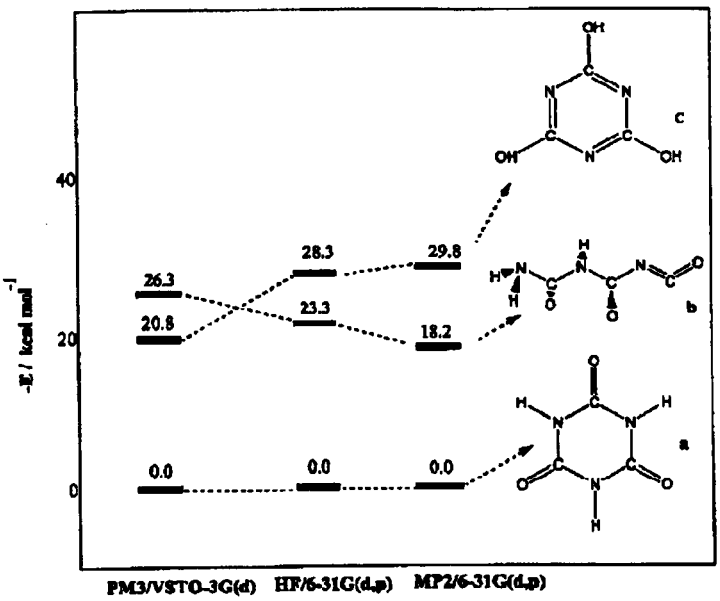

Figure1.28. Total energies of the isocyanic acid trimers in different structure, the oxo (keto) structure (a), open chain structure (b) and hydroxyl (enol) structure (c) [93].

Therefore with the most sTable isomers of trimer HNCO, it can be expected to find exclusively more cyanuric acid in the oxo (keto) from a mixture of different oligomers and polymers.

1.13 Isocyanates and their reactivity

Isocyanate is the chemical group of atoms –N=C=O which is different to cyanate, arranged as –O-C≡N. Some organic isocyanates are used as monomer feed stock for polyurethane production, such as toluene diisocyanate (TDI), methylene diphenyl 4,4′-diisocyanate (MDI), hexamethylene diisocyanate (HDI) and isophorone diisocyanate (IPDI).

These compounds are reactive and therefore toxic. Exposure of these isocyanate compounds and their vapours should be avoided [94].

The isocyanate group can react with hydroxyl functional group to form a urethane linkage. The reaction between a compound with two or more hydroxyl group (polyol) and a diisocyanate can produce long chain polymers called polyurethanes. Other important reaction products of diisocyanates include polyureas formed by their reaction with polyamines, the kinetic rate constants of the reactions a, b, c and d are K_a, K_b, K_c and K_d, Figure 1.29.

The reaction of isocyanate group with itself can lead to the compound known as biurets. Carbon dioxide is a product of the reaction between the isocyanate group and water and acts as a blowing agent in the production of polyurethane foams, Figure 1.30 [94].

A combination of ^{1}H and ^{13}C NMR and MALDI-TDF spectroscopies were used for analysis of the reaction products between isocyanates and alcohols.

Numerous compounds of higher molar masses have been identified as grafted di-or mono-urethanes. These grafted bonds and isocyanate, ending in allophanate linkages. Those molecules can further react with dissociated alcohol for example ending in branched molecules [94].

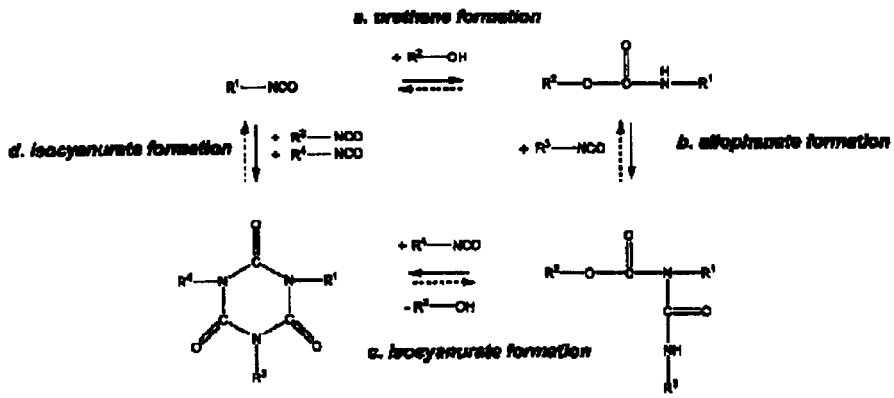

Figure1.29. The possible reactions between NCO and OH groups [94].

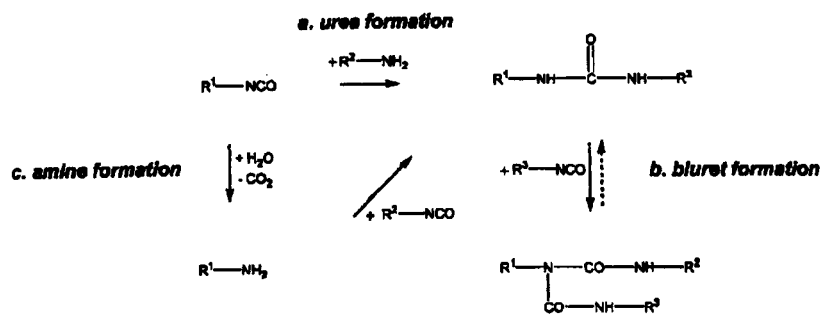

Figure1.30. The reactions of NCO groups in the present of water [94].

The allophonates are the main products of reaction between a di-urethane and di- or polyisocyanates at high temperature without any catalysts. Isocyanurate is not confirmed as a product of these reactions, but its presence in a very polar solvent has been verified.

At equimolar NCO/OH ratios, in the present of catalyst such as tin carboxylates and common tertiary amines when isocyanates react with alcohols, urethane is the main product ($K_a >> K_b \approx K_c$), Figure 1.29. In the present of other catalysts like aminals, amino alcohol and amidines, isocyanurate is formed as a final product ($K_a < K_b \approx K_c$). However at high NCO/OH ratios the same product is indicated via the urethane and allophanate formation as the intermediates identified products.

The stability of an allophonate depends on its structure and temperature. Aromatic allophonates are the least stable compounds and dissociate to a considerable extent in a short period of heating (only 10 minutes at 165°C – 210°C).

In fact at 160°C the allophonate crosslink would be relatively unstable. In the reaction between isocyanate and alcohols at an equimolar NCO/OH ratio, without catalyst, urethane is the main product [94].

1.14 The history of urea condensates and their applications

The reaction of phosphoric acid with urea has been investigated for a long time, beginning with a German patent [95], granted to Badische Anilin und Soda-Fabik (BASF) in 1914. In this work the urea phosphate as a fertilizer was produced by the reaction between one mole of urea and one mole phosphoric acid, the solution was cooled to crystallize.

A new inflammable type of cotton fabric as an electrical insulation has been introduced in 1937 [96], using a composition containing urea and phosphoric acid as the main ingredients. Reacting 1 mole phosphoric acid and 3 moles of urea with a soluble phenol formaldehyde resin at room temperature produced a dry product which could be dissolved in a suitable solvent such as alcohol at 50°C. The cellulose material was impregnated with this solution and then dried for 15 minutes at 110 - 120°C. During drying the "resol" resin was converted to an insoluble, infusible form. Preferably the best FR result was achieved from a solution containing 80% by weight of alcohol, 20% phosphate of urea and 15% resin. In this work no esterification of the cellulose was claimed, and indeed none would occur using this specific treatment.

In another work, a mixture of 2 parts of urea and 1 part of 75% phosphoric acid was used and pre-heated to 140-170°C, cooled, diluted with ammonia, and then treated with an aldehyde e.g. formaldehyde. The flame retardancy properties and the strength of the cellulose fabric was thus improved [97].

Further investigations in this field were carried out in 1945[98]; cotton fabric was treated with various types of urea/phosphoric acid products and application, drying and curing conditions optimized. In all these samples the mixture of urea/phosphoric acid (maximum molar ratio of urea/phosphoric acid was 2.7:1) was heated at 150°C for 5 minutes to 1 hour. In their compounds, the amounts of water-soluble and water-insoluble products were determined. The interesting point is that, in water-soluble products the presence of ammonium salts such as di-ammonium pyrophosphate, and in a water-insoluble product, the presence of cyanuric acid was confirmed. Phosphoric acid esterification of cellulose fabric was also indicated as a result of this work. It is proposed that because of the low amount of water-soluble products formed during the preparation of this type of urea condensate a less than satisfactory flame retardancy effect would have been achieved. In another work in 1956, the chemical structure of the "ammonium-phosphate-cellulose complex" (the designated name) has been discussed in detail [99]. However more uncertainty regarding the chemical structure was indicated especially after curing the fabric on cellulose. Since that time no further research in this area has been published.

Cellulose has also been sulphated readily by heating it with a mixture of sulfamic acid and urea similarly to the sulphation of starch [100] [101].

In the 1960s the application of a prepared complex of urea and sulphamic acid as a sizing agent for cotton fabric was reported [102]. In fact the urea condensate of sulphamic acid and urea were produced by reacting these products in various molar ratios, heating to 150°C, and make a solution from the products.

In another research sizing agents have been produced by mixing urea/phosphoric acid and other sulphur compounds [103] and heating. In one example 4000 g urea were mixed with 200 g sulphamic acid and 4200 g of water. The mixture was placed in a heating vessel and heated to 100°C; boiling was stopped and the pH raised to about 8. In fact the ammonia and ammonium salt were produced from the reaction between urea and the acid, selected from sulphamic acid, phosphoric acid, oxalic acid, methane-sulpuric acid, trichloroacetic acid, nitric acid and sulphuric acid. These sizing agents can be applied to paper.

It was not until a few years later, that the possibility of using the compound produced from urea and sulphamic acid as a flame retardant was investigated. No practical commercial application of such a product took place until the introduction of a prepared complex as a combined material for fire fighting [104], [105].

In this work, [105] the use of aqueous or powdered nitrogen containing compound urea condensate salt of sulphur oxyacid as the fire retardant has been announced. This product can be applied as a fertilizer agent and also for fire-fighting grass and forest fires.

In one example, 3 moles of ammonia were reacted with 1 mole carbon dioxide in a reactor at 160- 210°C, to form ammonium carbamate; after heating one mole of water was removed, to give an aqueous solution, containing 60 to 80% urea. At this stage one mole sulphuric acid was added to 4 moles of an aqueous solution of urea. An ammonium urea condensate salt of sulphuric acid, some urea sulphate and biuret sulphate can be identified in these products. The application of ammonium polyphosphate, phosphinic acid and some other phosphorus compound as additives has also been covered by this invention.

The production of urea phosphate continuously in a vacuum crystallization process was also proposed later [106]. The process utilized un-concentrated phosphoric acid and urea solution as a feed material and involved heating and evaporation of the solution to yield a super-saturated solution of urea phosphate. The temperature was kept constant at maximum 80°C, while the selected weight ratio of H_3PO_4 to urea on a water-free basis was less than 0.63 to 1.0.

The reaction of urea and phosphoric acid to form urea phosphate is shown by the following Scheme 59.

$$CO(NH_2)_2 + H_3PO_4 \longrightarrow CO(NH_2)_2\,H_3PO_4 \qquad (59)$$

The urea-phosphoric acid reaction and the crystallization of urea phosphate are both exothermic. To produce solutions containing polyphosphate, the solid urea phosphate first was heated by exothermal heat, to form urea-ammonium polyphosphate melt. This product can produce a solution of fertilizers [107].

Novel nitrogen and phosphorous containing salts, with a wide variety of potential uses have been claimed in 1976 [108]. A water soluble product contained at least one radical selected from the group consisting of borate, sulphate, sulphite and phosphite were produced, by mixing components of an organic ammoniating and condensating agent (urea), phosphoric acid, sulphuric acid, boric oxide, phosphorous acid and sulphurous acid.

Normally the temperature of the mixture was allowed to rise from 60°C to at least 100°C with stirring. After that, heating temperature raise to 135-160°C, when an exothermic reaction take place. As a result of this exothermic reaction the

temperature reached about 200°C; the products of the reaction were substantially in the form of foam. In one example, 355 parts of urea were added to a mixture of 500 parts of tetraphosphoric acid and 92 parts of boric acid with stirring. The mixture was heated to 135°C, whereupon an exotherm took place and dry foam of ammonium borophosphate was formed. These products were amorphous and rapidly soluble in water.

In the study of this invention by changing the type and the amount of required initial materials, the exothermic reaction acts differently and in some examples the formation of water insoluble products was indicated.

In another invention, the preparation of urea condensate has been claimed [109]. The invention is related to the composition of these compounds:

- At least a primary di- and or polyamide
- Urea
- At least one secondary amine and if appropriate one or more poly-alcohols

All these mixtures, at elevated temperature in the presence or absence of catalysts, can reacts together to produce a urea condensate following loss of ammonia gas. One example clamied mixing 58 parts of hexamethylendiamine, 60 parts of 3, 3′ dimethyl – 4, 4′ diaminodicyclo hexylmethane and 90 parts of urea, reacted at 160°C over 2 hours. During this procedure ammonia was eliminated above 120°C. The reaction mixture was initially liquid and then solidified to a white crystalline mass. The temperature was increased to 180°C, 193 parts dibutylamine were added, reaction continued at this temperature for 8 hours. A water-insoluble, colourless glassy-mass was produced. This product can be applied as a binder in various applications.

In a recent patent [110], cellulose fibres were treated with ammonium polyphosphate and urea, by heating to 140-200°C, then treated fibres formed into a nonwoven durable flame-retardant fabric.

The alkylated condensates are used as cross-linking resins and can be prepared by reacting a cyclic urea and glyoxal in stoichiometric amounts (glyoxal: cyclic urea, 0.8-1.2:1), around 50-60°C for two hours [111]. The water-soluble oligomers produced can be applied to textile materials in the present of catalysts include acids (such as hydrochloric, sulphuric, acetic or citric acid); metal salts (such as magnesium chloride, nitrate fluoroborate) and amine hydrochloride. The amount of catalyst generally is about 0.05 – 5% on the weight of padding liquor. The solvent may be water or/ and aliphatic alcohol.

"Flame retardant compositions utilizing amino condensation compounds" is the title of many patents with the name of Blount as an inventor. In all his research, he mixed or reacted the prepared complex of urea and organic compounds of aldehydes and fillers to produce a urea organic condensate composition which is incorporated in flammable organic compositions, such as polyurethane, polyester resin, vinyl resins and other resins [112], [113], [114].

In the basis of all his patents, the flame retardant compound were produced by heating urea with a nitrogen containing compound to above the melting point of urea, about 160°C for 1-3 hours. Upon heating above its melting point, urea can produce a very reactive isocyanic acid, which will react with itself or other organic or inorganic nitrogen containing compounds (in the case of nitrogen containing organic compounds, urea, urea derivatives, melamine, thiourea, polyamines, polyamide, amino sulphate and amino carbonate are the most suitable compounds, however in the case of inorganic compounds ammonium phosphate, ammonium polyphosphate and ammonium hydrogen sulphate can be classified.). To improve the flame retardancy effect a carbonization auxiliary (such as phosphorus acidic compounds, organic phosphoric compounds) can be added to the melt. The amino condensate may be further reacted with an aldehyde in the presence of a neutral acid, or base. It is important to note that all the above types of amino condensate products were water-insoluble.

After nearly one hundred years of study, no precise explanation regarding the chemical nature of the urea condensates has been published.

In recent work [115], the reaction between cyanate anion/isocyanic acid and phosphorous acid was studied and showed that mixing sodium cyanate and phosphorous acid resulted in the formation of O,O′-di-carbamoyl phosphate – this agent was applied to cotton fabric by a pad-bake process and shown to impart limited flame retardance due to covalent bonding of phosphorus. They also showed that much more promising flame retardance could be imparted on cotton fabric by treating it with polymethylphosphonic acids, such as ethylene diamine tetrakis(methylene phosphonic acid) [Briquest 422 – Albright and Wilson], in the presence of cyanamide – during baking the cotton was poly-esterified with the phosphonic acids and FR imparted.

1.15 Aims and objectives of this research

This research work describes a novel way to produce durable flame retardant agents from simple condensation products obtained by melting mixes of urea/sulphamic acid/phosphorus oxyacids. The main objective was that these condensates, when applied by pad-heat-cure processes, should be able to impart wash-durable flame retardance to cotton and other substrates.

Outstanding FR performance was achieved with selected optimised condensates. Detailed analysis was carried out to characterise the chemical nature of the polymeric condensates.

References – Chapter1

1. Horrocks, A.R. and Kandola, B.K.,"Flame Retardant Cellulosic Textiles", Fire Retardancy of Polymers: The Use of Intumescence, Ed: Camino, G., Bourbigot, S., Spring UC/RSC London 1998.

2. Ward, F., "The Principles and Practice of The Flame Proofing of Textiles", The Journal of Dyers and Colourists, 1955, 71, 10, 569-578.

3. Wikipedia Encyclopedia, Cellulose, [Online], [Accessed 10/4/09]. 2009. Available from http://en.wikipedia.org/wilki/cellulose

4. Encyclopedia Britannica, Cellulose, [Online], [Accessed 10/4/09]. 2009. Available from: http://www.britannica.com/EBchecked/topic/101633/cellulose

5. Carere, C.R., Sparling, R. and Cicek, N., "Third Generation Biofuels via Direct Cellulose Fermentation", International Journal of Molecular Science, 2008, 9, 1342-1360.

6. Kohel, R.J. and Lewis, C.F., Cotton, 1984, American Society of Agronomy, Wisconsin (USA)

7. Young, R. Cellulose Structure Modification and Hydrolysis, Publisher: Wiley New York, 1986.

8. McQueen, S.J., Mason, D.M., "Two Endogenous Protein that Induce Cell Wall Extension in Plants", Plant Cell, 1992, 4, 11, 1425-1433.

9. Perez, S. and Mackie, W., "Structure and Morphology of Cellulose", CERMAV-CNRS, 2001, Chapter IV., [online], [Accessed 10/4/2009].

10. Dieter, K. and Heablein, B., "Cellulose: Fascinating Biopolymer and Sustainable Raw Materials", Chem Inform, 2005, 36(36), Published Online Wiley Inter Science.

11. Sealey, II, "Process for Making a Composition for Conversion to Lyocell Fibre from an Alkaline Pulp Having Low Average Degree of Polymerization Values", 2006, US7083704.

12. Per, S., "Forest Products Chemistry Papermaking Science and Technology 3, Finland: Fapet OYP, (2000).

13. Salamone, J.C., "Concise Polymer Materials Encyclopaedia", Publisher CRC Press LCC (USA), (1999).

14. Wada, M. and Chanzy, H., "CelluloseIII_I Crystal Structure and Hydrogen Bonding by Synchrotron X-ray and Neutron Fibre Diffraction", Macromolecules, 2004, 37, 8548-8555.

15. Buleon, A. and Chanzy, H., "Single Crystals of Cellulose IV_{II}: Preparation and Properties", Journal of Polymer Science: Polymer Physics edition, 2003, 18, 6, 1209-1217.

16. Kamide, K. and Okajima, K., "Dissolution of Natural Cellulose into Aqueous Alkali Solution: Role of Supermolecular Structure of Cellulose", Polymer Journal, 1992, 24, 1, 71-86.

17. Zhankov, R.G. and Firsov, S.P., and Buslov, D.K., "Structural Physico-Chemistry of Cellulose Macromolecules Vibrational Spectra and Structure of Cellulose", Journal of Molecular Structure, 2002, 614, 117-125.

18. Sahin, H.T. and Arsian, M.B., "A Study on Physical and Chemical Properties of Cellulose Paper Immersed in Various Solvent Mixtures", International Journal of Molecular Sciences, 2008, 9, 78-88.

19. Beyler, C.L. and Hirschler, M.M., "Thermal Decomposition of Polymers", Chapter7: SFPE Handbook of Fire Protection Engineering", Online available, 1995.

20. Kuryla, W.C. and Papa, A.J., "Flame Retardancy of Polymeric Materials", 1987, 4, Publisher: Marcell Dekker INC.

21. Burge, S.J. and Tipper, C.F.H., "The Burning of Polymers", Combustion and Flame, 1969, 13, 5, 495-505.

22. Stuetz, D.E., Symposium on Flammability Characteristics of Polymeric Materials, University of Utah, 1971, Jun 21.

23. Horrocks, A.R., "An Introduction to the Burning Behavior of Cellulosic Fibres", Journal of Society of Dyers and Colourists, 1983, 99, 191.

24. Van Kervelen, D.W., "Some Basic Aspects of Flame Resistance of Polymeric Materials", Polymer, 1975, 16, 8, 615-20

25. Lewin, M. and Basch, A., "Structure Pyrolysis and Flammability of Cellulose", in "Flame Retardant Polymeric Materials",Edited by Lewin, M. and Atlas, S.M., 1978,Vol. II, Published by Plenum Press, New York, 1-14.

26. Basch, A. and Lewin, M., "The Influence of Fine Structure on the Pyrolysis of Cellulose. I. Vacuum Pyrolysis", Journal of Polymer Science A. Polymer Chemistry, 1973, 11, 12, 3071-3093.

27. Horrocks, A.R., "Fire Retardant Materials", Woodhead, Publishing Cambridge, 2001.

28. Creitz, E.C., "Inhibition of Diffusion Flames by Methyl Bromide and Trifluoromethyl Bromide Applied to the Fuel and Oxygen Sides of the Reaction

Zone,"Journal of Research of the National Bureau of Standards,1961, 65A, 4, 389–396.

29. Lewin, M., "On the Mechanism of Halogen's Flame-Supporting Properties.", Journal of Fire Science, 1979, 10, 69-77.

30. Noto, T. and Babushok, V., "Inhibition Effectiveness of Halogeneated Compounds.", Combustion and Flame, 1998, 112, 1-2, 147-160.

31. Brauman, S.K., "Phosphorous Fire Retardants in Polymers I. General Mode of Action", Journal of Fire Retardant Chemistry, 1977, 4, 18-37.

32. Rodering, C., Basch, A. and Lewin, M., "Crosslinking and Pyrolytic Behaviour of Natural and Man-Made Cellulose Fibre", Journal of Polymer Science-Polymer Chemistry, 1975, 15, 1921-1932.

33. Price, D. and Geoffrey, A., "Introduction: Polymer Combustion, Condensate Phase Pyrolysis and Smoke Formation", Fire Retardant Materials, Ed: Horrocks, A.R., and Price, D., Publisher Woodhead, 2001.

34. Gibou, K.M. and Shapovalova, L.N. and Zhubanov, B.A., "Movement of Destruction Products through the Carbonized Layer upon Combustion of Polymers, Fire and Materials, 1986, 10, 3-4, 133-135.

35. Imhof, L.G. and Stuebon, K.C., "Evaluation of the Smoke and Flammability Character of Polymer Systems", Polymer Engineering and Science, 2004, 13, 2, 146-152.

36. Kilzer, F.J. and Broido, A., "Speculation on the Nature of Cellulose Pyrolysis", Pyrodynamics, 1965, 2, 151-163.

37. Schwenker, R.F. and Beck, L.R., "Pyrolytic Decomposition of Cellulose by Gas Chromatography", Journal of Polymer Science – Part C, 1960, 2, 331-340.

38. Kurlya, W.C. and Papa, A.J., Flame Retardancy of Polymeric Materials, 1978, Vol. 5, Publisher Mercel Dekker Inc.

39. Golova, O.P., "New Data on the Bonds of Polysaccharide (Cellulose) Structure and the Course of Chemical Reactions Occurring During Thermal Decomposition", Doki, Akad.Nauk SSSR., 1957, 116, 419-421.

40. Basch, A. and Lewin, M.," Low Add-On Levels of Chemicals on Cotton and Flame Retardancy", Textile Research Journal, 1973, 43, 11, 693-694.

41. Honeyman, J., "A Fundamental Study of the Pyrolysis of Cotton Cellulose to Provide Information Needed for Improvement of Flame-resistant Treatments for Cotton. Final Progress Report Contract No. URE29 (20)9 – Sheirly Institute, Didsbury, Manchester, Englan, April 1964, 103-104.

42. Mack, C.H. and Danaldson, D.J., "Effects of Bases on the Pyrolysis of Cotton Cellulose", Textile Research Journal, 1967, 37, 12, 1063-1071.

43. Shafizadeh, F. and Fu, Y.L.,"Pyrolysis of Cellulose", Carbohydrate Research, 1973, 29, 113.

44. Brokowitz, J.B. Mattuck and Noquchi, T., "Pyrolysis of Untreated and APO-THPC Treated Cotton Cellulose During 1-sec Exposure to Radiant Flux Levels of 5-25 cal/Cm^2 sec.", Journal of Applied Polymer Science, 1963, 7, 709-725.

45. Horrocks, A.R., Price, D. and Akalin, M., "FTIR Analysis of Gases Evolved From Cotton and Flame Retardant Cotton Fabric Pyrolysed in Air.", Polymer Degradation and Stability, 1996, 52, 205-213.

46. Horrocks, A.R., "Flame Retardant Finishes and Finishing", Textile Finishing Vol. II, ed: Heywood, D., Bradford, UK, Society of Dyers and Colourists.

47. Kandola, B.K., Horrocks, A.R., Price, D. and Coleman, G.V., "Flame Retardant Treatments of Cellulose and their Influence on the Mechanism of Cellulose Pyrolysis", Journal of Macromolecular Science, Part C: Polymer Reviews (1532-1797), 1996, 36, 721-794.

48. Horrocks, A.R., "Developments in Flame Retardants for Heat and Fire Resistant Textiles- The Role of Char Formation and Intumescence", Polymer Degradation Stability, 1996, 54, 143.

49. Lewin, M. and Dweil, E., "Mechanism and Modes of Action in Flame Retardancy of Polymer, Chapter2", Fire Retardant Materials, ed: Horrocks, A.R., and Price, D., Publisher Woodhead, 2001.

50. Lyons, J.W., "The Chemistry and Use of Flame Retardants", Publisher: Wiley – Interscience, New York, 1970, 135-215.

51. Shen, C.Y, Stahlheber, N.E. and Dyroff, D.R., "Preparation and Characterization of Crystalline Long-chain Ammonium Polyphosphates", Journal American Society, 1969, 91-62-67.

52. Weil, E.D., "Phosphorus – Based Flame Retardants", Handbook of Organophosphorus Chemistry, ed: Engel, R.E., Publisher Marcel Dekker, New York 1992, Chapter 14.

53. Horrocks, A.R., "Flame Retardant Finishing of Textiles.", Rev Progress Coloration, 1986, 16, 62-101.

54. Vail, S.L., Daigle, D.J. and Frank, A.W.,"Chemistry of Hydroxymethyl Phosphorus Compounds. Part I Introduction", Textile Research Journal, 1982, 52, 671.

55. Donaldson, D.J. and Normand, F.L., "A Durable Flame Retardant Finish for Cotton Based on THPC and Urea", Journal of Industrial Textiles, 1974, 3, 4, 250-256

56. Davies, P.J., Horrocks, A.R., and Alderson, A., "The Sensitisation of Thermal Decomposition of Ammonium Polyphosphate by Selected Metal Ions and their Potential for Improved Cotton Fabric Flame Retardancy", Polymer Degradation and Stability, 2005, 88, 114-122.

57. Gilliland, B.F. and Smith, B.F., "Flame Retardant Properties and Thermal Behaviour of Selected Flame Retardant Cotton Fabrics", Journal of Applied Polymer Science, 1972, 16, 1801-1816.

58. Lewin, M., Flame Retardance in Fabrics: In Chemical Processing of Fibres and Finishes. Part B, Handbook of Fibre Science and Technology, Vol. II, (Ed: Lewin, M. and Sello, S.B.), Publisher: New York, Dekker, 1984, 1-143.

59. Kandola, B., Horrocks, A.R., Price, D. and Coleman, G., "Flame Retardant Treatments of Cellulose and their Influences on the Mechanism of Cellulose Pyrolysis", Revs Machromol Chem Phys, 1996, C36, 721-794.

60. Jones, D.M. and Noone, T.M., "Some Approaches to the Permanent Flame Proofing of Cotton: Systems Containing Phosphorus", Journal of Applied Chemistry, 1962, 12, 397-405.

61. Lawler, T.E., Drews, M.J. and Barker, R., "Pyrolysis and Combustion of Cellulose VIII, Thermally Initiated Reactions of Phosphono Methylamide Flame Retardants", Journal of Applied Polymer Science, 1980, 25, 243.

62. Willard, J.J. and Wondra, R.E.," Quantitative Evaluation of Flame Retardant Cotton Finishes by the Limiting - Oxygen Index (LOI) Technique", Textile Research Journal, 1970, 40, 203.

63. Reeves, W.A.,"Some Chemical and Physical Factors in Influencing Flame Retardancy", Textile Research Journal, 1970, 40, 223-231.

64. Barke, R.H. and Hendrix, J.E., "Flame Retardance of Cotton and Other Naturally Occurring Cellulosic Polymers", Flame Retardancy of Polymeric Materials, Vol.5, Ed: Kuryla, W.C. and Papa, A.J., Publisher Marcel Dekker, New York, 1979.

65. Tian, C.M., Guo, H.Z. and Zhange, H.Y., "Study on the Thermal Degradation of Cellulose Ammonium Phosphate and its Metal Complexes", Thermochimica Acta, 1995, 253, 243-251.

66. Weidong W. and Yang, C., "Comparison of Different Reactive Organophosphorus Flame Retardant Agents for Cotton: Part I, The Bonding of the Flame Retardant Agents to Cotton.", Polymer Degradation and Stability, 2006, 91, 2541-2548.

67. Faroq, A.A. and Price, D., "Thermogravimetric Analysis Study of the Mechanism of Pyrolysis of Untreated and Flame Retardant Treated Cotton

Fabrics under a Continuous Flow of Nitrogen", Polymer Degradation and Stability, 1994, 44, 323-333.

68. Horrocks, A.R., "An Introduction to the Burning Behaviour of Cellulosic Fibres", Journal of the Society of Dyers and Colourists, 1983, 99, 7-8, 191-197.

69. Price, D. and Horrocks, A.R., "Influence of the Flame Retardants on the Mechanism of Pyrolysis of Cotton (Cellulose) Fabrics in Air", Journal of Analytical and Applied Pyrolysis, 1997, 40-41, 511-524.

70. Gaan, S. and Sun, G, "Effect of Phosphorus and Nitrogen on Flame Retardant Cellulose: A Study of Phosphorus Compounds", Journal Annual Applied Pyrolysis, 2007, 78, 371-377.

71. Ahlsreom, D.A., Liebman, S.A. and Quinn, E., "A Summary of the Procedure of Soot Formation", Journal Polymer Prep. Amer. Chem, Society Div Poly Chem, 1973, 14, 1025.

72. Rayon fibre, Online, Accessed [4/4/09], Available from : http//www.fibresource.com/F-TUTOR/rayon.htm

73. Hall, M.E. and Horrocks, A.R., "The Flamability of Lyocell", Polymer Degradation and Stability, 1999, 64, 505-510.

74. Fink, H.P., Weigel, P., "Structure Formation of Regenerated Cellulose Materials from NMMO –Solutions", Progress in Polymer Science, 2001, 26, 1473-1524.

75. Lewin, M. and Sello, S.B., Handbook of Fibre Science and Technology, Vol.II, Publisher: Taylor and Francis Inc, 1984.

76. Filipasic, F., "Polymeric Phosphazenes", 1976, USP3990900.

77. Hupfl, J., "Manufacture of Flame –Retardant Regenerated Cellulose Fibres", 1977, USP4063883.

78. Leonard, E.A., "Flame Retardant Regenerated Cellulose", 1969, USP3455713.

79. Hilado, C.J., "Carbon Monoxide from Fibres with Fire Retardants", Journal of Industrial Textiles,1981, 10, 3, 225-231.

80. Hilado, C.J and Brauer, D.P., "Treated Viscose Fibres: Effect of Sand and Flame 5060 on Pyrolysis GAS Toxicity", Fire Safety Centre Sunnyvale California 94087.

81. Paren, A., "Product Containing Silicon Dioxide and a Method for its Preparation", 1993, W1OP Patent, WO/013249.

82. Paren, A., "Product Containing Silicon Dioxide and a Method for its Preparation", 1995, USP4417752.

83. Chen, S. and Zheng, Q-K," Fire Retardant Properties of the Viscose Rayon Containing Alkoxycyclotiphosphazene", Journal of Applied Polymer Science, 2006, 102, 1, 698-702.

84. Seddon, H., Hall, M. and Horrocks, A.R., "The Flame Retardancy of Lyocell Fibres", Polymer Degradation and Stability, 1996, 54, 401-402.

85. Lewin, M. "Unsolved problems and Unanswered Questions in Flame Retardance of Polymers.", Polymer Degradation and Stability, 2005, 88, 13-19.

86. Chivas, C., Guillaume, E. and Sainrat, A., "Assessment of Risks and Benefits in the Use of Flame Retardants in Upholstered Furniture in Continental Europe", Fire Safety Journal, 2009, 44, 801-807.

87. Toxicological Risks of Selected Flame-Retardant Chemicals, Subcommittee on Flame Retardant Chemicals, Committee on Toxicology, National Research Council, 2000, Online, [Accessed 01/04/2009]. Available from: http://www.nap.edu/catalog/9841.html.

88. Paciorek, K.J., Kratzer, R.H. and Kaufman, J., "Thermal Oxidative Degradation Studies of Phosphate Esters", American Industries Hygiene Assessment Journal, 1978, 39, 633.

89. Werner, E.A.,"The Chemistry of urea", Publisher: London; New York: Longmans Green and CO, 1923.

90. Stradella, I. and Argentero, M., "A Study of the Thermal Decomposition of Urea, of Related Compounds and Thiourea using DSC and TG-EGA., Thermochimi Acta, 1993, 219, 315-323.

91. Chen, J.P. and Isa, K., "Thermal Decomposition of Urea and Urea Derivatives by Simultaneous TG (DTA/) MS", Journal Mass Spectrum Society Japan, 1998, 46, 299-303.

92. Schaber, P.M., Colson, J. and Higgins, S., "Thermal Decomposition (Pyrolysis) of Urea in an Open Reaction Vessel", Thermochimica Acta, 2004, 424, 131-142.

93. Geith, J. and Klapőtke, T.M., "Ab Initio Calculations of the Polymerization Pathways of Isocyanic acid HNCO", Journal of Molecular Structure (Theochem), 2001, 538, 29-39.

94. Lapprand, A. and Boisson, F., "Reactivity of Isocyanates with Urethanes: Conditions for allophanates formation", Polymer Degradation and Stability, 2005, 90, 363-73.

95. Badische Anilin and Soda-Fabrik (BASF), 1914, German patent 28649195.

96. F. Groeb, "Electrical Insulation and Method of Making the Same", 1937, USP2089697

97. Ford, F.M. and Hall, W.P.," Flame-proofing of Fibrous Materials", 1949, USP2482756.

98. Davis, F.V., Findlay, J. and Rogers, E., "The Urea-Phosphoric Acid Method of Flame-proofing Textiles", Journal of the Textile Institute, 1949, 40, T839-854.

99. Nuessle, A.C. and Ford, M.F., "Some Aspects of the Cellulose-Phosphate-Urea Reaction", Textile Research Journal, 1956, 26, 1, 32-39.

100. Martin, I. and Wurzburg, O.B., "Amylaceous Esters of Sulphamic acid", 1958, USP2857377.

101. Thomas, J.C., "Process for the Preparation of Cellulose Sulphate", 1950, USP2511229.

102. Emerson, R.W., "Urea Containing Sizing Composition", 1977, USP402554.

103. Emerson, R.W., "Ammonia-Containing Sizing Compositions", 1977, USP4022634.

104. Rohringer, P., "Fire-Retardant, Intumescent Composition and its Use for the Flameproofing of Substrates, and as a Fire-Extinguishing Agent Comprising an Ammonium Salt, a Water-Soluble Nitrogen Compound as a Blowing Agent Dextrin", 1983, USP4382884.

105. Blount, D.H., "Urea Condensate Salt of Sulphur Oxyacid for Fire Control", 2005, USP6464903.

106. Keens, D., Improvements in or Relating to the Production of Urea Phosphate", 1969, British patent 1149924.

107. Lewis, H.T., "Production of Urea Phosphate", 1984, USP4461913.

108. Smith, R.A., "Novel Nitrogen and Phosphorus – Containing Salt", 1976, .USP3941896.

109. Schupp, E., "Process for the Preparation of Urea Condensate and their Use", 1986, USP4568729.

110. Fang, X., "Fire Resistant Fabric Formed From Treated Fibres", 2007, USP WO/095010.

111. Bernard, F.N and Rock Hill, S.C., "Glyoxal/Cyclic Urea Condensates", 1981, USP4284758.

112. Blount, D.H., "Flame retardant Compositions Utilizing Amino Condensation Compounds", 1998, USP5854309.

113. Blount, D.H., "Flame retardant Compositions Utilizing Amino Condensation Compounds", 2001, USP6258298.

114. Blount, D.H., "Flame retardant Compositions Utilizing Amino Condensation Compounds", 2001, USP6348526.

115. Morrison, G., "Novel Flame Retardant Systems for Cellulosics Based on Poly-functional Phosphorus Oxyacids and their Derivatives", PhD thesis, University of Leeds, 2006.

Chapter 2- Materials and Analytical Techniques

Introduction

In this study flame retardant properties were imparted to cotton fabric by the application of a sulphamic acid/phosphorous acid/urea condensate. The urea-containing condensates were produced by varying the ratio of various types of sulphating and phosphating agents heated together with urea.

The chemical structure of the condensates and that of the treated cotton fabrics were investigated using various modern analytical techniques, such as Fourier transform- infrared spectroscopy (FT-IR), Raman spectroscopy and nuclear magnetic resonance (NMR) spectroscopy. The physical performance characteristics of the treated fabrics were investigated by using differential scanning calorimetry (DSC), thermogravimetric analysis TGA, and a flammability test. In addition a scanning electron microscope (SEM) was used to analyse untreated and treated cotton fabric, and the EDX attachment used to indicate the distribution of phosphorus and sulphur elements on the surface.

The aims and objectives of this chapter are to describe the applied materials and the analytical techniques used through this work. Each method has been illustrated with theoretical information plus some details regarding the corresponding instrumentation.

2.1 Materials

2.1.1 Fabrics

The woven fabric, 100% cotton ($136g/m^2$), desized, scoured, bleached and mercerized, was supplied by Whalleys, Bradford in UK.

2.1.2 Chemicals:

The chemicals, sulphamic acid, sulphuric acid, urea, phosphoric acid, phosphorous acid, starch and polyvinyl alcohol (MW 12500) were all supplied in standard laboratory grade by Sigma-Aldrich, UK.

Non-ionic wetting agent Sandozin NIE was supplied by Clariant, UK.

2.2 Analytical techniques

2.2.1 Chemical analysis techniques

2.2.1.1 Electromagnetic spectra

An electromagnetic (EM) spectrum of an object is the characteristic distribution of electromagnetic radiation emitted or absorbed by that particular object. In Figure 2.1, all possible frequencies of electromagnetic radiation have been shown.

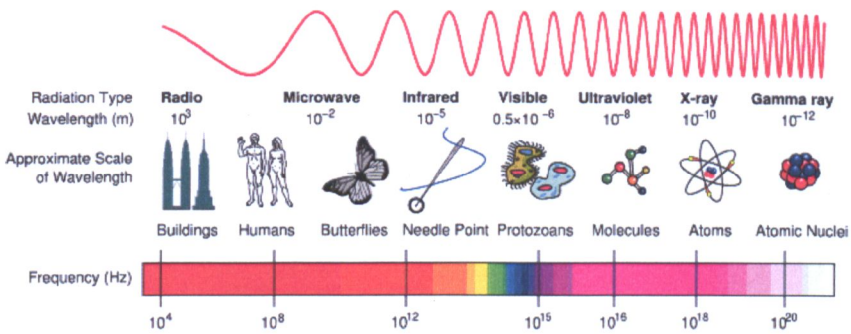

Figure2.1. All possible frequencies of electromagnetic radiation [1].

EM waves are typically described by any of the three physical properties, the frequency f, wavelength λ or photon energy E. Wavelength is inversely proportional to the wave frequency, while photon energy is directly proportional to the wave frequency. It means that, gamma rays have the highest energy of around billion electron volts with high frequency and radio waves have very low energy around femto electron volts. These relations are illustrated by the following equations [1]:

$$f = \frac{c}{\lambda} \quad \text{or} \quad f = \frac{E}{h} \quad \text{or} \quad E = \frac{hc}{\lambda}$$

Where:

c = 299,792,458 m/s (speed of light in vacuum) and

h = 6.626,068 × 10^{-34} J.s (Planck's constant).

2.2.1.1.1 Fourier-transform infrared spectroscopy (FT-IR)

Infrared spectroscopy is a subset of spectroscopy that works within the infrared region of the electromagnetic spectrum. Absorption spectroscopy can be used to identify specific chemical functional groups in compounds.

Each molecule has specific frequencies at which they rotate or vibrate corresponding to different vibrational modes, energy levels. In fact, the resonance frequencies are determined by the shape of the molecular potential surface energy, the masses of the atoms and by the associated vibration-based coupling. In another way, the resonant frequencies are related to the strength of the chemical bond and the mass of the atoms at either end of the bond. Therefore, the frequency of the vibrations is a characteristic of a particular bond type.

The infrared spectrum of a sample is collected by passing a beam of IR light through the sample. The interaction of this electromagnetic radiation, with an object, can be considered in terms of changes in the molecule dipoles corresponding with vibration and rotations. The position of atoms in a molecule joined by bonds with spring-like properties, are subject to a number of different vibration, stretching and bending properties.

Stretching means, a change in inter- atomic distance along the bond axis, while bending involves a change in bond angle. In Figure 2.2 and 2.3, various types of vibration modes for the atoms in a CH_2 group have been indicated [2].

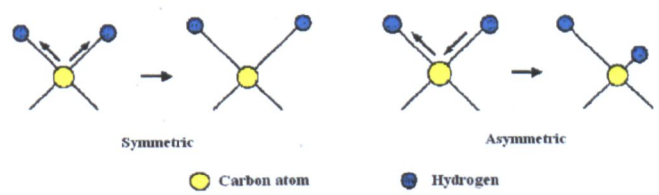

Figure2.2. Stretching vibrations in the atoms in a CH_2 group [2].

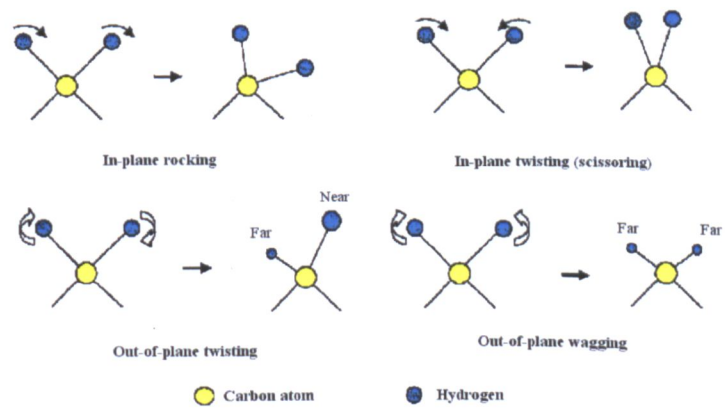

Figure2.3. Bending vibrations in the atoms in a CH_2 group [2].

The infrared region of the electromagnetic spectrum is divided into three sub-regions, the near, mid and far infrared.

The far-infrared, approximately 400-10 cm^{-1}(1000-30 μm) has low energy and may be used for rotational spectroscopy.

The mid-infrared, approximately 4000-400 cm^{-1} (30-2.5 μm) may be used to study the fundamental vibrations and associated rotational-vibrational structure.

The near-infrared, approximately 1400-4000 cm^{-1}(2.5-0.8 μm), with high energy, can excite overtone or harmonic vibrations [3].

In Fourier transform IR technique, the information at all frequencies is collected simultaneously, therefore measurement of a single spectrum is much faster than the older grating-based methods [2].

Instrumentation

A schematic representation of an FT-IR spectrometer is shown in Figure 2.4. It consists of the following elements: a light source, interferometer, a detector and also a recording or plotting device [4].

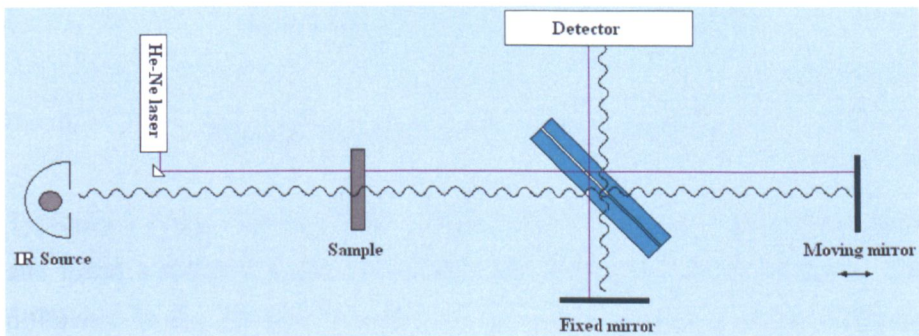

Figure2.4. Schematic representation of the FT-IR spectrometer.

The infrared vibration is passed to the sample through an interferometer before reaching a detector. A single incoming beam of light will be split into two identical beams by a grating or a partial mirror. Each beam will travel a different route, called a path. The difference in the distance travelled by each beam path difference creates a phase difference between them. This difference has an effect on light intensity received by the detector. Therefore an interference pattern between the initially identical waves is produced. Measuring the resulting intensity of the light received is known as homodyne detection [3], [5].

Light source

For the mid-infrared region two light sources are commonly in use: the Globar source which is constructed of silicon carbide and a Nernst filament, which is a mixture of the oxides of zirconium , yttrium and erbium [3].

The interferometer

In FT-IR the most common interferometer used is called the Michelson interferometer, Figure 2.5. It consists of two perpendicular mirrors one of them can move forward and backward, the other is fixed. Semi-refractive film, as a beam splitter, bisects the plane of the two mirrors, so that both mirrors receive light from the source.

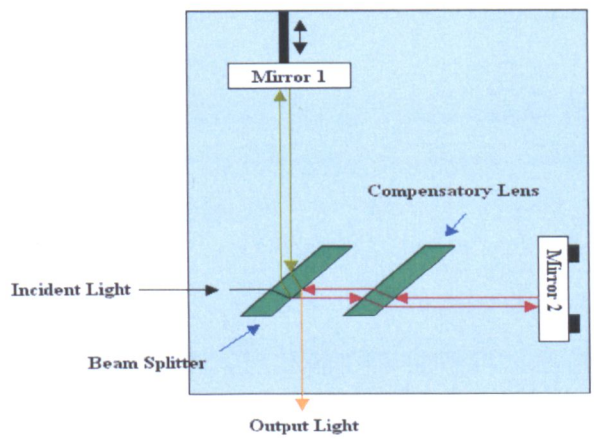

Figure2.5. Schematic of a Michelson interferometer.

Typically a single incoming beam of light will be split into two identical beams and travel a different route, before they are recombined at the detector. The difference in the distance travelled by each beam creates a phase difference between the two reflected waves and thus produces an interference pattern.

In mono-chromatic light, with specific wavelength, the recombination of the two beams at the splitter shows constructive or destructive interference, depending on the relative path length of both beams.

In the case of the path difference equal to an integral number of the monochromatic light's wavelength, the constructive interference will be produced. Therefore a bright beam reaches the detector. However in the destructive interference, if the path difference is equal to half of the wavelength, there is no radiation reaching the detector. In fact, the movement of the unfixed

mirror to the beam splitter can produce various light intensity values, through the samples [6].

The Detector

Thermal detectors and photo-conductive are two commonly used detectors in IR spectroscopy. In FT-IR pyroelectric devices with high sensitivity to heat are mainly used [3].

The Recording Device

The created pattern of radiation across a region can be represented as a function of position i(x, y), ie. an image. The pattern of incoming radiation i(x,y) can be transformed into the Fourier domains f(u,v). In the x, y domain, the phase difference between two points are measured in an interferometer, and correlated to a single point in the u,v domain.

A single beam detected by scanning through the x, y coordinates can build up a full image, and by using the interferometer to measure multiple points, a full picture in u, v space will be produced. This technique is called aperture synthesis [3].

Sampling Technique

In attenuated total reflectance (ATR) sampling technique, the IR ray was passed through a hemi-cylindrical prism of high refractive index, consists of zinc selenide (ZnSe) or germanium (Ge), thallium iodide or a diamond.

When the sample is in solid form, it is necessary to use a device which provides constant pressure on the sample, which ensures intimate contact with the prism, Figure 2.6.

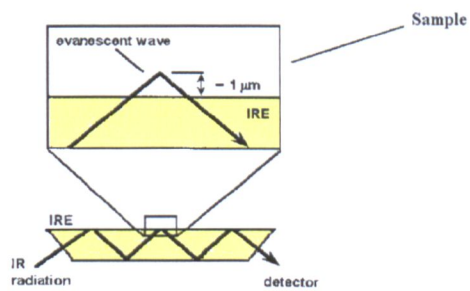

Figure2.6. A schematic representation of the ATR sampling device where IRE is the internal reflection element [7].

This beam penetrates a fraction of a wavelength beyond the reflective surface of the crystal. When a sample which selectively absorbs radiation, is in close

contact with the reflective surface, because of its refractive index, the beam loses its energy at a specific wavelength. The resultant attenuated radiation is subsequently measured and plotted as a fraction of the wavelength. Therefore the characteristic absorption spectrum of the sample can be produced as a function of the wavelength [7]. Infrared spectroscopy correlation tables, which attribute absorption wavelength to specific chemical groups, are available in the literature.

In this work, samples were run on the Perkin-Elmer 1740 Infrared Fourier Transform Spectrophotometer (PE instruments, UK) using a diamond ATR attachment.

Each spectrum was acquired using the following settings: $4cm^{-1}$ resolution, 100 scans per spectrum and a scan speed of $0.5cm.s^{-1}$. The Spectrum 5.0.1 software (PE Instruments, UK) was used to plot each spectrum.

2.2.1.1.2 Raman Spectroscopy

Raman spectroscopy named after C.V Raman is a spectroscopic technique used to study vibrational, rotational and other low frequency modes in a system. This instrument is based on the Raman Effect, which is the inelastic scattering of photons by molecules. The effect was discovered for the first time by the Indian physicist, C.V. Raman in 1928. The Raman Effect is very weak since only a very small fraction of the incident photons, about 1 in 10^7 are involved in inelastic scattering [8].

A schematic representation of Raman spectroscopy is shown in Figure 2.7.

This technique works with monochromatic light of a specific wavelength, usually from a laser in the visible, near infrared or near ultraviolet range of the spectrum. The laser light interacts with phonons or other excitations of the atoms within a molecule, and therefore, the energy level of the laser photons will be changed and shifted up or down. In fact by the shift in energy, some information regarding the photon mode is collected.

Typically, at the start of the procedure a laser beam as a light source is directed on to the sample, all the scattering light from the sample is collected by a lens and sent through a mono-chromator. In this section, the characteristic

wavelengths close to the laser line, related to elastic Rayleigh[1] scattering are filtered out meanwhile the rest of the collected light is dispersed on to a detector.

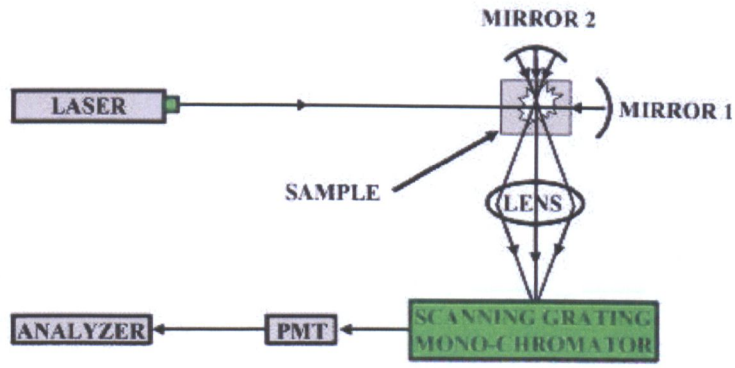

Figure2.7. A schematic representation of Raman spectroscopy [9].

The Raman effects occur when light impinges upon a molecule and interacts with the electron cloud and the bonds in that molecule. The molecule will be exited from the ground state to a virtual energy state, and relax into a vibrational excited state. The energy increase or decrease from the excitation is related to the vibrational energy spacing in the ground electronic state of the molecule.

Historically, in Raman spectroscopy, multiple dispersion stages are applied to produce a high degree of laser rejection. The photo-multiplier detectors used to record the spectrum sometimes require many hours to record a single spectrum [8].

Since the introduction of Raman spectroscopy, this new technology has provided different types of analysis techniques, including surface-enhanced Raman, tip-enhanced Raman, polarized Raman, stimulated Raman, transmission Raman, spatially-offset Raman and hyper Raman.

Raman spectroscopy is an effective analytical method used in chemistry, since vibrational information is specific to the chemical bonds and symmetry of molecules. Therefore this technique provides a fingerprint by which the molecule can be identified. For example, the vibrational frequencies of SiO_2, Si_2O_2 and Si_3O_3 were detected and assigned using Raman spectra. The finger print region of the Raman spectra is in the frequency range 500 – 2000 cm^{-1} [10].

1. In Rayleigh scattering, the emitted photon has the same wavelength as the absorbing photon.

Infrared (IR) and Raman spectroscopy both measure the vibrational energies of molecules but these methods are based on different selection rules. In fact, to have a vibration motion to be active in IR, the dipole moment of the molecule must be changed. Therefore the symmetric stretch in CO_2 with no change in the dipole moment is not IR active.

However for a transition to be Raman active there must be a change in polarizability of the molecule.

In Figure 2.8, the vibrational motion of the symmetric stretch in CO_2 is Raman active, because of the polarizability of the molecule changes, and various ellipsoid structure are indicated.

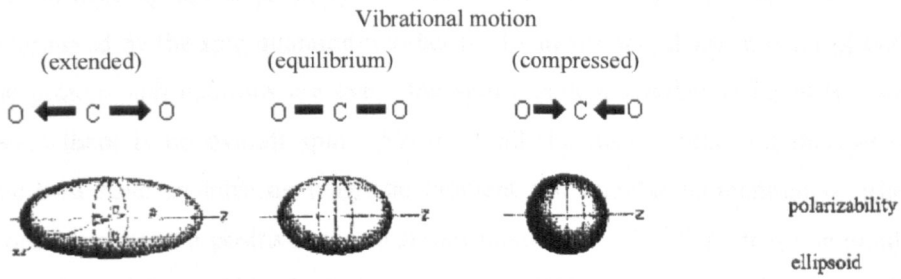

Figure2.8. Various vibrational motions due to the polarizability of the CO_2 molecule [11].

In addition, a vibration will be active in Raman, when the polarizability of the molecule changes via the vibrational motion [11].

Samples were run on a Perkin-Elmer System 2000 NIR FT-Raman Spectrometer (PE instruments, UK) using a Diode Pumped Nd: YAG Laser. Each spectrum was acquired using the following settings: $4cm^{-1}$ resolution, 100 scans per spectrum and a scan speed of $0.2cm.s^{-1}$. The power of the laser was set at 500 mV. The software used was Spectrum 5.0.1 software (PE instruments, UK).

2.2.1.3 Nuclear magnetic resonance (NMR)

In physics, the tendency of a system to oscillate at large amplitude at some frequencies than others is known as the system's resonance frequencies. At a resonant frequency, the frequency of oscillation does not change with changing

amplitude. In fact at these frequencies, because of the stored vibration energy in the system, even a small periodic driving force, can produce a large amplitude vibration.

Nuclear magnetic resonance (NMR) is the name given to a physical resonance phenomenon, which is based on the observation of specific quantum mechanical magnetic properties of an atomic nucleus in the presence of an applied external magnetic field.

Today NMR is a powerful technique that can provide detailed information on the topology, dynamic and three dimensional structures of molecules in solution and in the solid state [12].

Theory of nuclear magnetic resonance

All nucleons, that are neutrons and protons, comprising any atomic nucleus, have the intrinsic quantum property of spin. The overall spin of the nucleus is determined by the spin quantum number S. In an isotope, if the number of both the protons and neutrons are even, the spin quantum number is equal to zero, (S=0) there is no overall spin. However all the nuclei with odd number of nucleons have an intrinsic magnetic moment and angular momentum in other words they have a positive spin quantum number, $s > 0$. The most commonly studied nuclei are ^{1}H which is the most NMR-sensitive isotope after the radioactive ^{3}H and ^{13}C, however nuclei from isotopes of many other elements such as ^{2}H, ^{10}B, ^{11}B, ^{14}N, ^{15}N, ^{17}O, ^{19}F, ^{23}Na, ^{29}Si, ^{31}P, ^{35}Cl, ^{113}Cd, ^{195}Pt are studied by high-field NMR spectroscopy.

The resonance frequency of a particular substance is directly related to the strength of the applied magnetic field. In the case of a non-uniform magnetic field, the resonance frequencies of the sample's nuclei depend on where the sample is located. In fact the resolution of imaging techniques is related to how big the gradient of the field is, and more powerful magnets by using superconductors are usually produced.

The principle of NMR usually involves two sequential steps:

- The polarization of the magnetic nuclear spins in an applied constant magnetic field H_0.

- The perturbation of this alignment of the nuclear spins in the presence of an electromagnetic, usually radio frequency (RF) pulse. The constant magnetic field ($H_{0)}$ and also the nuclei of observation have an effect on the selected perturbing frequency.

Resonant absorption by nuclear spins will occur only when electromagnetic radiation with the required frequency is being applied to the energy difference between the nuclear spin levels in a constant magnetic field. The radiofrequency range of the electromagnetic spectrum is the best to apply in a constant magnetic field up to ~20 T[1].

The "shielding" effect of the surrounding electrons is also important for perturbation of the NMR frequency. In fact the magnetic field is reduced because of this electronic shielding. Therefore the difference in energy is reduced and the required frequency to achieve resonance is also reduced. This shift which is relevant to the electron's molecular orbital, is called the chemical shift. Therefore the ability of NMR spectroscopy to probe the chemical structure of molecules, which depends on the electron density distribution in molecular orbital, is elucidated.

In fact, in a specific chemical group with high electron density of its surrounding molecular orbital, the nuclear is shifted to a higher degree then its NMR frequency will be shifted up-field (that is a lower chemical shift). However in low electron density when its NMR frequency is shifted down-field a high chemical shift will be seen.

If the local symmetry of such molecular orbital is very high, it can lead to isotropic shift. In fact in regard to the external magnetic field, the orientation of the molecule has an effect on the shielding effects [12].

Instrumentation

An NMR spectrometer consists of an electromagnetic source, a magnet, a sample holder, a detector and a recording or plotting device. A schematic representation of the standard set up is illustrated in Figure 2.9.

1. The magnetic field intensity unit, Tesla (T).

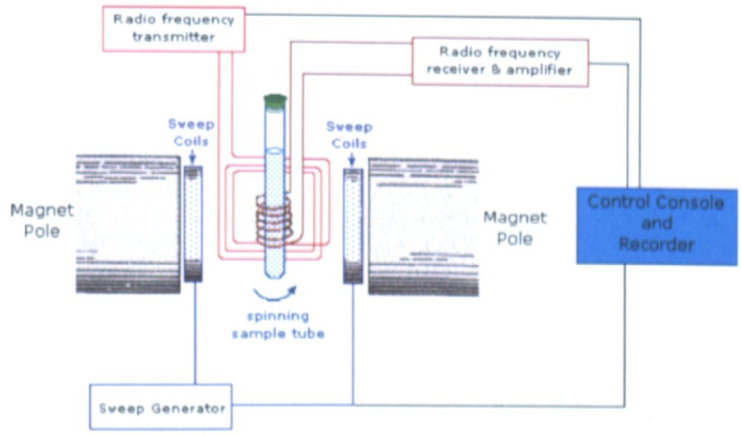

Figure2.9. Representation of a NMR spectrometer [14].

In a practical technique, sample containing protons (hydrogen nuclei) is placed in a strong magnetic field to produce partial polarization of the protons. In addition a strong radio frequency field is also imposed on the sample, therefore, some of the nuclear spins, excite into their higher energy state. When this strong RF signal is switched off, the spins tend to return to their lower state, and a small amount of radiation at the Larmor[1] frequency will be produced. The spin relaxation of the protons from their excited state has the main role on the emission of radiation. Therefore in a detector coil, a radio frequency signal is induced, which is applied to display the NMR signal.

In fact the Larmor frequency of the detected signal is related to the intensity of the applied magnetic field therefore, changing the magnitude of that field produces various detected frequencies. When a sample is placed in a magnetic field, the source of the proton NMR signal in a sample will be located easily. This idea is used in magnetic resonance imaging by an advanced NMR in medical imaging process [13, 14].

The Magnet

The required magnet in NMR has to provide an extremely stable and homogeneous magnetic field, which is usually ranged approximately from 1.5 to 12 T, which is given 60 to 500 MHz proton resonance frequency. In modern instruments, superconducting magnet is usually used capable of generating field

1. The Larmor frequency of the electron spin is in the microwave region of the electromagnetic spectrum and is used in electron spin resonance.

above 2.35 T (100 MHz). They are made of an alloy of nobium and titanium immersed in liquid helium at 4K (-269°C) [15].

The Electromagnetic Source

The radio frequency transmitter consists of a coil wound around the sample tube, to provide electromagnetic frequency. In fact, the sample is subjected to an additional weak oscillating magnetic field perpendicular to the applied magnetic field direction. The radio frequency absorbed by a nucleus is slightly different and depends upon the surrounding of the nucleus a range of radio frequency must be applied.

NMR spectrometers can work using the continuous wave or the pulse Fourier-transform principle.

In continuous wave spectroscopy (CW spectroscopy), a fixed frequency source is used and the current (and hence magnetic field) varied in an electromagnet to produce the resonant absorption signals. Alternatively the frequency of the transmitted weak radio frequency is varied continuously (frequency sweep) within the desired range and individual frequencies are recorded. At various frequencies, the relative size of absorption is measured and a simple spectrum is produced. Alternatively, the strength of the applied magnetic field may also be continuously varied, thus a sweep of the magnetic field strength also leads to NMR spectrum recording. The magnetic field strength is proportional to the energy gap between stationary states.

In the Fourier-transform spectrometer, a single radio frequency, pulse approximately 1-5 μs, from a strong field irradiating all frequencies simultaneously is applied to the sample. Principally the pulse is applied only for a few microseconds and therefore a large number of pulses of the signal average can be taken may be carried in a very short time. As a result, the signal-to-noise ratio of spectra will be improved and high quality proton spectra can be recorded within a few minutes [15].

The Detector

The detector consists of a coil perpendicular to the transmission coil and thus in crossed coil geometry. The magnetisation will be detected without interference from the applied variable field [15].

The Sample Holder

To facilitate a homogeneous magnetic field on sample, it is usually dissolved in deuterated solvent and is placed in a quartz tube which is spun about its axis in the spectrometer using an air turbine.

Nuclear Magnetic Resonance analysis was performed on a Bruker 400 Ultrashield instrumiatent (Bruker Companies, UK). The samples were dissolved in an appropriate amount of an appropriate deuterated solvent and scans 128 for ^{1}H and 2048 scans for ^{13}C NMR analysis respectively were collected at 20°C. Data were collected with XWin NMR 3.0 software (Bruker, UK) and processed using MestReC 2.3a software (MestReC, Spain).

2.2.1.5 Elemental analysis

Elemental analysis (C, H, N, S and P) was carried out on a Carlo-Erba 1106 Elemental analyser.

The elemental analysis was performed in the School of chemistry at the University of Leeds, UK.

2.2.1.6 Mass spectrometry

Mass spectrometry is an analytical technique used in elucidating the chemical structure of a compound, determining its chemical composition and isotope incorporation and identifying an organic compound by virtue of its fragmentation pattern [16]. A chemical compound is subjected to ionization using various techniques and the resultant ions are characterized on the basis of their different mass-charge ratio (m/z). The number of ions representing each mass/charge unit is recorded as mass spectrum [16].

Instrumentation

A mass spectrometer consists of three modules:

- An ion source which can convert gas phase sample molecule into ions
- A mass analyzer enables to sort the ions by their masses by applying electromagnetic fields.
- A detector; measures the value of an indicator quantity and provide data for calculating the considerable amounts of each ion present.

This technique can be used for qualitative and quantitative analysis. A schematic representation of a mass spectrometry instrument is shown in Figure 2.10.

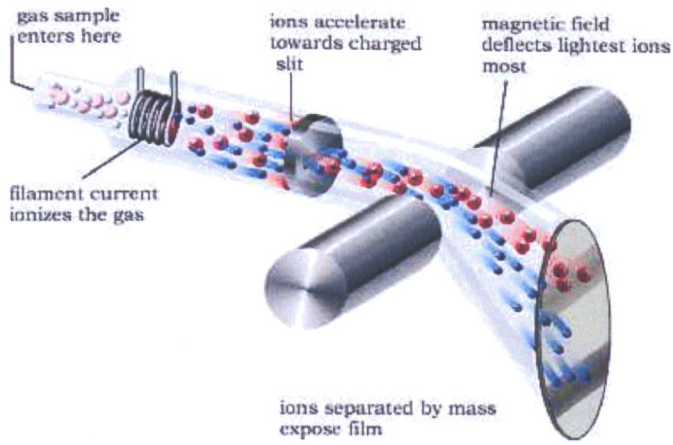

Figure2.10. Schematic representation of a mass spectrometry instrument [16].

The basic principle of mass spectrometry is quite simple. The sample is injected into to the ionization chamber by means of direct insertion or through some chromatographic technique, such as liquid chromatography or gas chromatography. The sample is ionized by various techniques, for example in electron impact ionization the gas phase sample is bombarded with high energy electrons. This ionization gives a molecular ion that can undergo fragmentation. As it is a radical cation, it can fragment to either radical or ion with even number of electrons or molecule or new ion. This fragmentation is very critical and quite predictable characteristic of a molecule and utilised for the identification of a chemical compound and elucidation of its structure [17].

In the electrospray technique, the sample solution in a polar volatile solvent is injected through a capillary at atmospheric pressure. The capillary is surrounded by nitrogen gas called the nebulizing gas and applied electric potential to form an aerosol of charged droplets. The nebulizing gas directs the charged sample towards the spectrometer [18]. The charged ions are separated using various ion separation methods and analysed on the basis of their mass-charge ratio (m/z). The detector detects the emerging ions from the analyser and measures their abundance covering ions into electrical signals.

A mass spectrum is a presentation of the masses of positively charged ions including the original molecular ion versus their relative abundances. The most

intense peak in the spectrum is called a peak and it is assigned value of 100%. The intensities of the other peaks are reported as percentages with reference to the base peak. The base peak may not be the molecular ion. The spectrum also provides information about the fragmentation pattern produced by ionization. These fragments can be investigated to study bond cleavage patterns [18].

Mass spectrometry analysis was performed using a Bruker Daltonics MicrOTOF[1] at the Mass Spectra service School of Chemistry, University of Leeds, UK, applying Electrospary (ES^+) Ionization technique. The spectra are reported as values in atomic mass unit followed by the peak intensity relative to the base peak (100%) using sodium formate as a standard.

2.2.2Thermal analysis technique

2.2.2.1 Differential scanning calorimetry (DSC)

Differential scanning calorimetry (DSC) is a thermoanalytical technique in which the difference in the amount of heat energy required to increase the temperature of a sample and a reference material are measured as a function of temperature. The technique was developed by E.S Watson in 1960 and commercially introduced in 1963. The main application of DSC is in studying phase transitions, such as melting point, Tg or exothermic decomposition. These physical and chemical transitions involve energy changes or heat capacity changes which can be detected by DSC with great sensitivity. A schematic representation of DSC instrument is shown in Figure 2.11.

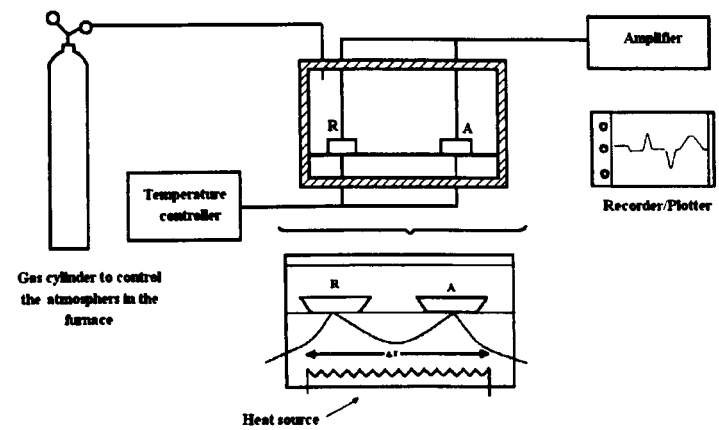

Figure2.11. Schematic DSC instrument [19].

The different types of technology used by the instrumentation to make the experiment, there are two different conventions; in one technique both the sample and reference are maintained at nearly the same temperature through the experiment. In fact the temperature of a sample holder increases linearly as a function of time [19].

When the sample undergoes a physical transformation such as a phase transition more or less heat will need to flow to it than the reference, to keep both at the same temperature. Therefore depending on whether the process is exothermic or endothermic, by observing the difference in heat flow between the sample and reference, DSC is able to measure the amount of heat absorbed or released during this transition. The result of a DSC experiment is a curve of heat flux versus temperature or time. The exothermic and endothermic transitions in the sample show with a positive or negative peak, Figure 2.12.

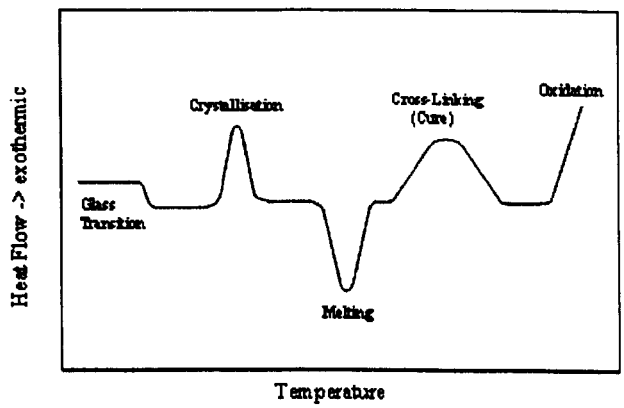

Figure2.12. Schematic DSC curve demonstrating the appearance of several common features [19].

In another technique, the amount of heat supplied can be adjusted to give various heating rates to the reference and sample chamber. Then instead of maintaining equal temperatures and measuring differential heat flow, it is possible to maintain in constant heat flow and measure the difference in temperature between the reference and sample chamber. The temperature difference will give a good measure of the heat capacity. In fact when the heat capacity of the sample chamber increases, because of a heat absorbing or endothermic transition, the temperature in the sample chamber is behind the reference chamber therefore the negative temperature differential can be

measured ($T_{sample} - T_{ref} < 0$). Conversely in exothermic transition, there will be a positive temperature differential ($T_{sample} \_ T_{ref} > 0$) [19].

The enthalpies of transition can be calculated using a DSC curve, using the following equation:

$$\Delta H = KA$$

where:

ΔH is the enthalpy of transition

K is the calorimetric constant

A is the area made by the curve.

The calorimetric constant will vary for each instrument, and can be refined for a well characterized sample with known transition enthalpies [19].

2.2.2.2 Thermogravimetric Analysis

Thermogravimetric analysis (TGA) provides a quantitative measurement of any weight changes associated with thermally induced transitions.

This technique involves heating a sample in an inert or oxidising atmosphere and measuring the weight. In fact the weight change over specific temperature ranges provides some information regarding the chemical composition of the sample and thermal stability. The applications of this technique include:

- Assessment of moisture and volatiles
- Assessment of composition
- Thermal stability
- Oxidative stability
- Decomposition kinetics

Such analysis relies on a high degree of precision in three measurements: weight, temperature, and temperature change. As many weight loss curves look similar, the weight loss curve may require transformation before results may be interpreted. A derivative weight loss curve can be used to tell the point at which weight loss is most apparent [20].

DSC and TGA analysis was performed using a DSC 2010 (TA instrument Ltd) under nitrogen atmosphere, from room temperature. Typically, 5 to 10 mg of sample was heated at a rate of $10^{\circ}C.min^{-1}$ with a purge gas flow of $200cm^3.min^{-1}$.. Data was recorded using Thermal Advantage software (TA Instruments Ltd).

2.3 Scanning Electron Microscope (SEM)

The scanning electron microscope (SEM) is a type of electron microscope that produces an image of the sample surface by scanning it with a high energy beam of electrons in a raster scan pattern. The electron beam interact the atoms on the surface of a sample, producing scattered electrons and X-ray signals that contain precise topographical information, chemical composition and other properties such as electrical conductivity. This technique provides the sufficient information for researcher in various areas of study such as the medical, materials and physical science communities [21].

The first SEM image was obtained by Max Knoll in 1935, of silicon steel, showing electron channelling contrast. Since that further investigation on beam specimen interaction and the physical principle of SEM were carried out until 1956 when the first SEM microscope was marketed by the Cambridge Instrument Company as the "Stereoscan".

Magnification in a SEM can be controlled over a range of up to 6 orders of magnitude from about X25 to X250,000 and exceptionally to 2 million times in the Hitachi S-5500 in-lens Field Emission SEM, imaging a specimen area about 60 nm wide with resolution up to 0.4 nm [21].

In SEM, from the interactions of the electron beam with atoms at or near the surface of the sample, various types of signals are produced, including secondary electron, back scattered electron (BSE), characteristic X-ray, light (cathodoluminescence), specimen current and transmitted electrons. To detect each type of signal, the specialized detectors are required and usually all present on a single machine.

In the most common or standard detection mode, secondary electron imaging or SEI, a high-resolution image of a sample surface is provided revealing details about 1 to 5 nm in size. SEM micrographs have a very large depth of field, which can produce a characteristic three dimensional appearance of a sample.

Back scattered electron (BSE) are beam electrons that are reflected from the sample by elastic scattering. BSE are often used in analytical SEM with the spectra made from the characteristic X-rays. The intensity of the BSE signal is related to the atomic number (Z) of the specimen. Therefore the BSE image can provide desirable information regarding the distribution of different elements in the sample. Characteristic X-rays are emitted when the electron beam removes

an inner shell electron from the sample and electron with higher energy fill the shell and release energy. These characteristic X-ray are used to identify the chemical composition of the sample and also measure the abundance of elements in the sample [21].

A schematic representation of SEM microscope is shown in Figure 2.13.

An electron beam is thermionically[1] emitted from an electron gun filled with a tungsten filament cathode. Tungsten is a cheap metal with a highest melting point and lower vapour pressure of all metals thereby it can be heated for electron emission.

The emitted electron beam has an energy ranging from a few hundred eV to 40 KeV, is focused by one or two condense lenses to a spot about 0.4 nm to 5nm in diameters. In the electron column, the beam passes through pairs of scanning coils or pairs of deflector plates, then in the final lens, which deflect the beam in the x and y axes. Therefore all over a rectangular area of the sample surface can be scanned in a raster fashion.

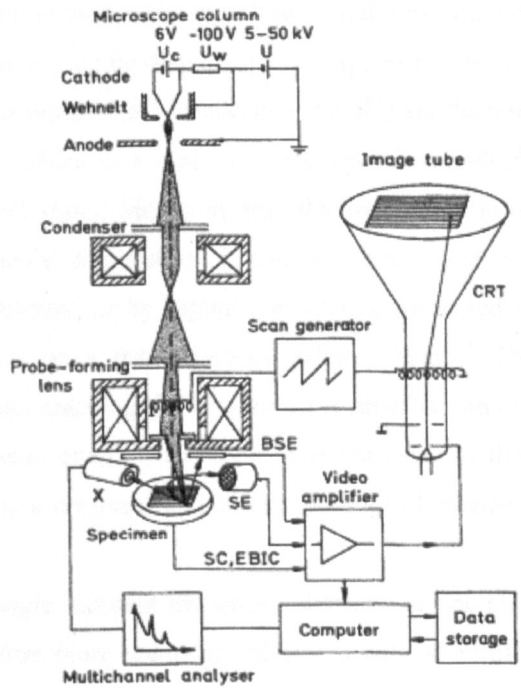

Figure2.13. Schematic representation of a scanning electron microscope (SEM) [22].

1. Thermionic emission means the emission of electrons into vacuum by a heated electronic conductor.

At this stage, when the primary electron beam interact, with the sample, by repeating random scattering and absorption within a tear drop shaped volume of the specimen, the electron will lose some energy. The interaction volume is usually extends from less than 100 nm to around 5μm into the surface.

In fact, the size of the interaction volume depends on the electron's landing energy, the atomic number of the specimen and also the specimen's density. The energy exchange between the electron beam and the sample can produce the reflection of high energy electrons by elastic scattering emission. The specimen absorbs some of the beam current, which can be also detected and create an image of the distribution of the specimen current.

Different types of electronic amplifiers are used to amplify the signals which are displayed as variations in brightness on a cathode ray tube. The raster scanning of the CRT display is synchronised with that of the beam on the specimen in the microscope. Therefore from the scanned area of the specimen, a distribution map of the intensity of the emitted signal will be produced in an image. This image can be captured by photography from a high resolution cathode ray tube or in modern microscope can be displayed on computer monitor.

The secondary electrons with low energy (<50 eV) are detected by an Everhart-Thornley detector which is a type of scintillator-photomultiplier system. The amplified electrical signal output by the photomultiplier is displayed as a two dimensional intensity distribution. It can be viewed and photographed on an analogue video display, or by digital conversion, displayed as a digital image. This process relies on a raster-scanned primary beam. The numbers of the secondary electrons reaching the detector have an effect on the brightness of the signal. If the beam enters the sample perpendicular to the surface, then the activated region is a uniform, and certain number of electrons escape from the sample.

As the incident angle increase the escape distance of one side of the beam will decrease. Therefore more secondary electrons will be emitted and in a created image, steep surface and edges tend to be brighter than flat surfaces, and well-defined three-dimensional image will be produced.

In this technique, producing an image resolution with less than 1 nm is also possible.

The back-scattered electrons can provide some information regarding chemical composition on the surface of specimen. Back-scattered electrons consist of high energy electrons that are reflected or back scattered out of the specimen interaction volume by elastic scattering interaction with the specimen atoms. In fact, heavy elements with high atomic number back-scatter electrons more strongly than light elements with low atomic number and thus appear brighter in the image. Back-scatter electron detectors are usually either of scintillator or semi-conductor types, can placed above the sample in a doughnut type arrangement, concentric with the electron beam, maximising the solid angle of collection. An electron back scattered diffraction (EBSD) image can be formed by back scattered electron that can be used to determine the crystallographic structure of the specimen.

All samples must be of an appropriate size to fit in the specimen chamber and are generally mounted rigidly on a specimen holder called a specimen stub. For imaging in the SEM, specimen must be electrically conductive at least at the surface to prevent the accumulation of electrostatic charge at the surface the ground connection for the specimen is required. Metal objects need little special preparation, except cleaning and mounting on a specimen stub. Non-conductive specimens tend to charge when scanned by the electron beam, because of that, scanning faults and other image artifacts might be seen. Therefore, an ultra-tin coating of electrically conducting material, commonly gold, deposited on the sample either by low vacuum sputter coating or by high vacuum evaporation [22].

A micrograph record of the untreated and treated cotton fabric with various chemical solutions was provided by JSM-820 scanning electron microscope from JEOL Company. In addition to the secondary imaging, back scattered electron, energy dispersive X-ray (EDX) analysis were also used for chemical analysis. Mapping elements distribution with in a given sample was carried out on the surface and also for the cross section of each fabric. Samples were attached to standard SEM stubs and silver coated in a Bio-Rad Diode sputter coating units [22].

2.3 Characterization

2.3.1 Flammability test

The procedure was carried out was according to the vertical strip test as BS EN ISO 6941/2 tests, in which a simple vertically orientated fabric subjected to a standard igniting flame source on the surface of the fabric for a specific time as 10 sec. For flame retarded fabric the properties measured after extinction of the ignition source, are the damaged (or char) length (D), size of the hole if present (F), time of after flame and after glow and nature of any debris and smoke etc, Figure 2.14.

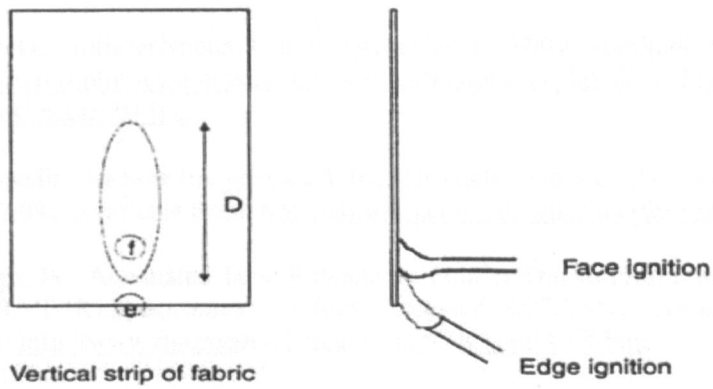

Figure2.14. A Schematic representation of a simple vertical strip test.

After glow time: The time after glow continues after the removal of the ignition source and the cessation of flaming.

Char length: The distance from the fabric edge which is directly exposed to the flame to the furthest point of visible fabric damage after a specific tearing force has been applied [23].

References Chapter-2

1. Pavia- Glampman, D. and Kriz, G., "Introduction to Spectroscopy", Publisher: Books/Cole, Thomson Learning, USA, 2001.

2. Sheffield Hallam University-School of Science and Mathematics, Infra-Red Absorption Spectroscopy – Theoretical Principle. Online, [Accessed 23/07/09], 1998, Available from: http://www.shu.ac.uk/schools/sci/chem/tutorials/molspec/irspec1.htm.

3. Stuart, B. , "Modern Infrared Spectroscopy", Chichester,Wiley and Sons, 1996.

4. Banwell, G.N. and Mc Cash, E.M." Fundamentals of Molecular Spectroscopy", 4th, London, Mc Grow – Hill Book Company, 1994.

5. Michelson Intreferometer, Online, [Accessed 23/07/09], Available from: http://www.physics.iitm.ac.in/courses_files/courses/gplab03_odd/Michelson_files/image004.jpg

6. Wikipedia, the Free Encyclopedia, Interferometry, Online, [Accessed 23/07/09], Available from: http://en.wikipedia.org/wiki/Interferometry

7. Phipps, W., Attenuated Total Reflectance Fourier Transform Infrared (ATR/FT-IR) Spectrometry, Online, [Accessed: 8/07/2009], Available from: http://www.microemanlytical.com/ATR_ken/ATR.htm.

8. Ferraro, J.R., Nakamoto, K and Brown, C.W., "Introductory Raman Spectroscopy", Publisher: Elsiver Science USA, 2003.

9. Wasatch Photonics – Raman Spectroscopy, Online, [Accessed: 30.07/2009], Available from: http://www.wasatchphotonics.com/applications/raman_spectroscopy.htm.

10. Markus, F, Markus, J. And Anderas, Z., "Raman – Spectroscopy of Oligomeric SiO Species Isolated in Solid Methane", Journal of Chemical Physics, 1999, 111, 17, 7881-7887.

11. Laserna, J.J., "Modern Techniques in Raman Spectroscopy", Publisher: John Wiley and sons, 1996.

12. Akitt, J.W. and Mann, B.E.,"NMR and Chemistry, an Introduction to Modern NMR Spectroscopy", Publisher: Standley Thornes, 2000.

13. Hollas, J.M., "Modern Spectroscopy", Publisher John Willey and Sons, 1987.

14. Nuclear Magnetic Resonance Spectroscopy, Online, [Accessed: 31/07/2009], Available from:

http://www.cem.msu.edu/~reusch/Virtual Text/ Spectrpy/nmr/nmr1.htm

15. Keeler, J., "Understanding NMR Spectrometry", Publisher: John Wiley and Sons, 2005.

16. Wikipedia, the Free Encyclopedia, Mass Spectrometry, Online, [Accessed: 10/10/2009], Available from: http://en.wikipedia.org/wiki/Mass_spectrometry

17. Hoffmann, E. and Stroobant,V., Mass Spectroscopy, Principal and Application. 3th Ed, West Sussex: John Wiley & Sons Ltd., 2007, 1-5.

18. Mass Spectroscopy, Online, [Accessed: 20/10/2009], Available from: http://antoine.frostburg.edu/chem/senese/101/atoms/slides/sld017.htm

19. Menczel, J. D. and Prime, R.B., "Thermal Analysis of Polymers, Fundamentals and Applications", publisher: John Wiley and sons, 2009.

20. Wikipedia, the Free Encyclopedia, Theromgravimetric Analysis, Online, [Accessed 25/07/2009], Available from: http://en.wikipedia.org/wiki/thermogravimetric_analysis

21. Goldstein, J.I., "Scanning Electron Microscopy and X-ray Microanalysis: a Text for Biologists, Materials Scientists and Geologists", Publisher: Plenum New York; London, 1981.

22. Transmission and Scanning Electron Microscopy, Online, [Accessed 20/07/2009], Available from: http://www.inano.au.dk/research/competences-and-facilities/nanotools/transmission-and-scanning-electron-microscopy/

23. Standard Test Method for Flame Resistance of Textiles (Vertical Test), D-6413-99, Annual Book of ASTM Standards 2000, 7, 2.

Chapter 3 – Preparation of Urea Condensed Products

Introduction

The objective and aims of this research were to make cheap, effective, wash-durable flame retardant agents for application to cellulosic fabrics from aqueous pad-liquors and to fix the finish by drying and baking. The potential flame retardant agents were based on urea condensates and produced by melt-reactions of urea with sulphating agents and phosphating agents.

Sulphuric acid and sulphamic acid were selected as sulphating agents while phosphoric acid and phosphorous acid were used as phosphating agents.

At a constant rate of heat input in an open reaction vessel, various types of urea condensates have been produced. To find the best type with appropriate molar ratio of the initial materials, some specific factors have been considered.

- The controllability of the exothermic reactions.
- The water solubility of the products.
- The starting and terminating temperature of the exothermic reaction.
- The cost of the initial materials

Therefore a study on the production procedures of the various types of urea condensates was undertaken to find the most controllable process, to give products with high water solubility and low cost. The exotherms involved were studied using the DSC thermo-analysis technique.

This chapter describes the chemical analysis of urea condensates, formed from heating urea alone or urea condensates formed from heating mixtures of urea with sulphamic acid, phosphorus acid and combinations of sulphamic acid/phosphorous acid – some condensates being water-soluble and others water-insoluble. The results of the various analytical techniques including conventional elemental analysis, mass spectrometry, NMR, FT-IR and also Raman spectroscopy are reported.

3.1 Thermal decomposition of urea

Preparation of each urea condensate was carried out by mixing the initial materials and heating up to the melt temperature. The effectiveness of urea and also the complicated reactions involved in this process are explained in detail. The FTIR spectra of the condensates were measured at different temperatures.

20 g of urea were placed in a beaker and heated at a constant rate of heat input. The phenomena observed on heating are:

- The urea started to melt at 45°C.
- Clear urea melts were produced at 120°C (the melting point of urea in different references is about 133 – 135°C).
- Molten urea started to boil slowly at temperatures above 120°C; some gas was evolved and temperature rose very quickly due to exothermic reactions.
- At 140°C, the mix boiled very intensively.

At 140°C the product when cooled and tested was still water soluble; the reactions, also confirmed in the literature, may be written as follows, (Scheme 3.1):

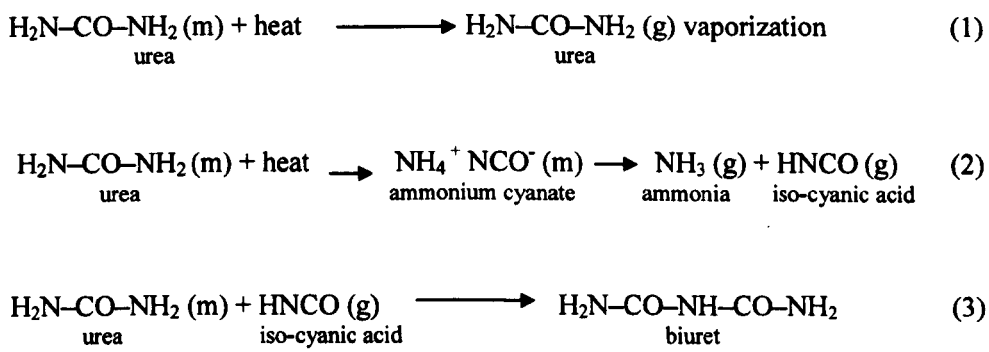

Scheme3.1. The reactions involved during the thermal decomposition of urea in an open vessel [1].

At 150°C still boiling intensively, some evaporation occurred, Reaction (1). From the study of thermal decomposition of urea by Schaber [1], at 152°C, urea decomposition begins and biuret production is first noted, Reaction (3).

At 160°C, with the mix still boiling, further gas evolved.

As found in this study, melting urea at 160°C gives a water insoluble compound, which is a new product.

3.2 Preparation of urea condensates

3.2.1 Preparation of the sulphamic acid/urea condensates [S/U]

Preparation of urea condensate 1S/2U using one mole of sulphamic acid and 2 moles of urea

Sulphamic acid, NH_2SO_3H, known to be an esterification catalyst, has a melting point and decomposition temperature of 205 °C.

To form a condensate 2 moles urea (120 g) and 1 mole sulphamic acid (97 g) were heated in a beaker at a constant rate of heat input, the temperature rose irregularly as shown in Figure 3.1.

At 50°C, the mixture started to melt; from 85° - 95°C, some gases evolved from the reaction; from 120° to 130°C, a clear melt was produced, and NH_3 evolved from the reaction; at 140°C the melt became viscose and some crystals appeared. After cooling to 120°C, the colourless melt became a very thick viscous fluid and some crystals were produced.

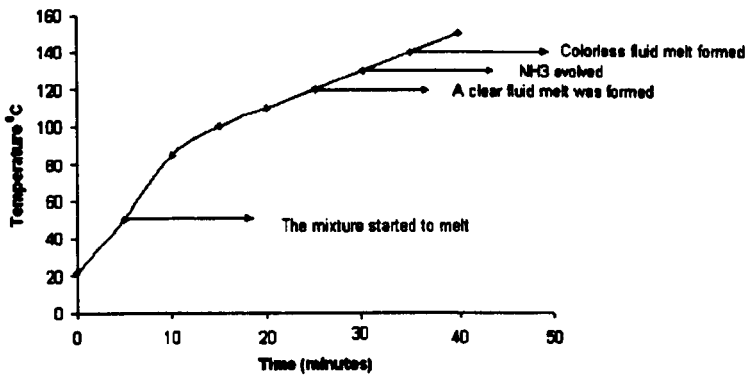

Figure3.1. Changes observed on heating 1 mole sulphamic acid and 2 moles of urea at a constant rate of heat input [1S/2U].

Preparation of urea condensate 1S/3U using one mole of sulphamic acid and 3 moles of urea

1 mole sulphamic acid (97 g) and 3 moles of urea (180 g) were heated at a constant rate of heat input, the temperature rose irregularly as shown in Figure 3.2.

At 50°C, the mixture started melting; at 110°C, complete melting occurred and some gas evolved from the reaction; from 120° to 155°C a clear melt was produced. After cooling to 60°C some small crystals formed at the surface of the liquid.

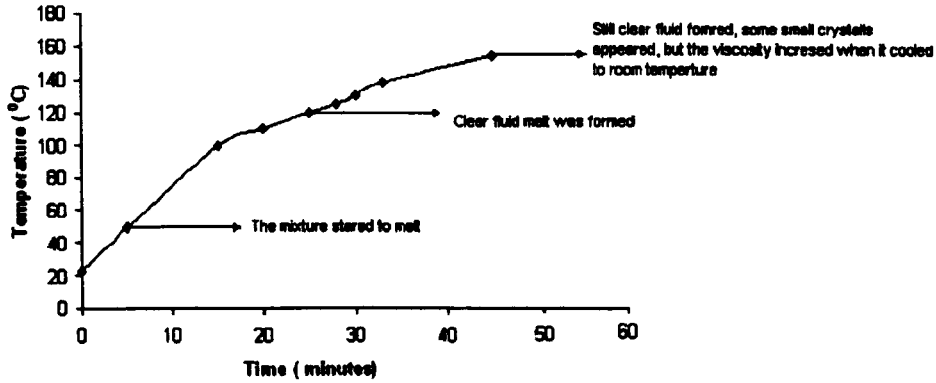

Figure3.2. Changes observed on heating 1 mole sulphamic acid and 3 moles of urea at a constant rate of heat input [1S/3U].

Preparation of urea condensate 1S/4U using one mole of sulphamic acid and 4 moles of urea

1 mole sulphamic acid (97g) was taken to the reaction with 4 moles of urea (240 g), by heating up the mixture at a constant rate. The temperature increased irregularly as indicated in Figure 3.3.

At 55°C, the mixture started to melt; at 110°C, the mix melted completely and some gas evolved from the reaction { a sample was taken at this stage (Sample 1)}; at 120°C a clear melt was formed, (Sample 2); at 130°C, a clear viscous fluid was produced, (Sample 3). The mix was clear when it cooled to room temperature, but remained a fluid of high viscosity. On further heating for ten more minutes, at 155°C, a clear fluid remained (Sample 4), but when cooled, some crystals precipitated in the reaction vessel, indicating some insoluble products were produced.

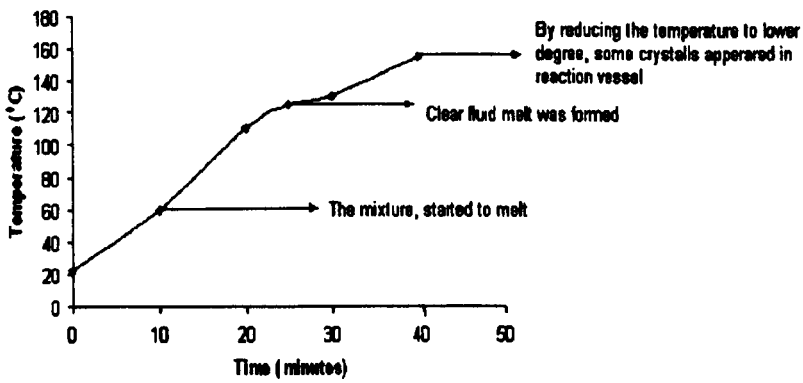

Figure3.3. Changes observed on heating 1 mole sulphamic acid and 4 moles of urea at a constant rate of heat input [1S/4U].

Preparation of urea condensate 1S/5U using one mole of sulphamic acid and 5 moles of urea

A similar procedure was used in this preparation. The observed changes are shown in Figure 3.4. The final product is white crystals.

The weight ratio of initial materials and also the yield of products have been provided in Table 3.1.

Table3.1. The weight proportion of initial material and the efficiency of products

Urea condensate	1S /2U	1S/3U	1S/4U	1S/5U
The weight ratio of urea to sulphamic acid	1.2	1.8	2.4	3.1
% Yield	90	94	98	99

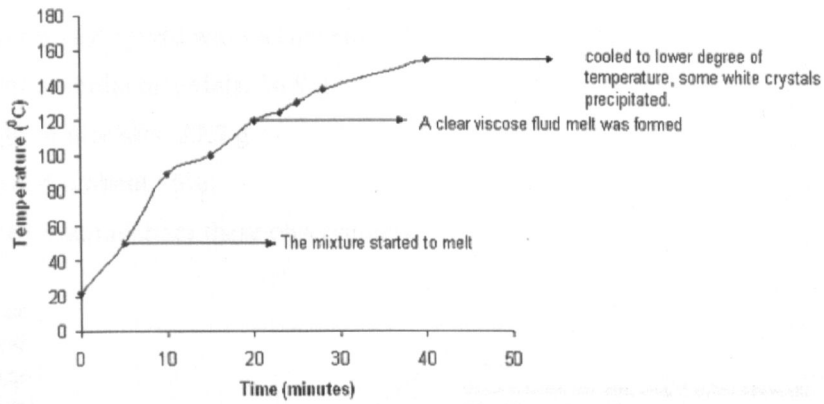

Figure3.4. Changes observed on heating 1 mole of sulphamic acid and 5 moles of urea at a constant rate of heat input [1S/5U]

It has to be mentioned that during the preparation of the various types of urea/sulphamic acid condensates, at the beginning of the process when the mixture is melted completely, the pH was acidic until it reached to the reaction temperature, the result of this chemical reaction change the pH to the higher degree approximately 7-8 (The pH was measured using the pH indicator paper.).

3.2.2 Preparation of the sulphuric acid/urea condensates

Sulphuric acid melts at 10 °C, and boils at 337 °C. In all the condensates various molar ratios of sulphuric acid and urea were used. Unfortunately the chemical reactions were highly exothermic and it was not possible to control the procedure; solid products were produced very rapidly and were not water soluble.

3.2.3 Preparation of the phosphorous acid/urea condensates [PH/U]

One mole of phosphorous acid and two moles of urea [1PH/2U]

The two initial materials were heated at a constant rate in a beaker at atmospheric pressure. Phosphorous acid, H_3PO_3 has a melting point of 73.6 °C and boils at 200 °C with decomposition.

The phenomena observed during the condensation reactions were as follows:

At 23 °C the mix started to become fluid; at 60°C the solution started to boil, and NH_3 was given off; at 100°C, the mix was quite fluid, but still boiling with evolving gases; an exotherm resulted in a spontaneous temperature rise to 142°C, the intensity of boiling reduced and a clear colourless fluid was produced; the temperature dropped to 125°C and remained constant for a few minutes; further cooling gave hard crystals which were water soluble.

The condensate yield was calculated:

Weight of initial materials: 36.9 g

Weight of products: 27.7 g

The yield is about 75%

Figure3.5 summarises these observations.

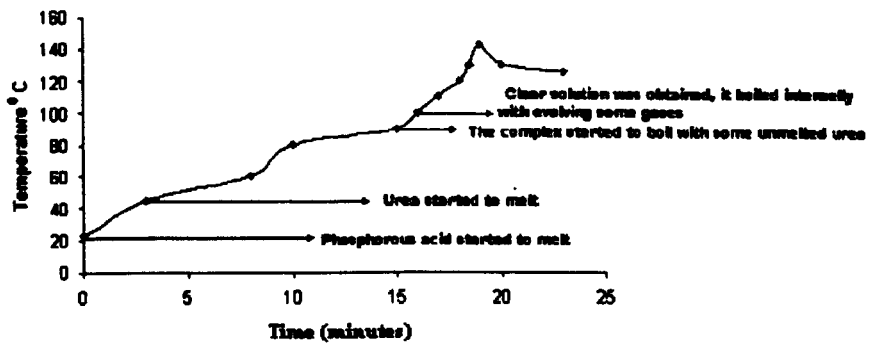

Figure3.5. Changes observed on heating 1 mole of phosphorous acid and 2 moles of urea at a constant rate of heat input [1PH/2U].

Preparation of condensate from one mole of phosphorous acid and 3 moles of urea [1PH/3U]

The observations were similar to those from the pervious condensate preparation; however the exotherm was greater, Figure 3.6. The product yield was approximately 89%.

Preparation of condensate from one mole of phosphorous acid and 4 moles of urea [1PH/4U]

The procedure was the same as for the 1PH/2U condensate explained previously, but the reaction time was different since the increased amount of urea needed more time to melt; however the product yield was higher at approximately 93%. It is very interesting that, by increasing the amount of urea in a reaction, the water solubility of the final condensates decreased.

Preparation of condensate from one mole of phosphorous acid and 5 moles of urea [1PH/5U]

The reaction process was as for the previous condensate. Increasing the temperature at a constant rate, the condensate was produced at a lower temperature (125°C). On cooling crystals formed very quickly; the solid was difficult to dissolve in cold water but dissolved readily in warm water at 60°C. The product yield was approximately 93.5 %.

The observed phenomena when heating different molar ratio of phosphorous acid and urea, are shown in Figure 3.6.

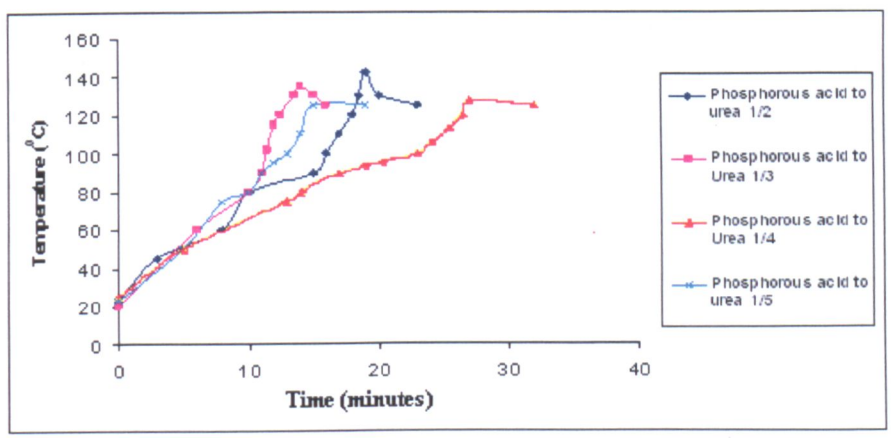

Figure3.6. Changes observed when heating different molar ratio of phosphorous acid and urea.

It is very clear, that for various molar ratios used to form urea condensates, the rate of reaction was different, but in all cases easy to control. According to the molar ratio used the temperature exotherm was different along with the rate of gas evolution from the reaction; always there was a sudden drop in the boiling intensity and the temperature also dropped very quickly, which indicates condensate

preparation was complete; also the indicator paper test showed that the pH changed from acidic condition to mildly alkaline.

3.2.4 Preparing of the phosphoric acid/urea condensates [PA/U]

In these experiments hemi-hydrate phosphoric acid with melting point at 29.32˚C and boiling point at 158˚C was used. One mole of phosphoric acid and 2, 3, 4 or 5 moles of urea were heated at a constant rate; the temperature rose irregularly as shown in Figure 3.7.

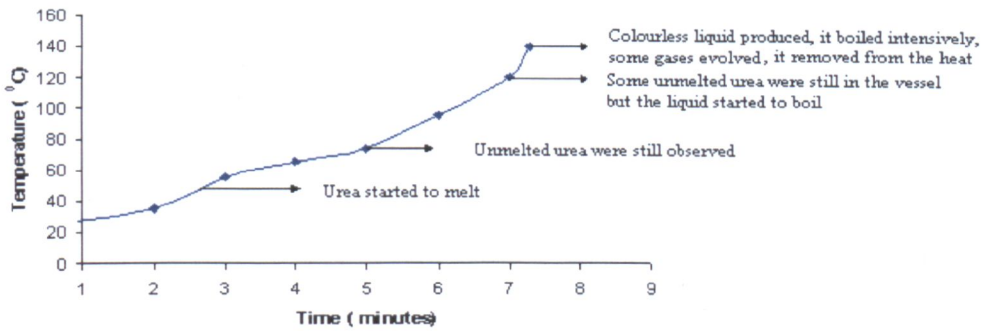

Figure3.7. changes observed on heating 1 mole of phosphoric acids and 2 moles of urea at a constant rate of heat input.

The temperature response differences between the reactions when forming the various condensates are shown in Figure 3.8; after removing the condensate from the heat, the temperature dropped very quickly and hard crystals were produced.

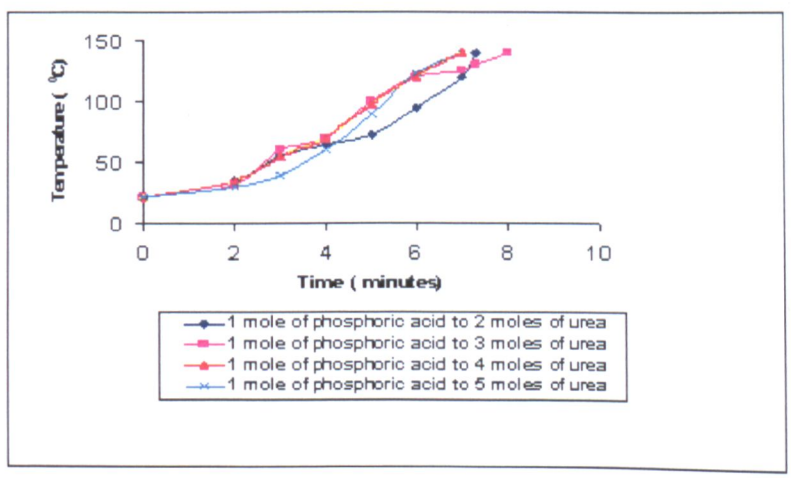

Figure3.8. Changes observed on heating 1 mole of phosphoric acids and different moles of urea at a constant rate of heat input.

By increasing the amount of urea, the exotherm increased but was controllable. The percentage yields obtained from each urea condensate reaction are summarised in Table 3.2.

When preparing the pad-liquor to use for fabric treatment (section 4.1.4) the prepared urea condensate was dissolved in water at the required concentration. By increasing the amount of urea in the condensate, the product water-solubility is reduced and it thus takes more time for the pad-liquor to be prepared.

Table3.2. The weight proportion of initial material and the efficiency of products.

The type of urea condensate	1PA/2U	1PA/3U	1PA/4U	1PA/5U
The weight ratio of urea to phosphoric acid	1.2	1.8	2.4	3.1
yield%	90	94	98	99

3.2.5 Preparation of the sulphamic acid/phosphorous acid/urea condensates [S/PH/U]

There is some possibility to reduce the cost of the flame retardant condensate produced by this method, by increasing the amount of urea and also to exploit the FR synergism between sulphamic acid and phosphorous acid. Therefore as an initial experiment, 1mole of sulphamic acid and 1 mole phosphorous acid were mixed with various molar ratios of urea (4, 6, 8, 10, 12, 14, 16, 18 and 20) to form a variety of condensates. Good solubility of the condensates in water was seen as desirable in all these processes; however by increasing the amount of urea, the reaction took place at higher temperature and harder crystals were produced. After applying the solution of each type of condensate to cotton fabric by a pad-dry-bake procedure, the flame retardancy properties of the treated fabrics were investigated; with the exception of the 20 moles of urea condensate, the other condensates provided sufficient durable flame retardancy performance on cotton fabric.

The product formed from 1 mole sulphamic acid, one mole phosphorous acid and 10 moles of urea was selected for chemical analysis. During the heating process, some valuable information was obtained:

The mix started to melt at 80°C. The molten mix started to boil intensively with gas evolution at 120°C and some gases were evolved from the reaction. Suddenly at 135°C, the intensive boiling changed to a calm process with small bubbles and the mix temperature remained constant for a few minutes; at this point the reaction was

removed from the heater. The pH (paper indicator) of the mix changed from acidic to mildly alkaline. The water solubility of the condensate was high and it was thus investigated as a flame retardant product for textile materials.

Two other S/PH/U condensates were investigated: heating a mixture of 1mole sulphamic acid, 2 moles of phosphorous acid and 10 moles of urea at a constant rate in an open beaker, and also 2 moles sulphamic acid 3 moles of phosphorous acid and 10 moles of urea; these condensates also gave promising FR properties following application to cotton fabrics. In fact by increasing the amount of phosphorous acid in the urea condensate, the reaction temperature was reduced; in the second product with three moles of phosphorous acid, the reaction was terminated at 120°C, approximately 10°C lower than for the 1mole phosphorous acid compound. The condensate of 2S/3PH/10U produced a gel, and remained in this condition for at least few hours, which is a valuable quality in industrial scale up process. As indicated previously, by taking the condensation reaction above 150°C, water in-soluble products were produced. Details from the chemical analysis of the various condensates are provided in the next section.

3.3 Elemental analysis of S/PH/U condensate

The elemental analysis report is provided for three urea condensate samples the water-soluble1S/1PH/10U (mixture heated to 135°C), the water-insoluble 1S/1PH/10U condensate (mixture heated to 180°C) and also the water-soluble 1S/2PH/10U condensate in Table 3.3.

Table3.3. Elemental analysis of the S/PH/U condensates.

Elements	Water-soluble 1S/1PH/10U (%)	Water-insoluble 1S/1PH/10U (%)	Water-soluble 1S/2PH/10U (%)
Carbon	14.2	15.25	12.65
Hydrogen	6.25	6.65	6.25
Nitrogen	37.3	33.1	34.85
Sulphur	4.75	1.6	3.2
phosphorus	3.3	1.8	6.85

In comparison between the two urea condensate products, 1S/1PH/10U and 1S/2PH/10U, the amount of carbon, nitrogen and sulphur elements were reduced in the 1S/2PH/10U condensate. In fact during the production of the urea condensate in

an open vessel, it is not possible to control the amount and the type of gases evolving from the reactions, therefore no similarity between the data for these two products could be expected.

In the water insoluble product, 1S/1PH/10U condensate, which has been produced at high temperature above 160°C, the amount of sulphur and phosphorus has been significantly reduced. This reduction may be due to the different types of gases evolved and needs to be studied more precisely.

3.4 Further analysis of the urea condensate reactions by DSC

Differential scanning calorimetry (DSC) is an analytical technique in which the difference in heat flow between a sample and inert reference material is measured as a function of time and temperature; both samples are subjected to a controlled environment of time, temperature, atmosphere and pressure. In Figure 3.9 the thermal decomposition of urea is shown. The melting process starts at 50°C and ends at 150°C; the endothermic effect centred at 137°C indicates the urea melting transition.

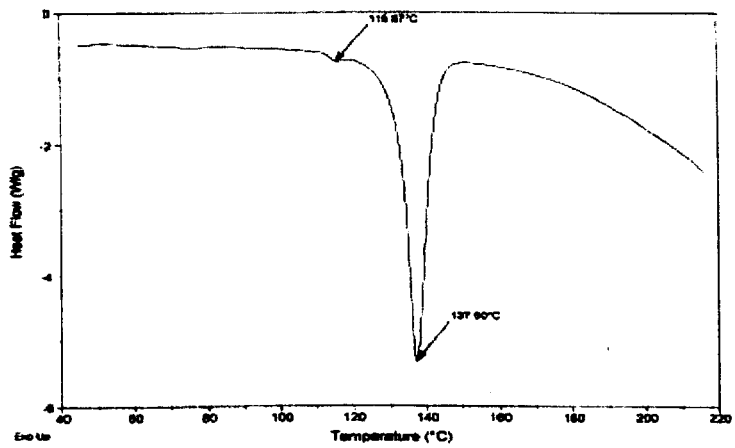

Figure3.9. The DSC thermogram of urea decomposition under nitrogen gas flow.

In Figure 3.10 the DSC thermogram from heating a mixture of one mole of sulphamic acid and 4 moles of urea, is shown.

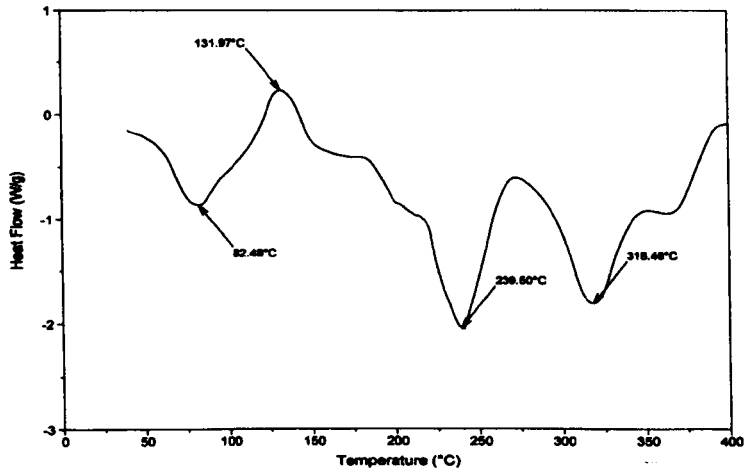

Figure3.10. DSC results for the mix 1:4 sulphamic acid/urea.

An exothermic effect is shown with onset temperature of 132°C. The exothermic peak is attributed to an interaction between the initial materials; following this temperature point further reactions are evident giving several products which show endotherms.

The same experiment was carried out on the phosphorous acid and urea mix, by mixing the initial materials in the appropriate molar ratio and then heating up at a constant rate in the DSC instrument. The thermogram from this study is shown in Figure 3.11. In this case the first exothermic effect began at 75°C and finished at 150°C and centred at 112°C as indicated in DSC curve. The lower melting point of phosphorous acid reduced the reaction temperature compared to the urea sulphamic acid system. By increasing the amount of urea in the reaction, this exothermic process occurs at a higher temperature. Further thermal reactions gave products which show two endotherms (224°C and 351°C) but these condensation temperatures were not used in our research.

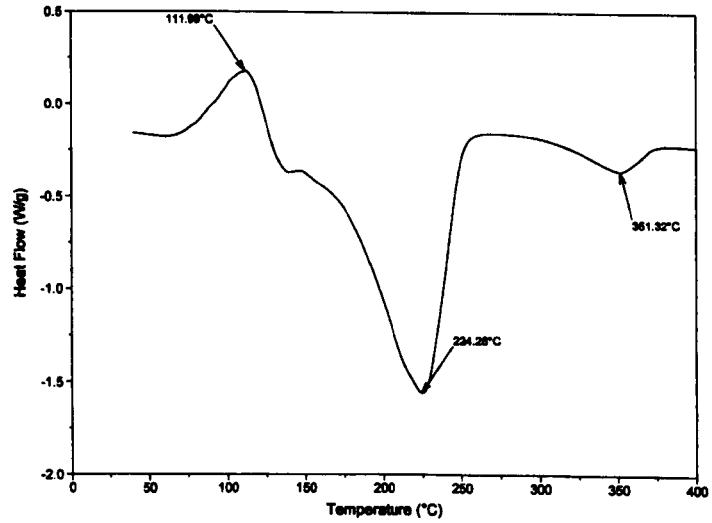

Figure3.11. DSC result for the sample of 1:3 phosphorous acid and urea.

The mix of phosphorous acid, sulphamic acid and urea to produce the urea condensate was also studied by DSC. In this case a mix of 1 mole sulphamic acid, 1 mole phosphorous acid and 10 moles of urea was used. The thermogram shows a very strong, sharp exotherm at 130°C signifying a precise chemical reaction is taking place between the initial materials, starting around 100°C and centred at 130°C.

The decomposition of the product is indicated by the endotherm, centred on 220°C. The DSC thermogram is shown in Figure3.12.

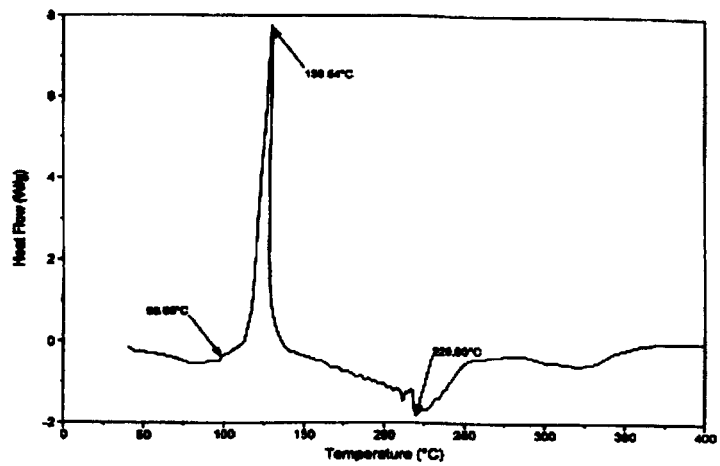

Figure3.12. DSC results for the initial materials 1 mole sulphamic acid and 1 mole phosphorous acid and 10 moles of urea.

The stability of the urea condensate products is also very important and can be examined by reheating the products using the DSC technique. Therefore, in the next

experiment, the sample which has been heated to 140°C was reheated at a constant rate to see the thermal decomposition of the products.

Figure 3.13 shows the DSC curve obtained from reheating the 1/1/10 molar ratio condensate of phosphorous acid, sulphamic acid and urea. The two endotherms effects at 123°C and 132°C, indicates at least two products are produced in the thermal decomposition procedure.

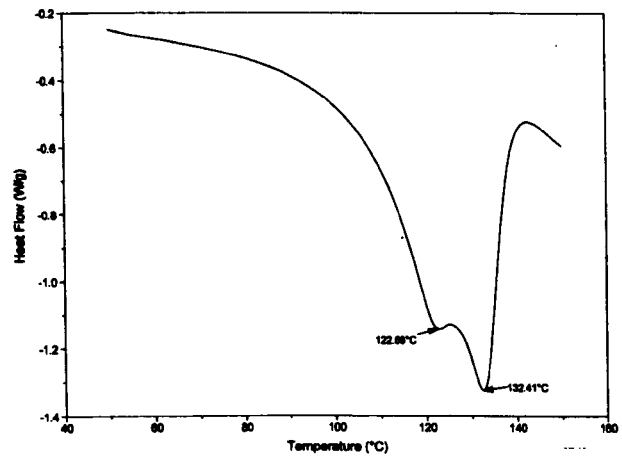

Figure3.13. The DSC reheating results for the 1S/1PH/10U condensate.

In the next experiment, the other urea condensate produced from 1mole sulphamic acid, 2 moles of phosphorous acid and 10 moles of urea was studied using DSC. The same procedure was carried out on initial materials and the DSC curve is shown in Figure 3.14. The first wide and small endotherm centred at 97°C represents the completion of the melting process for the initial materials; this is followed by an exotherm centred at 114°C with low enthalpy energy changes. The main chemical reaction occurred between 120°C to 135°C, centred at 126°C with a strong exotherm, representing the main new product.

To confirm the purity of our product (i.e. reaction completed), the reheating process was carried out on the sample heated up to 140°C. The DSC curve is illustrated in Figure 3.15.

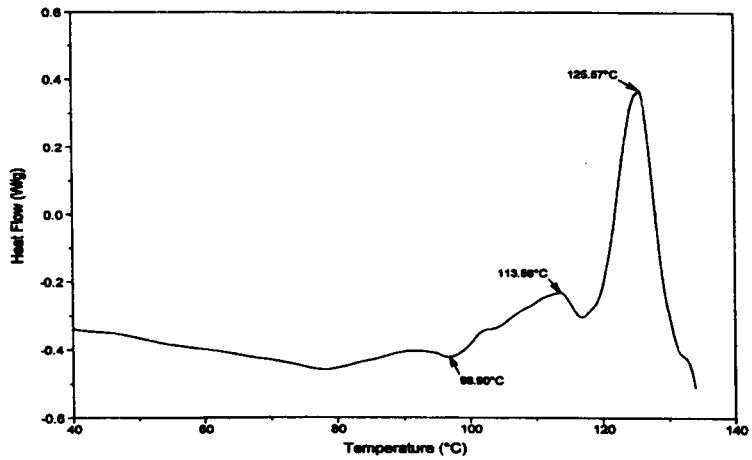

Figure3.14. The DSC result of heating up one mole sulphamic acid 2 moles phosphorous acid and 10 moles of urea at a constant rate.

A very clear endotherm centred at 125°C is good evidence for the full formation of the urea condensation products produced from the reaction of 1 mole sulphamic acid, 2 moles of phosphorous acid with 10 moles of urea.

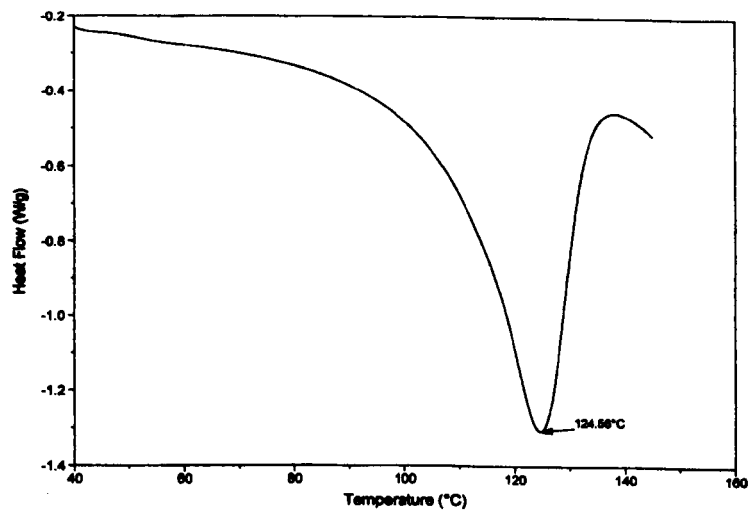

Figure3.15. The DSC result of reheating process on the 1S/2PH/10U condensate.

3.5 FT-IR spectroscopic analysis

3.5.1 FT-IR analysis of Urea

The difference between the FTIR spectrum of urea and that urea of heated at 140°C for about 5 minutes is shown in Figure 3.16.

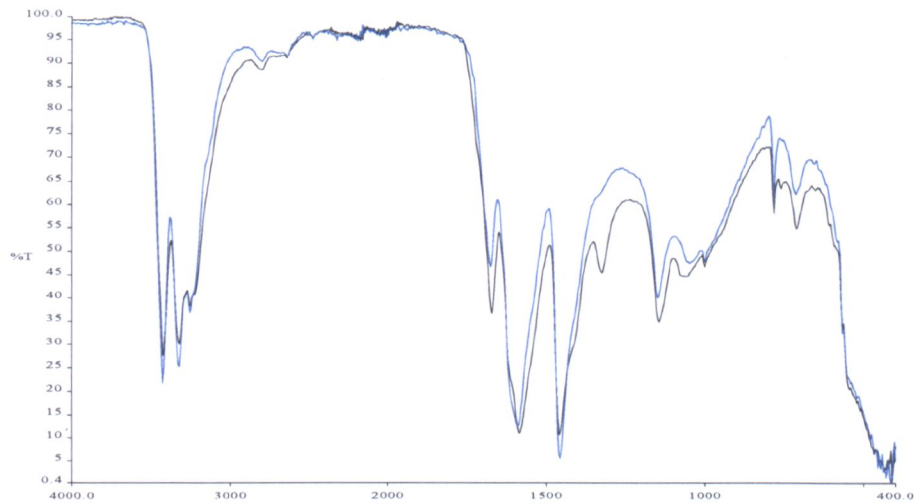

Figure3.16. FT-IR spectra of urea (98 %) [blue] and urea heated at 140°C [black].

The pre-heated urea shows a stronger band at 1678 cm^{-1} which suggests formation of new –NH–CO–NH– groups. A combination of bands of NH deformation and CN stretching vibration confirmed by the presence of a very strong absorption at 3436 cm^{-1} (S), 3325 cm^{-1} (S) and 3254 cm^{-1} (m), indicating the primary amide of urea. In the spectrum of the melted urea, medium absorption appeared at 1327 cm^{-1}, which can be mainly due to CNH in plane bending and CN stretching, respectively. Approximate IR absorbance frequencies for alkyl urea are indicated in Table 3.4.

Table3.4. Approximate IR absorbance frequency representing the alkyl urea functional groups.

Group	R_2N-CO-NR_2 cm^{-1}	RNH–CO–NHR cm^{-1}	R_2N–CO–NH_2 cm^{-1}	RNH–CO–NH_2 cm^{-1}
NH_2 anti-symmetric starch			3410	3430
NH stretch		3340		3350
NH_2 Symmetric stretch			3200	3220
C=O stretch	1640	1625	1660	1650
NH_2 deformation			1610	1600
CNH stretch – bend		1585 , 1535 w		1560

The properties of isocyanic acid, HNCO, and some of its derivatives have been described in section 1.12. However there has been some doubt regarding the thermal stability of HNCO, it forms very strong hydrogen bonds therefore the formation of dimers or other oligomers with the formula $(HNCO)_n$ are possible. These dimers should have bands in the same region as the fundamental of monomeric HNCO [1]. In fact at 140°C, the melted urea contains various products with amide linkage, the reaction of isocyanic acid with amines can produce polyureas or polyamides; some possible reactions are illustrated here, Scheme 3.2.

$H_2N–CO–NH_2$ (m) + HNCO (g) ⟶ $H_2N–CO–NH–CO–NH_2$
Urea iso-cyanic acid biuret

$H_2N–CO–NH–CO–NH_2$ + HNCO (g) ⟶ H_2N-CO-NH-CO-NH-CO-NH_2
biuret iso-cyanic acid ureas

H_2N-(CO-NH-CO)$_n$-NH_2
Ureas

Scheme3.2. The reactions of isocyanic acid with amines.

Through this work it was found that, when the urea is heated above its melting point to160°C, a water insoluble product will be produced, which needs to be analysed in more detail.

The polymerization of HNCO leads to a mixture of cyanuric acid (trimer of HNCO) and cyamelide, and these can react further to form chain-like polymers of fairly high molecular weight. The heating of urea in an open vessel to high temperature (160°C), leads to the liberation of NH_3 and also H_2O, the other possible reactions which can produce new products are shown in Schemes 3.3 to 3.8. The presence of ammonia and isocyanic acid in gas form, can also promote further reactions.

Urea reactions:

H_2N-CO-NH_2 (m) + heat ⟶ $NH_4^+NCO^-$ (m) ⟶ NH_3 (g) + NHCO (g)
Urea ammonium cyanate ammonia isocyanic acid

2HNCO (g) + H_2N-CO-NH_2 (m) ⟶ ammelide (s) + 2 H_2O (g)
isocyanic acid urea

2HNCO (g) + H_2N-CO-NH_2 (m) ⟶ ammeline (s) + 2H_2O (g)
isocyanic acid urea

Scheme3.3. Urea reactions.

Biuret reactions:

$H_2N\text{-}CO\text{-}NH\text{-}CO\text{-}NH_2$ (m) + HNCO (g) → CYA (s) + NH_3 (g)
biuret — cyanic acid — cyanuric acid — ammonia

$2H_2N\text{-}CO\text{-}NH\text{-}CO\text{-}NH_2$ (m) → CYA (s) + HNCO (g) + $2NH_3$ (g)
biuret — cyanuric acid — cyanic acid — ammonia

$2H_2N\text{-}CO\text{-}NH\text{-}CO\text{-}NH_2$ (m) → ammelide (s) + HNCO (g) + NH_3 (g) + H_2O (g)
biuret — cyanic acid — ammonia

$H_2N\text{-}CO\text{-}NH\text{-}CO\text{-}NH_2$ (m) + HNCO (g) → ammeline (s) + $2H_2O$ (g)
biuret — cyanic acid

Scheme3.4. Biuret reactions.

Triuret reactions:

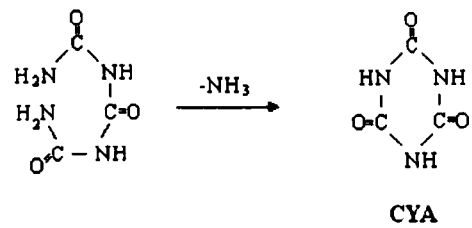

CYA

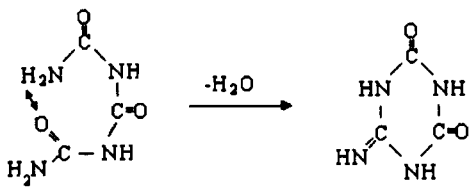

Ammelide

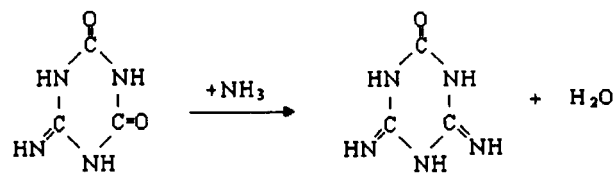

Ammelide **Ammeline**

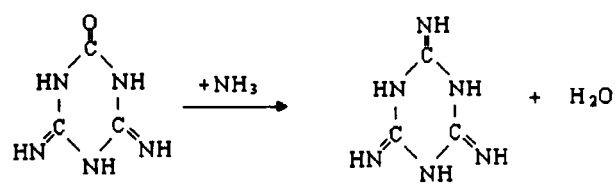

Ammeline **Melamine**

3 HNCO (g) ⟶ CYA (s)
Cyanic acid — cyanuric acid

CYA (s) + NH_3 (g) ⟶ ammelide (s) + H_2O (g)
Ammonia

Scheme3.5.

cyanate production:

NH_3 (g) + HNCO (g) ⟶ $NH_4^+NCO^-$ (s)
ammonia — cyanic acid — ammonium cyanate

Scheme3.6.

Urea cyanurate production:

H_2N-CO-NH_2 (m) + CYA (s) ⟶ H_2N-CO-$NH_3^+CYA^-$ (s)
urea — urea cyanurate

Scheme3.7

Biuret cyanurate production:

H_2N-CO-NH-CO-NH_2 (m) + CYA(s) ⟶ H_2N-CO-NH-CO-$NH_3^+CYA^-$(s)
biuret — biuret cyanurate

$3H_2NC \equiv N$ (g) ⟶ melamine (s)
cyanamide

Scheme3.8

The FT-IR spectra of melted urea at 140°C and also at 160°C are shown in Figure 3.17. It is clear, in specific regions, that new peaks appear representing new functional groups relevant to the chemical reactions which may take place at high temperature (160°C).

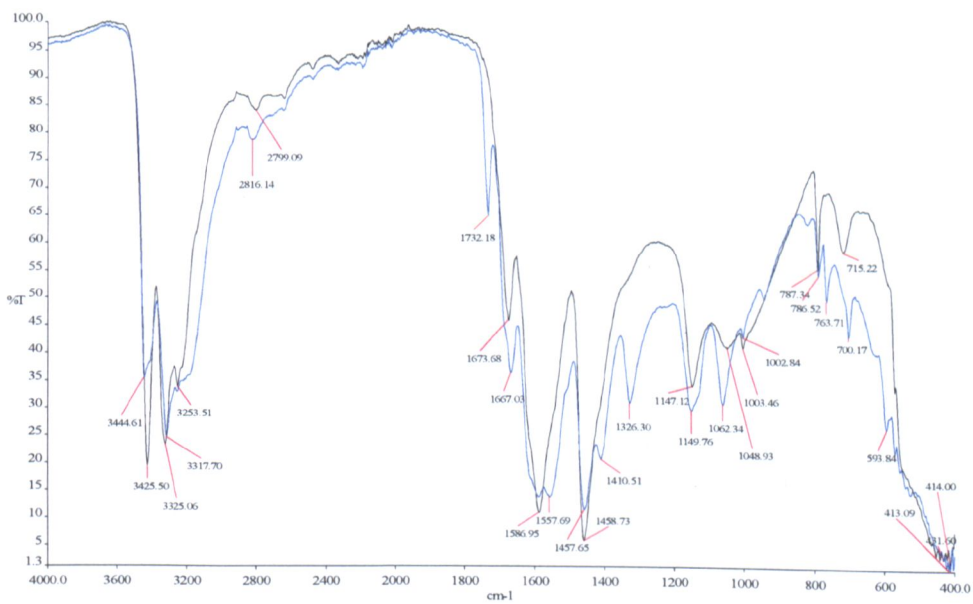

Figure3.17. The FT-IR spectra of urea heated up to140°C, above its melting point 138°C (water-soluble) [black], and the urea heated up to 160°C (water- insoluble) [blue].

In Table 3.5 the information regarding these functional groups and specific assigned peak frequency for each region are provided. However in some parts, the specific peak at particular frequency is not clear in the main FT-IR spectrum, therefore the second derivative spectrums are provided.

Table3.5. FT-IR spectral information regarding the possible functional groups that appeared in urea heated to 140°C.

*Functional Groups	Region cm^{-1}	**Specific Peak cm^{-1}	Intensity	Comments
Ureas	1680-1635	1674	s	C=O str, primary ureas, i.e. with NH_2 group
	3440-3200	3425 3325	m	NH str
	1605-1515	1587	s	amide II band
	1360-1300	1326	m	asym N-C-N str
	1190-1140	1147	m	sym N-C-N str
-$NHCONH_2$	3440-3400	3425	m	asym NH_2 str
	3360-3320	3325	m	NH str
	3240-3200	-	m	sym NH_2 str
	1605-1515	1587	s	NH_2 def vib
	1360-1300	1326	s-m	asym N-C-N str
	1190-1140	1147	m	sym N-C-N str
	620-530	594	v	NH_2 def vib
-NHCONH-	3360-3320	3325	m	NH str
	1585-1515	1558	v	NH def vib
	1360-1300	1326	s-m	asym N-C-N str
	1190-1140	1147	m	sym N-C-N str
Primary amides	1420-1400	1410	m	C-N str, known as amide III band
	~1150	1150	w	NH_2 in plane rocking vib, not always seen
	750-600	715	m	Br, NH_2 def vib
	600-550	-	m-s	N-C=O def vib
	500-450	-	m-s	C-C=O def vib

* These functional groups and their specific identified frequency regions are indicated in ref. [2].

** These specific peaks are determined from the main FT-IR spectrum of urea heated to 140°C.

The possible formation of cyanuric acid at high temperature after removing ammonia gas in an open vessel reaction was the first predicted compound in this reaction. Literature has cited the indication of the alkyl and aryl sym-triazines which have a strong band at 1580-1520 cm^{-1}, which may be a doublet [2], and at least one band at 1450-1350 cm^{-1} due to in-plane stretching vibrations, and one weak band at 860-775 cm^{-1} due to an out-plane deformation. The FT-IR spectrum of urea heated to 160°C shows two strong bands at 1558 cm^{-1} and 1587 cm^{-1} and also one band at 1411 cm^{-1} representing ring stretching vibration of cyanuric acid. In addition the other observation of the out-plane deformation band at 764 cm^{-1} can confirm the presence

of the cyclic trimer of isocyanic acid following heating urea at high temperature (160°C).

The vibrational assignments for all possible products that could be formed in heating urea at 160°C are indicated in Table 3.6.

Table3.6. FT-IR spectral information regarding the possible functional groups that appeared in urea heated to 160°C.

*Functional Groups	Region cm-1	**Specific Peak cm-1	Intensity	Comments
Sym-triazines	3300-3100	-	m	C-H str
	1580-1520	1557	vs	ring str, doublet
	1450-1350	1411	v	ring str, at least one
	1000-980		w	band
	860-775	787	w-m	ring str
		787		out-of-plane bending vib, at least one band
Cyclic ureas (five membered ring)				
(in solid phase)	1680-1635	1667	s	ketone groups in ring
(in solution)	1735-1685	1732	s	increase frequency
Hydroxyl-substituted triazines	1775-1675	1732	s	C=O str vibration of keto
	795-750	763	sharp-m	iso form
$\begin{matrix} R \\ R \end{matrix}\!\!>\!C=N-H$	1650-1640	-	s	C=N str vibrations
Ammelines and ammelides	2650~	-	w-m	br, ring NH…O=C vib
Cyanate ion, NCO^-	2225-2100	-	s	asy NCO str
	1335-1290	-	s	sy NCO str
	1295-1180		w	combination band
	650-600		s	NCO bending vib
Melamines	3500-3100	3444	v	NH_2 str
		3318		
	1680-1640	1667	m	NH_2 def
	1600-1500	1587	s	Ring str
		1558		
	1450-1350	1411	v	number of bands
	825-800	-	m	}Only one of the two is
	795-750	787	m	present
		787		

* These functional groups and their specific identified frequency regions are indicated in ref. [2].

** These specific peaks are determined from the main FT-IR spectrum of urea heated to 160°C.

Cyclic urea is also another suggestion, which has a specific band at 1680-1635 cm^{-1} frequency [2], with a strong band in the FTIR spectrum at 1667 cm^{-1} as shown in Figure 3.17. However this band also appears in the urea reaction at 140°C, representing the C=O stretching vibration. The second derivative spectra for the 1640-1760 cm^{-1} region shows new bands which can provide evidence of new products being formed.

The production of cyanuric acid and also triazine has been discussed previously but to study these in more detail, the second derivative spectrum in specific frequency regions was used. This work shows that melamine is formed at 160°C, although earlier work claimed this compound was only found, when urea was heated above 250°C.

A study of the thermal decomposition of urea, and related compounds using DSC and TGA measurements, together with evolved gas analysis (EGA) connecting to an FT-IR spectrometer [3], gave reasonable information regarding the type of gas evolved and also the specific frequency indicated for each product at specific temperature. It is interesting to note that at high temperature, approximately 160°C, NH_3, CO_2 and CO gases were detected and there was no indication of water evaporation in the analysis.

Figure 3.18 shows the second derivative spectrum of urea melted at 160°C, a new broad band appears at 3467 cm^{-1}, representing the NH_2 stretching vibration while two new bands at 3437 cm^{-1} and 3429 cm^{-1} are also representing the NH_2 stretching vibration of melamine which does not appear in the main spectrum. The bands at 3345 cm^{-1} and 3336 $cm^{-1}$are also observed at this region which may indicate the same vibration mode.

Cyanuric acid was detected showing bands at 1053 cm^{-1}, and also at 1778, 1703,1053 and 764 cm^{-1}[2]. The exact band at 1054 cm^{-1} and a new band close to it at 1045 cm^{-1} in the second derivative spectrum of melted urea at 160°C can provide sufficient information regarding the present of cyanuric acid in our melted product Figure 3.20. The new bands of the second derivative spectrum at 1715, 1722, 1743 cm^{-1} and 1752 cm^{-1} also representing the new products, all these bands produced a strong band at 1732 cm^{-1} in the main FT-IR spectrum and is related to the cyanuric acid and other triazine products at this temperature.

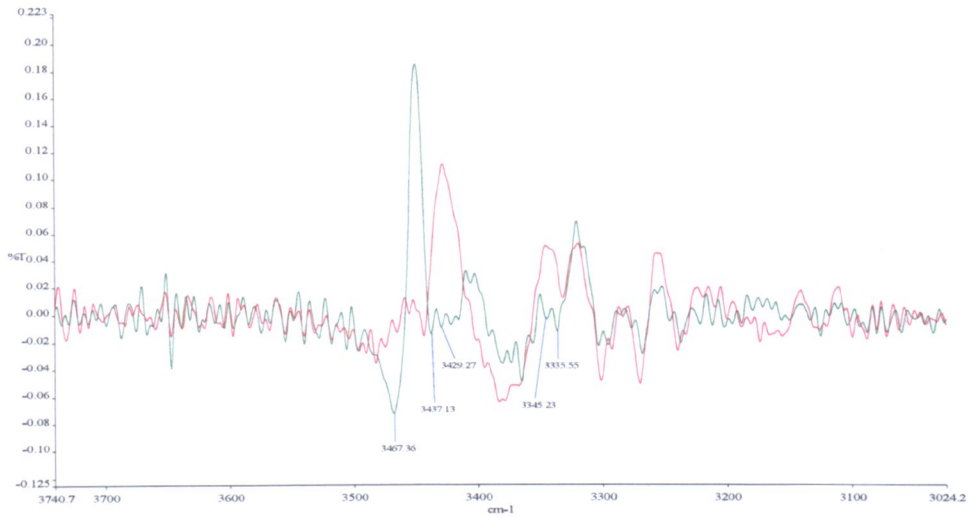

Figure3.18. The 2nd derivative spectra of urea heated to 140°C [red] and urea heated to 160°C [green].

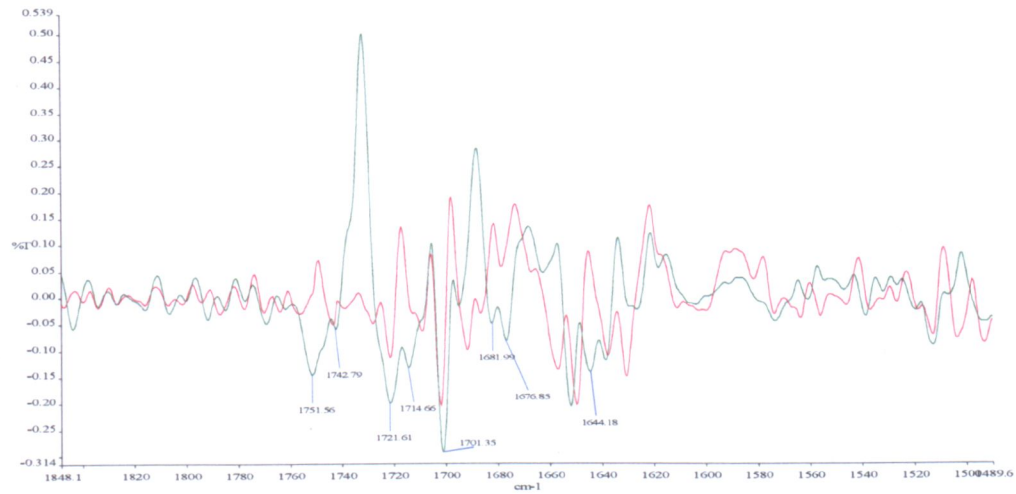

Figure3.19. The 2nd derivative spectra of urea heated to 140°C [red] and urea heated to 160°C [green].

The presence of biuret has been confirmed through the band at 1081 cm^{-1} [1], which is indicated at 1085 cm^{-1} in the second derivative spectrum of urea heated at 160°C. The other product, ammelide has a specific band at 1073 cm^{-1}[1], in the heated urea at 160°C this band is formed at 1076 cm^{-1} in Figure 3.20.

In Schaber's research [1] he indicated another band at 764 cm^{-1}, which in our work appeared at 771 cm^{-1}, (Figure 3.21).

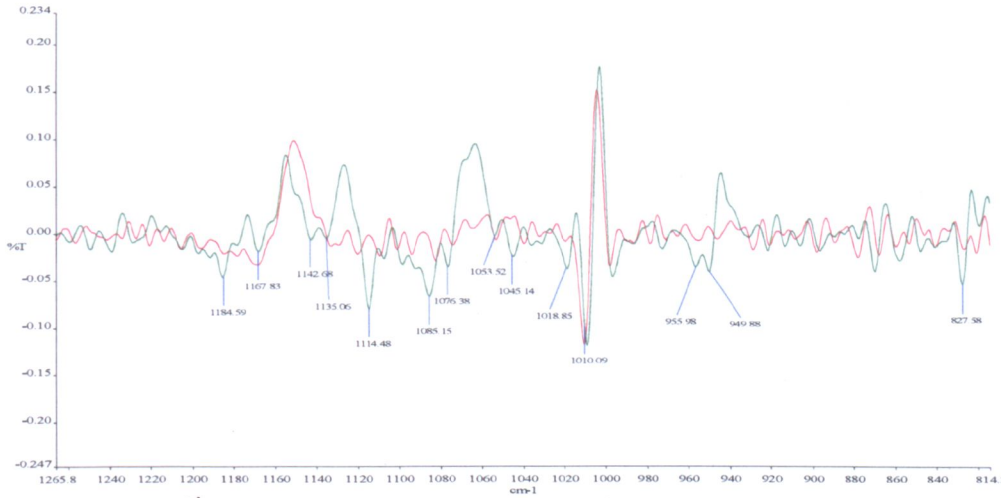

Figure3.20. The 2nd derivative spectra of urea heated to 140°C [red] and urea heated to 160°C [green].

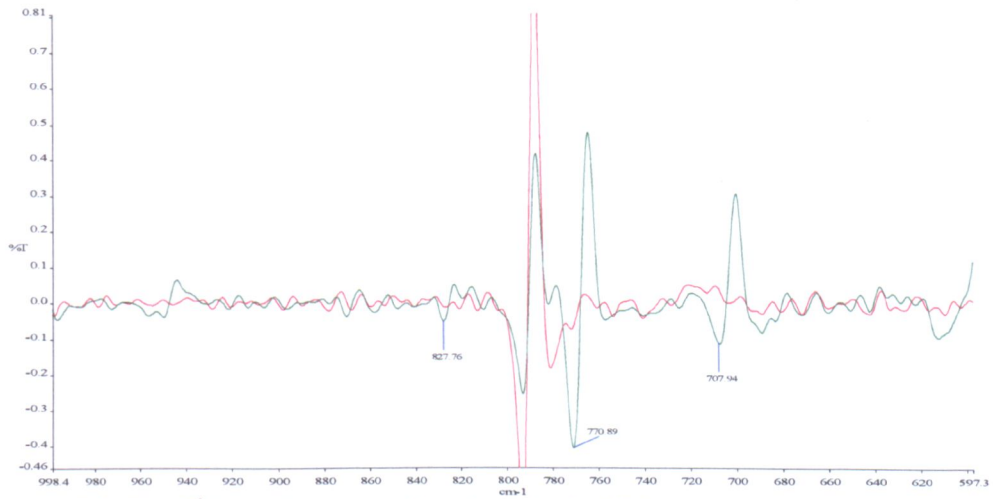

Figure3.21. The 2nd derivative spectra of urea heated to 140°C [red] and urea heated to 160°C [green].

The present of cyanate ion NCO- can be confirmed by the specific bands indicated at various frequency regions, Table 3.6. In the main FT-IR spectrum, Figure 3.17, the intensity reduction of two strong bands at 1323 cm^{-1} and 1335 cm^{-1} represent the symmetrical stretching vibration of the N-CO group detected by increasing the temperature of urea decomposition from 140 to 160°C. In the specific frequency region between 1295-1180 cm^{-1} no specific new bands appear. In the region 2225-2100 cm^{-1} relevant to the asymmetrical stretching vibration of N-CO group no specified bands are indicated in the main FTIR spectrum for both (140–160°C) urea thermal decomposition spectra.

3.5.2 Sulphamic acid / urea condensate (S/U)

To study the FT-IR analysis of the sulphamic acid/urea condensate the spectrum of sulphamic acid, heated urea at 140°C and also the urea condensate of 1 mole sulphamic acid and 4 moles of urea are compared in Figure 3.22. The new product can be seen which requires detailed analysis.

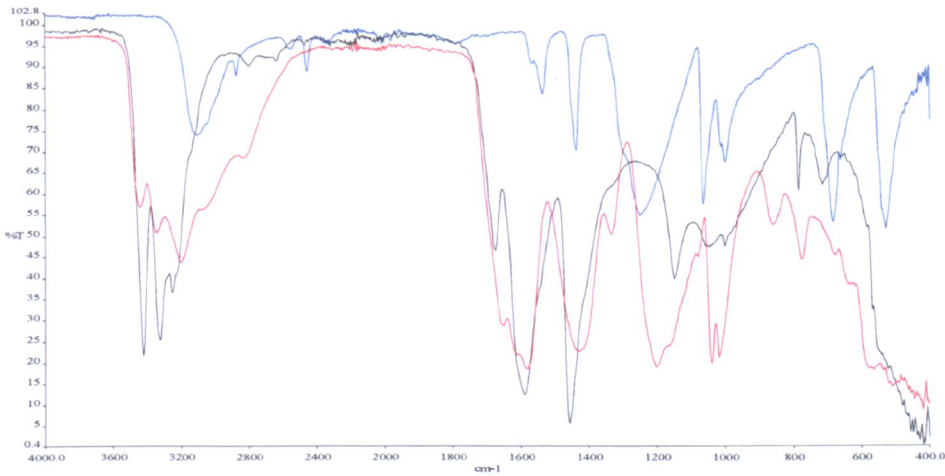

Figure3.22. The spectra of sulphamic acid/urea condensate [red] compared with that of the initial materials; heated urea at 140°C [black] and also sulphamic acid [blue].

During the preparation of sulphamic acid/urea condensate samples were removed at different temperatures. In Figure 3.23 the FT-IR spectrum of all the samples for 1 mole sulphamic acid and 4 moles of urea are indicated.

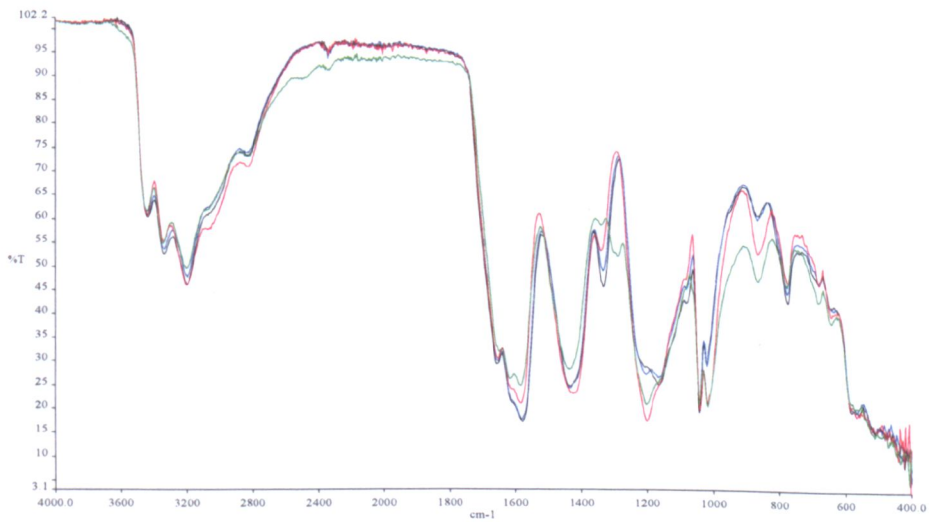

Figure3.23. Difference between the sulphamic acid/urea condensate (1S/4U) at various temperature, first sample which has been removed at 110°C [green], sample 2 removed at 120°C[red], sample 3 removed at 130°C [blue], sample 4 removed at 150°C [black].

It is clear that the two samples removed at 130°C and 150°C are similar, and therefore the reactions which have occurred between these two temperatures have been verified previously using the DSC thermal analysis.

The study of the two spectra for initial materials and sulphamic acid/urea condensate together provides adequate information relevant to the new products. In Figure 3.24 the spectra of urea condensate product and the melted urea at 140°C are shown. The main difference appears at particular regions, 3000-2400 cm^{-1}, 1300-900 cm^{-1} and 900-600 cm^{-1}; in Table 3.7 the positions and intensity of bands in specifics regions for urea are also indicated.

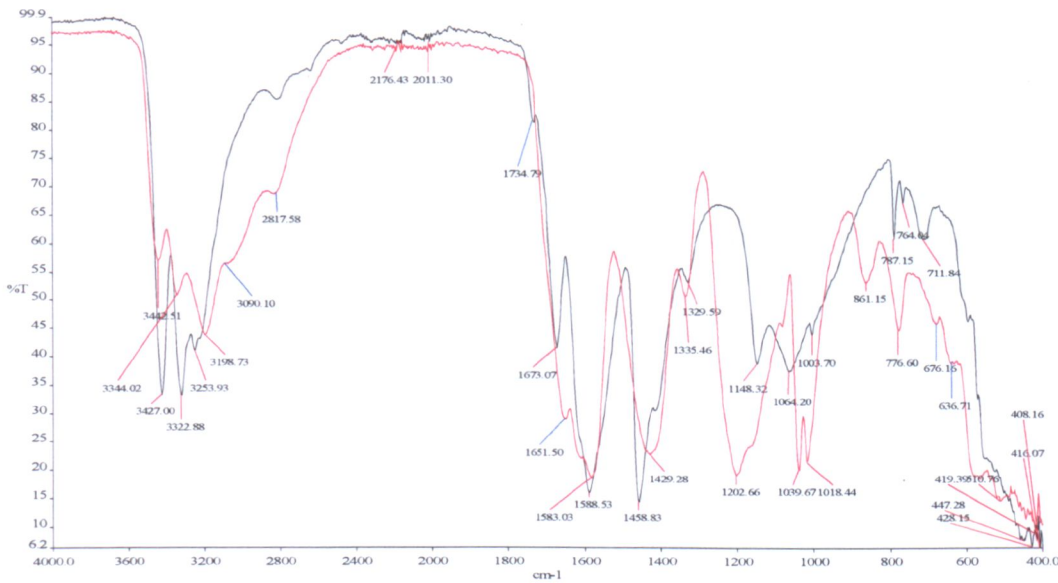

Figure3.24. FT-IR spectra of heated urea to 140°C [black] and 1S/4U condensate [red].

Consequently to be able to comprehend the chemical structure of the urea condensate, a comparison of FT-IR spectra of sulphamic acid as the initial material and product was made. In Figure 3.25 the two spectra are shown; details regarding particular overlapping frequencies and also specific new bands in the product are indicated.

The IR position and intensities of the bands relevant to sulphonamide and the other functional groups of the sulphamic acid/urea condensate are provided in Table 3.8.

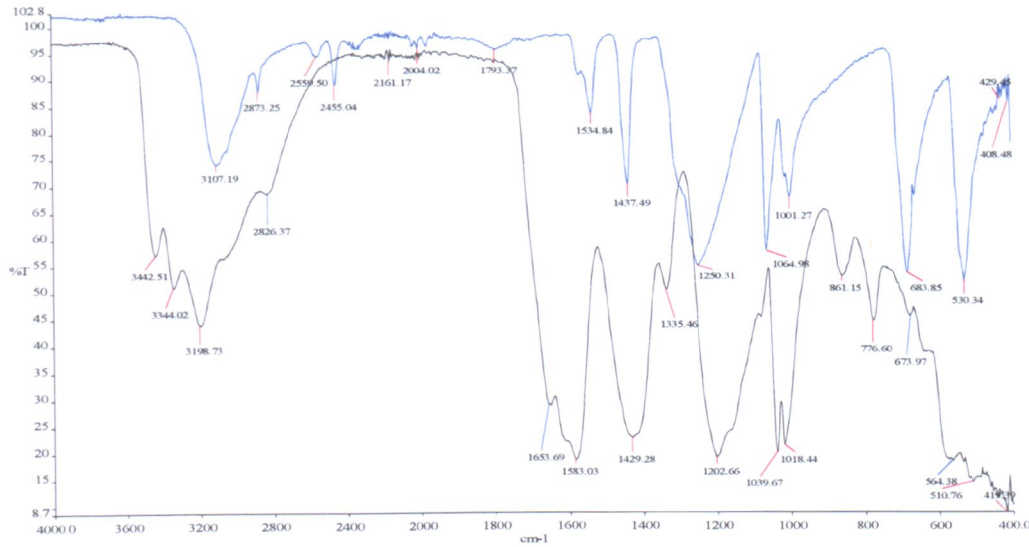

Figure3.25. The FT-IR spectra of sulphamic acid [blue] and 1S/4U condensate [black].

Table3.7. Assignment frequencies for ureas in FT-IR spectrum of 1S/4U condensate.

*Functional Groups	Region cm^{-1}	**Specific Peak cm^{-1}	Intensity	Comments
Ureas	1680-1635	1654	s	C=O str, primary ureas, i.e. with NH_2 group
	3440-3200	3344 3443	m	NH str
	1605-1515	1583	s	amide II band
	1360-1300	1335	m	asym N-C-N str
	1190-1140	-	m	sym N-C-N str
$-NHCONH_2$	3440-3400	3443	m	asym NH_2 str
	3360-3320	3344	m	NH str
	3240-3200	3199	m	sym NH_2 str
	1605-1515	1583	s	NH_2 def vib
	1360-1300	1335	s-m	asym N-C-N str
	1190-1140	-	m	sym N-C-N str
	620-530	564	v	NH_2 def vib
-NHCONH-	3360-3320	3344	m	NH str
	1585-1515	1583	v	NH def vib
	1360-1300	1335	s-m	asym N-C-N str
	1190-1140	-	m	sym N-C-N str
Primary amides	1420-1400	1429	m	C-N str, known as amide III band
	~1150	-	w	NH_2 in plane rocking vib, not always seen
	750-600	674	m	Br, NH_2 def vib
	600-550	564	m-s	N-C=O def vib
	500-450	511	m-s	C-C=O def vib

* These functional groups and their specific identified frequency regions are indicated in reference [2].

** These specific peaks are determined from the main FT-IR spectrum of 1S/4U urea condensate.

Table3.8. The FT-IR spectrum information regarding the possible functional groups appears in 1S/4U condensate.

*Functional Groups	Region cm^{-1}	**Specific Peak cm^{-1}	Intensity	Comments
Primary sulphonamides, - SO_2NH_2 (hydrogen bonded or solid phase)	3390-3245	3344	s	Two bands due to asym and sym N-H str
	1650-1550	1583	m-s	NH_2 def vib
	1360-1310	1335	s	Asym SO_2 str
	1190-1130	-		NH_2 rocking vib
	1165-1135	-		Sym SO_2 str
	935-875	861	m	N-S str
	730-650	676	w-m	NH_2 wagging vib,br
	630-510	637		SO_2 def vib
	560-480	-		SO_2 wagging vib
	490-400	419-416		SO_2 twisting vib
	415-290	408	s	NH_2 twisting vib
N-Mono-substituted sulphonamides – SO_2NH- (hydrogen bonded or solid phase)	3335-3205	-	s	N-H str, one band only
	1420-1370	1429	m	NH def vib
	1360-1300	1335	s	Asym SO_2 str
	1190-1130	-	s	Sym SO_2 str
	975-835	861	w-m	N-S str
	700-600	676	w,br	NH def vib
	600-520	-	w-m	SO_2 def vib
	555-445	447	w-m	SO_2 wagging vib
	480-400	428		SO_2 twisting vib
	~350	-		SO_2 rocking vib
	~280	-		CNS def vib
Covalent sulphonates, R-SO_2-OR	1420-1330	1335	s	Asym SO_2 str
	1235-1145	1203	s	Sym SO_2 str
	1020-850	1018	s	SO asym str
	830-690	777	m	SO sym str
	700-600	-	w	S-C str
	610-500	-	m-w	SO_2 def vib, usually two bands
Alkyl sulphonates, RO-SO_2-R	1360-1350	1335	m-s	
Alkyl sulphonic acids (anhydrous), RSO_2-OH	3000-2800	2818	s	Br, O-H str
	2500-2300	2359	w-m	Br, O-H str
	1355-1340	-	s	Asym SO_2 str
	1200-1100	1203	s	Sym SO_2 str
	1165-1150	1058***	s	Br, S-O str
	1080-1040	-	w	
	910-890	-	s	S-O str
	700-600	676	w	S-C str
		637		

* These functional groups and their specific identified frequency regions are indicated in reference [2].

** These specific peaks are determined from the main FT-IR spectrum of 1S/4U urea condensate.

*** This specific peak is determined from 2nd derivative spectrum, figure 3.26.

The analysis of the spectra from S/U condensates to explain specific frequency, relevant to the functional groups found in the initial starting materials and in the product together with new peaks observed for the urea condensate is given below:

3500-3000 cm^{-1}

The intensity of three strong bands at 3427 cm^{-1}, 3323 cm^{-1} and 3254 cm^{-1} are relevant to the NH stretching vibration of ureas have been reduced to the medium intensity and appear in the main urea sulphamic acid condensate spectrum.

3000-2300 cm^{-1}

The two medium bands in sulphamic acid spectrum at 2459 cm^{-1} and 2874 cm^{-1} are attributed to the OH stretching vibration of alkyl sulphonic acid anhydrous RSO_2-OH also appears in the urea condensate product.

1700-1400 cm^{-1}

The ureas C=O stretching vibration band is found at 1673 cm^{-1} in the urea spectrum while in the product it appears at 1661 cm^{-1}. The other strong band at 1589 cm^{-1} are due to NH stretching vibrations which occur in urea and also in the urea condensate product. In the urea spectrum a very broad and strong band at 1459 cm^{-1} is observed however in the product spectrum it appears again as a broad band centred at 1429 cm^{-1} attributed to the NH deformation vibration of secondary amides. In the sulphamic acid FT-IR spectrum this relevant band is observed differently as a very strong and sharp band at 1438 cm^{-1}.

1400- 1100 cm^{-1}

In the melted urea spectrum Figure 3.24 the asymmetric N-C-N stretching vibration are confirmed with the band at 1330 cm^{-1} while the symmetric stretching vibration is observed at 1148 cm^{-1}. These two bands are also found in the urea/sulphamic condensate at 1335 cm^{-1} and also a wide band centred at 1222 cm^{-1}. It needs to be mentioned that a very strong band at 1245 cm^{-1} in the sulphamic acid spectrum is due to the asymmetric and symmetric vibration of SO_2 stretching, this also appears in the condensate with a change in shape of the band to a broad band.

1100-800 cm^{-1}

The strong band at 1040 cm^{-1} in Figure 3.25, representing the NH-SO_3H group [2], in sulphamic acid shows two very strong peaks at 1065 cm^{-1} and 1001 cm^{-1} due to

S-O stretching vibration which can also be assigned in the urea condensates at 1018 cm^{-1} and 1040 cm^{-1}.

1000-600 cm^{-1}

The two strong bands in the sulphamic acid spectrum which appear at 684 and 530 cm^{-1} are due to the NH_2 wagging vibration and SO_2 wagging vibration respectively. Both of these peaks with medium intensity are also found in the urea condensate. The bands due to the NH deformation vibration of primary amide of urea appear at 764 cm^{-1} and 712 cm^{-1} and in the product are observed at 777 cm^{-1}. A new band at 861 cm^{-1} in the urea condensate due to the N-S stretching vibration appears which is not observed in the sulphamic acid spectrum.

As indicated in Table 3.7, some specific peaks relevant to the functional groups at particular frequencies are provided, but the information is not completely clear hence the second derivative spectra can clarify this fact.

In Figure 3.26 the second derivative spectra for specific frequency ranges for sulphamic acid and sulphamic acid/urea condensate are shown.

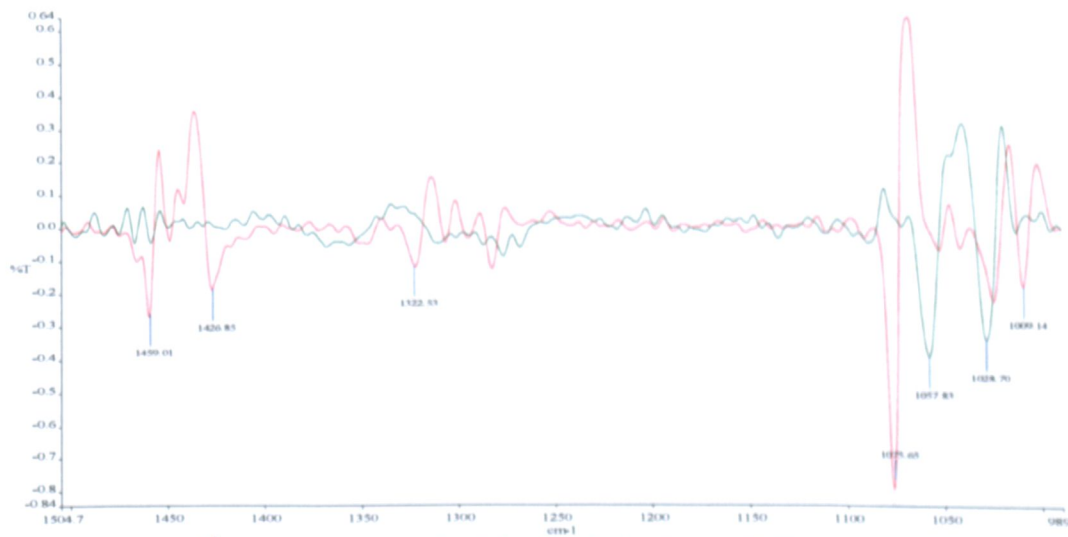

Figure3.26. The 2nd derivative spectra of sulphamic acid [red] and 1S/4U condensate [green].

The very strong band at 1076 cm^{-1} in the sulphamic acid spectrum is relevant to the alkyl sulphonic acid RSO_2-OH which appears as two new bands at 1058 cm^{-1} and 1029 cm^{-1} in the product. Also the intensity of two bands at 1427 cm^{-1} and 1459 cm^{-1} which are due to $-SO_2NH$ and NH deformation vibration are reduced in the product.

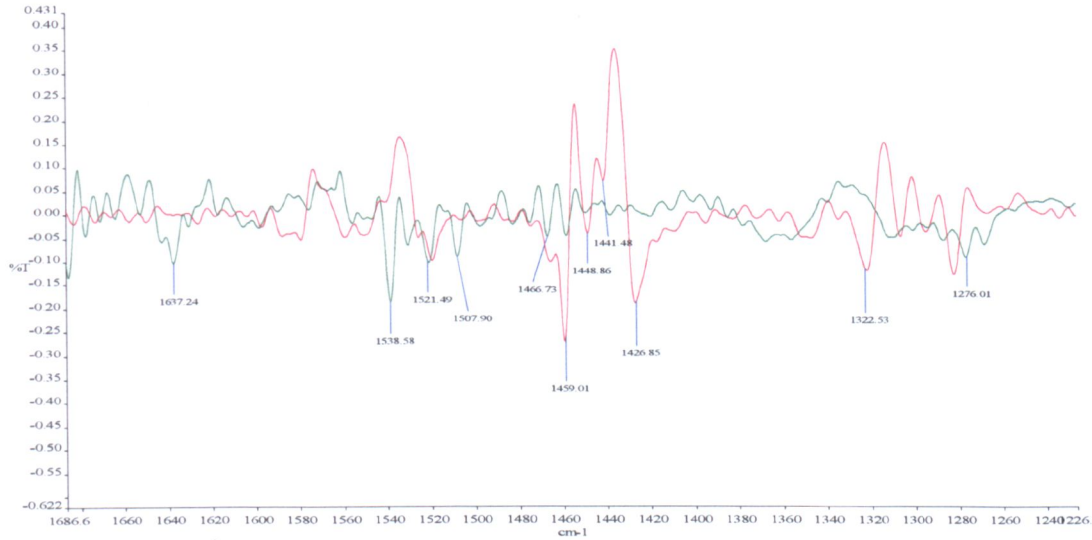

Figure3.27. The 2nd derivative spectra of sulphamic acid [red] and 1S/4U condensate [green].

In Figure 3.27 the intensity of two strong bands at 1427 cm^{-1} and 1459 cm^{-1} due to -SO_2NH- and NH deformation vibration are reduced in the product while some bands with high intensity are produced at 1539 cm^{-1} and 1508 cm^{-1}. These new bands are attributed to the NH_2 deformation vibration of urea. The other band at 1637 cm^{-1} is assigned to the C=O stretching vibration of the primary NH_2 group of urea.

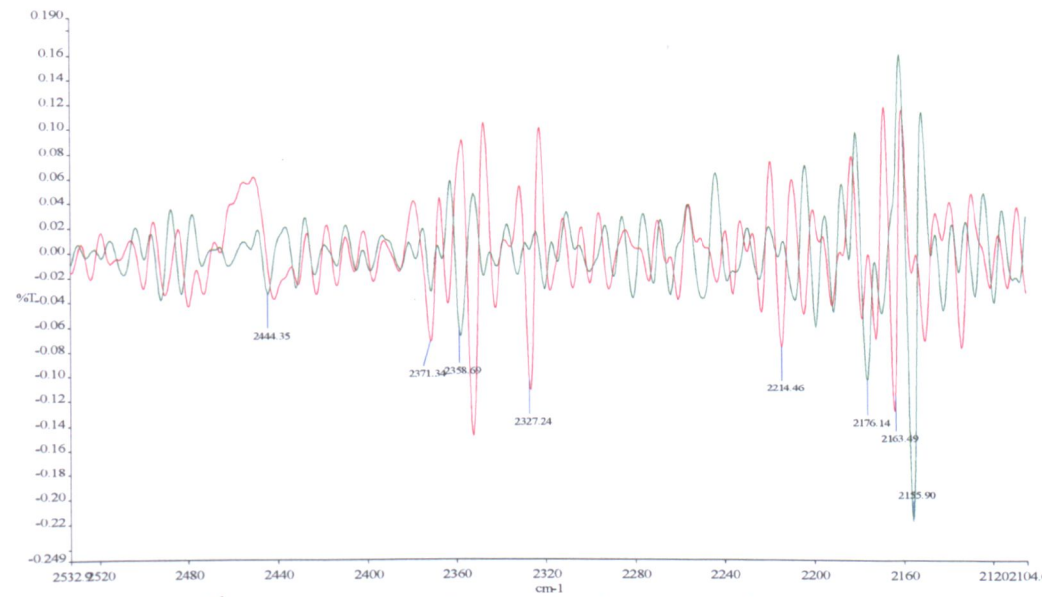

Figure3.28. The 2nd derivative spectra of sulphamic acid [red] and 1S/4U condensate [green].

In Figure 3.28 the intensity of two bands in the sulphamic acid at 2327 cm^{-1} and ~ 2348 cm^{-1}, relevant to the OH stretching vibration of sulphamic acid RSO_2OH, are reduced in

the condensate product. Also bands at 2156 cm^{-1} and 2163 cm^{-1} which could be attributed to the cyanate ion NCO-, appear in both spectra. However the intensity of these two bands in the main spectrum is very weak.

According to the information provided from the FT-IR analysis, the possible chemical reactions may be elucidated. At high temperature when the urea is melted in the present of sulphamic acid, thermal analysis shows significant amounts of isocyanic acid gas. Therefore the reaction starts with the generation of isocyanic acid which reacts with the amine and hydroxyl groups of sulphamic acid to produce the new products indicated below, Scheme 3.9.

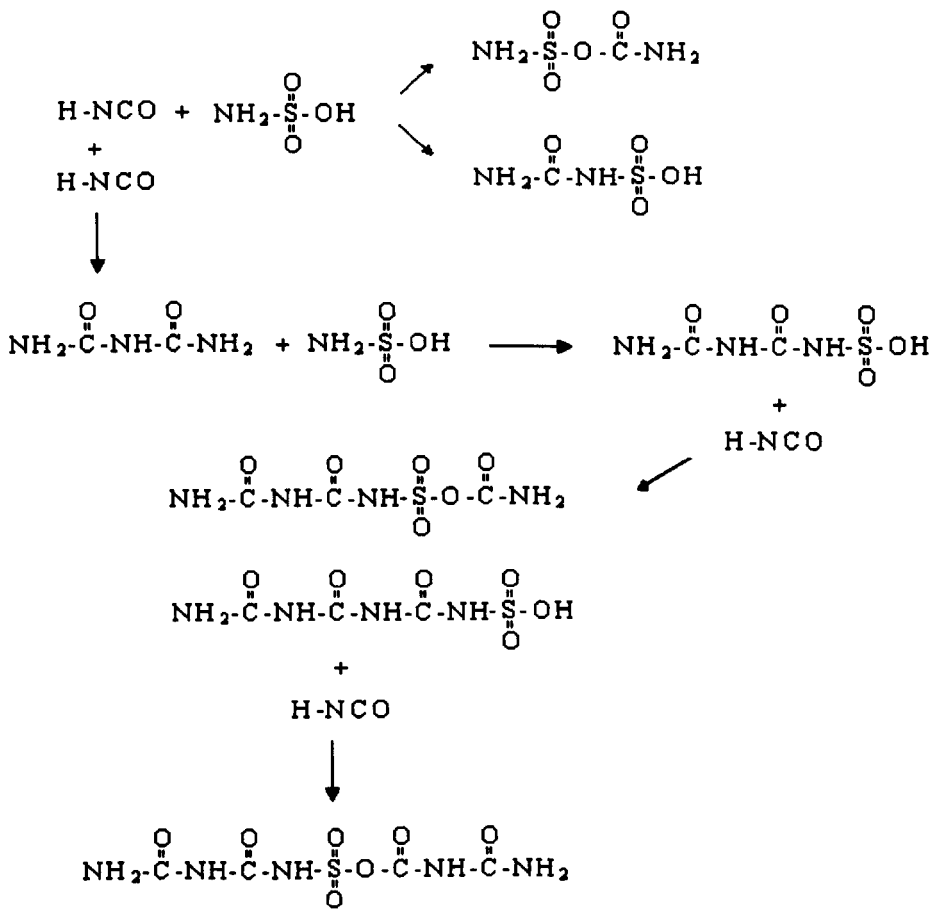

Scheme3.9. Possibility of some products produced in S/U condensate.

3.5.3 Phosphorous acid/ urea condensate

The urea/phosphorous acid condensate was prepared by mixing in various molar ratios; the condensate of one mole phosphorous acid and 3 moles of urea was analysed using FT-IR to determine the structure of the main product. The spectra of urea and phosphorous acid and the products are overlapped in Figure 3.29.

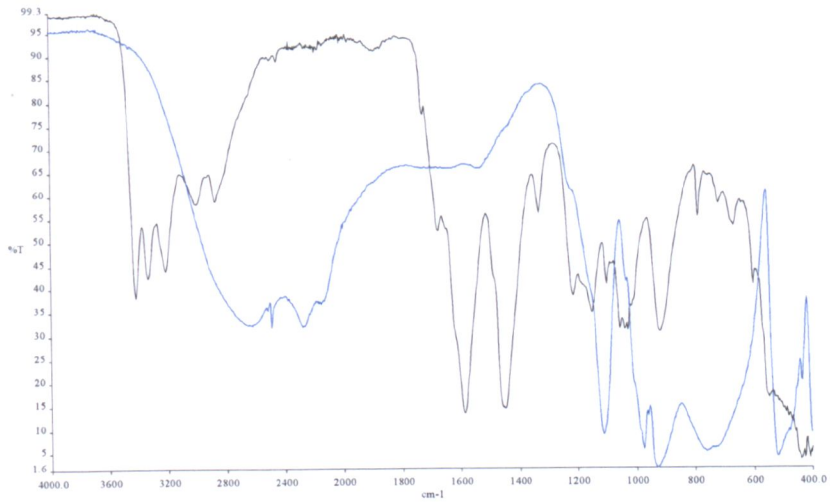

Figure3.29. The FT-IR spectra of phosphorous acid [blue] and 1PH/3U condensate [black].

At first the FT-IR spectrum of urea and phosphorous acid condensate prepared from one mole of phosphorous acid and various molar ratio of urea are compared, Figure 3.30.

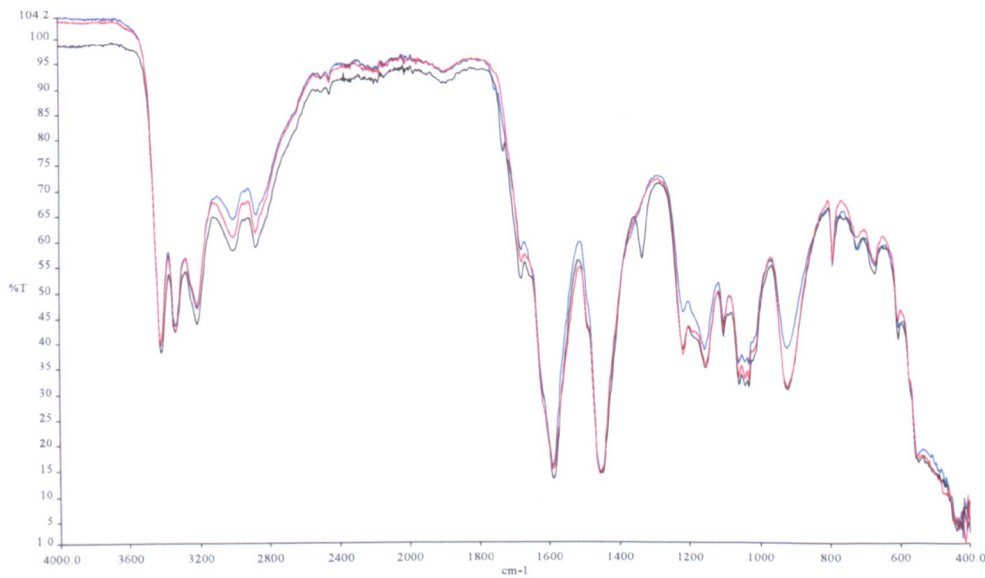

Figure3.30. The spectra of urea condensates from phosphorous acid and urea at various molar ratios [phosphorous acid: urea], red 1:5, blue 1:4 and black 1:3.

The differences attributed to the asymmetric (1360-1300 cm^{-1} region) and symmetric (1190-1140 cm^{-1}) stretching vibration of N-C-N in ureas can be identified in the products. The medium intensity peak at 1329 cm^{-1} appears in the FT-IR spectrum of the urea/phosphorous acid condensate, prepared from one mole of phosphorous acid and 3 moles of urea. There is no further considerable difference between the products, therefore it seems that, they will all be expected to have the same performance when they are applied to the cotton fabric, and subjected to the flame retardancy test.

The FT-IR spectrum of urea / phosphorous acid condensate [one mole phosphorous acid: three moles of urea] has been analysed in detail, Figure 3.31.

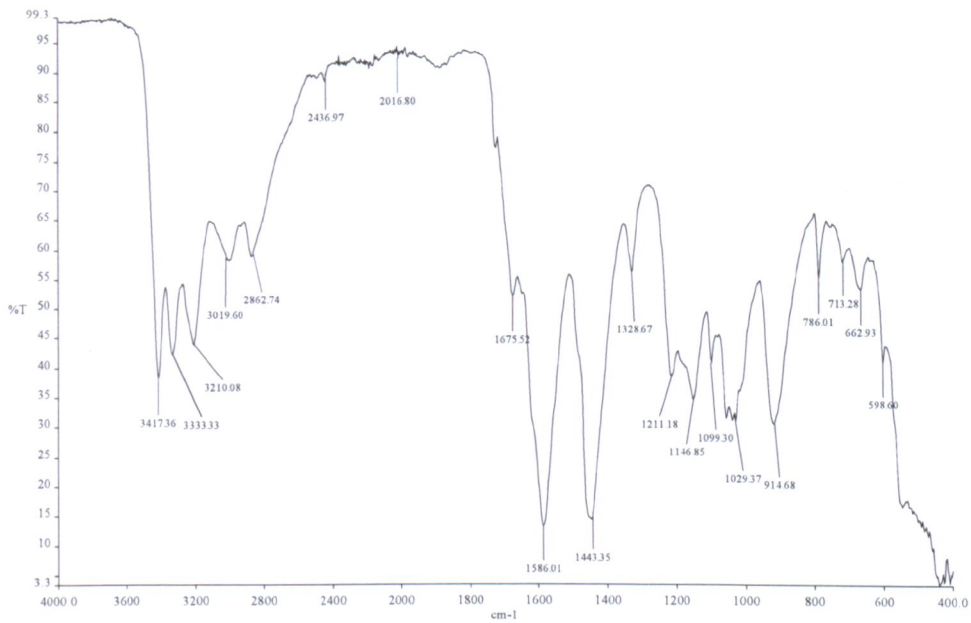

Figure3.31. The FTIR spectrum of phosphorous acid and urea condensate 1PH/3U.

The P– NH_2 bands appear at three different frequency regions relating to stretch and deformation, respectively. The band at 3425- 3012 cm^{-1} region is assigned to NH_2 stretch and 1575 – 1538 cm^{-1} to the NH_2 bend and also at 976 – 922 cm^{-1} to the P- N stretch [4], [5].

The FT-IR spectrum of the product shows three strong bands at 3417, 3333 cm^{-1} and 3210 cm^{-1} which are attributed to the NH_2 stretching of P-NH_2 group. The band at 1586 cm^{-1} is very strong compared to that of urea; a small shoulder can also be due to the NH_2 bending and also a strong band at 915 cm^{-1} can be related to the P-N stretch.

A salt of phosphorus acid containing the $(PO_3)^{2-}$ group absorbs strongly in the IR at 1242 – 970 cm^{-1} due to out of phase stretch (two components), and a medium/strong 1021-893 cm^{-1} in phase stretch [4], [5]. In Figure 3.30, the strong bands at 1099, 1029 cm^{-1} and also the band at 915 cm^{-1} are characteristic of phosphorous acid.

Salts of acids containing the PO^{2-} group have two strong IR bands in the regions 1323 – 1092 cm^{-1} (out of phase stretch) and 1164 – 995 cm^{-1} (in phase stretch) [4], [5]. In the PH/U urea condensate, a strong band appears at 1147 cm^{-1} and 1211 cm^{-1} which can be attributed to this PO^{2-} group.

In Table 3.9 the characterization absorptions of phosphorous compounds are indicated.

Table3.9. FT-IR spectral information regarding the possible functional groups appeared in phosphorous acid/urea condensate.

*Functional Groups	Region cm^{-1}	**Specific Peak cm^{-1}	Intensity	Comments
P-N Vibration	1110-930	915	m-s	Probably asym P-N-C str
	750-680	713	m-s	Sym P-N-C str
P-NH	3200-2900	3020-3210	m	NH str
	1145-1075	1099	w-m	C-N str
	1110-930	-	m-s	P-N-C asym str
P-O-C vibration	1050-970	1029		P-O-C asym str vib
P-H Vibration	2500-2225	2437	m	P-H str
	1150-965	1029-1099	w-m	P-H def vib
P-OH Vibrations	2700-2560	-	w-m	O-H str
	2300-2100	-	w-m	O-H str
	1040-910	1029	m-s	P-O str vib
P=O vibration:				
P=O un-associated	1350-1175	1147	vs	P=O str
P=O associated	1250-1150	1211	vs	P=O str
(RO)(OH)HP=O	1215-1200	1211	vs	P=O str
R(OH)HP=O	1175-1135	1147	vs	P=O str
RPO_3^{2-}	1125-970	1029	s	Asym PO_3^{2-} str
	1000-960	1099	m	Sym PO_3^{2-} str

* These functional groups and their specific identified frequency regions are indicated in reference [2].

** These specific peaks are determined from the main FT-IR spectrum of 1PH/3U condensate.

The P-OH stretching vibration has disappeared in the urea phosphorous acid condensate product which indicates that the main reaction takes place following the evaporation of water from the open reaction vessel.

The other bands relevant to the urea structure can be explained briefly in Table 3.10.

The amount of urea in the product can predict the presence of specific functional groups relevant to the urea compound, which are easily identified in the products spectra.

Table3.10. The range and position of the maximum absorption of urea functional groups and the relevant specific bands are observed in the 1PH/3U condensate.

*Functional Groups	Region cm^{-1}	**Specific Peak cm^{-1}	Intensity	Comments
Ureas	1680-1635	1676	s	C=O str, primary ureas, i.e. with NH_2
	3440-3200	3333- 3417	m	group
	1605-1515	1586	s	NH stre
	1360-1300	1329	m	amide II band
	1190-1140	1147	m	asym N-C-N str
				sym N-C-N str
-$NHCONH_2$	3440-3400	3417	m	asym NH_2 str
	3360-3320	3333	m	NH str
	3240-3200	3210	m	sym NH_2 str
	1605-1515	1586	s	NH_2 def vib
	1360-1300	1329	s-m	asym N-C-N str
	1190-1140	1147	m	sym N-C-N str
	620-530	599	v	NH_2 def vib
-NHCONH-	3360-3320	3333	m	NH str
	1585-1515	1586	v	NH def vib
	1360-1300	1329	s-m	asym N-C-N str
	1190-1140	1147	m	sym N-C-N str
Primary amides	1420-1400	1443	m	C-N str, known as amide III band
	~1150	1147	w	NH_2 in plane rocking vib, not always seen
	750-600	663	m	Br, NH2 def vib
	600-550	599	m-s	N-C=O def vib
	500-450	-	m-s	C-C=O def vib

* These functional groups and their specific identified frequency regions are indicated in reference [2].

** These specific peaks are determined from the main FT-IR spectrum of 1PH/3U urea condensate.

The possible reactions involved are shown in Scheme 3.10.

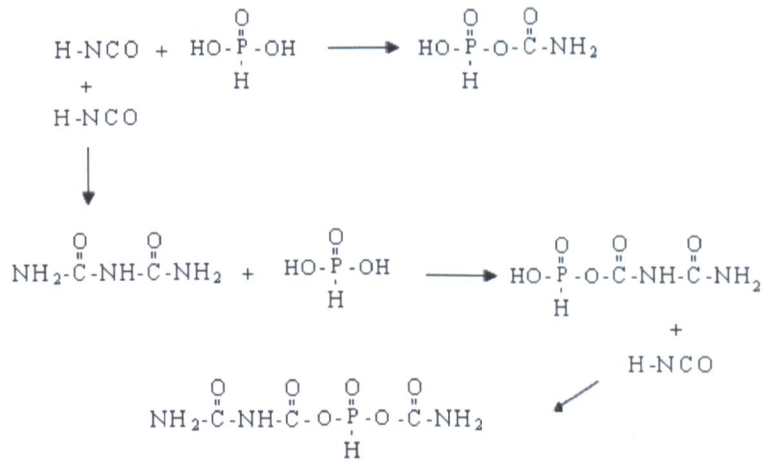

Scheme3.10. Possible products produced in PH/U condensate.

3.5.4 The sulphamic acid / phosphorous acid / urea condensate

As mentioned previously in this chapter, section 3.2.5, various molar ratios of urea were used with one mole of phosphorous acid and 1 mole sulphamic acid mixed condensates. In Figure 3.32 the spectra of all the sulphamic acid/phosphorous acid/urea (S/PH/U) products are shown.

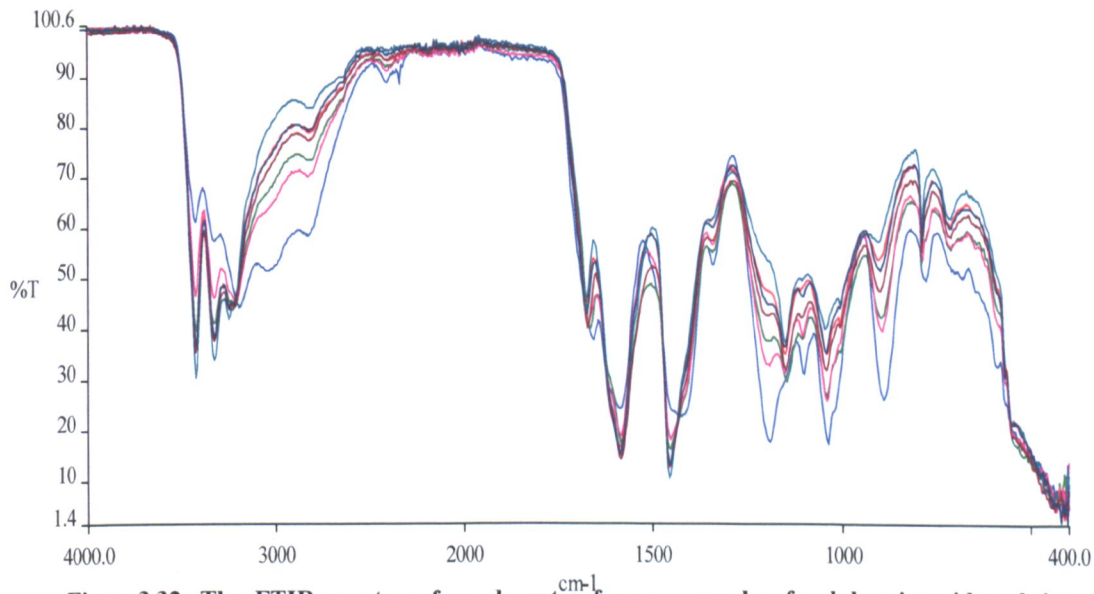

Figure3.32. The FTIR spectra of condensates from one mole of sulphamic acid and 1 mole of phosphorous acid and different molar ratios of urea; 8 moles of urea [blue], 10 moles of urea [red], 12 moles of urea [green], 14 moles of urea [pink], 16 moles of urea [Teal], 18 moles of urea [brown] and 20 moles of urea [navy].

To study the FT-IR spectrum of each product, it is obvious that only those specific frequency regions relevant to the urea functional groups appear differently, these have been highlighted previously. In Figure3.33 the spectrum of four products from the U/S/PH are compared.

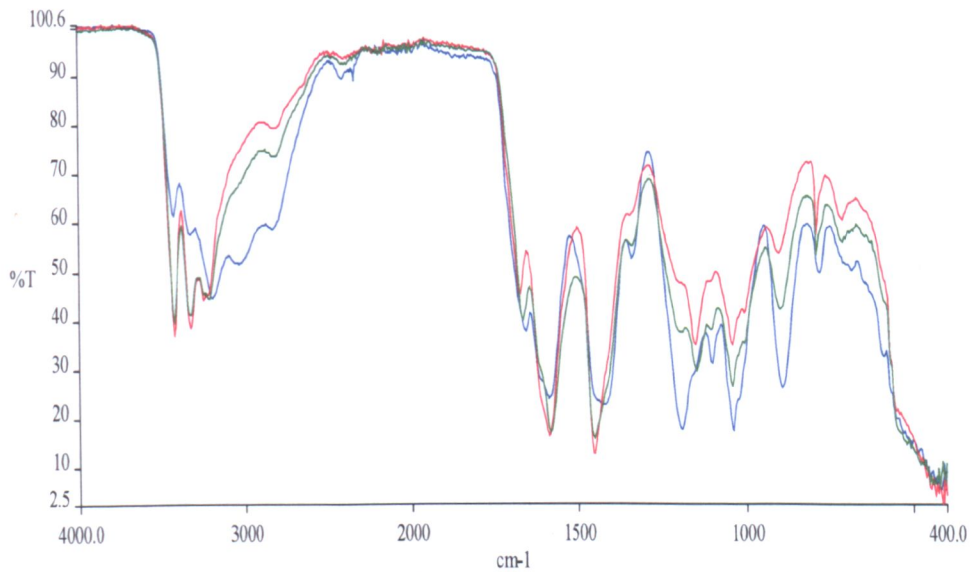

Figure3.33. The FTIR spectra of urea condensates from one mole sulphamic acid/one mole of phosphorous acid and different moles of urea; 8 [blue], 10 [red], 12 [green].

3500-3000 cm^{-1}

The three bands appearing in this region are relevant to the asymmetric and symmetric NH_2 stretching and also NH stretching of urea. These bands show lower intensity for the product containing a lower molar ratio of urea 1 mole sulphamic acid, 1 mole phosphorous acid and 8 moles of urea.

3000-2500 cm^{-1}

P-OH vibration of phosphorous acid has several bands in this region which are reduced in intensity when the amount of urea is increased in the product.

1500-1400 cm^{-1}

In this region, by increasing the amount of urea, the specific band attributed to the C-N stretching vibration, known as amide III band of ureas, changed from a broad peak to a sharp peak.

1300-900 cm^{-1}

The intensity of the bands in this region is reduced because of the high amount of urea in the product. These bands have been explained previously in Tables 3.8 and 3.9; they are due to P=O and S=O stretching vibrations and also P-N-C asymmetric and symmetric vibrations.

900-500 cm^{-1}

In this region a similar effect to that of 1300-900 cm^{-1} is seen, in fact the intensity of all specific bands relevant to the sulphur compound is reduced.

3.5.4.1 FT-IR analysis of urea condensate of 1S/1PH/10U

To analyse the FT-IR spectrum of the product in greater detail, the urea condensation product was prepared from one mole sulphamic acid, 1 mole phosphorous acid and 10 moles urea. The main FT-IR spectrum of 1S/1PH/10U is shown in Figure 3.34.

The overlapping spectra of this product and melted urea at 140°C are compared in Figure 3.35. To study in more detail, the overlapping of the product spectrum with two other urea sulphamic acid condensates (1S/3U), Figure 3.36 and 1PH/3U condensate Figure 3.37 are shown.

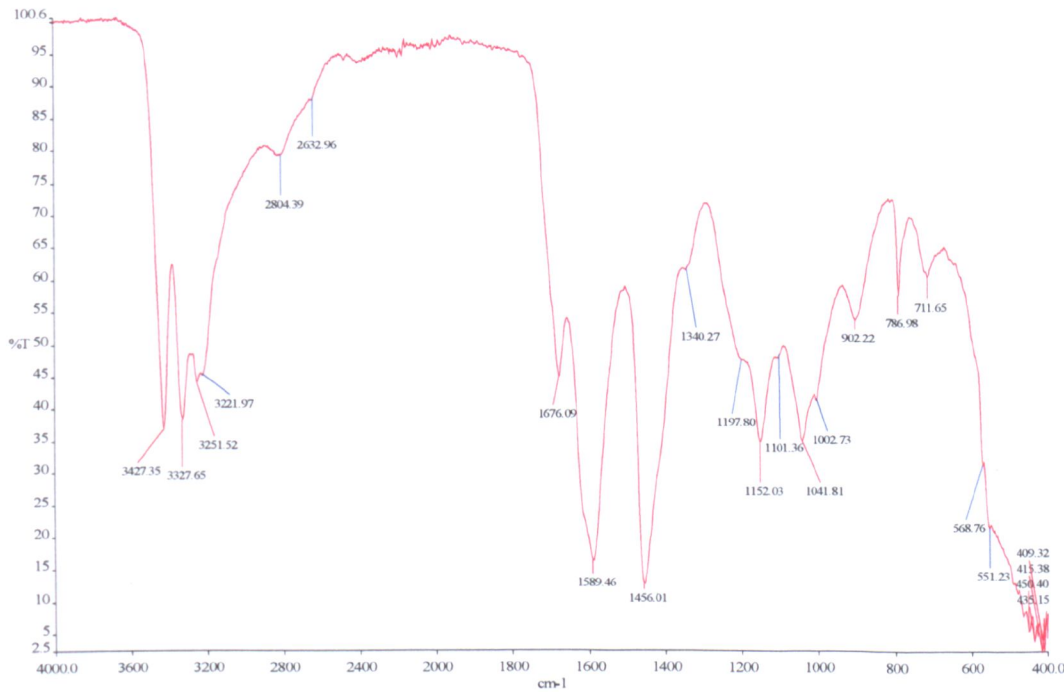

Figure3.34. The FT-IR spectrum of 1S/1PH/10U product.

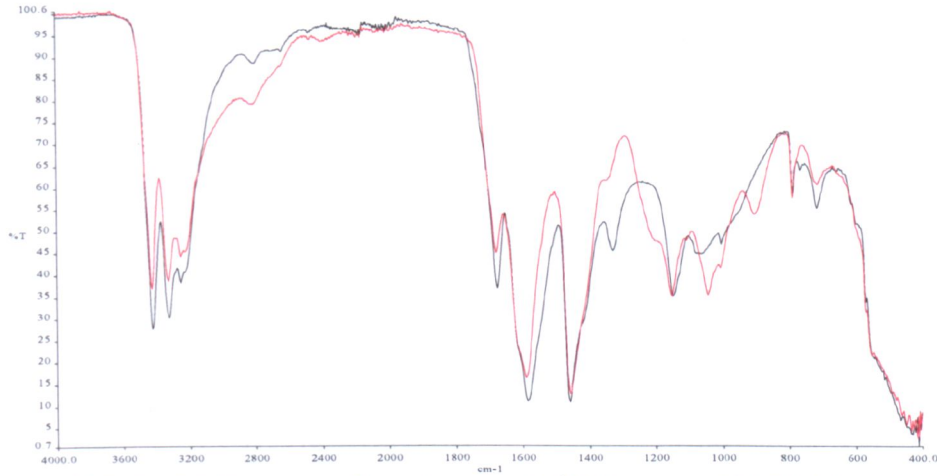

Figure3.35. The FT-IR spectra of heated urea to 140°C [black] and 1S/1PH/10U condensate [red].

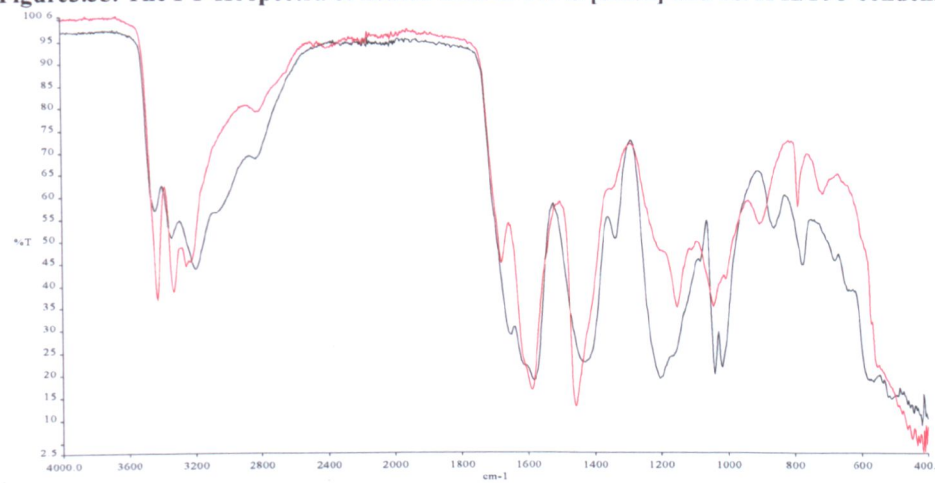

Figure3.36. The FT-IR spectra of the 1S/3U condensate [black] and 1S/1PH/10U condensate [red].

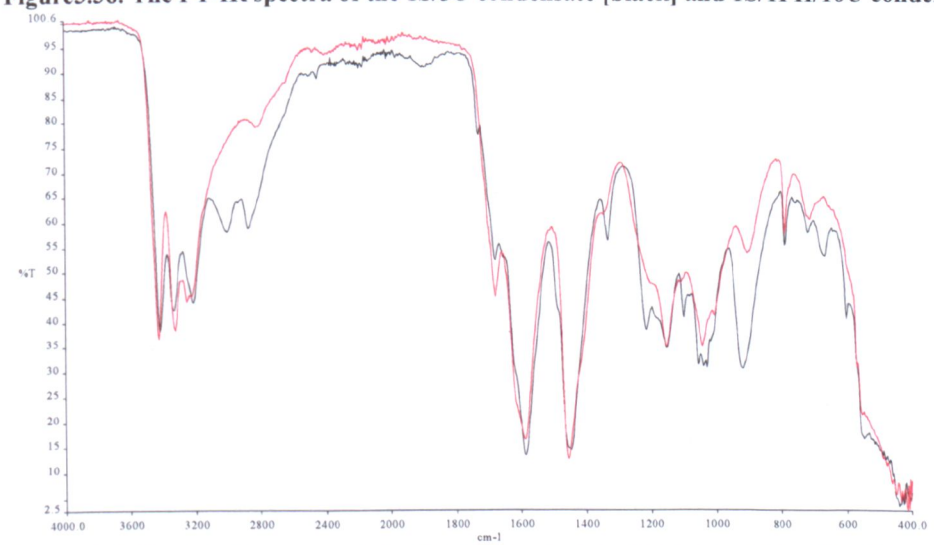

Figure3.37. The FT-IR spectra of the 1PH/3U condensate [black] and 1S/1PH/10U condensate [red].

Table3.11. The analysis of FT-IR spectrum of 1S/1PH/10U condensate

Specific peak cm^{-1}	Relevant functional group	Comment
3427 3328 3252 3222	NH str NH str Asym NH_2 str Sym NH_2 str	These peaks appear in urea and urea compound
1676	C=O str, primary ureas, i.e.with NH_2 group	The same band appears in melted urea and PH/U
1589	Amide II band, NH def vib	The same band appears in melted urea and PH/U
1456 1340	Asym N-C-N str and Asym SO_2 str	The intensity reduced in S/PH/U
1198	P=O str (RO)(OH)HP=O Sym SO_2 str R-SO_2-OR	The intensity in PH/U and S/U condensate reduced
1152	P=O str (R(OH))HP=O Sym N-C-N str	It exactly seen in PH/U and urea melted
1101	P-H def vib Asym PO_3^{-2} str	It appears in S/U with higher intensity
1042 1003	P=O str vib S-O asym str	The intensity of these bands in S/PH/U are lower than in S/U and PH/U
902	P-N vib probably asym –P-N-C str	This band appears in PH/U with higher intensity
787	NH2 def primary amine	It exactly appears in melted urea and PH/U
712	Sym P-N-C st, Br NH_2 def vib	It appears in melted urea and also PH/U
569	N-C=O def vib	It appears in Urea and PH/U spectrum

Interpretation of the main FT-IR spectrum of the 1S/1PH/10U condensate is indicated in Table 3.11, second derivative spectroscopy for some specific regions was used to determine further details of the products.

The second derivatives of S/HP/U product and S/U condensate are compared in Figure 3.38. The intensity of the bands in the region 3600-3000 cm^{-1}, relevant to the primary and secondary amide, NH_2 and NH stretching vibration are changed.

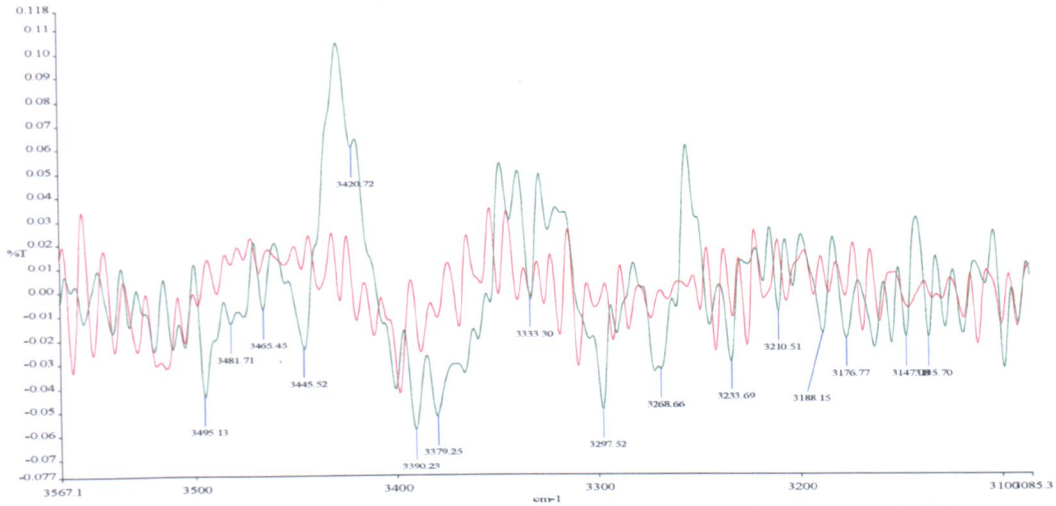

Figure3.38. The 2nd derivative spectra of 1S/1PH/10U condensate [green] and 1S/3U condensate [red].

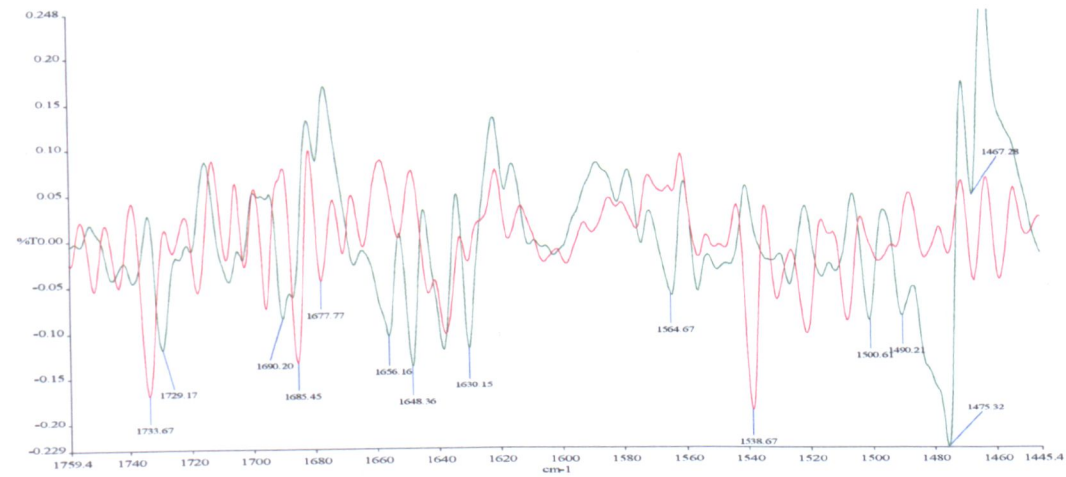

Figure3.39. The 2nd derivative spectra of 1S/1PH/10U condensate [green] and 1S/3U condensate [red].

In the main FT-IR spectrum of urea condensate S/PH/U, Figure 3.34 the combined C=O stretching and NH_2 vibration of the amide groups appears with two sharp bands at 1456 cm^{-1} and 1589 cm^{-1}. Primary amide shows a very strong band due to the C=O stretching vibration at 1690 – 1670 cm^{-1} in the solid phase [2]. Secondary amides absorb strongly at 1680 – 1630 cm^{-1} and also have a band in the region 1790 – 1720 cm^{-1} [2], which appears in both compounds due to the presence of urea. In Figure 3.39 the second derivatives in the region 1760-1440 cm^{-1}, present various bands for both urea condensates relevant to this functional group.

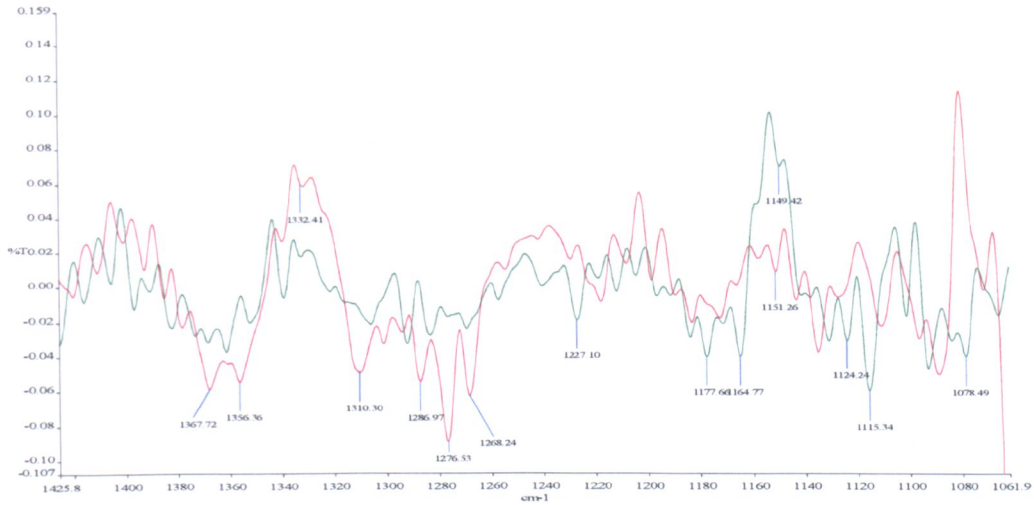

Figure3.40. The 2nd derivative spectra of 1S/1PH/10U condensate [green] and 1S/3U condensate [red].

In the Figure 3.40 the specific region from 1426 cm^{-1} to 1061 cm^{-1} with information regarding the sulphur and phosphorus compounds has been clarified previously. The intensity reduction of specific bands relevant to the sulphonamides can be identified in the second derivative spectrum at 1310 cm^{-1}, 1356 cm^{-1} and 1368 cm^{-1}, while several new peaks due to P=O stretching appear at 1227, 1178 $cm^{-1}$and 1165 cm^{-1} frequency. The new bands at 1149 cm^{-1}, due to the P=O stretching vibration of R (OH) HP=O were identified in the main FT-IR spectrum at 1152 cm^{-1}. The other bands at 1124, 1115 cm^{-1} and 1078 cm^{-1} are attributed to the P-NH, NH, CN and also P-N-C stretching vibrations which appear in the second derivative spectra of U/S/PH. In the main spectrum, Figure 3.34, the peak at 1101 cm^{-1} is due to these functional groups respectively.

In Figure 3.41 the intensity values of two bands at 1058 cm^{-1} and 1028 cm^{-1}, relevant to the alkyl sulphonic acids, RSO_2OH, are reduced in the new product of the S/PH/U urea condensate.

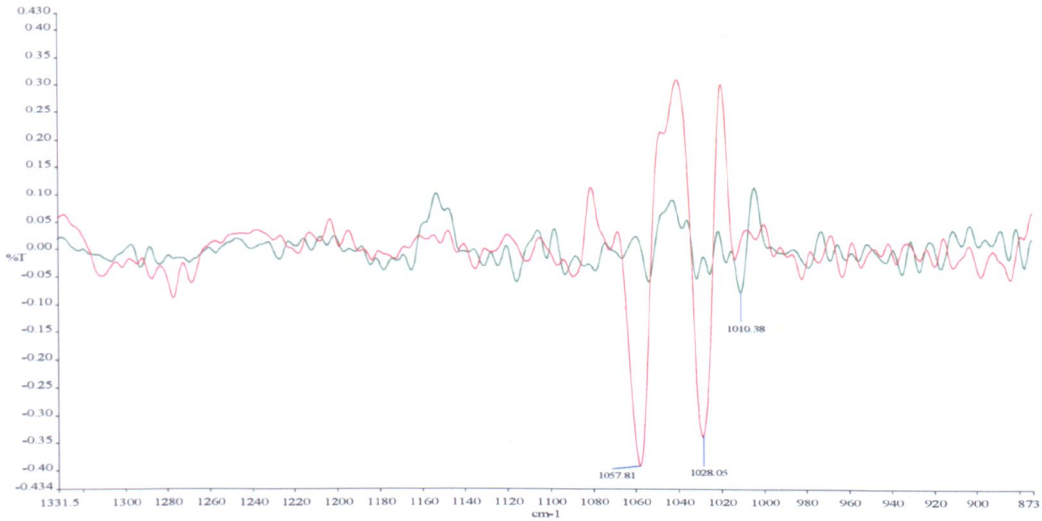

Figure3.41. The 2nd derivative spectra of 1S/1PH/10U condensate [green] and 1S/3U condensate [red].

Table 3.12 highlights some relevant functional groups with specific details.

Table3.12. Functional groups in FTIR spectrum of the S/PH/U condensate.

Functional groups	Regions cm^{-1}	Intensity	Comment
Sulphonamides	1360 – 1315	s	Asymmetric stretching vibration of the SO_2 group
(RO)(HO)HP=O	1215 – 1200	vs	P=O stretching
P-H	1150 – 965	w-m	P – H deformation vibration
P – O – C	1050 – 970	s	Asymmetric stretching vibration of the P – O - C
			SO_2 symmetrical stretching
Covalent sulphonate	830 – 690	m	S – C stretching
R – SO_2 - OR	700 – 600	w	SO_2deformation vibration
	610 – 500	m – w	

The overlap of two second derivative spectra, for various frequency regions, from the new product S/PH/U and the PH/U condensate will be discussed in this section. In the main FT-IR spectrum of phosphorous acid/urea condensate (Figure 3.31), the presence of two medium bands at 3020 cm^{-1} and 2863 cm^{-1} needs to be studied in further detail; therefore the second derivative spectrum was used to highlight specific peaks in this particular region. In Figure 3.42 the two peaks at 2899 cm^{-1} and 2909 cm^{-1} in PH/U condensate relevant to the P-NH stretching vibration have now disappeared; however another band in this region, at 2829 cm^{-1}, is seen in the product with a different intensity. In fact a band of medium to strong intensity, due to stretching vibration of the C-H bond

of the N-C-H group, occurs near 2820 cm^{-1} for amine absorption [2]. This has been identified in both products in the second derivative spectrum and also with different intensity in the main FT-IR spectrum.

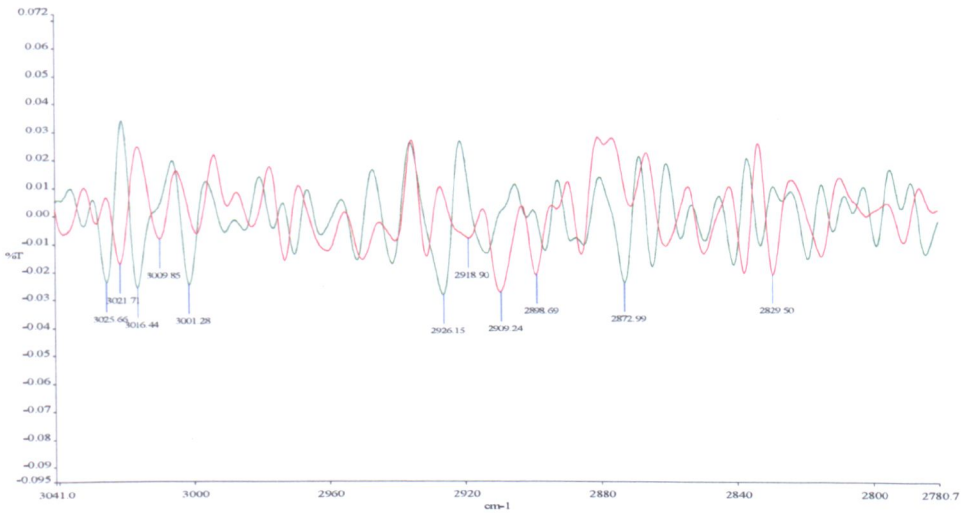

Figure3.42. The 2nd derivative spectra of 1S/1PH/10U condensate [green] and 1PH/3U condensate [red].

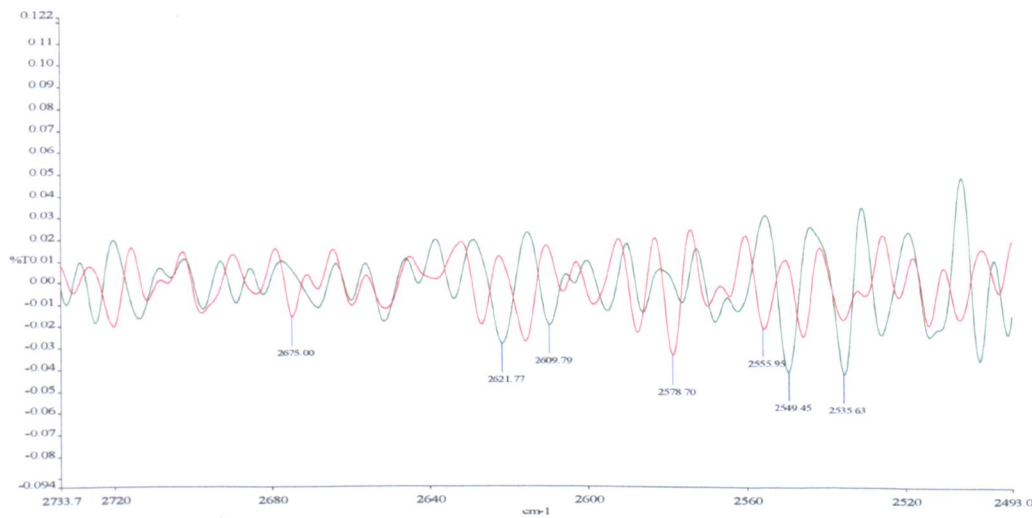

Figure3.43. The 2nd derivative spectra of 1S/1PH/10U condensate [green] and 1PH/3U condensate [red].

Bands of weak to medium intensity, due to the stretching vibration of the O-H bond in the phosphorus compounds occurs at 2700-2560 cm^{-1} and 2300-2100 cm^{-1} [2]; these are clearer in the second derivative spectrum, Figure3.43. In this region, the intensity values of a few bands are reduced, for example the band at 2579 cm^{-1}, some bands have disappeared, namely the bands at 2556 cm^{-1} and 2675 cm^{-1}.

However new bands at 2536 and 2549 cm^{-1} in the S/PH/U product can provide further confirmation of the presence of the P-H bonds in the new product. In fact the stretching vibration of the P-H group gives rise to a sharp band of medium intensity in the region 2500- 2225 cm^{-1}. For the aliphatic and aryl phosphines, this band occurs in a much narrower region: 2285-2265 cm^{-1} [2]. In Figure 3.44, at the region, 2204-2411 cm^{-1} the intensity of a sharp band at 2362 cm^{-1} is reduced in the new product, also the bands at 2339 cm^{-1} and 2329 cm^{-1} in the urea phosphorous acid condensate appear with the same effect. In the specific region for the aliphatic phosphine, the bands at 2278 cm^{-1} and 2268 cm^{-1} in PH/U condensate FT-IR spectrum presenting P-H stretching of the phosphorous compound, these two bands are observed in the new product but with some peak shift.

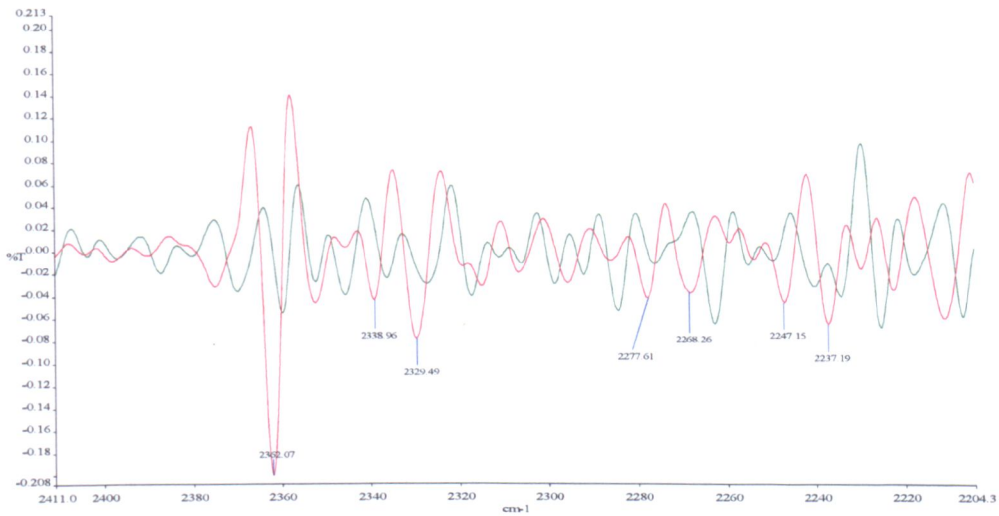

Figure3.44. The 2nd derivative spectra of 1S/1PH/10U condensate [green] and 1PH/3U condensate [red].

In Figure 3.45, the region at 1453-1103 cm^{-1} shows all the specific bands relevant to the phosphorus and sulphur compounds. In fact by overlapping these two spectra, it is simple to identify each particular band relevant to the phosphorus compound.

In phosphorus compounds, the P=O stretching vibration occurs in the frequency range from 1234 to 1404 cm^{-1}. Many of the phosphate esters exhibit a doublet band due to the existence of rotational conformers, and the frequency separation for these two bands varies between 7 and 29 cm^{-1} [5]. In Figure 3.45, the specific bands at 1197 cm^{-1} and 1241 cm^{-1} are attributed to the P=O stretching vibration, which are found in the S/PH/U

product although with lower intensity absorption. The two other bands at this region, 1344 cm^{-1} and 1391 cm^{-1} also indicate the P=O stretching vibration. In the new product the intensity of all these bands are reduced.

For aliphatic phosphorus compounds, the asymmetric stretching vibration of the P-O-C group gives a very strong broad band, normally found in the region 1050-970 cm^{-1} [2]; in the second derivative spectrum of the urea/phosphorous condensate the two strong bands at 1021 cm^{-1} and 1032 cm^{-1} are attributed to this stretching vibration. However, at this region, 1040-910 cm^{-1}, a medium to strong band due to the P-O stretching vibration are also expected [2]. In Table 3.9 the P-N vibration of the P-N-C asymmetric stretching has been identified at 1110-930 cm^{-1} frequency region [2], thus the presence of a few sharp and strong bands at this region is acceptable. Therefore it is possible to identify the other bands at 1048 cm^{-1} and 1067 cm^{-1} as P-N-C stretching vibrations. The RPO_3^{2-} functional group also has a band relevant to the asymmetric PO_3^{2-} stretching at 1125-970 cm^{-1} frequency regions [2] which have been identified in the main PH/U spectrum previously at 1029 cm^{-1}.

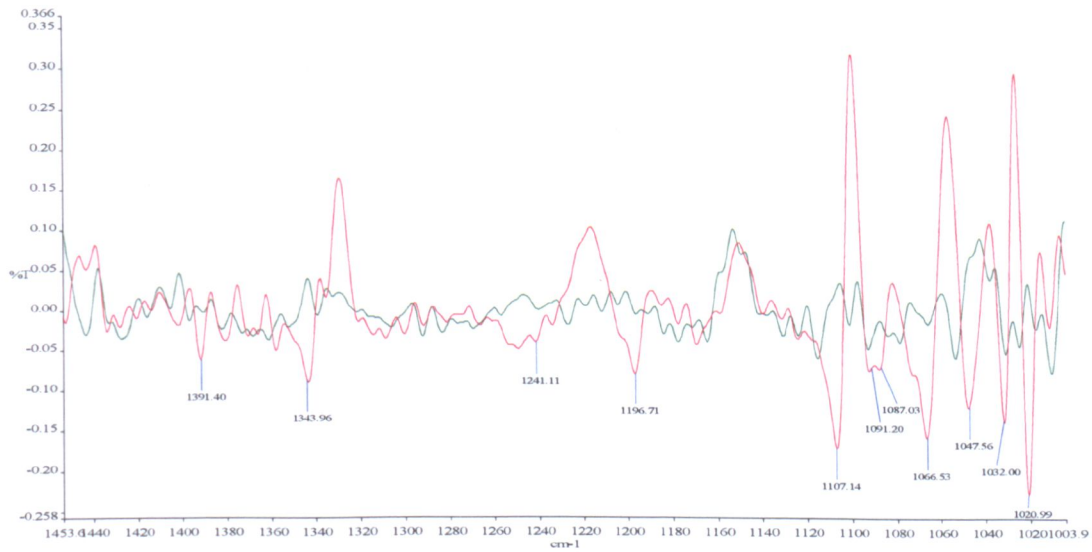

Figure3.45. The 2nd derivative spectra of 1S/1PH/10U condensate [green] and 1PH/3U condensate [red].

In the second derivative of the S/PH/U condensate, Figure 3.45 a shoulder appears on the peak at 1067 which can be identified as the PO_3^{2-} functional group however some other bands also appear at this region, a doublet band at 1087 cm^{-1} and 1091 cm^{-1} and also a strong band at 1107 cm^{-1} which can also verify the presence of this group

respectively. It is obvious that the intensity of all these bands is reduced in the S/PH/U condensate product.

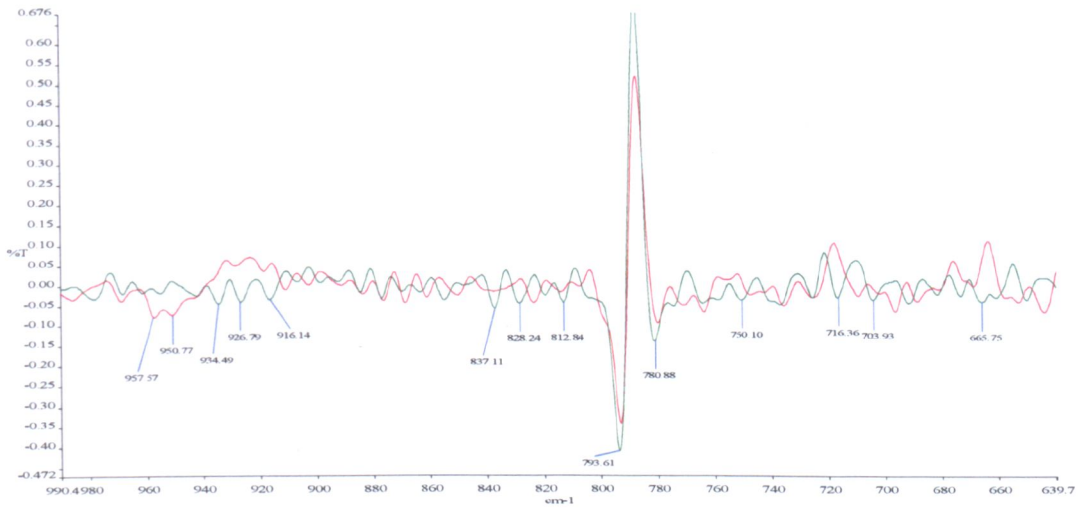

Figure3.46. The 2nd derivative spectra of 1S/1PH/10U condensate [green] and 1PH/3U condensate [red].

According to the reference [2], the P-O-H vibration of phosphorus acid has a medium to weak intensity peak at 1040-910 cm^{-1} region which was identified in the main spectrum of urea/phosphorous acid condensate at 915 cm^{-1}, but in the main FT-IR spectrum of the S/PH/U condensate the intensity of this band is reduced. In the second derivative of these two spectra overlapped in this frequency region, Figure 3.46, the bands at 951 cm^{-1} and 958 cm^{-1} in the PH/U condensate and also the bands at 934 cm^{-1}, 927 cm^{-1} and 916 cm^{-1} represent the P-O stretching vibration of the phosphorus condensate product.

Some of the possible products produced from the reaction of one mole sulphamic acid, 1 mole phosphorous acid and 10 moles of urea, are indicated in Scheme 3.11.

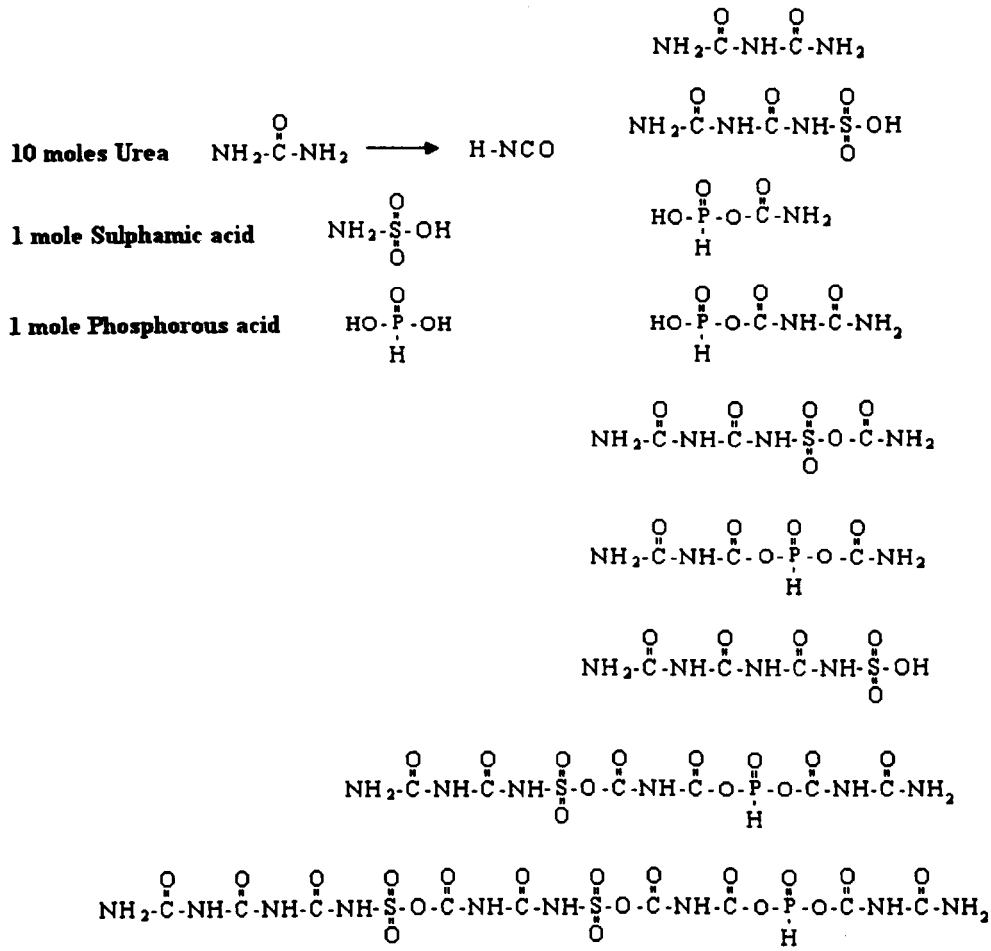

Scheme3.11. The possible products predicted in the reaction of one mole sulphamic acid, 1 mole phosphorous acid and 10 moles of urea condensate.

3.5.4.2. The urea condensate of 1S/2PH/10U

To study this new product, it is beneficial to analyse the spectra of 1S/1PH/10U and 1S/2PH/10U together. The overlap of the two spectra is shown in Figure 3.47. By comparing the specific bands at various frequencies, no remarkable difference is indicated, only a few bands show that a possible reaction occurs in the new product 1S/2PH/10U. In fact by increasing the amount of phosphorous acid in the condensate, the intensities of bands in specific regions are increased; in this way it is possible to identify all the relevant phosphorus compound bands.

Table 3.13 details the analysis of the FT-IR spectrum of 1S/2HP/10 U.

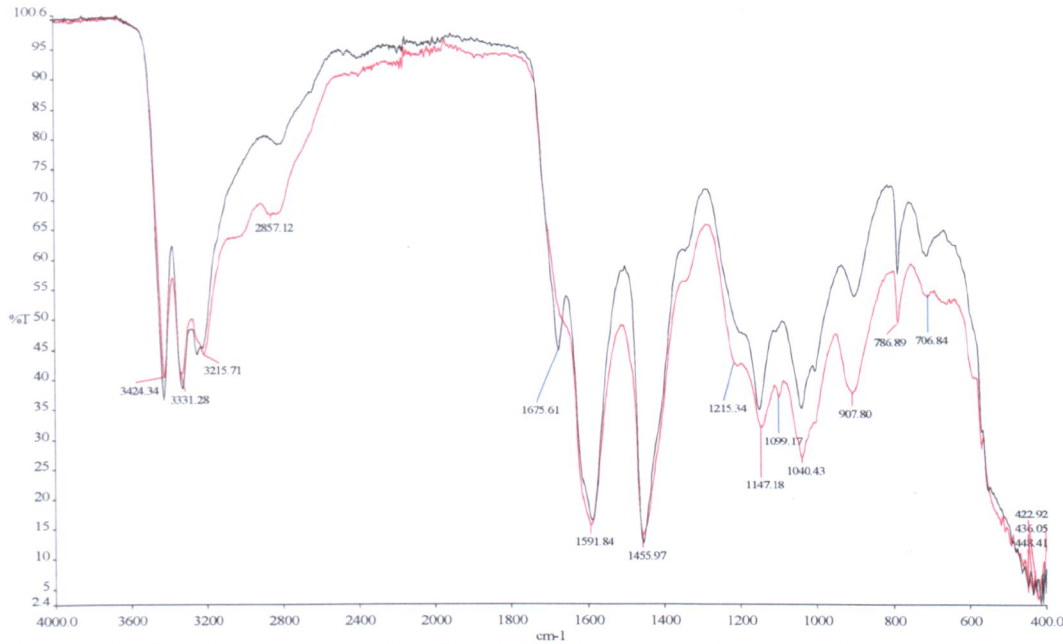

Figure3.47. The FT-IR spectrum of 1S/1PH/10U condensate [red] and 1S/2PH/10U condensate [black].

The information derived from the main FT-IR spectrum in Table 3.13 shows no particular difference between 1S/2PH/10U and 1S/1PH/10U condensates, therefore second derivative spectroscopy was required.

Table3.13. FT-IR spectrum of 1S/2PH/10U condensate.

Functional group	Specific bands cm^{-1}	Comments
Urea functional groups	3424	NH str
	3331	NH str
	3216	sym NH_2 str
	1676	C=O str, primary ureas, i.e.with NH_2 group
	1592	Amide II band, NH def vib
	1456	Secondary amide N-H bending vib
	787	NH_2 def primary amine
Phosphorus and sulphure compound groups	2857	P-N str vib
	1215	P=O str (RO)(OH)HP=O Sym SO_2 str R-SO_2-OR
	1147	P=O str (R(OH))HP=O Sym N-C-N str, SO_4 str
	1099	P-H def vib
	1040	Asym PO_3^{-2} str
	908	P-N vib probably asym-P-N-C str
	707	sym P-N-C st, br NH_2 def vib

In Figure 3.48 three specific bands relevant to the P-N stretching vibration are seen in the 1S/2PH/10U condensate at 2759, 2852 cm^{-1} and 2906 cm^{-1}.

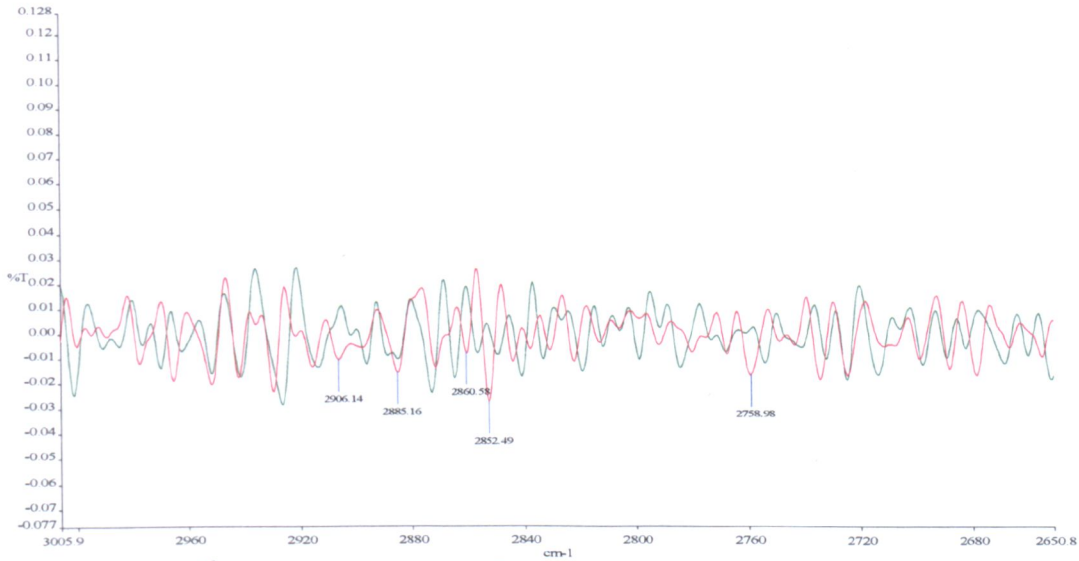

Figure3.48. The 2nd derivative spectra of 1S/1PH/10U [green] and 1S/2PH/10U condensate [red].

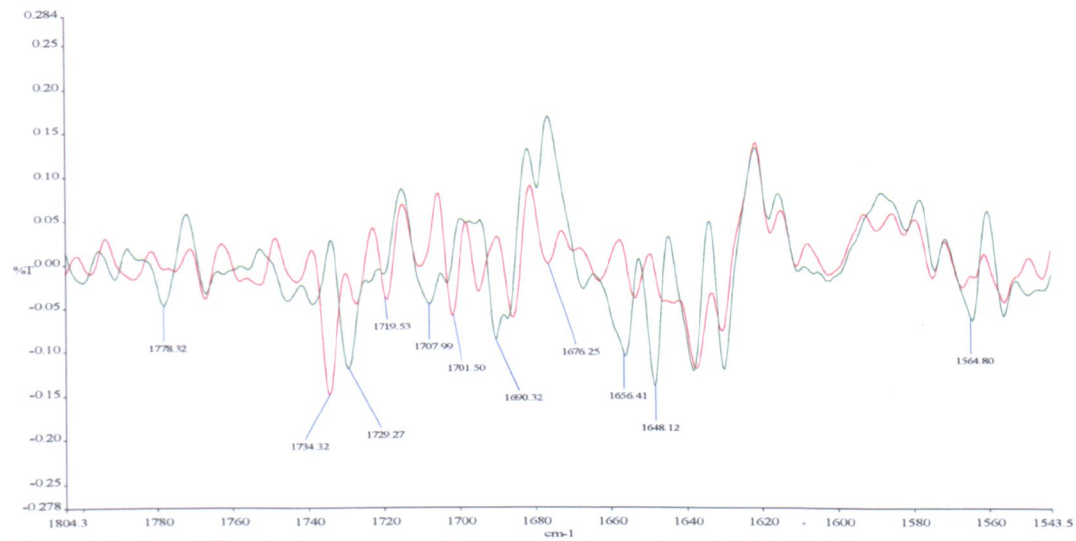

Figure3.49. The 2nd derivative spectra of 1S/1PH/10U [green] and 1S/2PH/10U condensate [red].

In Figure 3.49 the new product, 1S/2PH/10U condensate, the intensity values of two bands at 1648 cm^{-1} and 1656 cm^{-1} are reduced; these are attributed to C=O stretching vibration in the primary urea. In fact by increasing the amount of the phosphorous acid in the product, the effect of the primary amide functional group in the product is

reduced. The other bands at 1729 cm^{-1} and 1734 cm^{-1} in both compounds are similar with only 5 frequencies different representing the OH deformation vibration of the phosphorus acid compound.

In this new urea condensate product 1S/2PH/10U new functional groups are expected. The phosphonic anhydrides, have a medium to weak band at 1270-1250 cm^{-1} frequency region due to the P=O stretching vibration and also another band with similar intensity at 930-915 cm^{-1} relevant to the asymmetric P-O-P stretching vibration [2]. In Figure 3.50 in the second derivative spectrum of the product the new band at 1266 cm^{-1} can be attributed to P=O stretching of this functional group. A few new bands also appear at this region 1199, 1105, 1088 cm^{-1} and 1072 cm^{-1} which all of them can be interpreted as asymmetric stretching vibration of PO_3^{2-} group in the new product.

In Figure 3.51 the bands at 903 cm^{-1} and 912 cm^{-1} are attributed to the asymmetric stretching vibration of the P-O-P of a new anhydride phosphonic functional group which may be produced during the urea condensate reaction.

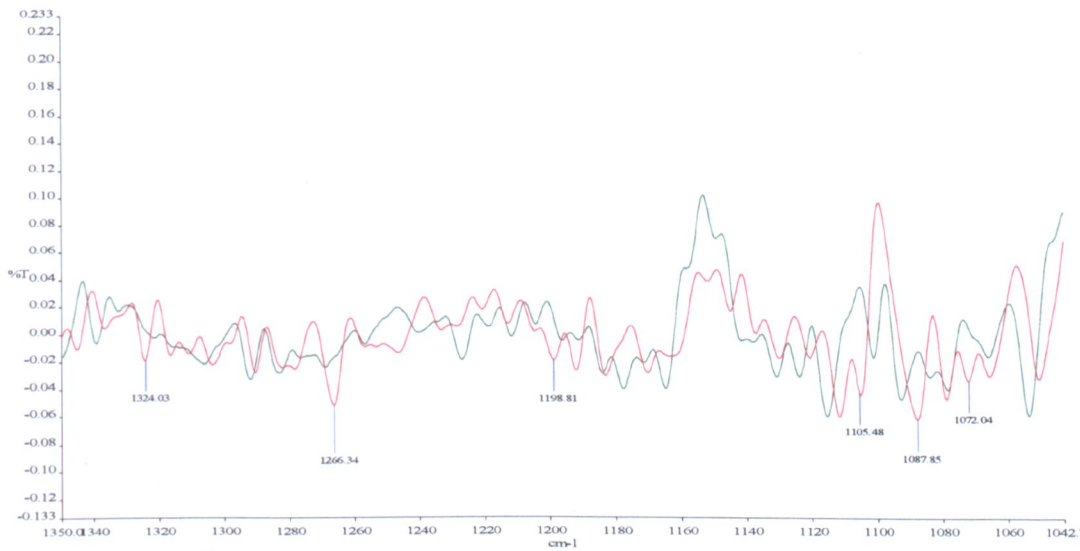

Figure3.50. The 2nd derivative spectra of 1S/1PH/10U [green] and 1S/2PH/10U [red].

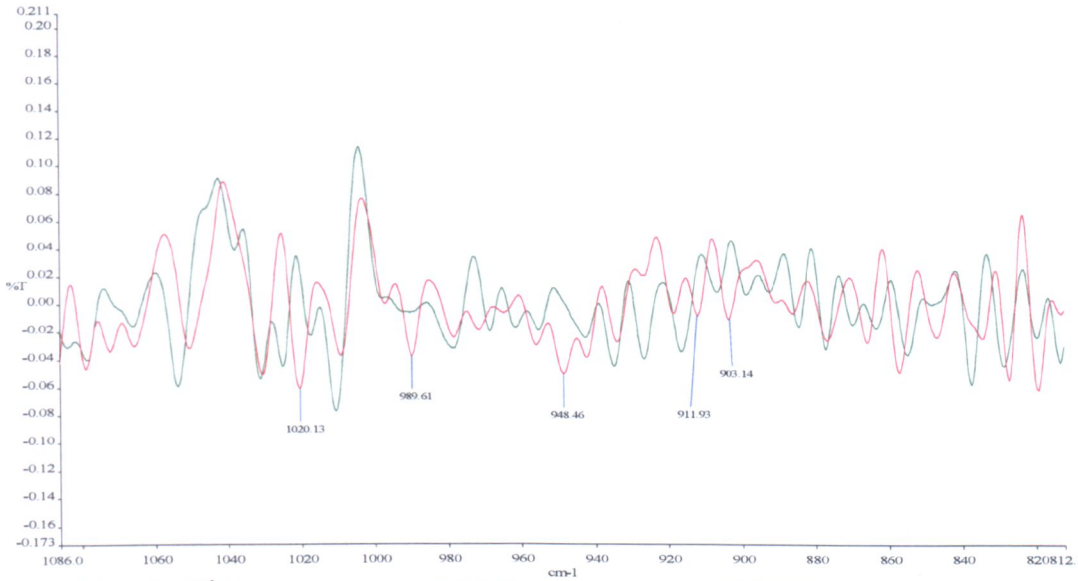

Figure3.51. The 2nd derivative spectra of 1S/1PH/10U [green] and 1S/2PH/10U [red].

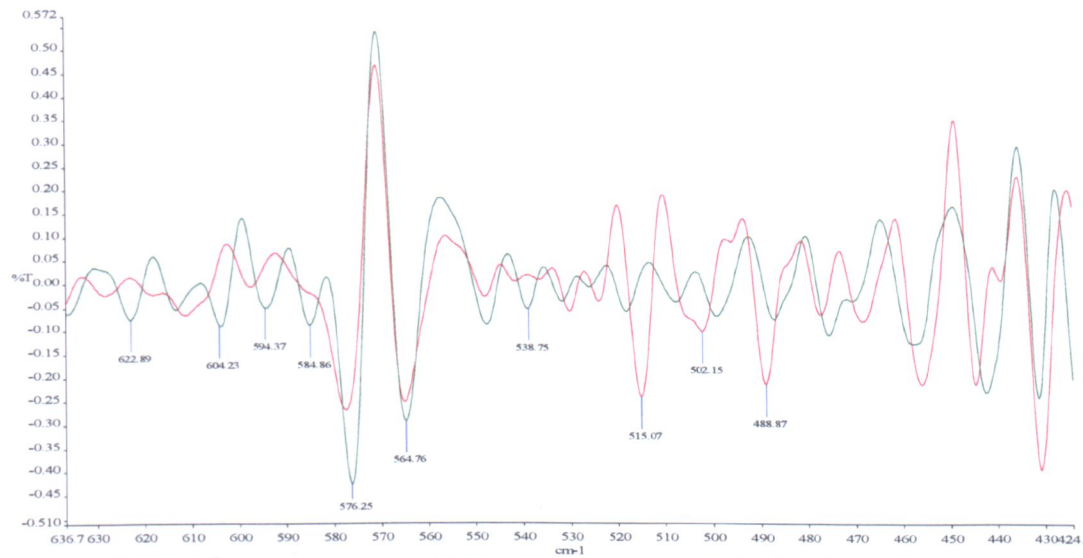

Figure3.52. The 2nd derivative spectra of 1S/1PH/10U [green] and 1S/2PH/10U [red].

The possible functional groups in the new product 1S/2PH/10U are indicated in Table 3.14, all the specific peaks are determined from the second derivative spectra.

Table3.14. Predicted functional groups in the FT-IR spectrum of 1S/2PH/10U condensate.

Functional Groups	Region cm^{-1}	Specific Peak cm^{-1}	Intensity	Comments
P-O-S	930-815	908		Asym P-O-S str
Sulphate ion, SO_4^{2-}	1200-1140 1130-1080 1065-955 680-580 530-405	1199 1088 990 - 502- 515	m vs w m - 	 Br, with shoulder, SO_4 str Sh, not always present Several bands
Phosphonic anhydrides R(RO)P-O-P(RO)R O O	1270-1250 930-915	1266 912	vs s	P=O str Br, asym P-O-P
P-O-P	1025-870	1020	s	Usually broad, asym str often found in region 945-925cm^{-1} (a weak band also near 700cm^{-1})

Some of the possible products produced in 1S/2PH/10U condensate are indicated in Scheme 3.12.

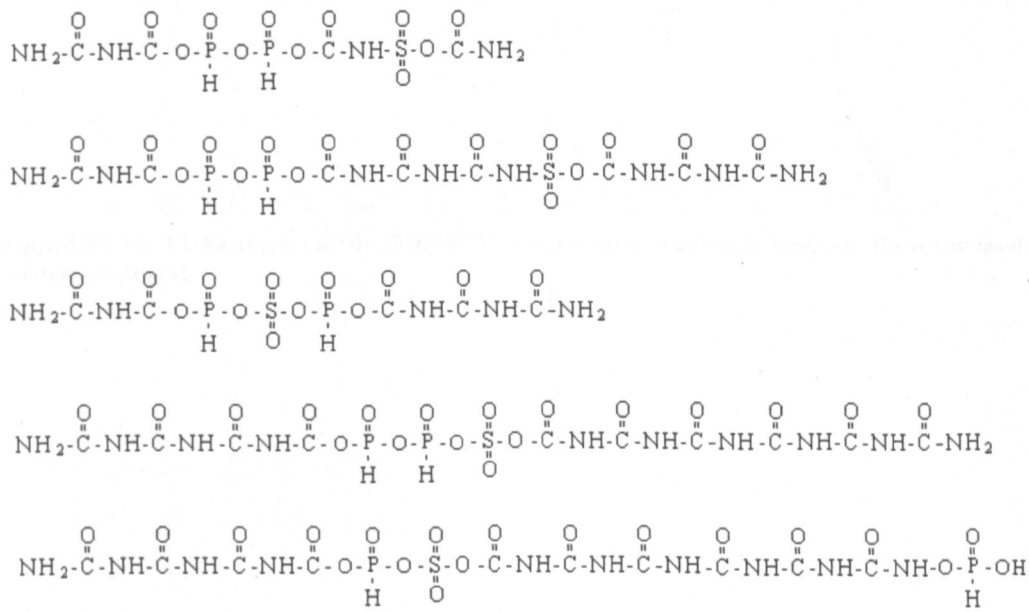

Scheme3.12. The possible products predicted in the reaction of one mole sulphamic acid, 2 moles phosphorous acid and 10 moles of urea condensate.

3.5.4.3 The water-insoluble product from the 1S/1PH/10U condensate

In preparation of the 1S/1PH/10U urea condensate, when the reaction temperature is raised from 140°C to 160°C, a new product will be produced; the water-soluble urea condensate changes to a water-insoluble product. To study the chemical reaction involved during this process, FT-IR and Raman analysis were carried out on the two products. In Figure 3.53 compares the two FT-IR spectra and Figure 3.54 compares the two Raman spectra.

It can be seen that the main bands relevant to the functional groups of the water-soluble urea compound produced at 140°C are quite different when the condensation temperature is raised to 160°C; the urea linkage in the aliphatic polyamide compound is modified and the specific bands due to the sulphur and phosphorus groups, in the frequency region 1000-1200 cm^{-1}, are still present.

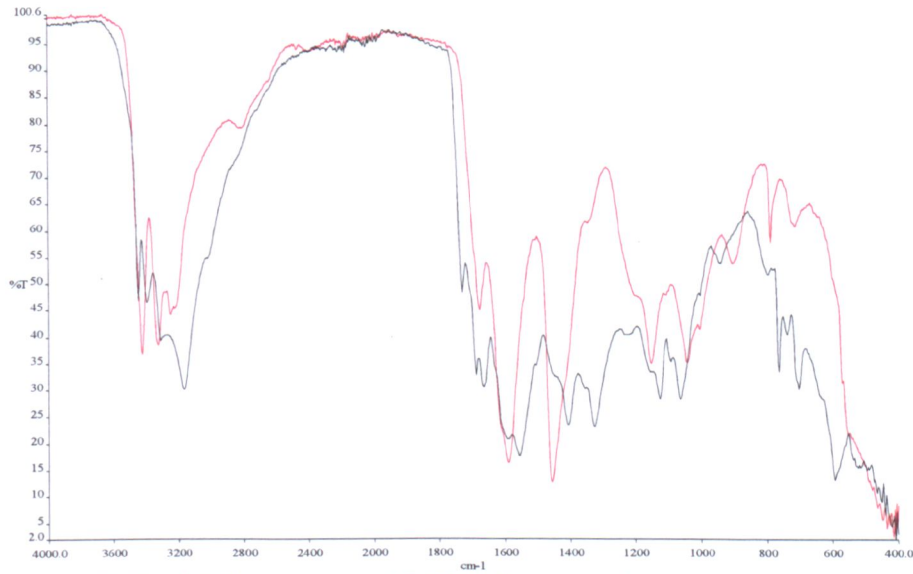

Figure3.53. The FT-IR spectra of the 1S/1PH/10U water-soluble condensate [red] and the water-insoluble condensate [black].

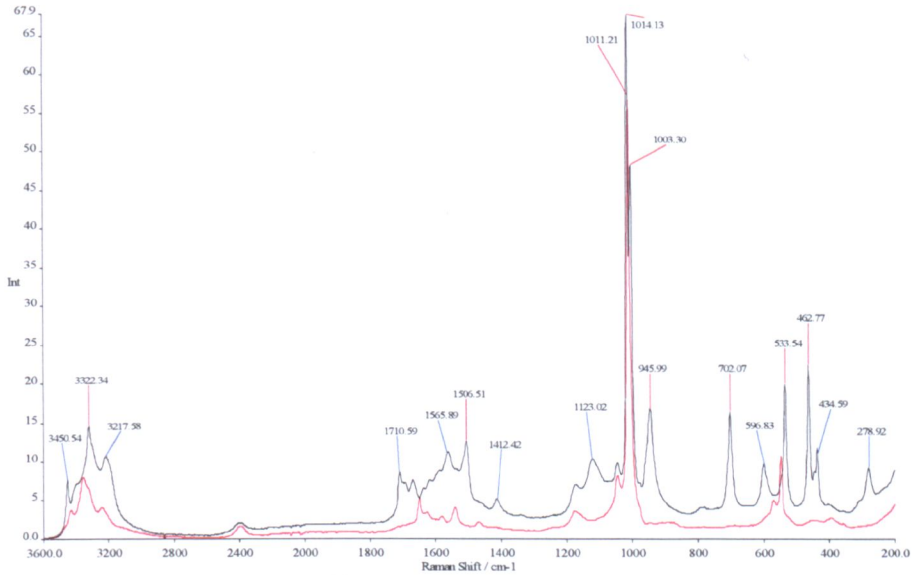

Figure3.54. The Raman spectra of the 1S/1PH/10U water-soluble condensate [red] and the urea water-insoluble condensate [black].

In this exothermic thermal reaction some specific observations need to be highlighted. During the thermal reaction in an open reaction vessel at high temperature, above 160°C, the evolution of gases is evident. To determine the nature of the new water-insoluble product using FT-IR and Raman spectrum analysis, it is valuable to predict all the possible products that may be produced at this high temperature. Therefore by indicating each specific band present at a particular frequency, the possible functional groups may be identified. In Table 3.15, the expected products were indicated with all the relevant information regarding the quality of the bands presence in both the FT-IR and Raman spectrum.

The specific bands are determined from the two spectra in Figures 3.55 and 3.56.

In some specific frequency regions second derivative spectra of the water-soluble and water-insoluble products were also required. In Table 3.16, the new functional groups expected to be found in the product after gas liberation is defined from these spectra. Since an excess of urea (10 moles) was used in the production of this urea condensate, there was similarity between this insoluble product and the sample obtained by heating only urea at 160°C. In the second derivative spectra, cyanuric acid and melamine appear with the same intensity at the exact specific frequency as in the urea only system.

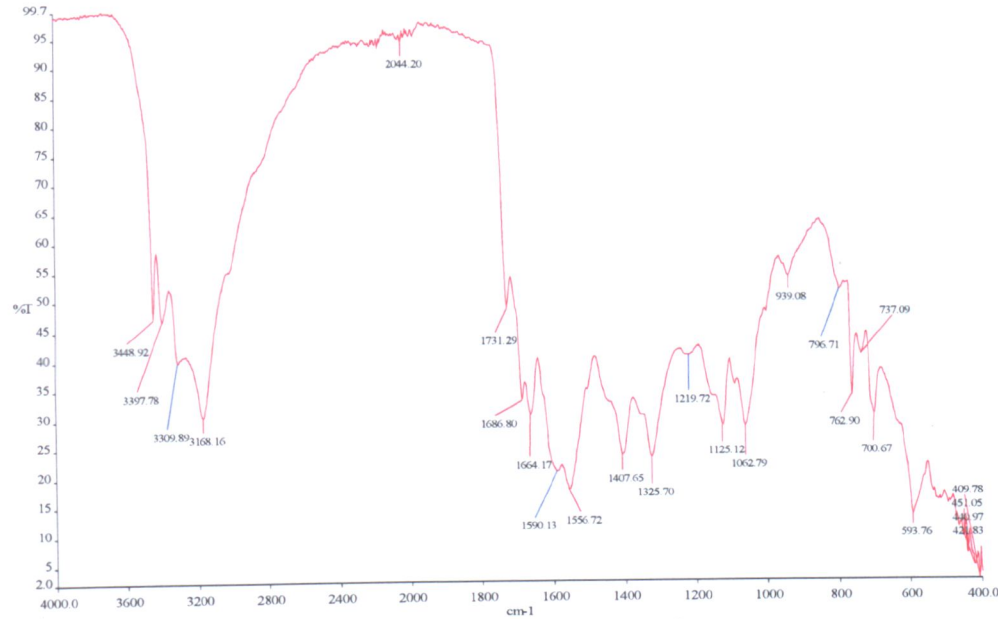

Figure3.55. The FT-IR spectrum of 1S/1PH/10U water- insoluble condensate.

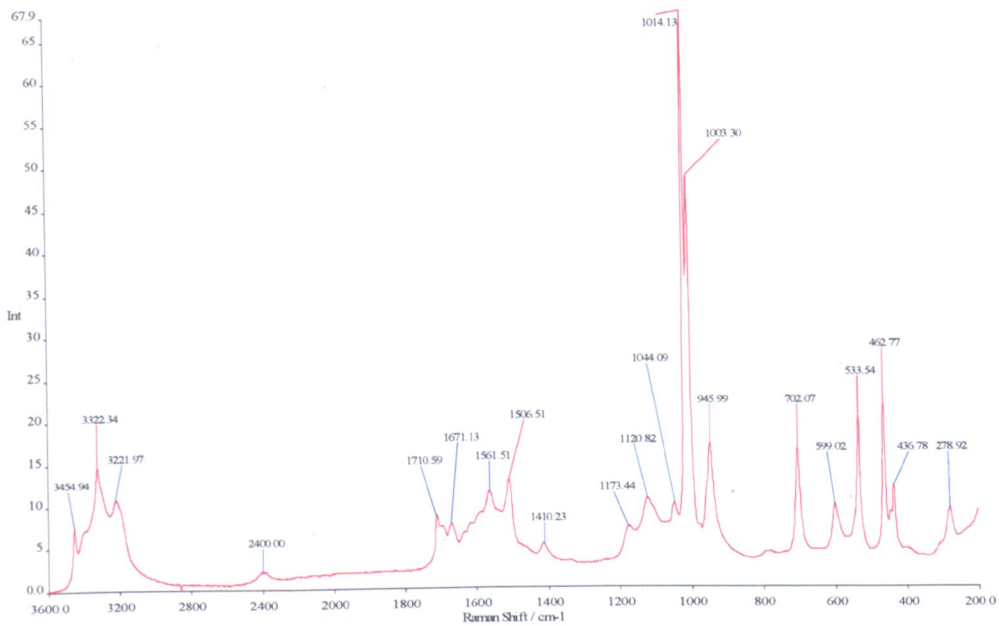

Figure3.56. The Raman spectrum of 1S/1PH/10U water-insoluble urea condensate.

Table3.15. The functional groups of various products expected in the 1S/1PH/10U water-insoluble condensate.

Functional Groups	Region cm^{-1}	FT-IR		Raman		Comments
		Specific Peak cm^{-1}	Intensity	Specific peak cm^{-1}	Intensity	
Sym-triazines	3300-3100	3168- 3310	m	3222	M, p	C-H stre
	1580-1520	1557-1590	vs	1562	m-w	ring str, doublet
	1450-1350	1408	v	1410	w-d	ring str, at least one band
	1000-980	?	w	1003	s, p	ring str
	860-775	797	w-m	-		out-of-plane bending vib, at least one band
Cyclic ureas (five membered ring)						
(in solid phase)	1680-1635	1664	s	1671	w-m	keton groups in ring increase
(in solution)	1735-1685	1731	s	1711	w-m	frequency
Hydroxyl-substituted triazines	1775-1675	1687	s	1711	-	C=O str vibration of keto
	795-750	737	sharp-m	-	-	iso form
$\begin{matrix} R \\ R \end{matrix}\!\!>\!C=N-H$	1650-1640	-	s	-	s	C=N str vibrations
Ammelines and ammelides	2650~	-	w-m	-	-	br, ring NH…O=C vib
Cyanate ion, NCO^-	2225-2100	-	s	-	w-m	asy NCO str
	1335-1290	1326	s	-	ms, p	sy NCO str
	1295-1180	1220	w	-		combination band
	650-600	594	s	599	w	NCO bending vib
Melamines	3500-3100	3168- 3310	v	3222-3322	m-w	NH_2 str
		3398-3449		3455		
	1680-1640	1664	m	1671	w	NH_2 def
	1600-1500	1557-1590	s	1507-1562	m-s	Ring str
					m	
	1450-1350	1408	v	1410		sh, number of bands
	825-800	-	m	-		}Only one of the two is present
	795-750	763	m	-		

Table3.16. The functional groups expected in the 1S/1PH/10U water-insoluble condensate.

*Functional Groups	Region cm^{-1}	**FT-IR		**Raman		Comments
		Specific Peak cm^{-1}	Intensity	Specific peak cm^{-1}	Intensity	
R-SO2-OH	1355-1340	1326	s	-	s-m	Asym SO_2 str
Sulphondiamides >N-SO$_2$-N	1340-1320 1145-1140	1326 1141 (2^{nd} derivative)	vs vs	- -	m-w s	Asym SO_2 str Sym SO_2 str
Monothiol esters −C(=O)−S−	1035-930	997 or ~1005 (2^{nd} derivative)	s	1015 or 1003 (2^{nd} derivative)	s	C-S str
P=O associated	1250-1150	1220	vs	-	m-w	P=O str
R(OH)HP=O	1175-1135	1125	vs	1121	m-w	P=O str
P-NH	3200-2900 1145-1075 1110-930	3168 1125 1063	M w-m m-s	- 1044 946	M M -	NH str C-N str P-N-C asym str
Aromatic disulphides	540-400	470 – 534 (2^{nd} derivative)	w-m	534 – 462 (2^{nd} derivative)	Vs-m,p	S-S str, two bands due to rotational isomeration

* These functional groups and their specific identified frequency regions are indicated in reference [2].

** These specific peaks are determined from the main FT-IR spectrum and second derivative spectra of 1S/1PH/10U condensate produced at 160° C.

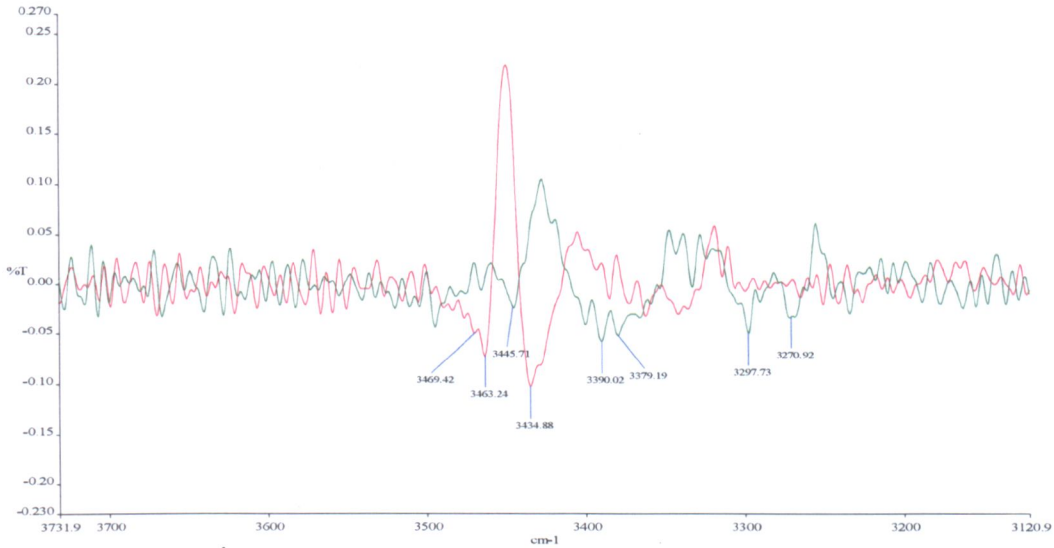

Figure3.57. The 2nd derivative spectra of 1S/1PH/10U water-soluble condensate [green] and the water- insoluble condensate [red].

In Figure 3.57, the two strong bands at 3469 cm^{-1} and 3435 cm^{-1} with shoulder, appear in the 1S/1PH/10U water-insoluble product, are attributed to the NH_2 and also CH stretching vibration of cyanuric acid and melamines which were identified previously in the urea insoluble product heated to 160°C in section 3.5.1. The band at 3446 cm^{-1} in the water-soluble product is not seen in the insoluble product. The intensity of some bands in this region have also reduced, 3390, 3379 cm^{-1}, 3298 cm^{-1}; these all represent NH_2 and NH functional groups in urea.

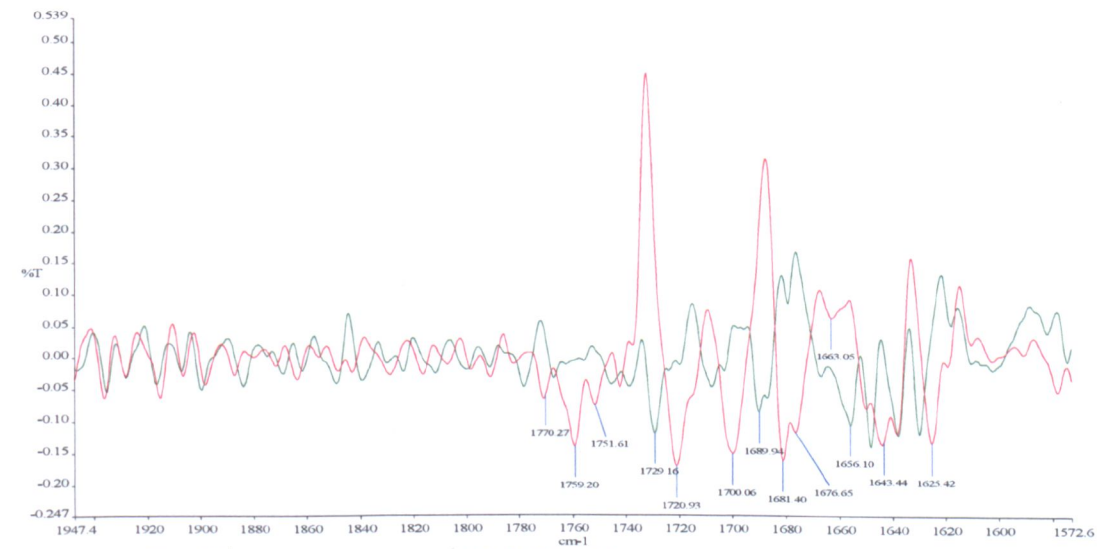

Figure3.58. The 2nd derivative spectra of 1S/1PH/10U water-soluble condensate [green] and the water- insoluble [red].

In Figure 3.58 a significant change can be seen at the particular region of 1947-1572 cm^{-1}. The bands relevant to C=O stretching of carbonyl group of different classes of compounds, appear in this region. These new strong bands present sufficient information relevant to the new compound with a new chemical structure. Similar bands at the same frequencies are observed in the urea heated to 160°C therefore the same products can be expected in the water insoluble product. The carbonyl group from tautomerization of hydroxy substituted triazines is evident in the 1775-1675 cm^{-1} region [2]. All these new bands at this specific region could be relevant to the present of cyanuric acid in the product.

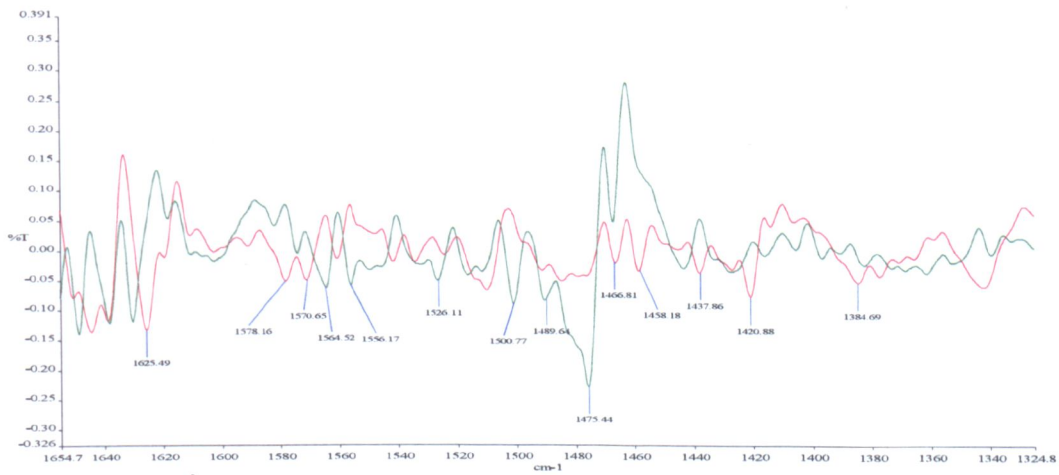

Figure3.59. The 2nd derivative spectra of 1S/1PH/10U water-soluble condensate [green] and the water- insoluble condensate [red].

In Figure 3.34 in the main spectrum of the water-soluble product, 1S/1PH/10U, in the frequency region from 1600-1450cm^{-1}, the two very strong bands at 1589 and 1456 cm^{-1} represent the secondary amide and NH deformation vibration of the urea group. In Figure 3.59, the band at 1589 verified as three bands in this region, at 1565, 1556 cm^{-1} and also a very sharp strong band with a shoulder at 1475 cm^{-1}. In the new insoluble product, these bands disappear completely.

In the water insoluble product two new bands at 1578 and 1570 cm^{-1} are attributed to the ring stretching vibration of symmetrical triazine. However some new bands, at 1467, 1458, 1438 cm^{-1} and 1421 cm^{-1} could also be verified as the melamine and triazine ring stretching vibration which could be expected in the at high temperature compound.

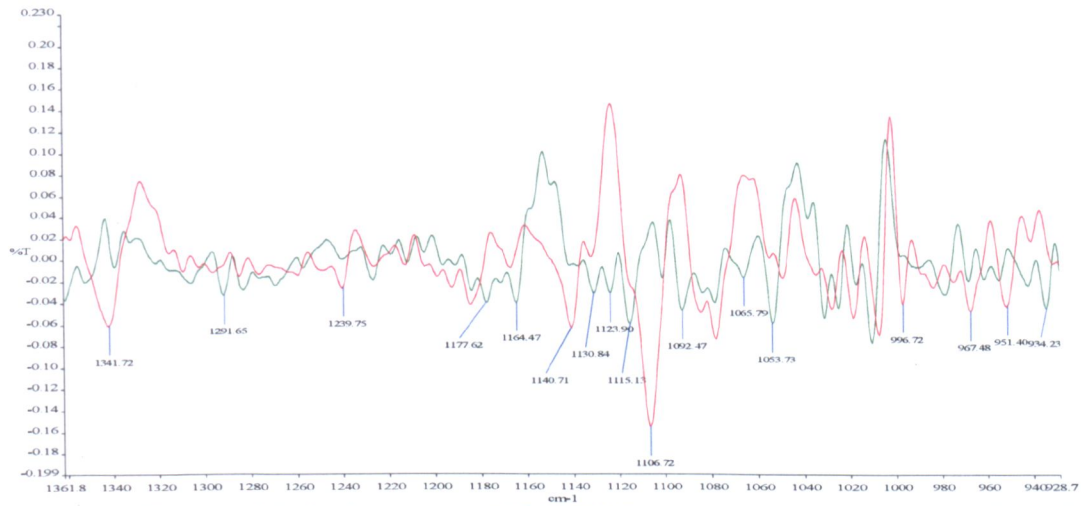

Figure3.60. The second derivative spectra of 1S/1PH/10U water-soluble condensate [green] and the water- insoluble condensate [red].

In Figure 3.60 in the specific frequency region, from 1362-9288 cm^{-1} all the bands relevant to the phosphorus and sulphur compounds appear. A significant difference can be seen by heating the product 1S/1PH/10U to high temperature. In the water-insoluble product a strong wide band, with high absorption intensity, at 1342 cm^{-1} is attributed to the asymmetric stretching vibration of the SO_2 functional groups. However the intensity of two bands at 1066 cm^{-1} and 1058 cm^{-1} due to the alkyl sulphonic acid RSO_2-OH are reduced. The intensity changes can be affected from the new neighbouring atoms/groups or from inter-molecular and intra-molecular bonding interactions.

In this region, the three new bands in the second derivative spectrum at 951, 967 cm^{-1} and 997 cm^{-1} are relevant to the ring stretching vibration of triazines. In the water-soluble product, the bands attributed to the P=O stretching vibration of phosphorus compound at 1131, 1124 cm^{-1} and 1115 cm^{-1} appear which are not seen in the water insoluble product. In fact two further bands at 1141 cm^{-1} and 1107 cm^{-1} represent the P=O stretching vibration of R(OH)HP=O appear with high absorption intensity in the new high temperature compound. These two bands together show a specific band at 1125 cm^{-1} in the main water-insoluble product, Figure 3.55.

In Raman spectrum, at approximately 1000 cm^{-1}, two very strong sharp bands appear in the new high temperature product, at 1014 cm^{-1} and 1003 cm^{-1}, are attributed to the CN stretching vibration of urea compound and also symmetric triazine. However in the S/U sulphamic acid product, the presence of a band at this frequency, relevant to the S-O

asymmetric stretching vibration is also indicated. The monothiol esters have a band representing the C-S stretching vibration at this specific region. In Figure 3.61 the second derivative of the Raman spectrum at this particular region enables these two bands to be identified.

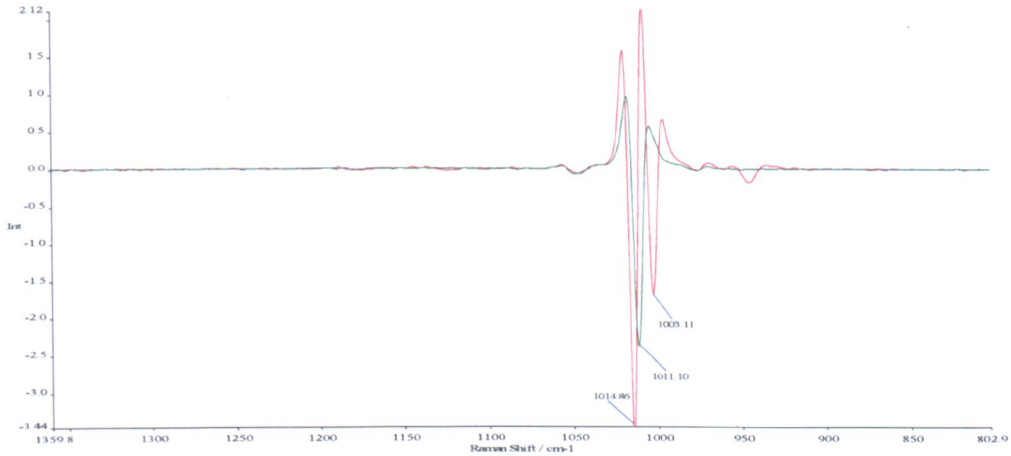

Figure3.61. The 2nd derivative Raman spectra of 1S/1PH/10U water-soluble [green] and the water-insoluble [red].

Increasing the absorption intensity of the band at 1220 cm^{-1} in the urea insoluble product, representing the P=O stretching vibration shows another band relevant to the phosphorous compound which does not appear in the Raman spectrum.

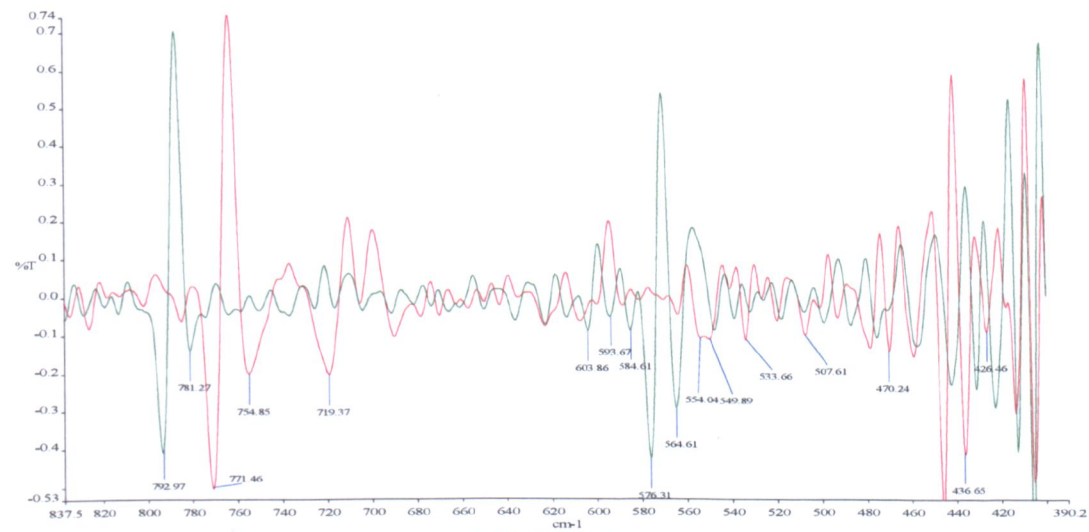

Figure3.62. The 2nd derivative spectra of 1S/1PH/10U water-soluble condensate [green] and the water- insoluble condensate [red].

The out-of-plane bending vibration of the symmetrical triazine has a band at a particular frequency region of 860-775 cm^{-1}, however for the melamine structure this region is

approximately indicated at 795-750 cm^{-1}[2]. In the main spectrum of the water insoluble product, two characteristic bands relevant to this effect are identified in Table 3.15. In Figure 3.62 the second derivative spectrum in this region shows a few sharp new bands, the band at 771 cm^{-1} could be relevant to the triazine structure and the other two bands, at 755 and 719 cm^{-1} represent melamine. In the urea water soluble product spectrum, several bands relevant to NH_2 deformation vibration of urea groups at 576, 565, 585 and 594 cm^{-1} disappear in the spectrum of the new product.

In Figure 3.63 in the Raman spectrum at this particular region from 837-390 cm^{-1}, a specific characteristic band can be identified which appears clearly in the second derivative spectrum. The two bands attached together at 534 cm^{-1} and 462 cm^{-1} could be identified as disulfides in an aromatic structure which needs further study in greater detail.

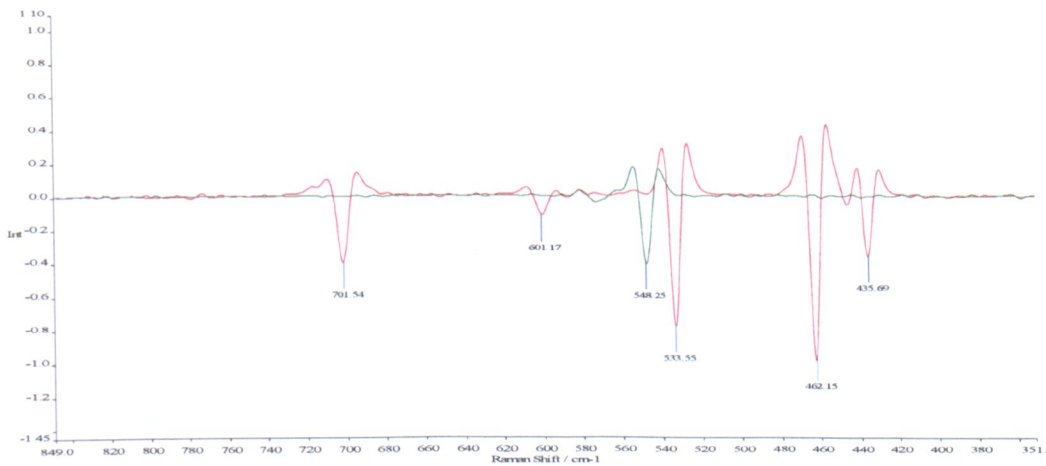

Figure3.63. The 2nd derivative Raman spectra of 1S/1PH/10U water-soluble [green] and the water-insoluble [red].

During the exothermic thermal reaction in an open vessel when the urea condensate 1S/1PH/10U was heated to 160°C, to produce the water insoluble products, some gases evolve. The main gases which are evolved during the reactions can be identified as NH_3, CO_2 and also water vapour. The likely reactions involved are shown in Scheme 3.13.

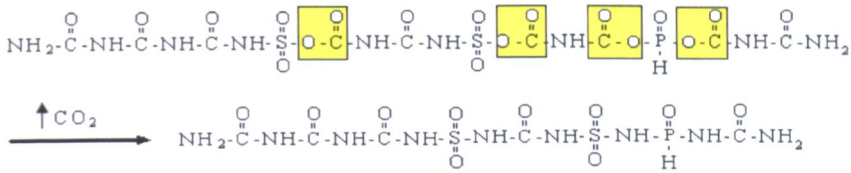

Scheme3.13. The possible gas evolved from the reaction vessel at 160°C.

The expected products after removing NH_3 have been explained in section 3.1. These compounds in combination can produce the complicated chemical structures proposed in Scheme 3.14.

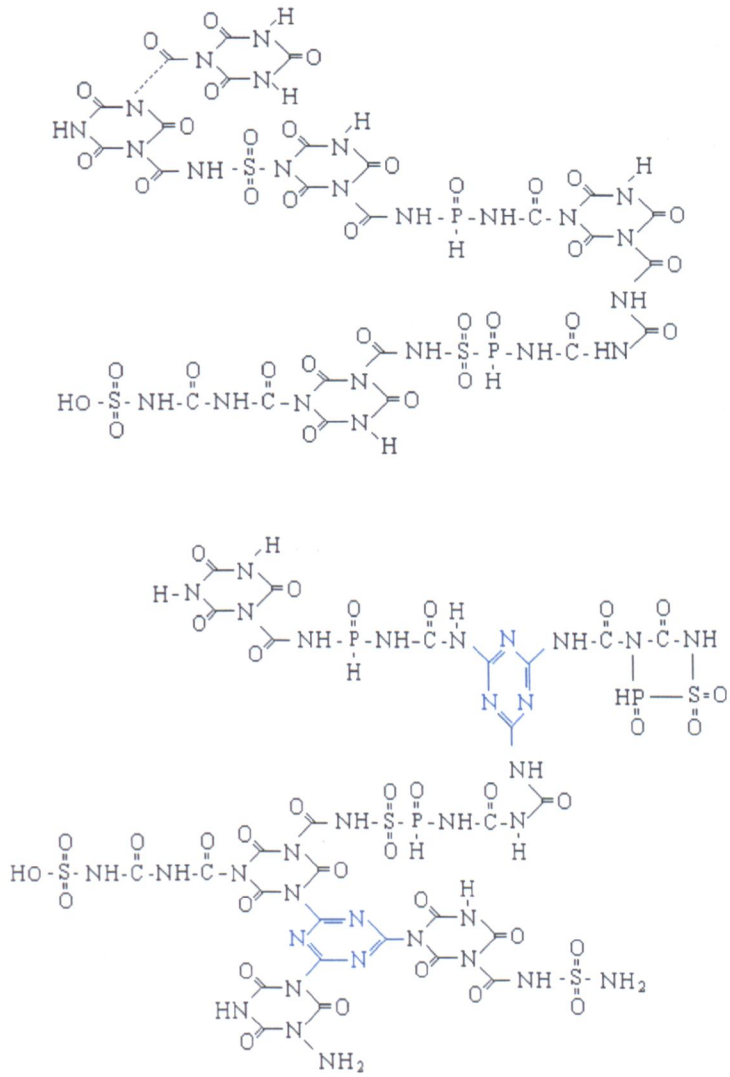

Scheme3.14. The predicted chemical structure for the water-insoluble 1S/1PH/10U condensate.

3.6 Mass spectrometry

Mass spectra results for both products 1S/1PH/10U and 1S/2PH/10U condensate are provided in Figures 3.64 and 3.65. These products have been produced at low temperature 140°C. The formation of various high molar mass oligomers with different chain lengths can be confirmed from these results. There is no sign of initial materials in the products, especially urea and the minimum molecular weight is indicated at approximately 120, which can be determined from the formation of biuret. The main products molecular weights have been reported to be 169, 207, 250 and also 314.9. From the NMR results provided in section 3.7.2, the urea linkage is the main functional group identified in the water soluble products. Therefore the formation of polyurea with various monomers can be claimed as the main products at this stage of production.

These suggested products are completely in agreement with the molecular weight performed in mass spectra results, Scheme 3.15.

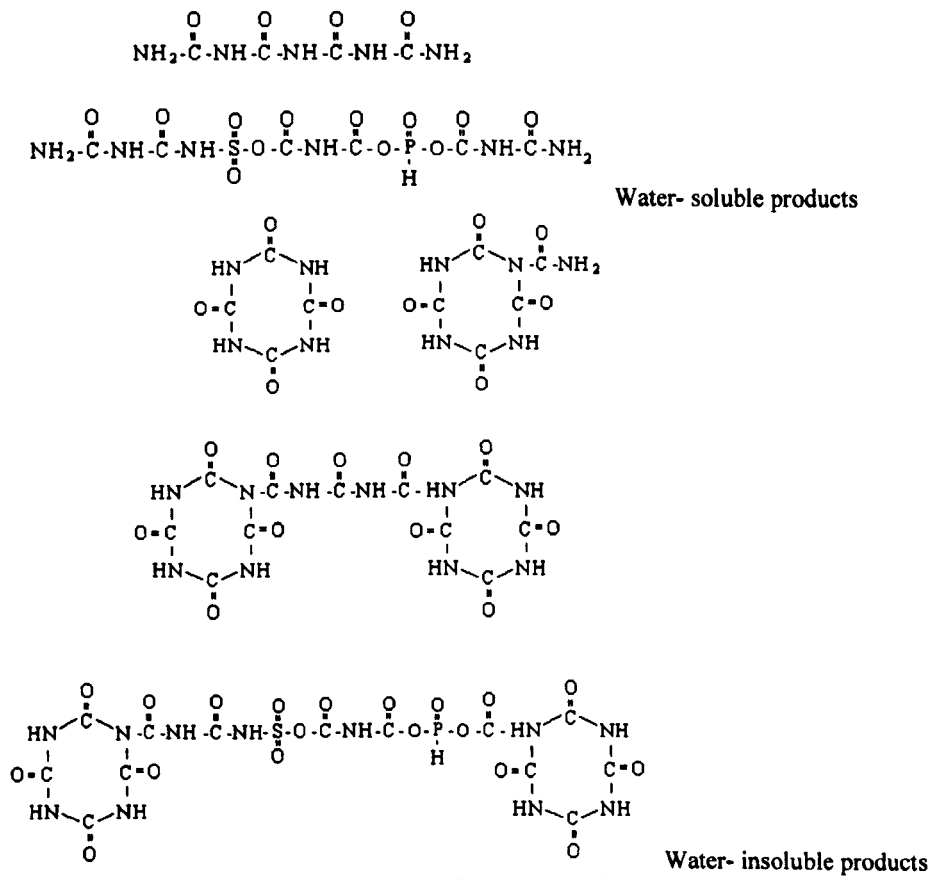

Scheme3.15. The possible products produced in urea condensate of sulphamic acid and phosphorous acid.

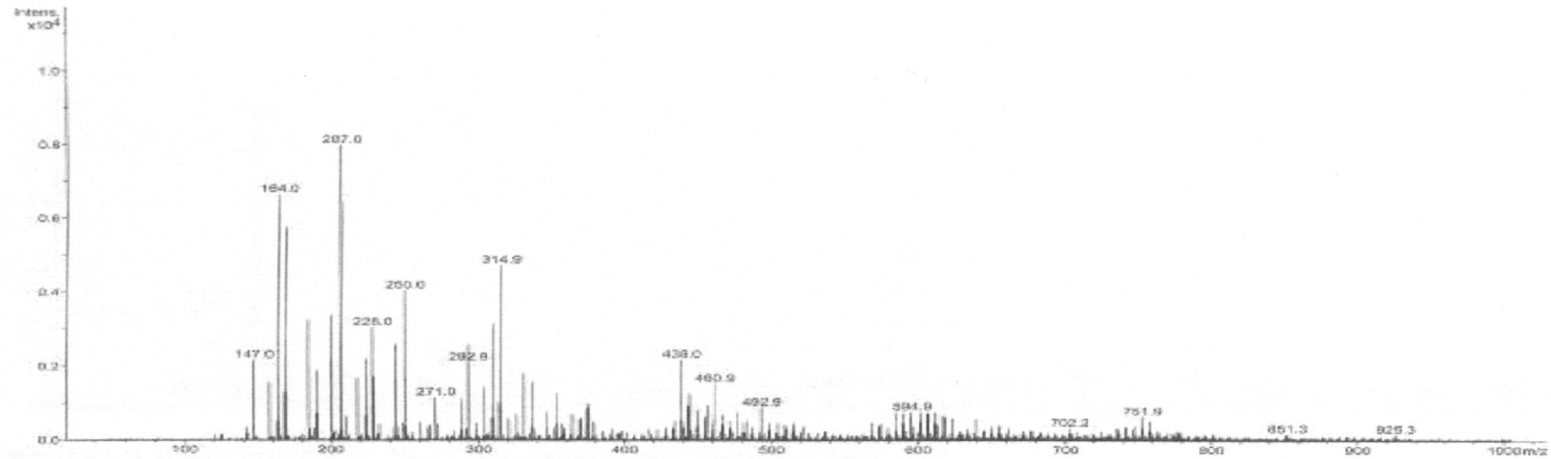

Figure3.64. Mass spectrum result of the 1S/1PH/10U condensate produced at 140°C.

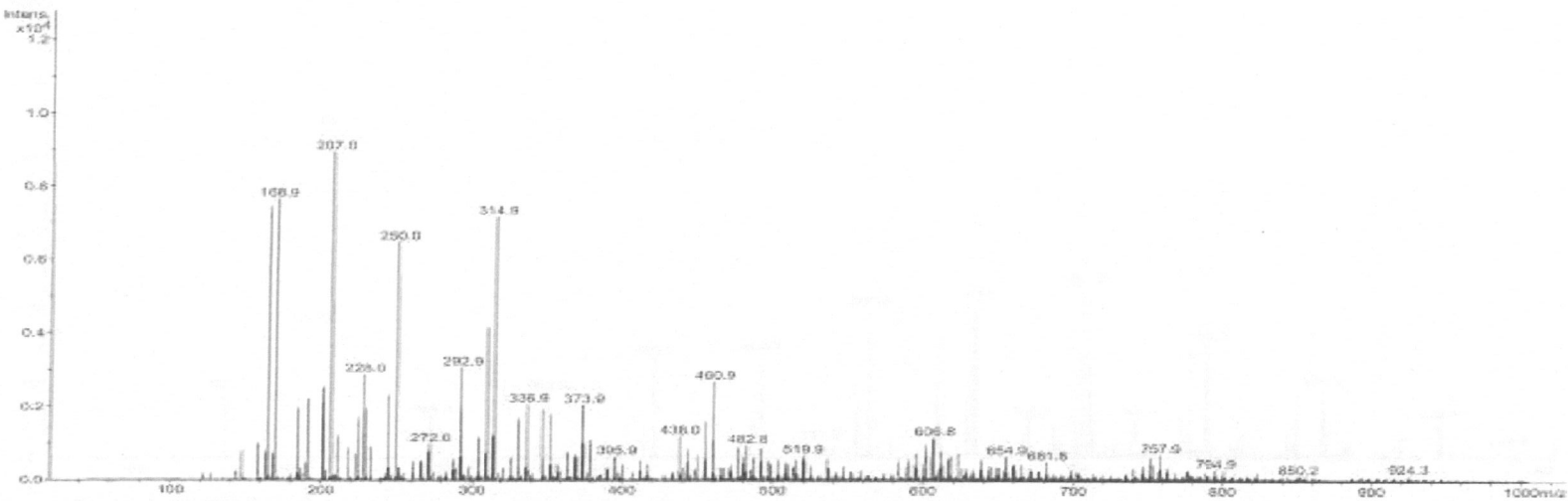

Figure3.65. Mass spectrum result of the 1S/2PH/10U condensate produced at 140°C.

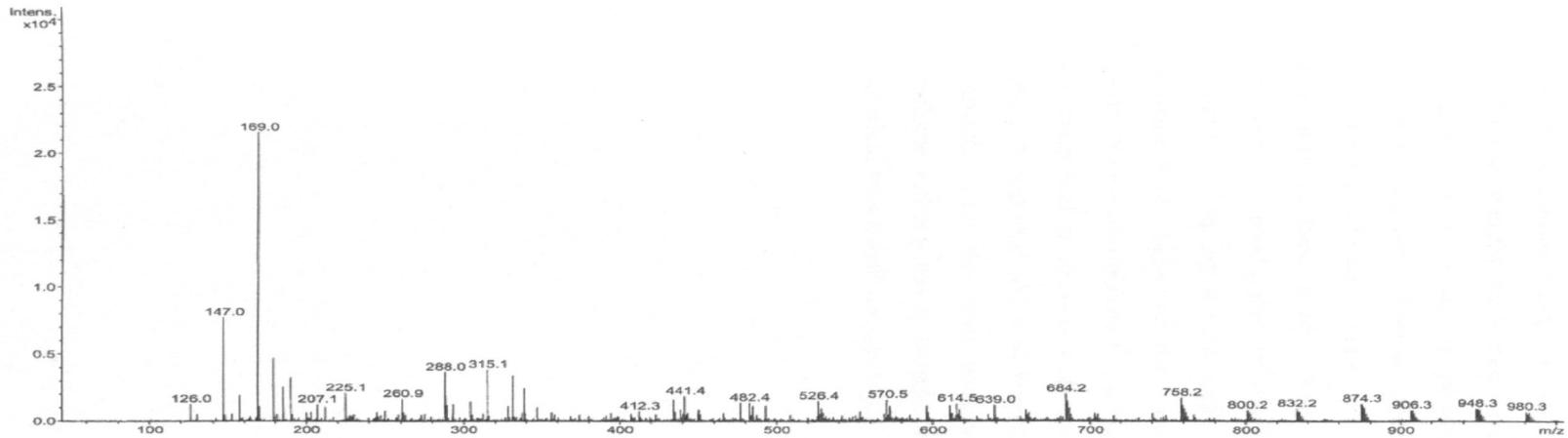

Figure3.66. Mass spectrum result of the 1S/1PH/10U condensate produced at 160°C.

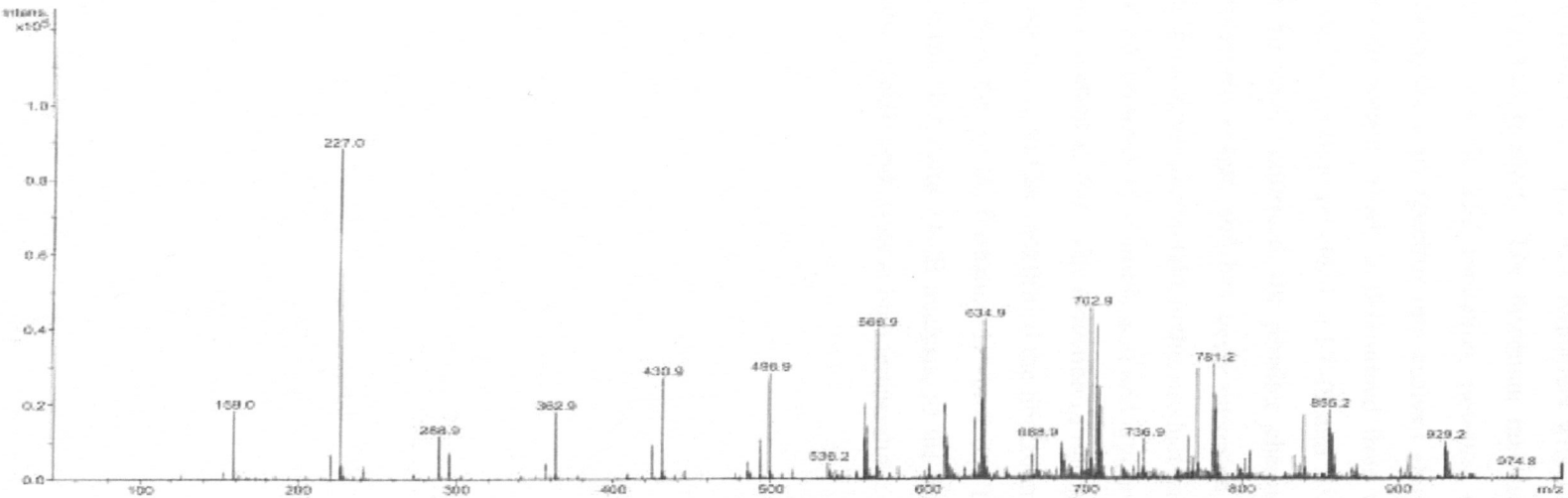

Figure3.67. The highlight of some part of the mass spectrum results of 1S/1PH/10U condensate produced at 160°C.

The mass spectrometry results for the urea condensate of 1S/1PH/10U produced at high temperature 160°C are shown in Figure 3.67. The new oligomers with high molecular weight have been reported for this product. The minimum molecular weight is 126, which is possibly due to cyanuric acid formation, however the fragments on the chemical structure during the mass spectroscopy analysis should also be considered. The main molecular weight which is determined from the insoluble products is 169. Relevant to the information provided in FT-IR and NMR analysis the production of cyclic urea has been confirmed, the possible chemical structure is in agreement with this molecular weight and has been suggested in Scheme 3.14. However the formation of high molecular weight in this product leads to other new complicated structures with the presence of cyanuric acid and aryl urea, the main high molecular weight oligomers centred at 700. The reduction of nitrogen elements reported in the elemental analysis result, section, confirmed the liberation of ammonia from the main structure and thus the cyclic formation is verified. The urethane linkage has also indicated from the NMR and FT-IR analysis, as the main chemical functional groups in the structure of urea condensate at high temperature.

3.7 NMR analysis

To further study the chemical components of the urea condensates, NMR analysis was used. The ^{1}H, ^{13}C and ^{31}P NMR spectra were obtained from the solution of the water-soluble urea condensates in D_2O and water-insoluble condensate in DMSO-d_6.

3.7.1 NMR analysis of urea

Urea as the main initial material needs to be analysed precisely. In Figure 3.68 the NMR proton (^{1}H) spectra of urea in D_2O is shown. This spectrum is characterized by two resonances or special regions, associated with the proton of the urea at 5.74 ppm and the D_2O solvent at 4.68 ppm respectively.

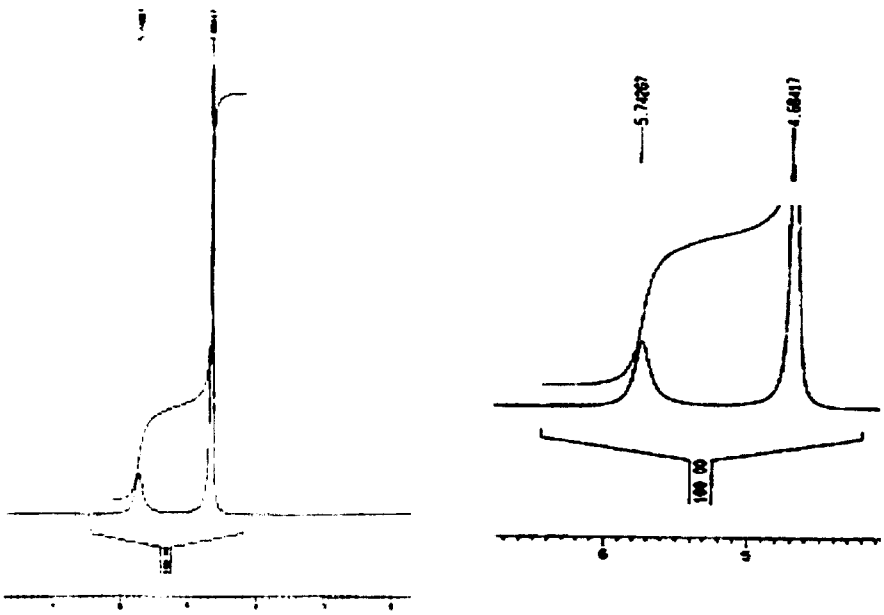

Figure3.68. ^{1}H NMR spectrum of urea in D_2O.

The ^{13}C results of urea (original), urea heated to 140°C (above its melting point) and also urea heated to 160°C to form the water-insoluble compound is shown in Figure 3.69. After condensation at temperatures above 140°C, the presence of isocyanic acid has been confirmed [1]; the reaction between highly reactive isocyanic acid leads to the production of various products, such as biuret, and triuret and cyclic ureas. The carbonyl group of urea attached to two NH_2 groups and also NH functional groups could be observed in all various types of products. In ^{13}C NMR results, the positions of these two carbon resonances are at the same frequency (~163 and ~157 ppm) for

urea and urea heated to 140°C; however in the water-insoluble urea condensate peaks with a 2 ppm shift can be observed. The integration of the resonance attributed to the carboxyl group attaching to NH functional group is different in urea. The formation of long chain poly-urea with urea linkage can be confirmed in the ^{13}C NMR spectra.

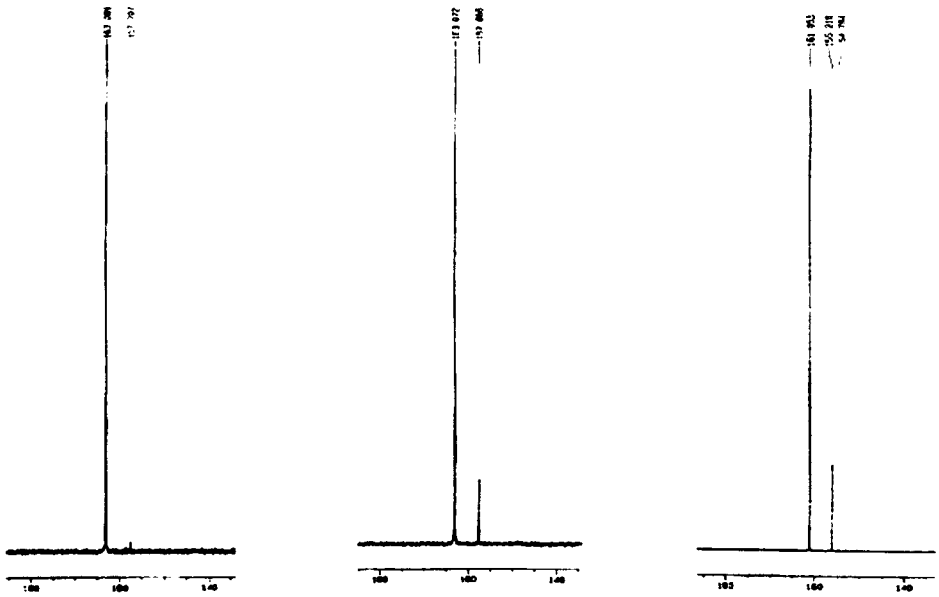

Original urea | Urea heated to 140°C (water-soluble) | Urea heated to 160°C (water- insoluble)

Figure3.69. ^{13}C NMR spectra of urea at various heating temperature.

In recent work [6] a solid state NMR study of a cyanuric acid / melamine system gave identified resonances at the same frequency found in the urea water-insoluble product.

3.7.2 NMR analysis of the water-soluble urea condensates

In this study various types of urea condensates produced at low temperature <150°C have been analyised; the ^{13}C, ^{1}H and ^{31}P spectra for the two main products, 1S/1PH/10U and 1S/2PH/10U have been reported.

3.7.2.1. ^{1}H NMR analysis

The proton NMR spectrum of the 1S/1PH/10U condensate is shown in Figure 3.70. D_2O as a solvent has a resonance at 4.6 ppm, also the protons of phosphorous acid appear in two triplet signals centred at 7.6 and 5.9 ppm. The other protons relevant to NH attached to the P=O at 5.8 ppm and NH attached to the sulphur group appear at

7.4 ppm, however the proton of NH attaching to the carbonyl group of urea is indicated at 7.1, 7.0 and 6.8 ppm.

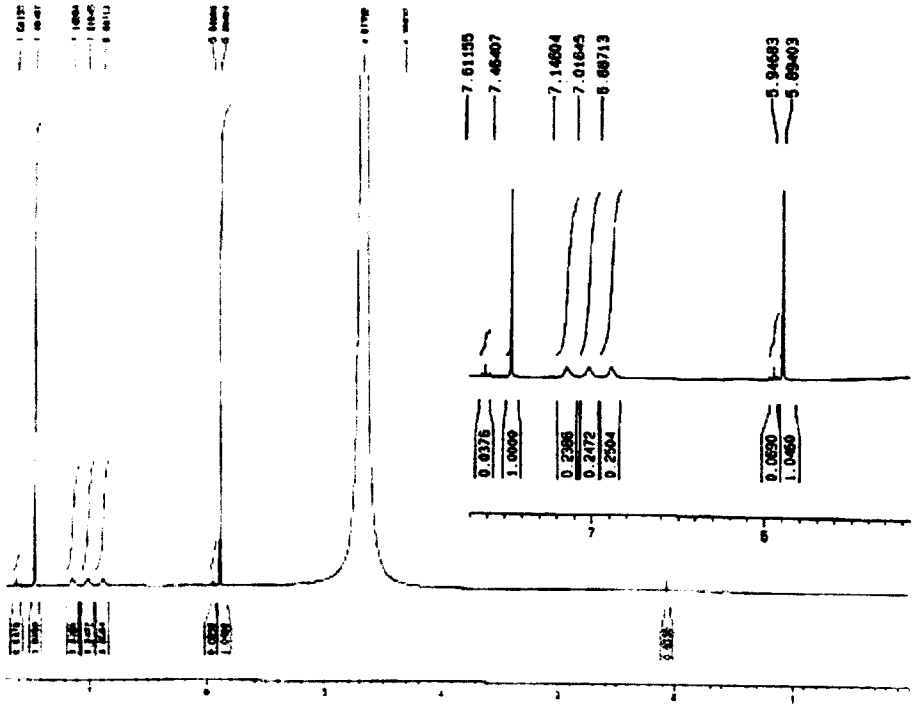

Figure3.70. Proton (^{1}H) NMR result from the 1S/1PH/10U condensate solution in D_2O.

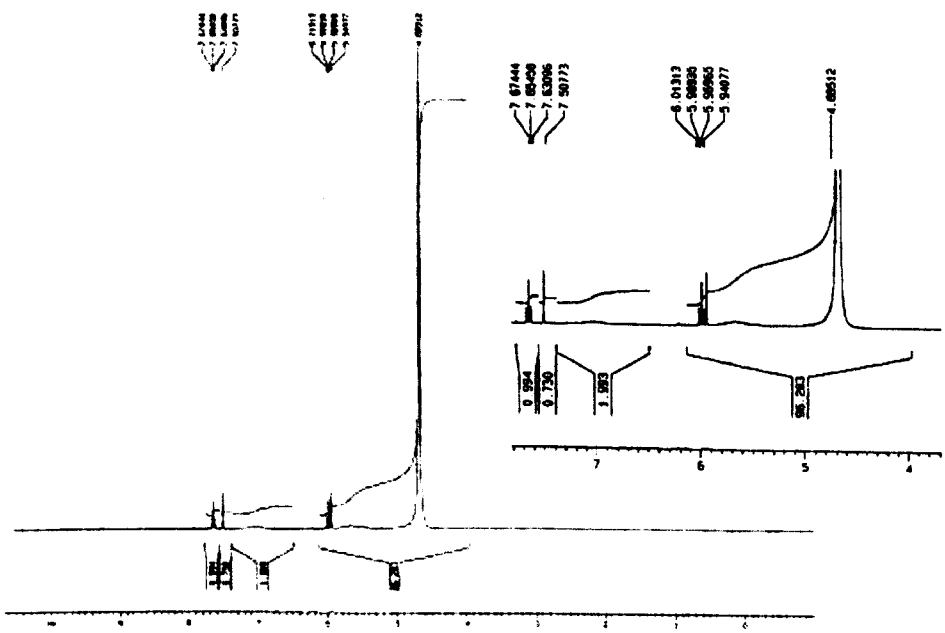

Figure3.71. Proton (^{1}H) NMR result from the 1S/2PH/10U condensate solution in D_2O.

In Figure 3.71, the ^{1}H NMR spectrum from 1S/2PH/10U condensate, the similar results has been indicated. The phosphorus protons appear clearer and also the two other NH protons are present. The proton attached to the urea carbonyl group does not appear in Figure 3.71, because of phosphorous acid, the present of these peak are not indicated.

In further study, the proton NMR spectra for the 1S/1PH/6U and 1S/2PH/16U condensates have been compared.

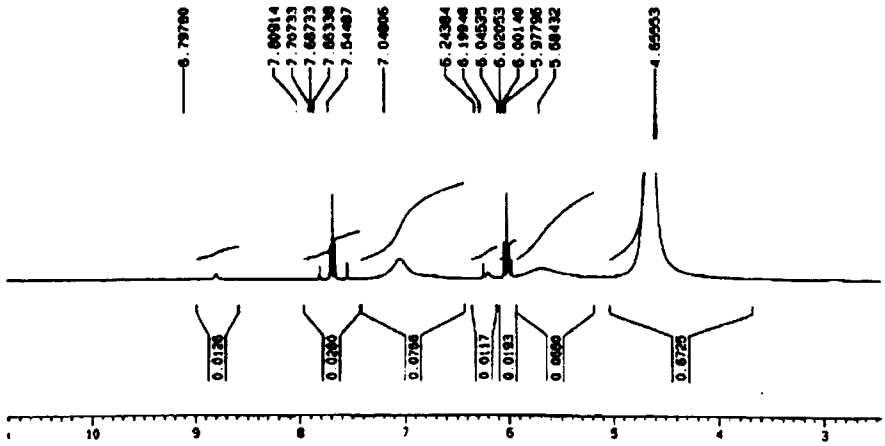

Figure3.72. Proton (^{1}H) NMR result from the 1S/1PH/6U condensate solution in D_2O.

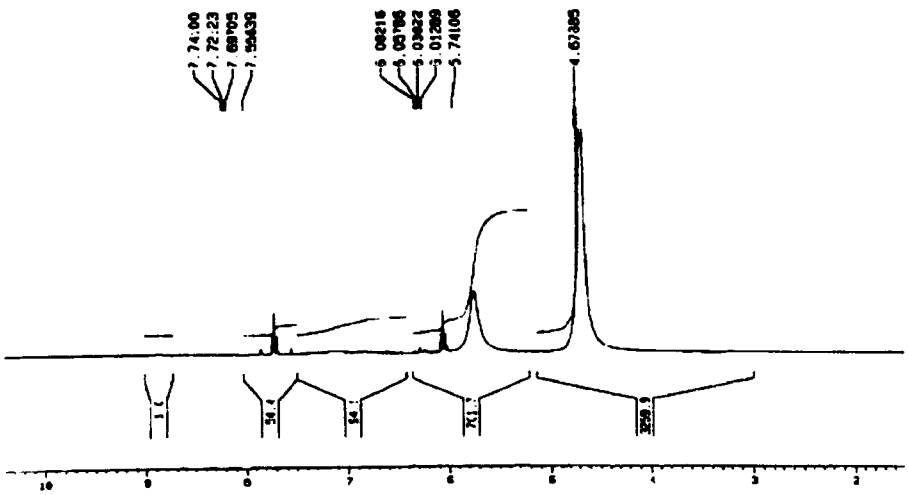

Figure3.73. Proton (^{1}H) NMR result from the 1S/2PH/16U condensate solution in D_2O.

The resonance relevant to the NH of the polyurea linkages appears at 7.0 ppm in proton NMR of the 1S/1PH/6U condensate which has not been clearly found in the other products. However the proton resonance representing the un-reacted urea can

only be identified precisely at 5.7 ppm in ^{1}H NMR spectrum of the 1S/2PH/16U condensate Figure 3.73, which is also not found in the other urea condensate spectra.

3.7.2.2 ^{13}C NMR analysis

To study the effect of the urea amount in urea condensate, the ^{13}C NMR spectra for 1S/1PH/6U, 1S/1PH/10U and 1S/1PH/16U are compared in Figure 3.74. The NMR spectrum of 1S/1PH/6U was selected as the background spectrum. In all three products the main resonance represents the carbonyl group attached to the NH_2, the main urea resonances are present with the same integration. However the second resonance shows that the carbon of carbonyl group bonded to the NH appears in various integrations for all three products. In fact, by increasing the amount of urea in the urea condensate, the molar ratio balance between the initial materials, urea, phosphorous and sulphamic acid is not in a specific order.

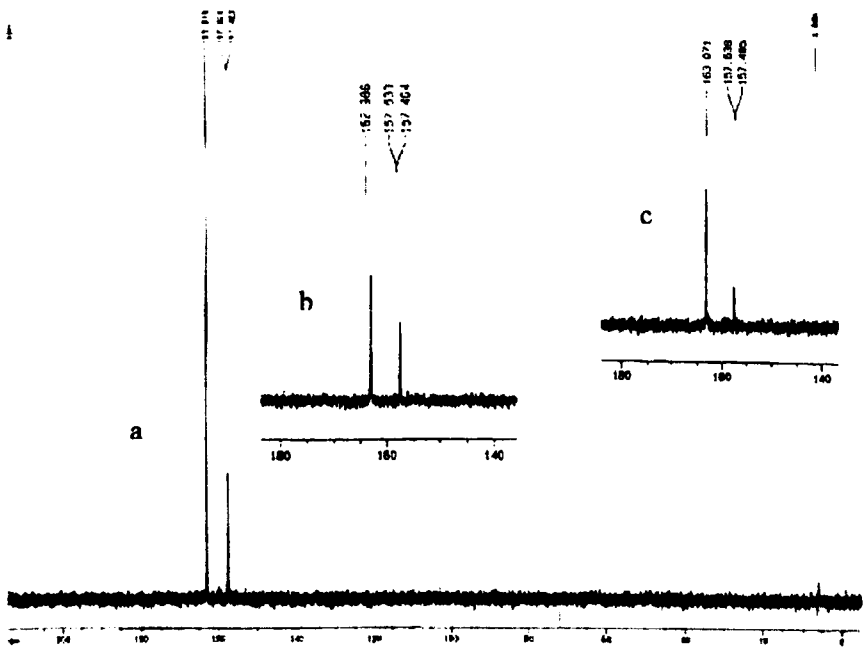

Figure3.74. ^{13}C NMR spectra for (a) 1S/1PH/6U, (b) 1S/1PH/10U and (c) 1S/2PH/16U condensates solution in D_2O.

3.7.2.3 ^{31}P NMR analysis

The ^{31}P NMR result from the 1S/1PH/10U condensate prepared at 140°C (water-soluble) shown in Figure 3.75. ^{31}P chemical shift for the $O{=}P(OR)_3$ is indicated at -20

to 0 ppm shift range, however the other functional groups, $(RO)_2POH$ also has a resonance in the shift range from 0 to 20 ppm [7]. Therefore it is very simple to determine the possible formation of the new structure in the urea condensates. In the literature the main resonance for phosphorous acid has been identified at 3.2 ppm [8], however in the urea condensates, this peak is due to the chemical reaction which occurs and indicates a new substitution on phosphorus hydroxyl groups. This result is in complete agreement with the information provided in FT-IR analysis. The main phosphorus resonance appears in three signals at 3.35, -2.48 and -4.43 ppm, which are attributed to these functional groups, $O=P(OR)_2H$. The presence of three resonances may explain the formation of the three functional groups in one chain molecule or it is possible to appear in three various chain molecules with various neighbouring substitutions. By increasing the concentration of phosphorous acid in the urea condensate, these segments appear at the same frequency shift, except the quantity of each functional group is increased in the 1S/2PH/10U condensate. ^{31}P-NMR results from various types of condensates, with this chemical shift and the quantity of each resonance has been also provided in Table 3.17.

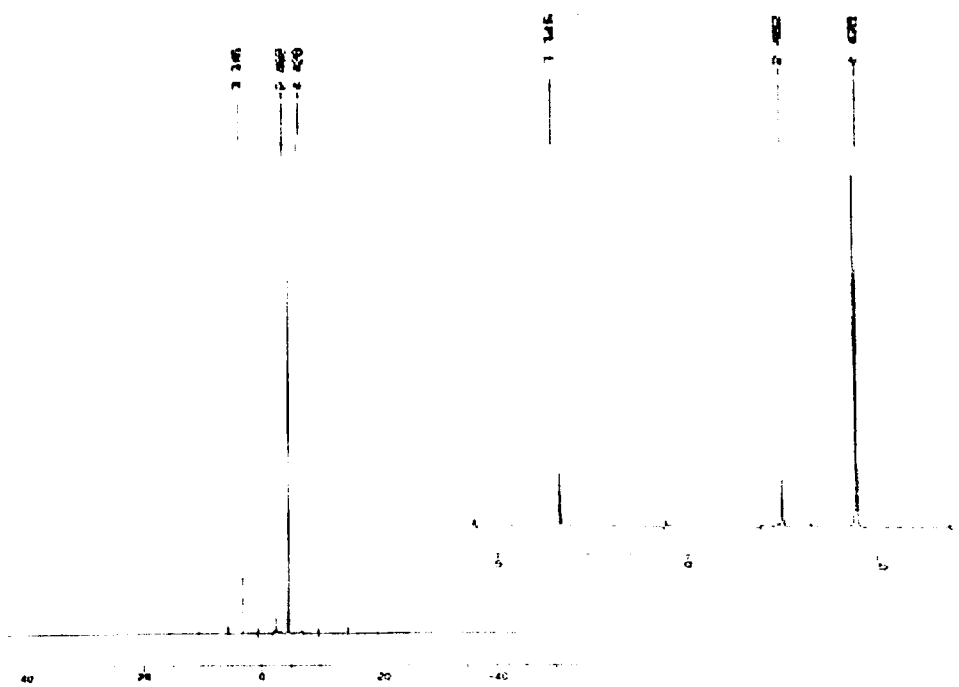

Figure3.75. The ^{31}P NMR result from the 1S/1PH/10U condensate solution in D_2O, prepared at 140°C.

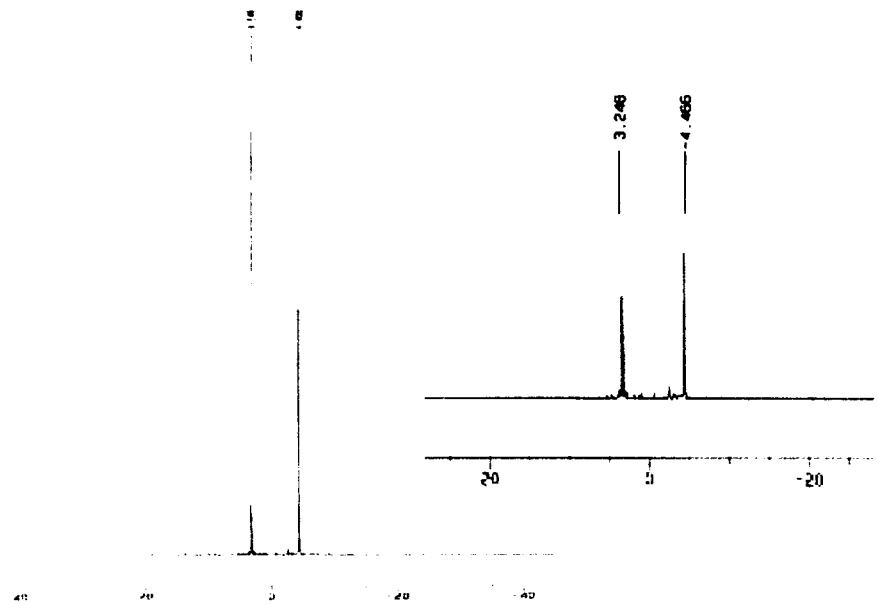

Figure3.76. The ^{31}P NMR result from the 1S/2PH/10U condensate solution in D_2O, prepared at 140°C.

3.7.3 NMR analysis of the water-insoluble urea condensates

3.7.3.1 ^{31}P NMR analysis

The spectra of ^{31}P NMR for water-insoluble condensates produced at >160°C are shown in Figures 3.76. Three new resonances appear at 0.92, -7.6 ppm and -8.51 ppm which may be attributed to the new functional groups produced in the urea condensate. However in the ^{31}P chemical shift information provided in references [7], the only functional groups indicated in this specific range (0 to -20 ppm) is $O=P(OR)_3$ and also in 0 to 20 ppm region, $(RO)_2POH$. In the FT-IR analysis the new formation of NH-PO-NH functional groups have been identified but in NMR analysis it is not possible to confirm it respectively. To study in more detail the use of model compounds is required, to determine the exact nature of phosphorus groups in the new chemical structure.

Table3.17. ^{31}P NMR results from the two urea condensate, 1S/1PH/10U and 1S/2PH/10U.

1S/1PH/10U condensate				1S/2PH/10U condensate			
Water-soluble		Water-insoluble		Water-soluble		Water-insoluble	
Chemical shift	Intensity	Chemical shift	Intensity	Chemical shift	Intensity	Chemical shift	Intensity
3.34	1.83	-0.93	14.00	3.24	14.00	-0.96	4.86
-2.48	1.68	-7.60	1.04	-4.46	8.05	-7.63	1.90
-4.43	14.00	-8.52	6.04			-8.54	14.00

Table 3.17 compares the quantity of each resonance in the two water-soluble and water-insoluble products; the intensity of a phosphorus functional group has been changed from one resonance to the other one. It is important to indicate that, for the 1S/1PH/10U condensate approximately 3.5 positive shift movements can be determined while the quantity of both peaks are still the same. However for the 1S/2PH/10U condensate, there is a negative shift of approximately 11.78 ppm between water and water-insoluble condensate. These chemical shifts confirm the new structure for the phosphorus group in the water-insoluble products which is relevant to the type of gas evolved from the160°C condensates. Regarding the information provided from the elemental analysis of the two water-soluble and water-insoluble condensate of 1S/1PH/10U a lower content of nitrogen, phosphorus and sulphur has been indicated after heating the products to the high temperature (section 3.3). The new structure which is formed at high temperature maintains the sulphur and phosphorus elements inside of the chemical bonding of the product formed. In Scheme 3.16 when the phosphorus acid is reacted with isocyanic acid and it is placed at the end of the chain structure, water solubility of this polyamide structure is possible. Therefore with this information regarding the new products at high temperature, a new position for the phosphorus element in the chain structure can be predicted which has been confirmed in the ^{31}P NMR results.

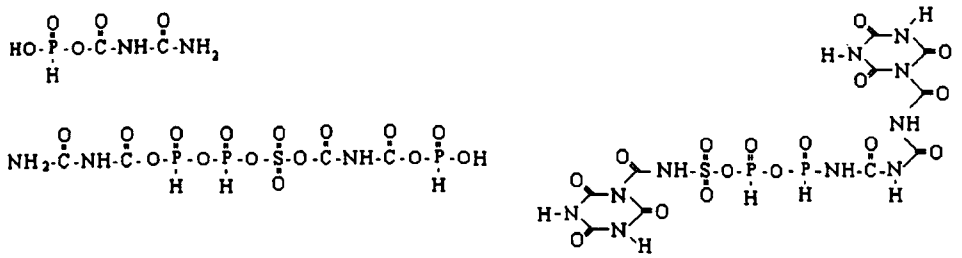

Water-soluble 1S/2PH/10U

Produced < 140°C

Water-insoluble 1S/2PH/10U

Produced > 160°C

Scheme3.16. The possible formation of urea condensates at < 140°C and > 160°C.

The high intensity of the signal relevant to the formation of phosphorous acid in the urea condensate 1S/2PH/10U at (δ=3.24) has been determined which can be verified in the Scheme 3.16. However these new phosphorus functional groups have also been identified in the FT-IR analysis (section 3.5.4.1 and 3.5.4.3).

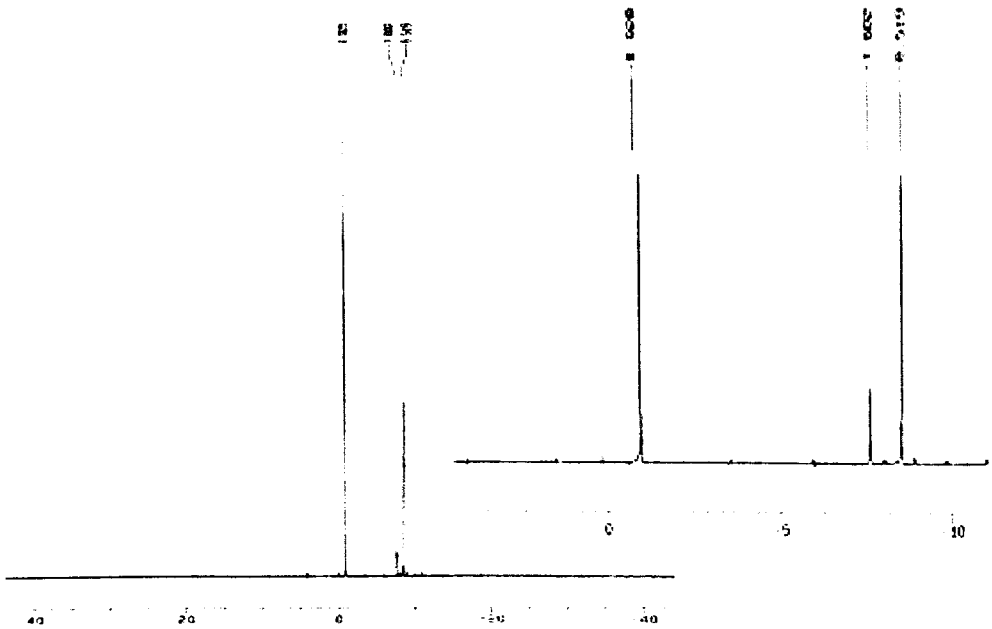

Figure3.77. The ^{31}P NMR result from the 1S/1PH/10U condensate solution in DMSO, prepared at 160°C (water-insoluble).

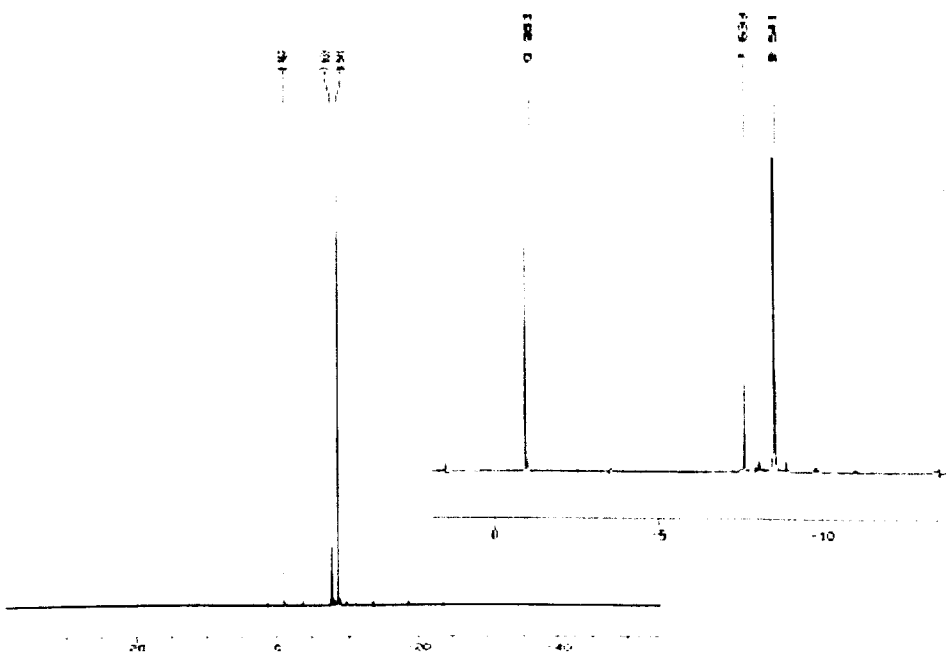

Figure3.78. ^{31}P NMR result from the 1S/2PH/10U condensate solution in DMSO, prepared at 160°C (water-insoluble).

3.7.3.2 ^{1}H NMR analysis

The ^{1}H NMR spectrum of water-soluble products has been studied in the previous section 3.7.2.2. The proton NMR spectra of the two water-insoluble products of 1S/1PH/10U (Figure 3.79) and 1S/2PH/10U (Figure 3.80) are shown. A significant difference can explain the new products which produced at high temperature. The chemical shifts and their intensity for these products are indicated, Table 3.18.

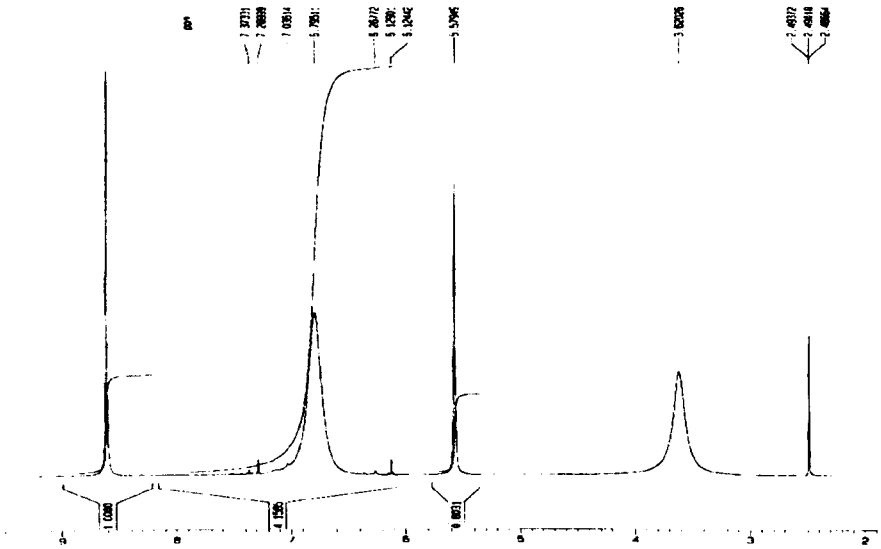

Figure3.79. ^{1}H NMR spectrum of the 1S/1PH/10U condensate solution in DMSO, prepared at 160°C (water-insoluble).

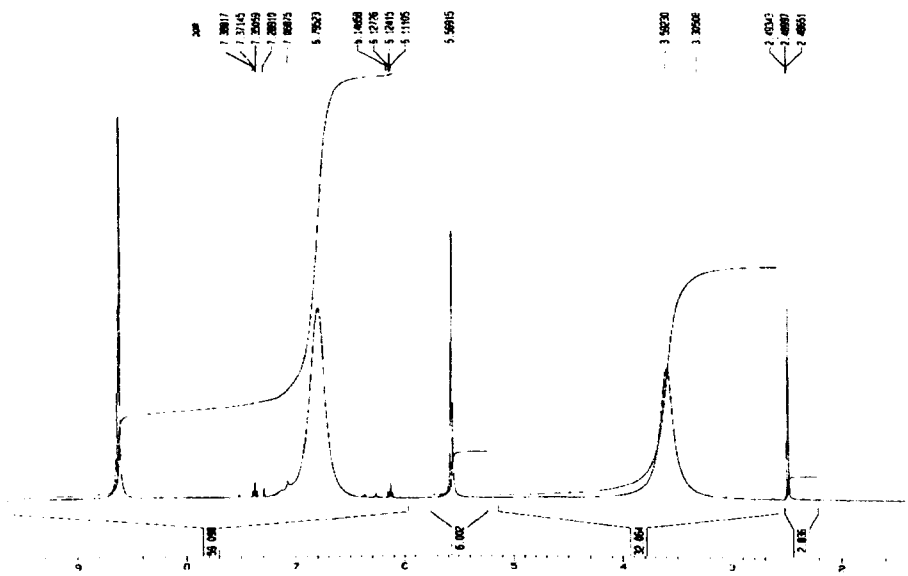

Figure3.80. ^{1}H NMR spectrum of the 1S/2PH/10U condensate solution in DMSO, prepared at 160°C (water-insoluble).

Table3.18. ^{1}H NMR results of the urea condensate products produced at 160°C (water-insoluble).

Functional groups	1S/1PH/10U		1S/2PH/10U	
	Chemical shift (ppm)	Intensity	Chemical shift (ppm)	Intensity
NH aryl-aryl urea and alkyl-aryl urea	8.61	14.00	8.62	14.00
Phosphorous acid	7.37 7.28 7.036	0.19 0.10 0.54	7.38 7.37 7.35 7.28 7.06	0.24 0.53 0.25 0.33 0.58
-NH-	6.79	5.61	6.79	6.32
Phosphorous acid	6.26 6.12	0.15 0.53	6.14 6.11	0.20 0.54 0.19
-NH2	5.57	10.65	5.56	8.84
-NH-O-	3.62	3.56	3.59 3.30	4.44 0.21

The similarity of chemical structure of these two products can be seen from the data provided in Table 3.18; showing the exact resonance with the same chemical shift and intensity for each product. Only the intensity of the peaks relevant to the phosphorous acid has changed due to the higher concentration of phosphorous acid in the urea condensate of 1S/2PH/10U.

3.7.3.3 ^{13}C NMR analysis

The ^{13}C NMR spectra for the two water-soluble 1S/1PH/10U and 1S/2PH/10U condensates have been provided in Figures 3.81.

Regarding all the information provided from the FT-IR analysis of these two compounds, it is possible to identify the other resonances which appear at 162.66, 159.98 ppm in 1S/1PH/10U condensate and also 159.97, 159.20 and 155.39 ppm, in the 1S/2PH/10U condensate as an amide groups which are attached to the phosphorus and sulphur groups in the main structure. It is possible to determine each one precisely by NMR analysis of the other urea condensate products such as 1S/4U, and 1PH/4U. Although, the quantity of all these resonances is very low, the NMR technique is a very powerful method and is able to indicate each carbon group in the structure. Higher concentration of phosphorous acid in the urea condensate

1S/2PH/10U gave further information relevant the resonance at 155.39 ppm; this is attributed to the carbonyl amide attached to the phosphorous acid.

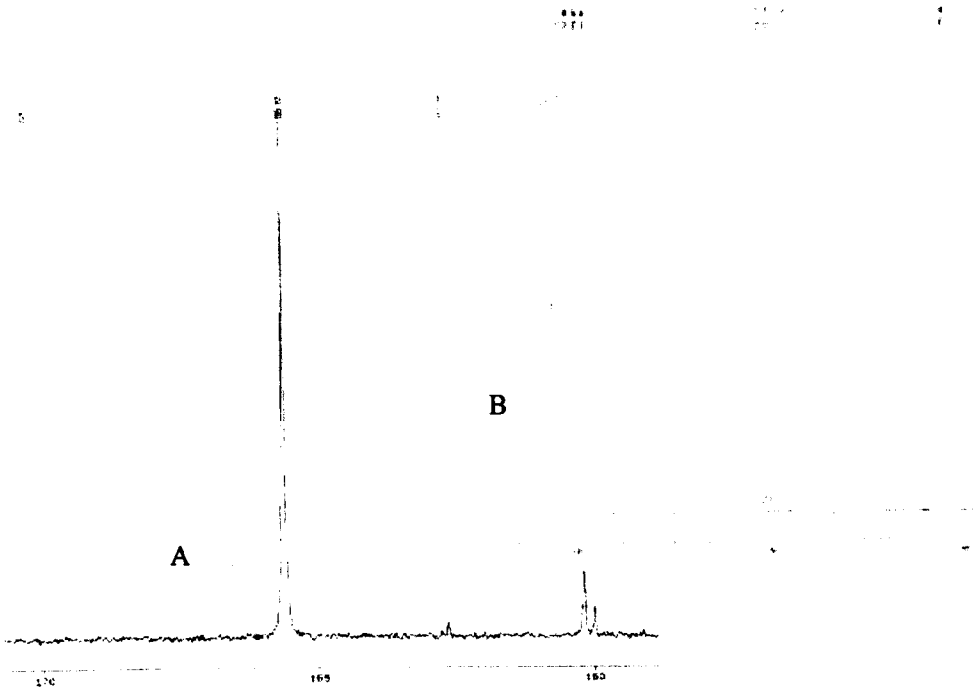

Figure3.81. ^{13}C NMR spectra of the 1S/1PH/10U [A] and the 1S/2PH/10U [B]condensates solution in D_2O, prepared at 140°C (water-soluble).

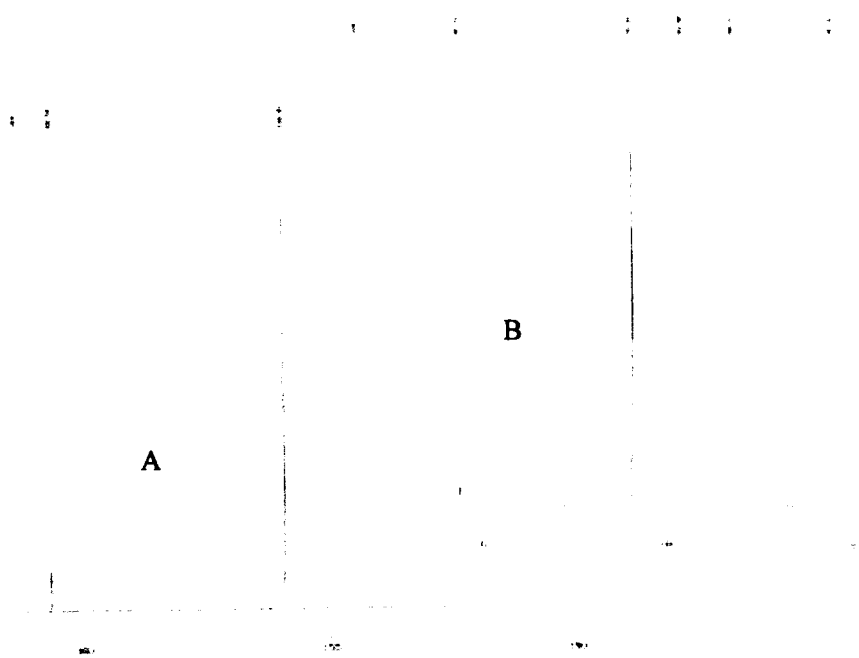

Figure3.82. ^{13}C NMR spectra of the 1S/1PH/10U [A] and the 1S/2PH/10U [B]condensate solution in DMSO, prepared at 160°C (water-insoluble).

Table3.19. ^{1}H NMR results of the urea condensate products produced > 160°C (water-insoluble).

Functional groups	1S/1PH/10U		1S/2PH/10U	
	Chemical shift (ppm)	Intensity	Chemical shift (ppm)	Intensity
NCON	160.64	1.58	160.59	1.06
Biuret linkage CO alakyl-aryl urea	155.93	14.00	155.91	14.00
Urethan functions	154.57	0.12	154.55	0.10
	153.16	0.11	153.16	0.12
	150.45	0.10	150.50	0.29

The ^{13} C NMR spectra for the two water-insoluble 1S/1PH/10U and 1S/2PH/10U condensates are shown in Figures 3.82.

In the ^{13}C NMR the difference between the two products, water soluble and water insoluble, is very clear. The 140°C condensate forms mainly the urea linkage however in the 160°C water-insoluble product, the biuret linkage, -NH-CO-NH-CO-NH-, is more abundant. This later structure can be a chain polymer with higher length. The possible formation of cyclic structure is also predicted. In recent work on the use of isocyanic acid to produce allophanates and polyurethanes [9], the presence of carbonyl groups of alky-aryl ureas has been identified at approximately 155 ppm. In addition these functional groups have also been determined in ^{1}H NMR results. The presence of allophanates, –NH-CO-NH-CO-O-, has been discussed with two different C=O peaks well separated with the same intensity in the region between 150.0-156.0 ppm, which can be identified in the ^{13}C spectra of both water-insoluble products. In other words, the urethane linkage attached to sulphur and phosphorus can be determined from the results provided in Table 3.19. Due to the higher concentration of phosphorous acid in the 1S/2PH/10U condensate, it is possible to verify these two resonances which appear at 150.45 ppm in the 1S/1PH/10U condensate spectum and 150.50 ppm in the 1S/2PH/10U condensate.

Conclusions:

The production of isocyanic acid, as the main thermo-decomposition products above its melting point (130°C), has been confirmed. The reaction of urea with various types of inorganic acid, such as sulphamic, phosphoric and phosphorous acid, is

always exothermic. Water soluble urea condensates were produced at temperatures between 125-140°C. These exothermic reactions occurred over a very short range of temperature; specific points to be noted:

- The rate of heat input, the type of reaction vessel (closed or open), under pressure or atmospheric pressure, all have an influence on the type of urea condensate produced.
- The type and the molar ratio of the selected initial materials can change the exothermic reaction; therefore the controllability of the reaction is a main point if industrial production is envisaged. From all the information provided in this chapter it is possible to indicate the most suitable process with regards to exotherm controllability:

1S/1PH/10U > 1S/2PH/10U > 1S/1PA/10U > 1PH/U (various moles of urea) > 1S/U (various moles of urea) > 1PA/U (various moles of urea)

- In the combination 1 mole sulphamic acid: 4 moles of urea, a very viscous gel form of compound was produced while for the other selected molar ratio reactions, a white water-soluble crystal was produced.
- In the case of phosphorous acid/urea condensates, by increasing the amount of urea, the exothermic reaction starts at a higher temperature and less water-soluble products were produced.
- By increasing the amount of phosphorus acid in the urea condensate, the exothermic reaction occurred at a lower temperature but more gas liberation from the reaction was seen.
- In the mixture of sulphamic acid, phosphrous acid and urea, the same effects have been seen. The condensate from one mole sulphamic acid/one mole phosphorus acid/10 moles of urea produced the desired flame retardant finish when applied to cotton. Therefore to reduce the cost of the products, higher amounts of urea were used in the condensate formulation while maintaining the same amounts of phosphorous and sulphamic acid. On increasing the amount of urea, the exothermic occurred at higher temperatures, however products having lower water solubility were produced; thus to prepare the flame retardant solution for application to fabric, warm water (50°C) was required to dissolve the agent.
- In the preparation of the urea condensate, 2 moles sulphamic acid/3 moles phosphorus acid/10 moles urea, a gas was evolved with a garlic odour indicating that the gas contained sulphur.

Chemical analysis results showed that the water soluble products produced are high molecular weight aliphatic chain ureas. By increasing the heat input to higher temperatures, above 160°C, in all the various urea condensates, water-insoluble products were formed. Further information from chemical analysis showed the presence of cyclic ureas in combination with cyanuric acid, melamines and other substituted triazines. In Scheme 3.17, the predicted chemical structure for the 1S/1PH/10U condensate formed above 160°C is shown.

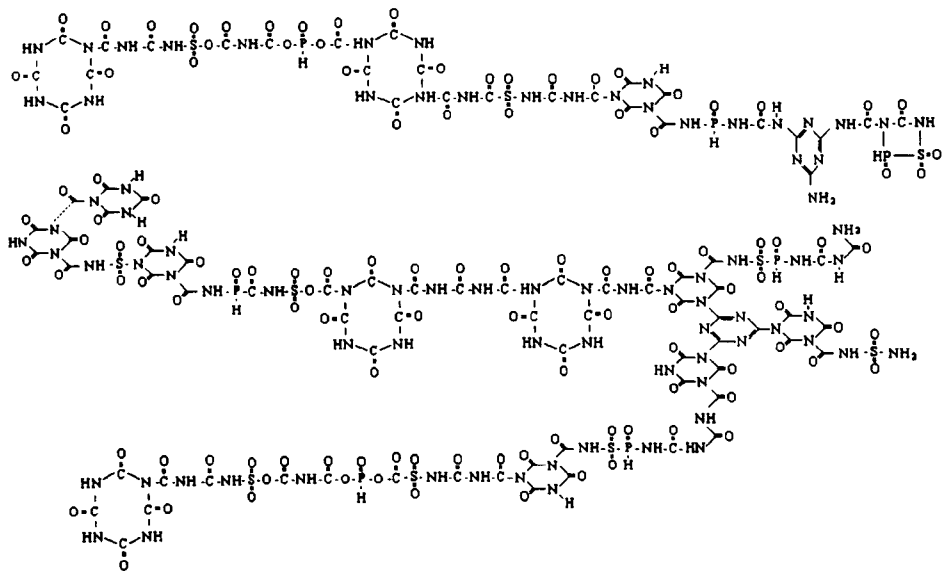

Scheme3.17. The predicted chemical structure for the water-insoluble products from the 1S/1PH/10U condensate.

References –Chapter 3

1. Schaber, P.M, Colson, J and Higgins, S, "Thermal Decomposition (Pyrolysis) of Urea in an Open Reaction Vessel", Thermochimica Acta, 2004, 424, 131-142.

2. Socrates, G., "Infrared and Raman Characteristic Group Frequencies", Publisher: John Wiley and Sons, LTD, 2001.

3. Stradella, L. and Agentero, M., "A Study of the Thermal Decomposition of Urea of Related Compounds and Thiourea Using DSC and TG-EGA", Thermochimica Acta, 1993, 219, 315-323.

4. Nyquist, R.A. and Muelder, W.W., "An Infrared Study of Organophosphorus Compounds-1, Rotational Isomers and Assignments", Spectrochimica Acta, 1966, 22, 9, 1563-1569.

5. Thomas, L.C., "Interpretation of the Infrared Spectra of Organophosphorus Compounds", Publisher: Heyden, London, 1974.

6. Damadaran, K. and Sanjayan, G.J, "Solid State NMR of Molecular Self-Assembly: Multinuclear Approach to the Cyanuric Acid-Melamine System", 2001, Organic Letters, 3, 12, 1921-1924.

7. Some Common ^{31}P Chemical Shifts, Online, [Accessed 20/11/2009], Available from: http://mutuslab.cs.uwindsor.ca/schurko/nmrcouse/chemical shifts/31P chemical shift.htm.

8. Platova, E.V., "Synthesis of Phosphorous acid and its Derivatives Based on the Reaction of Elemental Phosphorus (P_4) and Aqueous Solution of Choline in the Presence of the Hydroxides of Earth Alkali Metals, Hetroatom Chemistry, 2008, 19, 5, 517-519.

9. Lapprand, A, Boisson, F. and Delolme, F., "Reactivity of Isocyanates with Urethanes: Conditions for Allophanate Formation", Polymer Degradation and Stability, 2005, 90, 363-373.

Chapter 4 – Application of Urea Condensate products

Introduction

The aim of this chapter is to study the application procedure for various types of urea condensates to cotton fabric in order to maximise FR efficiencies and performance on the treated fabrics. To compare the effects of different type of urea condensate the same application concentration [500g/l] was selected for all products. At the beginning of the treatment the effect of curing conditions were examined on two selected urea condensates and it was found that 80% wet pick up, followed by a 2 minutes drying at 80°C and curing 2 minutes at 170°C were the optimum treatment conditions for all samples. The flame retardancy fabric face test was according to the selected standard, (section 2.3.1); using further information regarding char length, the most promising urea condensates would be selected.

Durability of the flame retardancy of the treated fabrics was also studied. All samples were washed in alkaline conditions, hard water (tap water) provided in 20:1, L:R, containing 2 g/l of sodium carbonate and 2 g/l of non-ionic wetting agents, washing at the boil for 20 minutes. This wash-durability test is equal to the results of 10 washing cycles in a commercial washing machine with colour care powder.

The results of each urea condensate after 13 times of washing have been provided. Some scanning electron micrographs are also provided showing elemental distribution of phosphorus and sulphur elements before and after wash-testing.

Differential scanning calorimetry (DSC) of the treated cotton samples with was carried out on selected treated samples. An exothermic curve for the treated samples can provide valuable information regarding the changes occurring on thermal decomposition of samples in the reaction with flame retardant agents. However the shift in TGA curve can provide more precise results regarding cellulose dehydration and char formation in case of treated samples with flame retardants.

The FT-IR and Raman analysis were reported only for selected samples such as: urea alone, sulphamic acid solution, 1S/4U, 1PH/3U 1S/1PH/10U and 1S/2PH/10U condensate treated cotton fabrics. The high reactivity of urea

condensates with materials containing hydroxyl groups was confirmed by studying their application to starch and polyvinyl alcohols.

4.1 The chemical treatment of cotton fabric

4.1.1 Treatment of cotton fabric with urea solution

Cotton fabric was impregnated with an aqueous solution of urea (500 g/l) using a laboratory pad set to give 80% wet pick up, dried for 84 seconds at 70°C and cured at 170°C for 2 minutes.

4.1.2 Treatment of cotton fabric with sulphamic acid solution

Cotton fabric was impregnated at 80% wet pick-up with 250g/l sulphamic acid solution (adjusted to pH 7 with ammonium hydroxide (35%)). The padded fabric was dried at 70°C, for 84 seconds and cured at 160°C for 2 minutes. It was observed that during the curing process the fabric discolored to a light brown.

4.1.3 Treatment of cotton fabric with S/U condensate

Fabric samples were impregnated with an aqueous solution of the S/U condensate on a laboratory pad at 80% wet pick-up, dried at 80 °C and cured at 170°C for 2 minutes.

The pad-liquor contained:

500 g/l of prepared urea condensate

10 g/l of wetting agent (Sandozine NIE, Clariant)

The treated fabrics were boil-washed for 20 minutes, with water containing 2 g/l of sodium carbonate and 1g/l of non-ionic wetting agent, the liquor ratio was 20:1, (pH ~11). The fabrics were then rinsed with cold water, and left to dry overnight at room temperature.

To determine the effectiveness of the flame retardant finishes, the burning test was performed on each fabric using the procedure described in Section 2.2.5. All the treated fabrics exhibited partial flame retardancy.

The effect of curing temperature and time on flame retardancy of the fabrics

The urea condensate from 1 mole of sulphamic acid and four moles of urea was selected. Fabric was treated using the same procedure as explained above of this section, but varying the curing temperature as explained in Table 4.1.

After fabrics were treated with the S/U condensate at various curing temperatures the fabrics were subjected to the flame test. All the treated fabrics had an after glow when the flame was removed, and a small hole was present on each sample. For comparison of the results of flame retardancy test, the size of each hole was measured and is indicated in Table 4.1. Photographs from the treated fabric with various type of the S/U condensate after the flame test are also provided in Figure 4.1.

Table4.1. The condition of drying and curing of cotton fabric treated with 1S/4U condensate.

Fabric code	Drying temperature ℃	Time of drying (second)	Curing temperature ℃	Time of curing (second)	Size of hole cm
S/U-1	70	84	165	140	3.5
S/U-2	70	84	170	140	3.5
S/U-3	70	84	175	140	3.3
S/U-4	70	84	180	140	3.0
S/U-5	70	84	185	140	3.2
S/U-6	70	84	190	140	3.0

The FT-IR analysis spectrum has been carried out on one fabric sample (1S/4U) and is discussed in section 3.5.2.

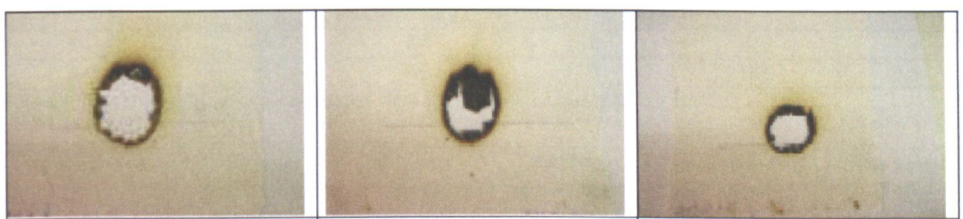

Cotton fabric treated with 1S/2U condensate hole size: 3.5 cm	Cotton fabric treated with 1S/3U condensate hole size: 3.5 cm	Cotton fabric treated with 1S/4U condensate hole size: 3.5 cm

Figure4.1. The flame retardancy results from fabrics treated with the S/U condensates.

4.1.4 Treatment of cotton fabric with urea condensate of PH/U

To produce good flame retardant materials, it is necessary to determine, how many moles of urea can be reacted with the phosphorous acid to achieve the desired flame retardancy result. Therefore various molar ratios of phosphorous acid/urea condensates were produced by mixing 1 mole phosphorous acid and different moles of urea, 2, 3, 4, 5, 6, 8, 10 and 12. Increasing the amount of urea in a mixture can facilitate the control of exothermal reaction but a hard crystalline compound will be produced with lower water solubility. The application of the urea condensates and washing process were carried out in the same procedures as

explained at the beginning of section 4.1.3. Fabric samples were impregnated with an aqueous solution of each urea condensate (section 3.2.3.) using a laboratory pad at 80% wet pick–up, dried on a frame and cured for the time and at the temperature specified in the Table 4.2.

The pad-liquor contained: 500 g/l of the prepared urea condensate, and 10 g/l of non-ionic wetting agent. The pH of the pad liquor has been measured and reported in Tables 4.2.

Table4.2. Drying and curing conditions for the cotton fabric treated with PH/U condensates.

Fabric code	Drying temperature ℃	Time of drying (second)	Curing temperature ℃	Time of curing (second)	The length of char cm
P-1-1	Pad and curing for 240 sec at 170℃				2.5
P-1-2	Pad and curing for 180 sec at 170℃				2.2
P-1-3	70	84	160	210	2
P-1-4	70	84	170	140	1.8

The fabric samples have been treated with the 1PH/2U condensate, (pH 5.2).

Fabric code	Drying temperature ℃	Time of drying (second)	Curing temperature ℃	Time of curing (second)	The length of char
P-2-1	Pad and curing for 240 sec at 170℃				2.8
P-2-2	Pad and curing for 180 sec at 170℃				2.5
P-2-3	70	84	160	210	3.4
P-2-4	70	84	170	140	3.5

The fabric samples have been treated with the 1PH/3U condensate, (pH 5.2).

Fabric code	Drying temperature ℃	Time of drying (second)	Curing temperature ℃	Time of curing (second)	The length of char
P-3-1	Pad and curing for 240 sec at 160℃				3.5
P-3-2	70	84	160	120	3.5
P-3-3	70	84	170	120	3.5

The fabric samples have been treated with the 1PH/4U condensate, (pH 5.6)

Fabric code	Drying temperature ℃	Time of drying (second)	Curing temperature ℃	Time of curing (second)	The length of char
P-4-1	70	84	160	120	3.5
P-4-2	70	84	160	210	3.5
P-4-3	70	84	170	105	3.5

The fabric samples have been treated with the 1PH/5U condensate, (pH 6.2).

All the treated fabrics passed the flame test some photographs of these samples are shown in Figure 4.2. They all exhibited very good flame retardancy performance, no after glow was observed and no holes were found in the tested fabrics.

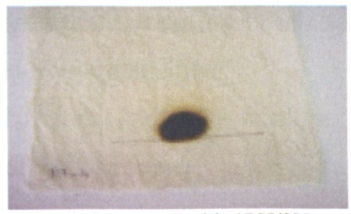

Fabric treated with 1PH/2U
Char length 2 cm

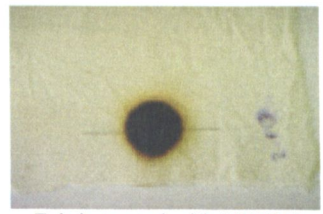

Fabric treated with 1PH/3U
Char length 2.5 cm

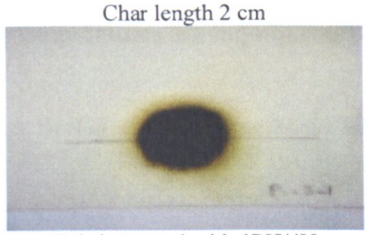

Fabric treated with 1PH/4U
Char length 3.5 cm

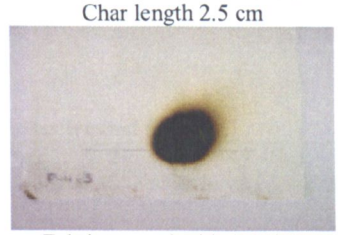

Fabric treated with 1PH/5U
Char length 3.5 cm

Figure4.2. The flame test results from fabrics treated with the PH/U condensates.

The samples containing up to 10 moles of urea passed the flame test and the samples with higher concentration of urea failed the flame test. No after glow and no holes were found in the treated fabrics that passed the flame test, the physical strength of the fabrics was acceptable and no change in their appearance can be observed. The treated fabric was very soft and exhibited crease resist properties. The maximum weight added on to the fabric from the FR treatments was approximately 10% before the washing stage. Photographs from the flame tests are shown in Figure 4.3.

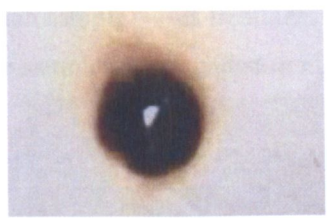

Fabric treated with 1PH/6U condensate
Char length: 3.5 cm

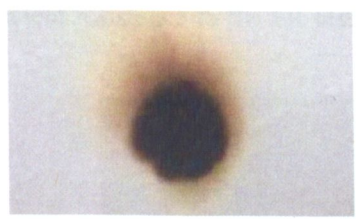

Fabric treated with 1PH/8U condensate
Char length: 3.7 cm

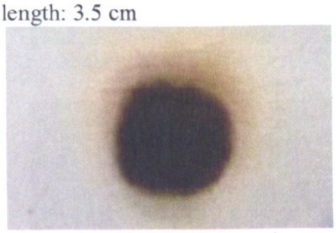

Fabric treated with 1PH/10U condensate
Char length: 3.8 cm

Figure4.3. The flame test results from the fabrics treated with one mole phosphorous acid and various moles of urea.

4.1.5 Treatment of cotton fabric with PA/U condensate

The pad-liquor contained:

500 g/l of urea condensate solution

10 g/l of wetting agent

The wet pick up was 80%. All the samples were dried at 70℃ for 84 seconds the curing temperatures are highlighted in Table 4.3.

Table4.3. Drying and curing conditions for PA/U condensates treated fabric.

Prepared condensate	Fabric code	Curing temperature ℃	Time of curing (second)	The length of char cm
1 mole of phosphoric acid to 2 moles urea [1PA/2U]	PA-1-1	165	140	3.8
	PA-1-2	160	120	3.7
1 mole of phosphoric acid to 3 moles of urea [1PA/3U]	PA-2-1	165	120	3.8
	PA-2-2	160	120	3.7
1 mole of phosphoric acid to 4 moles of urea [1PA/4U]	PA-3-1	165	120	4.0
	PA-3-2	160	120	3.5
1 mole of phosphoric acid to 5 moles of urea [1PA/5U]	PA-4-1	165	120	4.5
	PA-4-2	160	120	4.4

After the application of urea condensates, all the samples were washed with hard water containing 2 g/l of sodium carbonate (pH ~11) and 1 g/l wetting agent, at a liquor ratio of 20:1, for 20 minutes at 100℃. The flame test was then carried out on each sample. This treatment gave sufficient resistance to the FR test, pictures of the samples are provided in Figure 4.4.

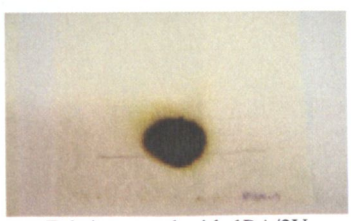

Fabric treated with 1PA/2U
Char length 3.8 cm

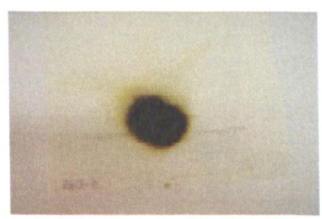

Fabric treated with 1PA/3U
Char length 3.5

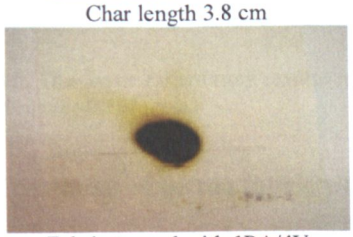

Fabric treated with 1PA/4U
Char length 3.5 cm

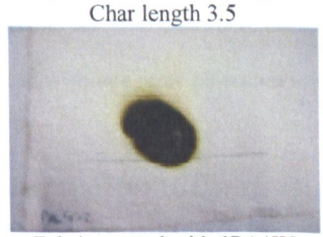

Fabric treated with 1PA/5U
Char length 4.4 cm

Figure4.4. The flame retardancy results from fabrics treated with the PA/U condensates.

To achieve the desirable flame retardancy properties on cotton fabric, the required amount of urea in the phosphoric acid urea condensate needs to be determined. A series of condensates containing PA/6U, 1PA/8U, 1PA/10U, 1PA/12 and 1PA/14U were prepared. As explained previously in section 3.2.4, by increasing the amount of urea in the mixture, the exothermic reaction can be controlled; however the cold water solubility of these products was insufficient but these urea condensate solution could be prepared using warm water (50°C). The application of these urea condensates were carried out in the same procedure described in 4.1.3. All the samples were washed under alkaline conditions as explained previously (section 4.1.3).

The FR test was carried out on all samples; the fabrics which were treated with pre-condensates of 1PA/6U, 1PA/8U and 1PA/12U all showed acceptable flame retardancy properties but the other samples failed this test. Photographs of the flame tested fabric are shown in Figure 4.5.

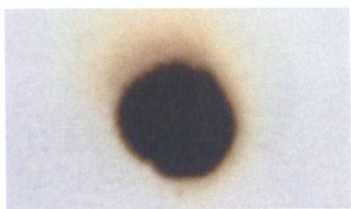

Fabric treated with 1PA/6U condensate
Char length: 3.5 cm

Fabric treated with 1PA/8U condensate
Char length: 4.5 cm

Fabric treated with 1PA/10U condensate

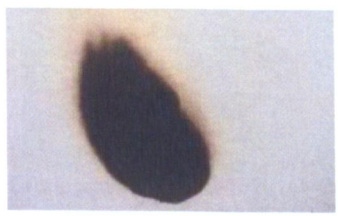

Fabric treated with 1PA/12U condensate
Char length: 8.5 cm

Figure4.5. The flame retardancy results from fabrics treated with one mole phosphoric acid and various moles of urea.

4.1.6 Treatment of cotton fabric with urea condensate of S/PH/U

This treatment was carried out in the same manner as the other products the fabric was impregnated at 80% wet pick up using 500 g/l of the S/PH/U solution and 10

g/l of wetting agent. Various urea condensates with 1 mole of sulphamic acid, 1 mole phosphorous acid and different molar ratios of urea were applied to the substrates. The drying and curing process was the same for all samples, 2 minutes drying at 80°C, and 2 minutes curing at 160°C.

The FT-IR spectra are provided for all samples. The flame test results from all treated fabrics are indicated in Figure 4.6. Only the fabric treated with 1S/1PH/20U failed the test.

Figure4.6. The flame test results from the fabrics treated with various molar ratios of S/PH/U condensates.

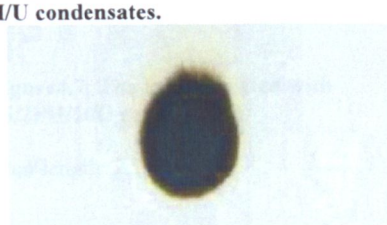

Fabric treated with 1S/1PH/6U condensate
Char length:4 cm

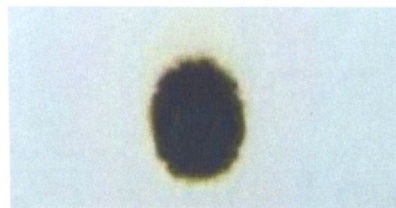

Fabric treated with 1S/1PH/8U condensate
Char length:4 cm

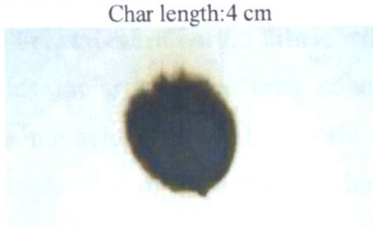

Fabric treated with 1S/1PH/10U condensate
Char length:4.5 cm

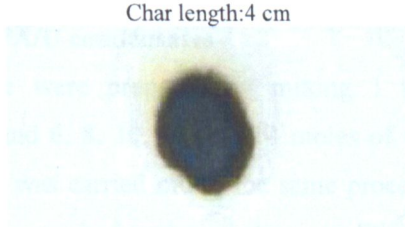

Fabric treated with 1S/1PH/12U condensate
Char length:4 cm

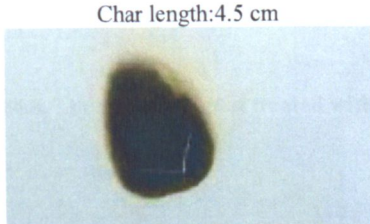

Fabric treated with 1S/1PH/14U condensate
Char length:4.5 cm

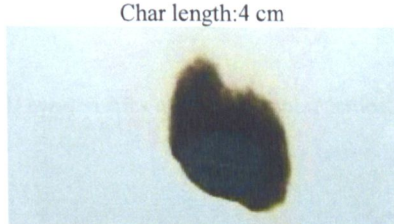

Fabric treated with 1S/1PH/16U condensate
Char length: 7 cm

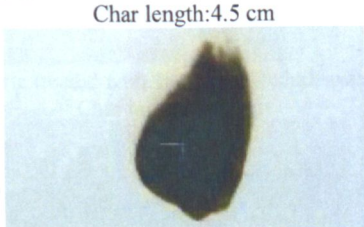

Fabric treated with 1S/1PH/18U condensate
Char length: 5.7

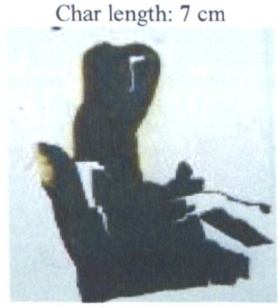

Fabric treated with 1S/1PH/20U condensate
The fabric burned completely, but the fabric structure was still kept.

The effect of phosphorous acid in the urea condensate

To improve the flame retardancy behaviour, a higher molar ratio of phosphorous acid was used to make the condensates. The urea condensate 1S/2PH/10U was produced, as stated in section. The application procedure in section was carried out to apply the condensate to the cotton fabric. The fabric was washed as described in section 4.1.3. The FT-IR analysis is provided in section 3.5.4.2. After the flame test, the fabric treated with this condensate performed significantly better than the fabric treated with the previous condensate; the char length was reduced Figure 4.7.

Figure4.7. The fabric treated with 1S/2PH/10U condensate.

Char length: 2.5 cm

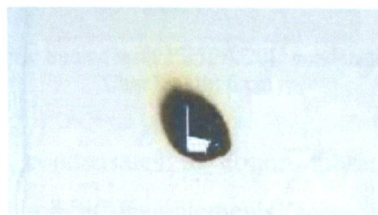

4.1.7 Treatment of cotton fabric with S/PA/U condensates

Various molar ratio of urea condensate were prepared by mixing 1 mole sulphamic acid, 1 mole phosphoric acid and 6, 8, 10, 12 and 14 moles of urea. The application of these urea condensates was carried out in the same procedure described in 4.1.3. All the samples were washed under alkaline conditions as explained previously (4.1.3).

Figure4.8. The fabric samples treated with S/PA/U condensates at various molar ratios.

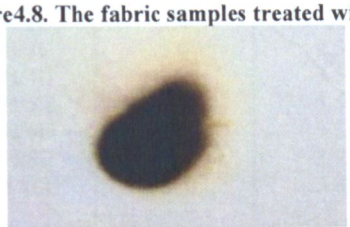

Fabric treated with 1S/1PA/6U condensate
Char length: 2.8 cm

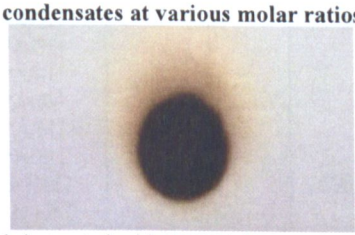

Fabric treated with 1S/1PA/8U condensate
Char length: 3.5 cm

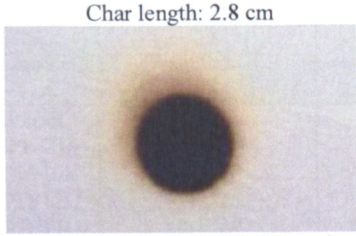

Fabric treated with 1S/1PA/10U condensate
Char length: 3.4 cm

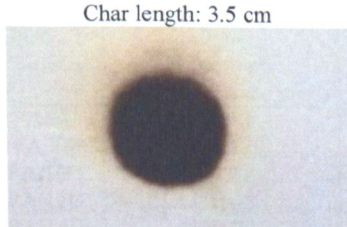

Fabric treated with 1S/1PA/12U condensate
Char length: 3.7 cm

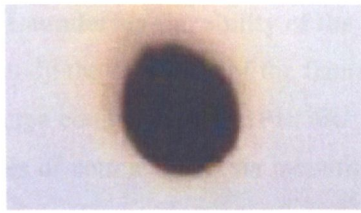

Fabric treated with 1S/1PA/14U condensate
Char length: 4 cm

Fabric treated with 1S/1PA/16U condensate
Char length: 4 cm

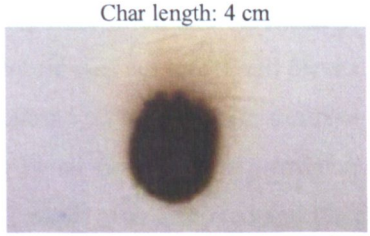

Fabric treated with 1S/1PA/18U condensate
Char length: 4 cm

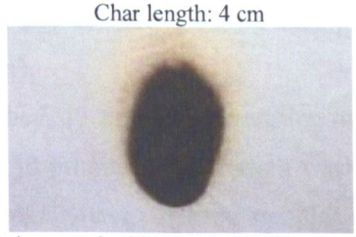

Fabric treated with 1S/1PA/20U condensate
Char length: 6 cm

The application of various types of urea condensates to cotton fabric, the relationship between the phosphorus, sulphur and nitrogen elements (according to the molar ratios of the initial materials applied at the beginning for urea condensate production) and char length produced on the treated fabric after flame test are reported in Table 4.4.

Table4.4.The relationship between the required elements for the production of urea condensate and char length produced after the flame test on cotton fabric treated with the urea condensate.

Phosphorous acid/Urea Condensate			Phosphoric acid/Urea Condensate		
Urea condensate	Phosphorus: Nitrogen	Char length cm	Urea condensate	Phosphorus: Nitrogen	Char length cm
1PH/2U	1:4	2	1PA/2U	1:4	3.8
1PH/3U	1:6	2.5	1PA/3U	1:6	3.5
1PH/4U	1:8	3.5	1PA/4U	1:8	3.5
1PH/5U	1:10	3.5	1PA/5U	1:10	4.4
1PH/6U	1:12	3.5	1PA/6U	1:12	3.5
1PH/8U	1:16	3.7	1PA/8U	1:16	4.5
1PH/10U	1:20	3.8	1PA/10U	1:20	Burned
			1PA/12U	1:24	8.5
Sulphamic acid/Phosphorous acid/urea Condensate			Sulphamic acid/ Phosphoric acid/Urea Condensate		
Urea condensate	Sulphur: Phosphorus: Nitrogen:	Char length cm	Urea condensate	Sulphur: Phosphorus: Nitrogen	Char length cm
1S/1PH/6U	1:1:13	4	1S/1PA/6U	1:1:13	2.8
1S/1PH/8U	1:1:17	4	1S/1PA/8U	1:1:17	3.5
1S/1PH/10U	1:1:21	4.5	1S/1PA/10U	1:1:21	3.4
1S/1PH/12U	1:1: 25	4	1S/1PA/12U	1:1: 25	3.7
1S/1PH/14U	1:1: 29	4.5	1S/1PA/14U	1:1: 29	4.0
1S/1PH/16U	1:1:33	7	1S/1PA/16U	1:1:33	4.0
1S/1PH/18U	1:1:37	5.7	1S/1PA/18U	1:1:37	4.0
1S/1PH/20U	1:1:41	Burned	1S/1PA/20U	1:1:41	6.0
1S/2PH/10U	1:2:21	2.5			

4.2. Laundering durability of the flame retardant fabrics

To study the durability of the flame retardancy of pilot plant scale treated fabrics, the urea condensates 1S/1PH/10U and 1S/2PH/10U were applied to two 5 meter pieces of cotton fabric via a continuous method. The pad liquors contained 500 g/l of condensate, 10 g/l of wetting agent (Sandozine NIE). The impregnated fabrics were dried and cured for 3 minutes at 165°C. After curing each piece of the fabric was cut into small pieces (33×25 cm).

The flame retardant fabric samples were washed, 13 times, in a washing machine with Persil Colour Care powder at 40°C for 30 minutes. After each wash-cycle one sample was removed for the flame retardancy test. All the samples treated with 1S/1PH/10U condensate, passed the flame test, but treatments with the 1S/2PH/10U condensate gave variable results - a few samples failing the flame test. This variation can be explained by uneven curing since one sample passed the flame test even after 13 cycles in a washing machine. Photographs of the tested pieces are provided in Figure 4.9 and 4.10. After 10 washing cycles the handle of the fabric had changed to a slightly harsh handle. It appears that some material has been removed from the surface of the fabric affecting the fabric handle. This is clear from the SEM photograph in section 4.6.

The FT-IR analysis is provided for the washed fabrics in section 4.8.6.

Figure4.9. The durability performance of fabric flame retardancy to laundering, fabrics treated with 1S/1PH/10U condensate in continuous method.

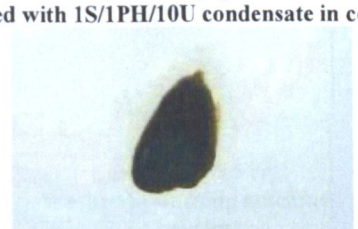

Char length: 4.8 cm
Washed in washing machine
1 cycle

Char length: 5.5 cm
Washed in washing machine
2 cycles

Char length: 6 cm
Washed in washing machine
3 cycles

Char length: 7 cm
Washed in washing machine
4 cycles

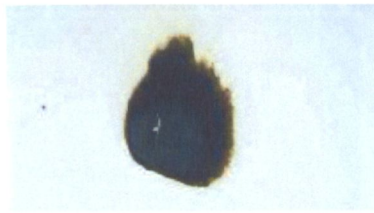

Char length: 6 cm
Washed in washing machine
5 cycles

Char length: 7.3 cm
Washed in washing machine
6 cycles

Char length: 5 cm
Washed in washing machine
7 cycles

Char length: 8.5 cm
Washed in washing machine
8 cycles

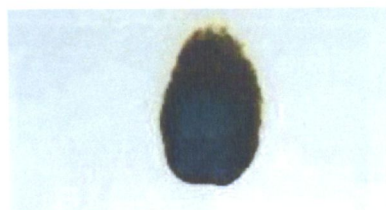

Char length: 5.8 cm
Washed in washing machine
9 cycles

Char length: 7.3 cm
Washed in washing machine
10 cycles

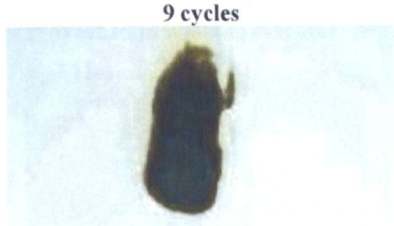

Char length: 5.5 cm
Washed in washing machine
11 cycles

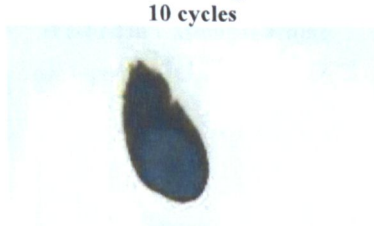

Char length: 4.8 cm
Washed in washing machine
12 cycles

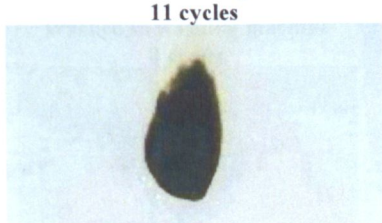

Char length: 5.0 cm
Washed in washing machine
13 cycles

Figure4.10. Performance of fabric flame retardancy to laundering, fabrics treated with 1S/2PH/10U condensate in continuous method.

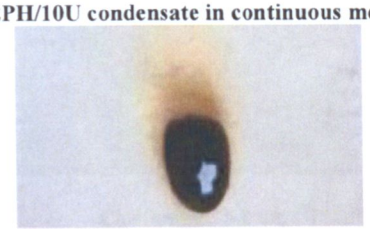

Char length: 4 cm
Washed in washing machine
1 cycle

Char length: 4.9 cm
Washed in washing machine
2 cycles

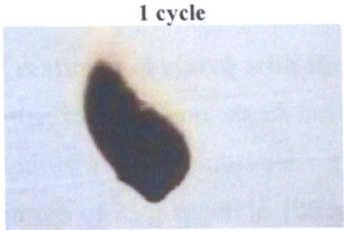

Char length: 7 cm
Washed in washing machine
4 cycles

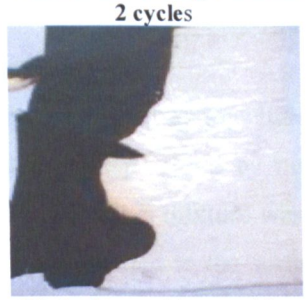

Washed in washing machine
5 cycles

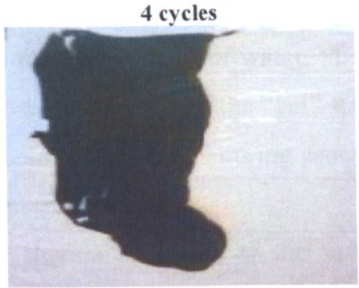

Washed in washing machine
6 cycles

Washed in washing machine
7 cycles

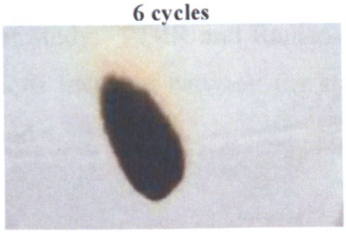

Char length: 4.8 cm
Washed in washing machine
8 cycles

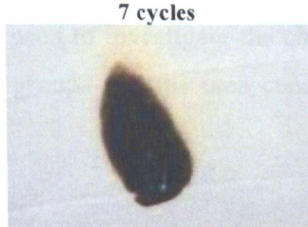

Char length: 5.5 cm
Washed in washing machine
9 cycles

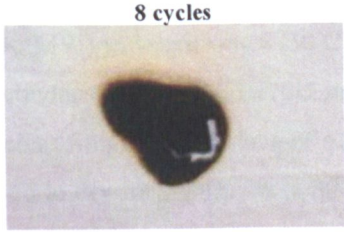

Char length: 3.5 cm
Washed in washing machine
10 cycles

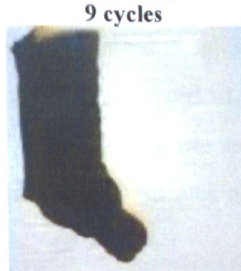

Washed in washing machine
11 cycles

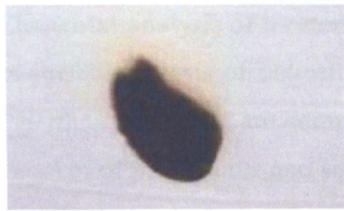

Char length: 5.2 cm
Washed in washing machine
12 cycles

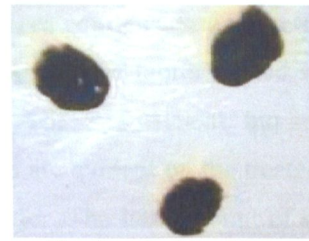

Char length: 6.0 – 6.5 cm
Washed in washing machine
13 cycles

4.3. Treatment of starch with the S/PH/U condensate

In further investigation, starch having a similar chemical structure to cellulose was selected as a model substrate. The starch solution was prepared by making a suspension of 25 g starch in 100 ml of water (25% g/l). This mixture was heated to 80°C to make a viscous solution. A thin layer was applied to the surface of a glass slide and allowed to air dry. The application of 1S/2PH/10U to the starch was carried out by preparing a mixture of 3.5 g starch, 3.5 g of 1S/2PH/10U in solid form and 15 ml of water, this mixture was heated to 80°C to obtain a "gel" from starch. A film of the "gel" starch was produced by coating a glass slide with this compound. In the curing process both coated slides were heated at 165°C for 4 minutes in a stenter.

DSC thermal analysis of the urea condensate treated starch was carried out (section 4.7.3). This reaction produced a flame retardant starch which needs further study. FT-IR and Raman analysis were used to investigate the chemical reactions involved between the starch hydroxyl groups and the urea condensate (section 4.9.)

4.4. Treatment of polyvinyl alcohol with the 1S/2PH/10 condensate

A 30% polyvinyl alcohol solution was prepared by dissolving polyvinyl alcohol (12500 MW) in warm water (50°C). To 10 cc of the viscous solution, 3 grams of urea condensate of 1S/2PH/10U in solid form was added and mixed to produce a very clear film on the surface of a flat glass slide. The coating on the surface was allowed to dry for 2 minutes at 80°C and the slide cured for 2 minutes at 160°C in a laboratory stenter (slide was stuck on fabric).

Both untreated and treated polyvinyl alcohol films were analysed by FT-IR; DSC thermal analysis was also performed on each sample (sections 4.10 and 4.7.4).

4.5. Elemental analysis of treated fabric with urea condensate products

The elemental analysis of untreated cotton fabric and the fabric treated with the 1S/1PH/10U condensate are compared in Table 4.5. A sufficient, but still very low, amount of phosphorus and sulphur elements are evident on the treated fabric which are able to produce a flame retardant fabric. The low amount of nitrogen may be due to the liberation of ammonia as the main gas which is evolved during the curing process.

Table4.5. Elemental analysis of untreated cotton fabric and treated fabric with 1S/1PH/10U.

Analysed elements	Untreated cotton fabric	1S/1PH/10U treated cotton fabric
Carbon	44.0	41.5
Hydrogen	6.45	6.15
Nitrogen	T/N*	1.0
Sulphur	T/N	0.45
phosphorus	T/N	1.75

*T/N= Trace or nil (<0.3%)

The actual amount of each elements were applied on fabric has been calculated from the 500g/l of urea condensates solution and 80% wet pick up. These results have been provided in Table 4.6.

To study the durability of the treatment to laundering process, the elemental analysis of two fabrics treated with 1S/1PH/10U after 1 cycle and 10 cycles of washing in a washing machine with Persil Colour Care powder are indicated in Table 4.7.

Table 4.6. Elemental analysis calculations from the amount of pad liquor applied to the treated fabrics, with 1S/1PH/10U and 1S/2PH/10U condensates.

Analysed elements	Treated fabric with 1S/1PH/10U %	Treated fabric with 1S/2PH/10U %
Nitrogen	6.5	6.5
Sulphur	1.39	1.39
phosphorus	1.4	2.8

An acceptable result for phosphorus and sulphur content after laundering process was achieved and can confirm the durability of urea condensate treatment to washing process. The unexpected result for phosphorus can be explained due to the uneven curing process in continuous treatment, section 4.2.

Table4.7. Elemental analysis of treated fabric with 1S/1PH/10U after one and 10 washing cycles in a washing machine.

Analysed elements	1S/1PH/10U treated cotton fabrics washed in a washing machine	
	Washed 1cycle	Washed 10 cycles
Carbon	40.6	40.6
Hydrogen	5.65	5.95
Nitrogen	T/N	T/N
Sulphur	0.9	0.5
phosphorus	0.8	1.05

4.6. Scanning electron microscopy

In this research some micrographs from the untreated cotton fabric and also fabric treated with various types of urea condensate solutions are provided. The magnification was fixed at X750 for all the micrograph samples and EDX elemental analysis was used to show the distribution of different elements on treated fabrics.

Untreated cotton fabric

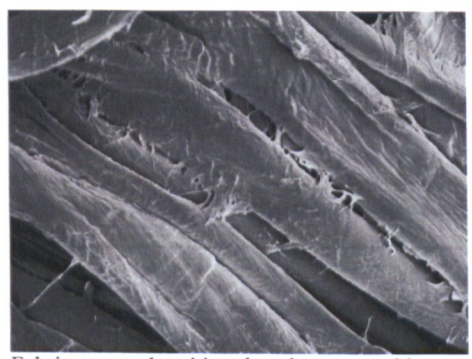

Fabric treated with phosphorous acid urea condensate , fabric code P-2-2

Fabric treated with 1S/4U condensate solution.

Figure4.11. Micrographs of untreated cotton fabric and fabric treated with urea condensates.

The coated polymer on the surface of the treated fabric is very clear, even after all the fabrics had been boiled in alkaline water for 20 minutes as indicated

previously. The fabric treated with phosphorous acid/ urea condensate exhibited excellent flame retardancy. The fabric treated with sulphamic acid/urea condensate showed only partial flame retardancy.

The elemental distribution map is also provided in Figure 4.12 and 4.13.

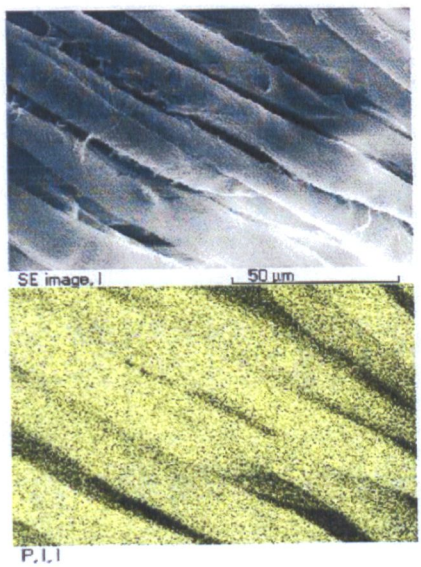

Figure4.12. Distribution of phosphorus on fabric treated with phosphorous acid urea condensate, 1PH/3U.

The yellow dots indicate the distribution of phosphorus on the surface of fabric.

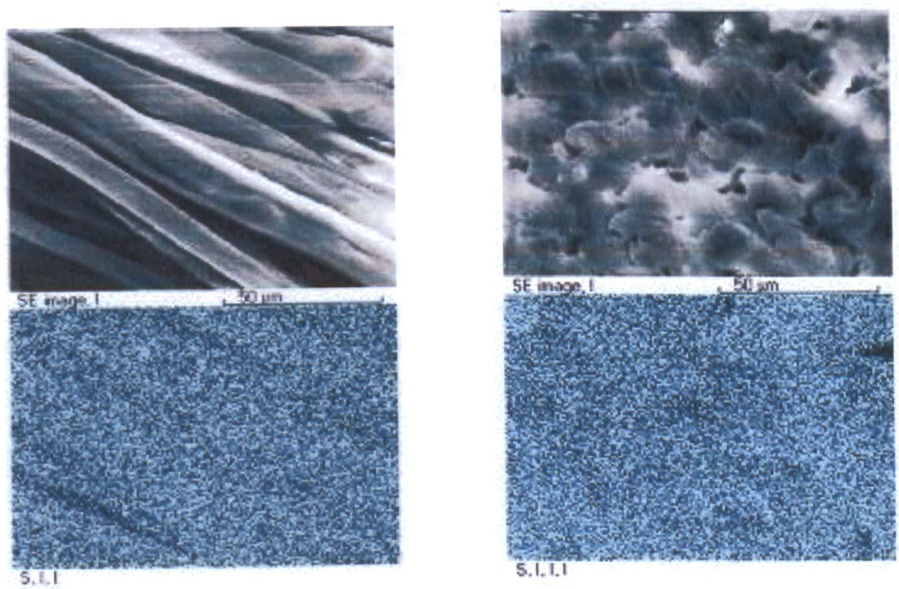

Figure4.13. Distribution of sulphur on the surface and cross section of fabric treated with the sulphamic acid urea condensate, 1S/4U.

The elemental analysis record is also shown in Figures, 4.14 and 4.15.

In comparison, the amount of phosphorus on the fabric treated with the phosphorous acid urea condensate is much higher than the amount of sulphur on the fabric treated with the sulphamic acid urea condensate.

Homogeneous distribution of sulphur and phosphorus elements is evidence that element has penetrated into the centre of the fibre therefore it can reinforce the durability of this treatment to multi-washing processes.

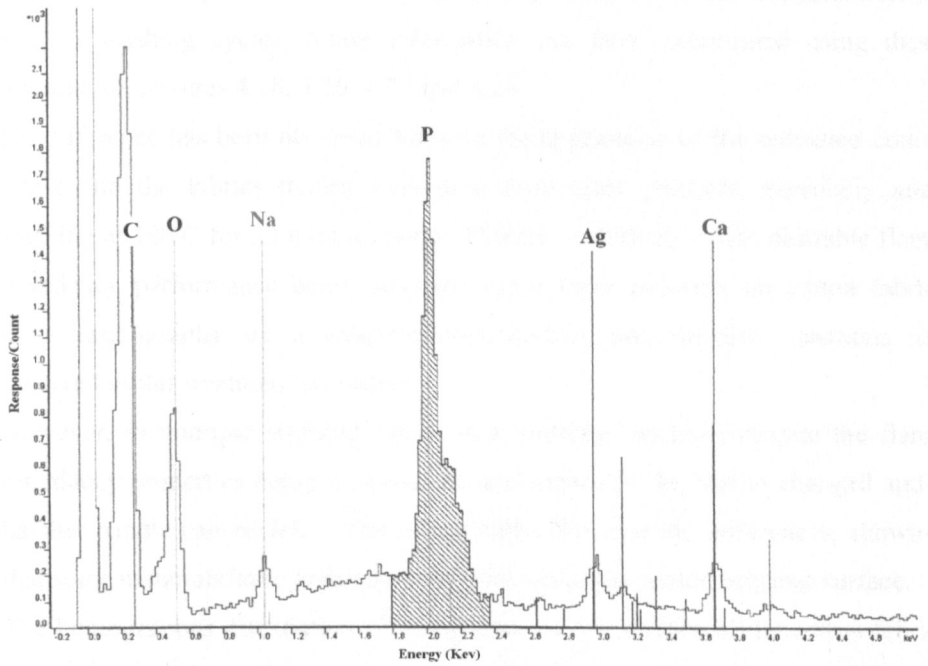

Figure4.14. Elemental analysis of treated fabric with phosphorous acid condensate, 1PH/3U.

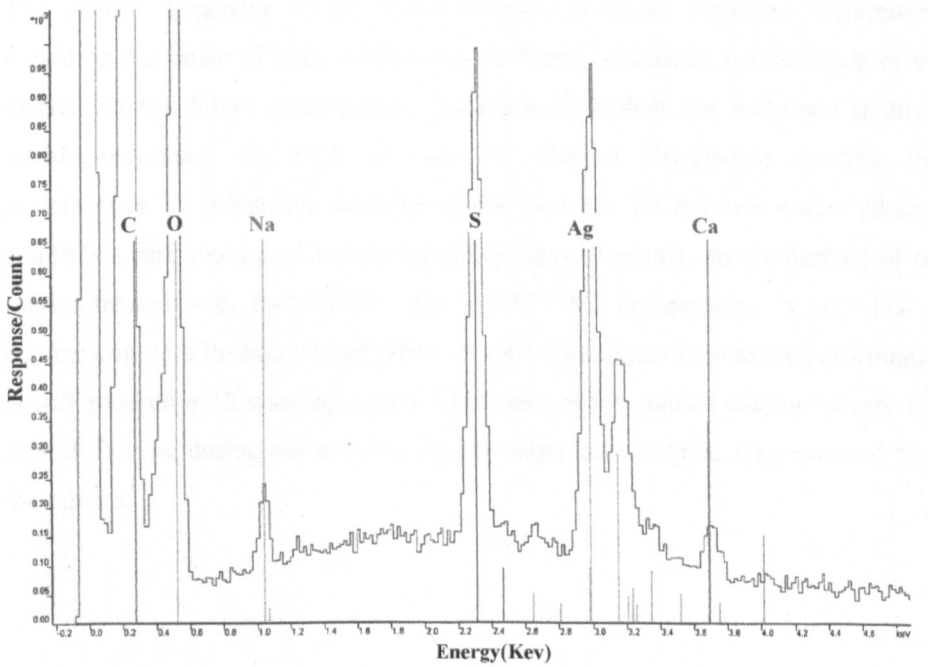

Figure4.15. Elemental analysis of treated fabric with sulphamic acid/urea condensate, 1S/4U.

The characteristic analytical results from the urea condensate treated fabrics were compared comparing to results from the commercial fabric treated with Proban (THPC/Ammonia). The treated fabrics of 1S/1PH/10U and 1S/2PH/10U were washed in washing machine with Persil Colour Care powder and analysed after 10 and 13 washing cycles. Some information has been determined using these micrograph pictures 4.18, 4.20, 4.22 and 4.24.

No difference has been observed between the appearance of the untreated cotton fabric and the fabrics treated with urea condensate products, especially after washing at 100°C for 20 minutes under alkaline conditions. With desirable flame retardancy performance being achieved using these products on cotton fabric, these micrographs are a valuable confirmation that chemical reactions are involved in this treatment procedure.

However, in multiple washing cycles in a washing machine, despite the flame retardancy properties being retained, the appearance of the fabrics changed and a harsher handle can be felt. The micrographs illustrate the differences, showing that some materials have been removed from the fabric coated polymer surface.

The homogeneous distribution of phosphorus on the surface of the cotton fabric, following washing, also confirms that chemical reactions occurred between cellulose and urea condensates.

The energy dispersive X-ray micro analysis provides sufficient information regarding the effect of each element on the flame retardancy performance of the fabric. Cotton fabric commercially treated with Proban can withstand multiple laundry-processes; the high amounts of retained phosphorus confirm this performance. Following washing at the boil for 20 minutes under alkaline conditions, the amount of remaining phosphorus elements, on the surface of the fabrics treated with 1S/1PH/10U and 1S/2PH/10U condensates, is very low in comparison with Proban treated fabric. Even so, the flame retardancy performance is still good after 13 washing cycles. The amount of retained sulphur is very low in both fabrics; during the washing process significant sulphur was removed from the fabrics.

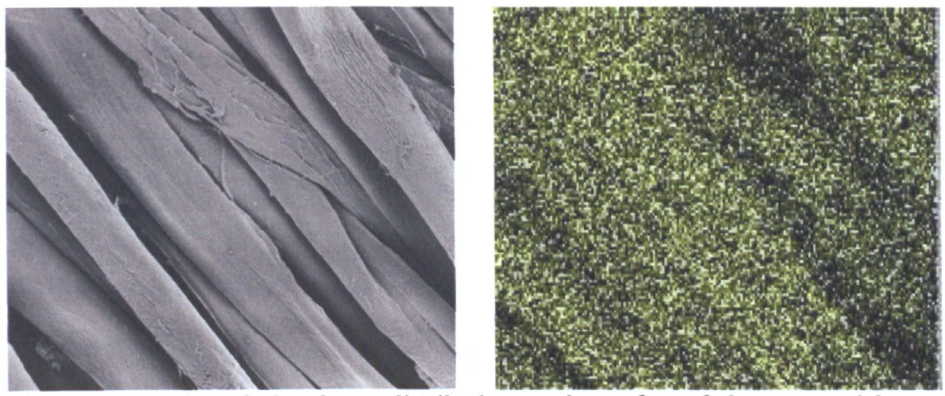

Figue4.16. Mapping of phosphorus distribution on the surface of the commercial cotton fabric treated with Proban.

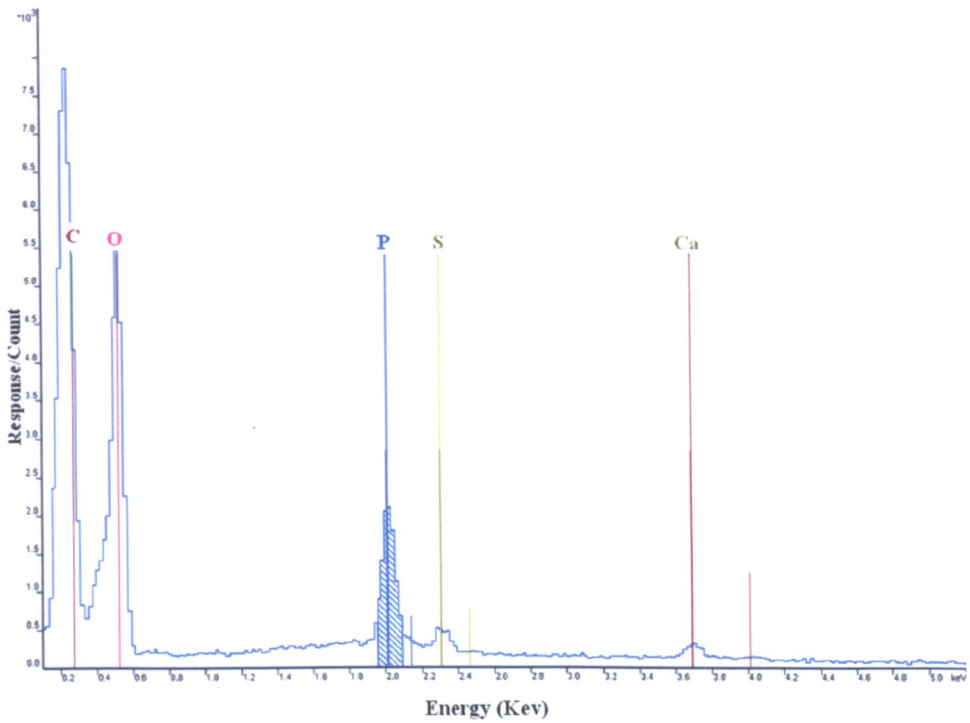

Figure4.17. Energy dispersion X-ray micro analysis for the elements distributed on the surface of commercial cotton fabric treated with Proban.

Table4.8. The elemental analysis obtained using the energy dispersion X-ray analysis technique on the surface of commercial cotton fabric treated with Proban.

Element	P	S	C	O	Ca	Mg
Atomic %	2.81	0.54	36.11	60.13	0.41	-

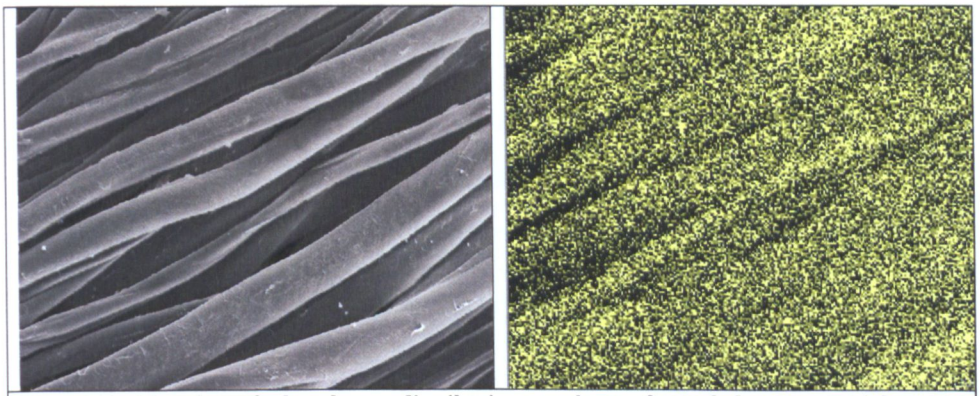

Figue4.18. Mapping of phosphorus distribution on the surface of the commercial cotton fabric treated with Proban, washed in a washing machine with Persil powder after 4 washing cycles.

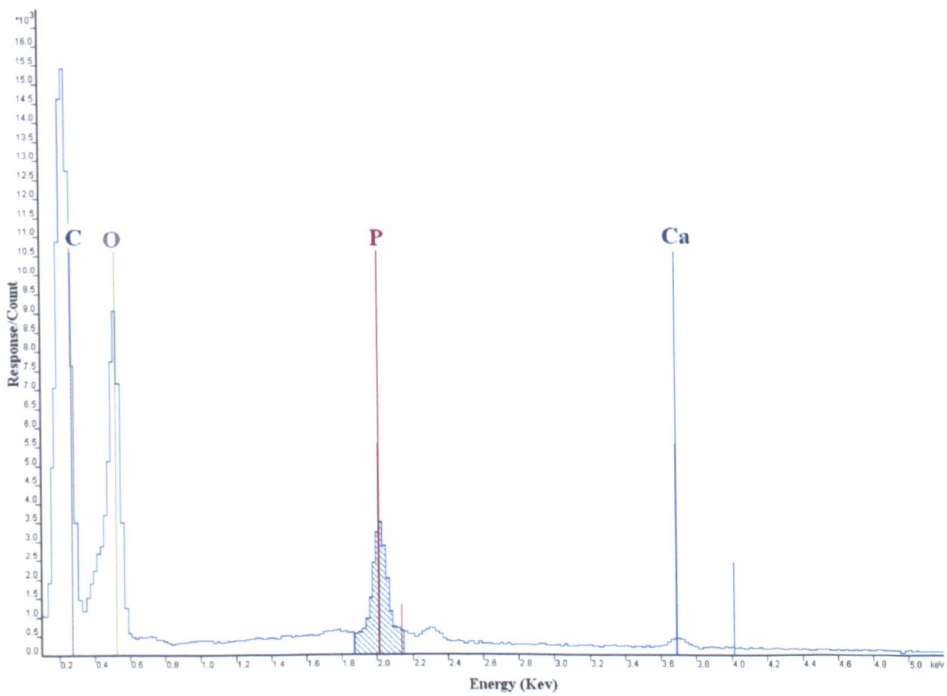

Figure4.19. Energy dispersion X-ray micro analysis for the elements distributed on the surface of commercial cotton fabric treated with Proban, washed in a washing machine with Percil powder after 4 washing cycles.

Table4.9. The elemental analysis obtained using the energy dispersion X-ray analysis technique on the surface of commercial cotton fabric treated with Proban, washed in a washing machine with Percil powder after 4 washing cycles.

Element	P	S	C	O	Ca	Mg
Atomic %	3.16	-	38.13	58.31	0.4	-

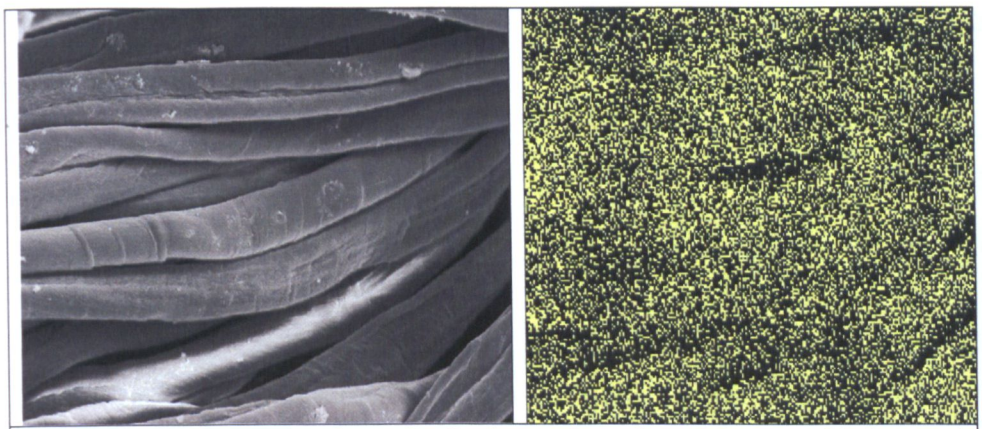

Figure4.20. Mapping of phosphorus distribution on the surface of the cotton fabric treated with the 1S/1PH/10U condensate, unwashed sample.

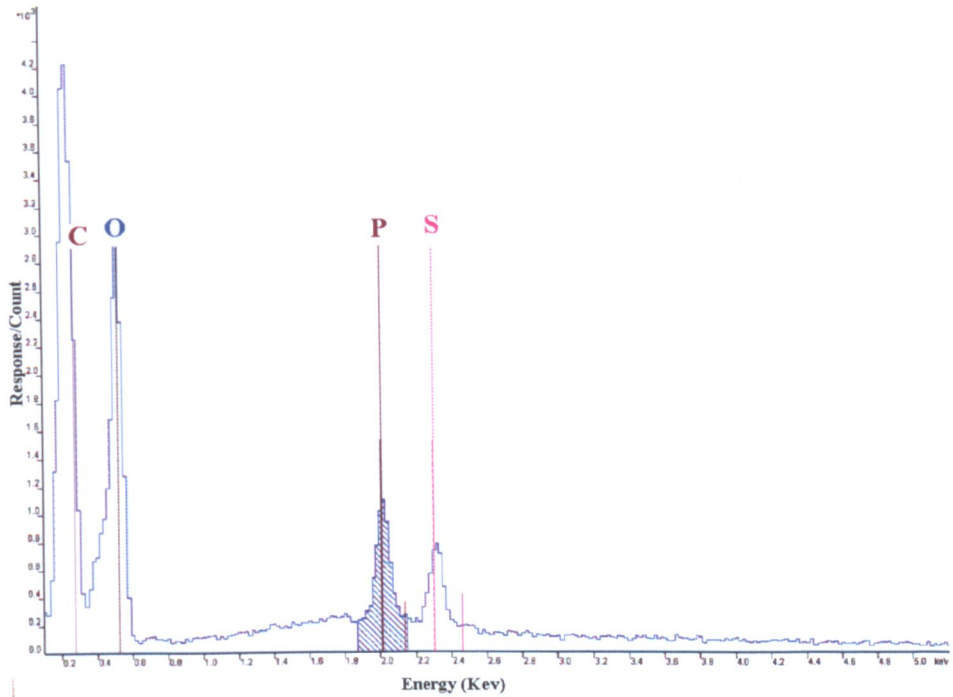

Figure4.21. Energy dispersion X-ray micro analysis for the elements distributed on the surface of the cotton fabric treated with the 1S/1PH/10U condensate, unwashed sample.

Table4.10. The elemental analysis obtained using the energy dispersion X-ray analysis technique on the surface of the cotton fabric treated with the 1S/1PH/10U condensate, unwashed sample.

Element	P	S	C	O	Ca	Mg
Atomic %	1.90	1.40	35.11	61.59	-	-

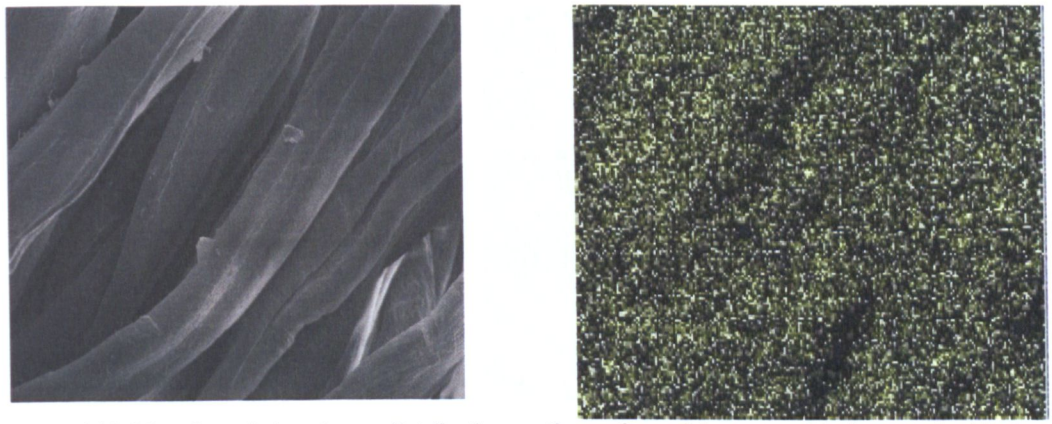

Figure4.22. Mapping of phosphorus distribution on the surface of the cotton fabric treated with the 1S/1PH/10U condensate, washed at boil temperature for 20 minutes in alkaline condition.

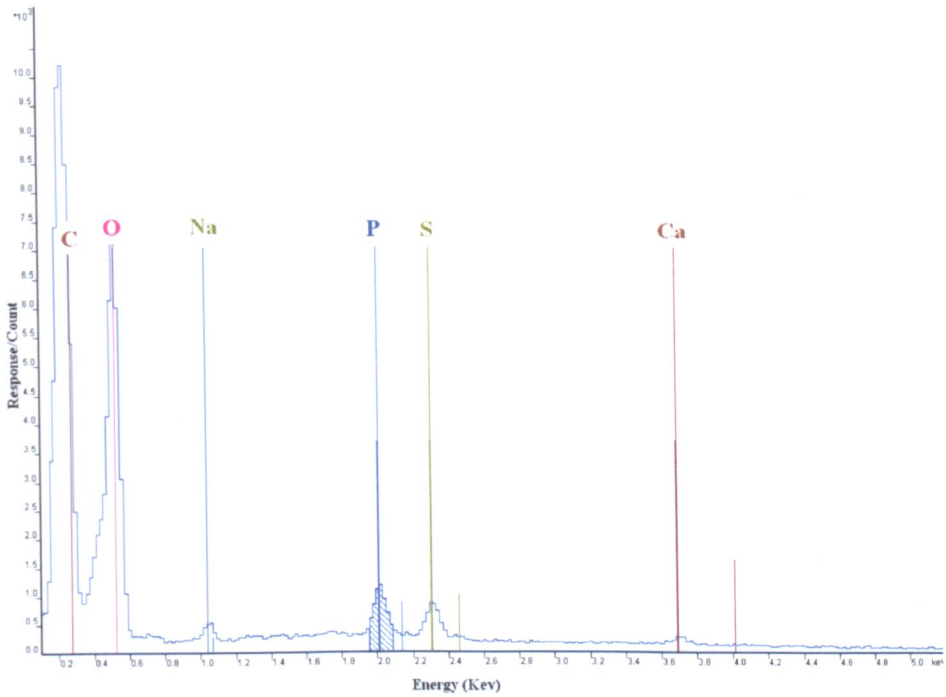

Figure4.23. Energy dispersion X-ray micro analysis for the elements distributed on the surface of the cotton fabric treated with 1S/1PH/10U condensate, washed for 20 minutes in alkaline condition at 100°C.

Table4.11. Elemental analysis obtained using the energy dispersion X-ray analysis technique on the surface of the cotton fabric treated with 1S/1PH/10U condensate, washed for 20 minutes in alkaline condition at 100°C.

Element	P	S	C	O	Ca	Na
Atomic %	1.15	0.90	35.96	60.64	0.26	1.08

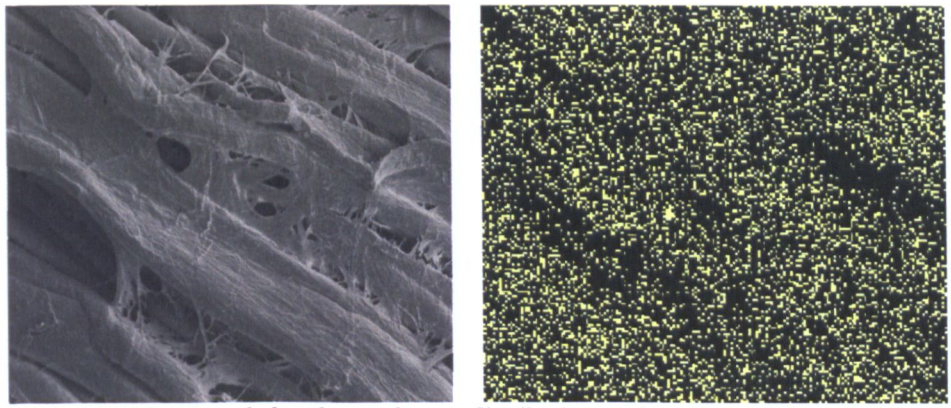

Figure4.24. Mapping of phosphorus element distribution on the surface of the cotton fabric treated in continuous method with the 1S/1PH/10U condensate, washed in a washing machine with Persil powder after 10 washing cycles.

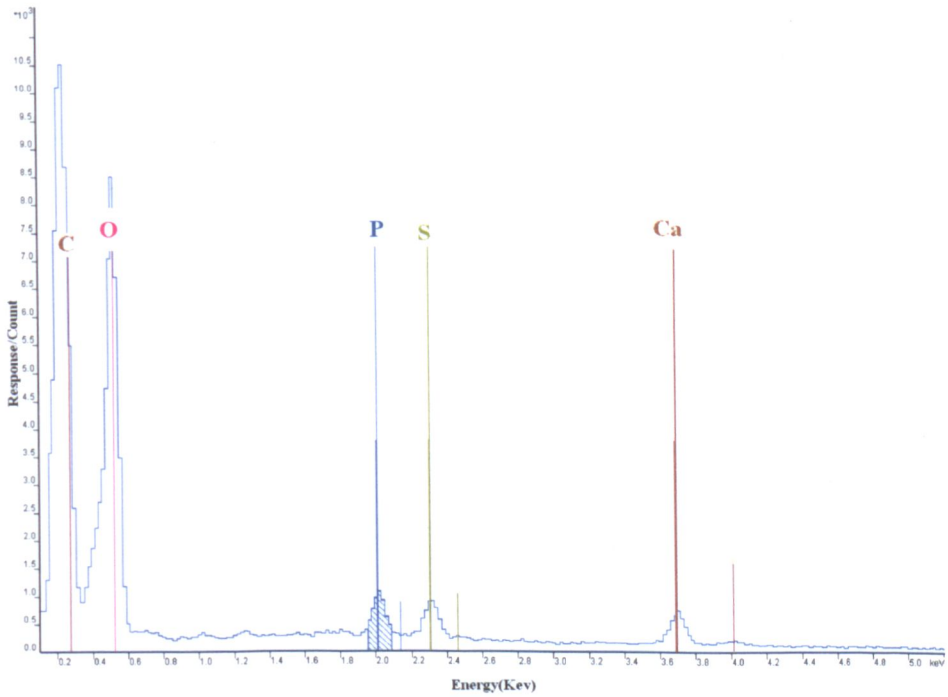

Figure4.25. EDX-ray micro analysis for the elements distributed on the surface of the cotton fabric treated in continuous method with the 1S/1PH/10U condensate, washed in a washing machine with Persil powder after 10 washing cycles.

Table4.12. The elemental analysis obtained using the ED X-ray analysis technique on the surface of the cotton fabric treated in continuous method with the 1S/1PH/10U condensate, washed in a washing machine with Persil powder after 10 washing cycles.

Element	P	S	C	O	Ca	Na
Atomic %	1.06	1.07	34.32	62.47	1.08	-

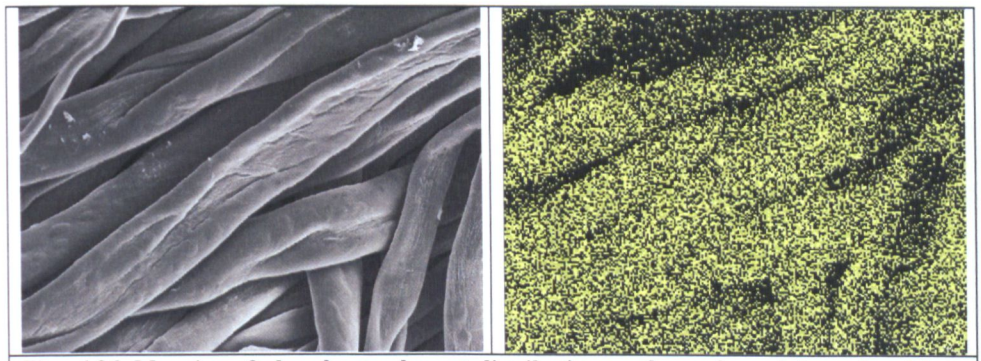

Figue4.26. Mapping of phosphorus element distribution on the surface of the cotton fabric treated with the 1S/2PH/10U condensate, unwashed sample.

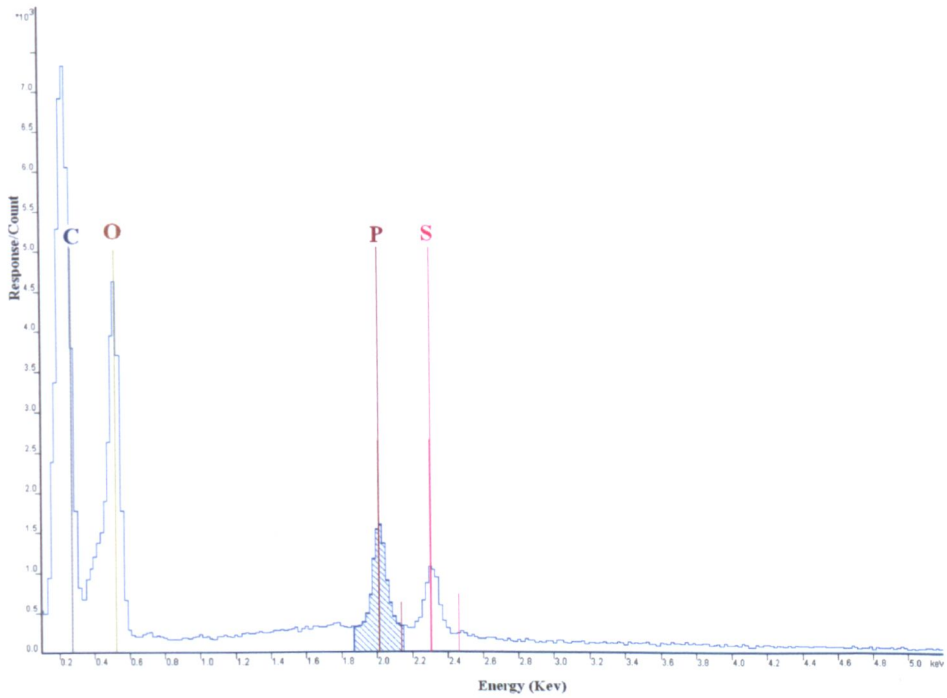

Figure4.27. Energy dispersion X-ray micro analysis for the elements distributed on the surface of the cotton fabric treated with the 1S/2PH/10U condensate, unwashed sample.

Table4.13. The elemental analysis obtained using the energy dispersion X-ray analysis technique on the surface of the cotton fabric treated with the 1S/2PH/10U condensate, unwashed sample.

Element	P	S	C	O	Ca	Mg
Atomic %	2.43	1.77	36.23	59.59	-	-

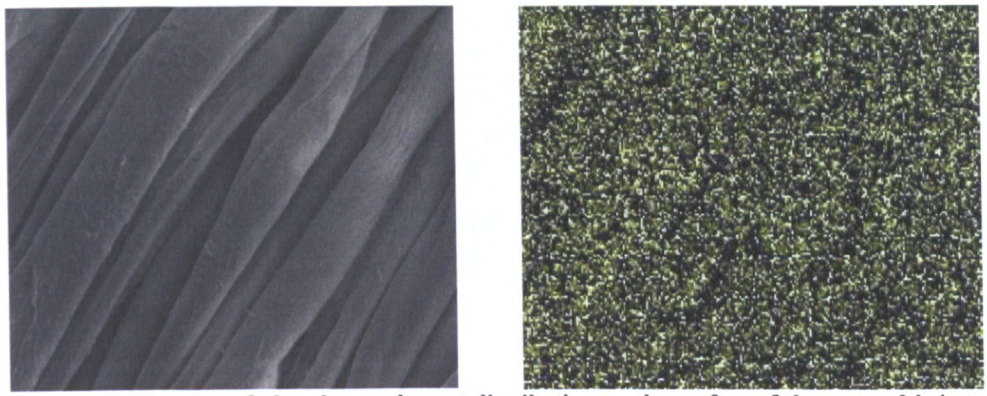

Figure4.28. Mapping of phosphorus element distribution on the surface of the cotton fabric treated with the 1S/2PH/10U condensate, washed at the boil for 20 minutes in alkaline condition.

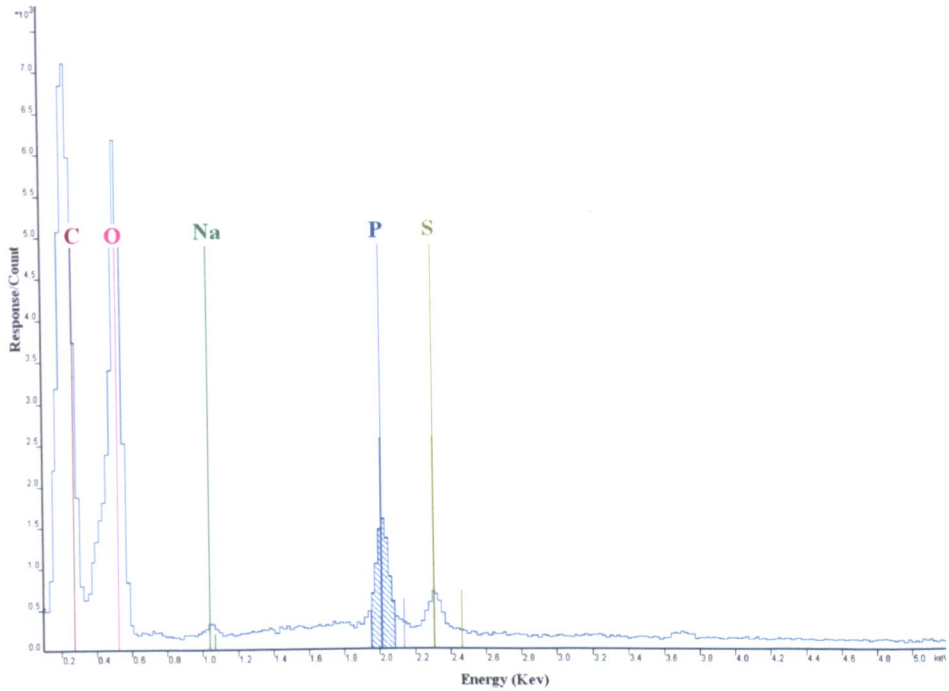

Figure4.29. Energy dispersion X-ray micro analysis for the elements distributed on the surface of the cotton fabric treated with 1S/2PH/10U condensate, washed for 20 minutes under alkaline conditions at 100°C.

Table4.14. The elemental analysis obtained using the energy dispersion X-ray analysis technique on the surface of the cotton fabric treated with 1S/2PH/10U condensate, washed for 20 minutes under alkaline conditions at 100°C.

Element	P	S	C	O	Ca	Na
Atomic %	1.51	0.54	33.56	64.05	-	0.34

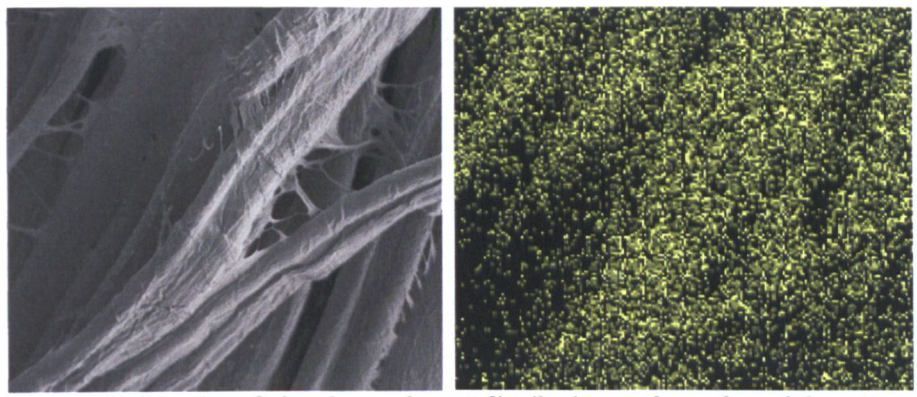

Figure 4.30. Mapping of phosphorus element distribution on the surface of the cotton fabric treated in continuous method with the 1S/2PH/10U condensate, washed in a washing machine with Persil powder after 13 washing cycles.

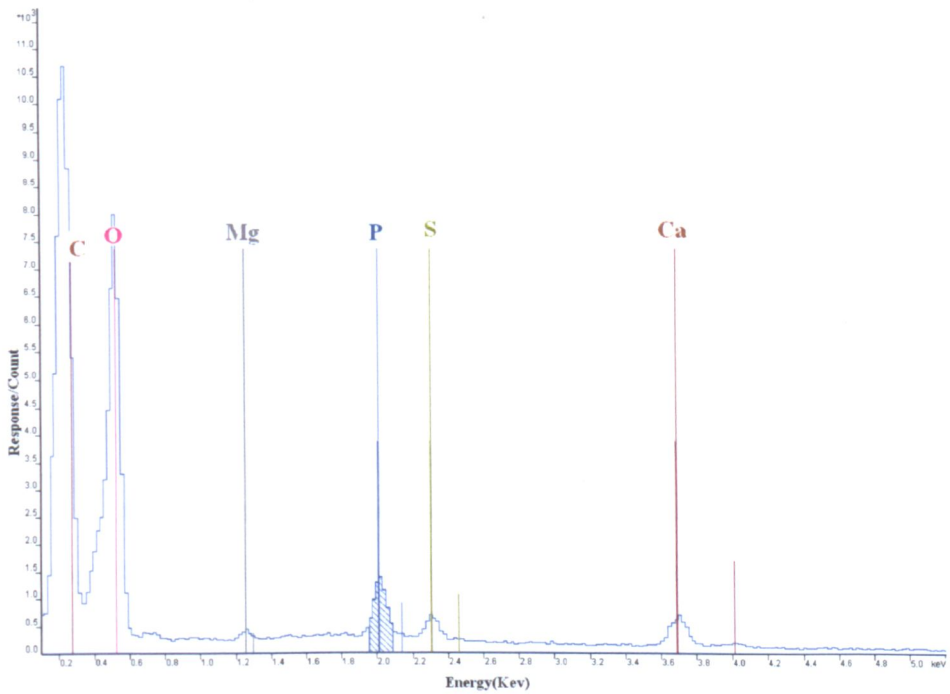

Figure4.31. EDX-ray micro analysis for the elements distributed on the surface of the cotton fabric treated in continuous method with the 1S/2PH/10U condensate, washed in a washing machine with Persil powder after 13 washing cycles.

Table4.15. The elemental analysis obtained using the ED X-ray analysis technique on the surface of the cotton fabric treated in continuous method with the 1S/2PH/10U condensate, washed in a washing machine with Persil powder after 13 washing cycles.

Element	P	S	C	O	Ca	Mg
Atomic %	1.36	0.62	35.15	61.66	0.97	0.23

4.7. Thermal analysis using Differential scanning calorimetry (DSC)

Thermal analysis of treated materials with the urea condensate solution has been carried out using Differential Scanning Calorimetry (DSC). In this instrument a sample and inert reference are heated in a controlled environment for specific time, temperature, atmosphere and pressure. The difference in heat flow between the sample and the inert reference is measured as a function of time and temperature range from - 180°C to 725°C.

To study the effects of the prepared urea condensate on cotton fabrics, the thermal decomposition of treated fabric with various PH/U condensates and also the untreated cotton fabric was compared.

The DSC result for the thermal decomposition of cotton fabric is shown in Figure 4.32.

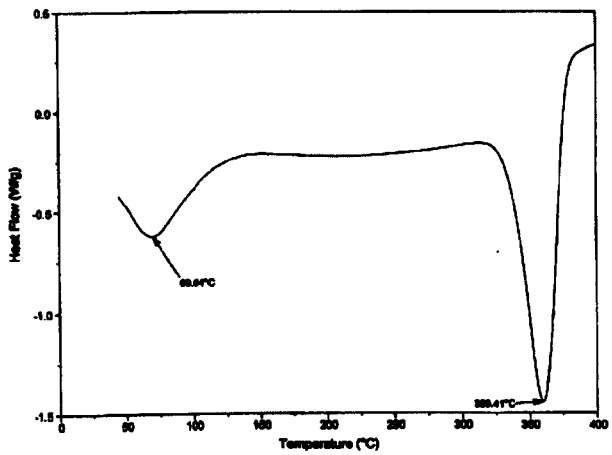

Figure4.32. DSC curve from the thermal decomposition of cotton fabric.

In the DSC curve of the cotton fabric, the first endotherm is related to the water content of the fabric and is centered at 69.0°C; the second endotherm is related to the main decomposition of the fabric centered at 359 1°C.

4.7.1. DSC analysis of treated fabric with PH/U condensates

The DSC results of cotton fabric treated with various types of PH/U condensates are compared in Figure 4.33.

The flame retardant behavior of the treated fabric can be analysed from the various exotherms shown in DSC. The decomposition enthalpy of the fabrics and also the main exotherms are provided in Table 4.16.

Table4.16. Enthalpy results from decomposition of fabrics, treated with PH/U condensate.

Urea condensate	1PH/2U	1PH/3U	1PH/4U	1PH/5U
Fabric code	P-1-2	P-2-2	P-3-1	P-4-2
ΔH (J/g)	137.0	114.2	99.6	86.8
Exothermic temperature	274	280	278	282

The chemical modification of cotton fabric with various PH/U condensates can cause the difference between the three exothermic curves.

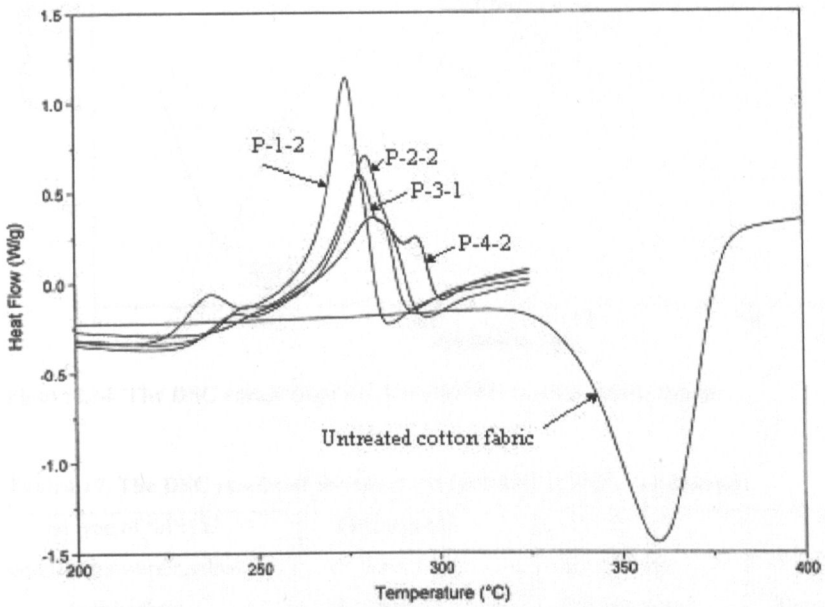

Figure4.33. DSC curve of the thermal decomposition of the fabric treated with various types of PH/U condensates.

All the treatments produce obvious new exotherms compared to untreated cotton. In fact; by increasing the amount of urea new products are formed and exotherms become apparent especially in the case of the fabric treated with the prepared condensates with 4 and 5 moles of urea.

4.7.2. DSC analysis of treated cotton fabric with S/PH/U condensates

The thermal decomposition of the flame retardant fabric treated with 1S/1PH/18U condensate is shown in Figure 4.34. The first endothermic effect under 100˚C can be attributed to the water content of the fabric, while the two exothermic effects provide sufficient information regarding the flame retardancy behavior of the fabric. A broad exotherm follows the sharp 320˚C

exotherm indicating a slow thermal decomposition of the main polymer on the treated cotton fabric. The DSC data from the thermal analysis of fabric treated with various types of S/PH/U condensates is provided in Table 4.17.

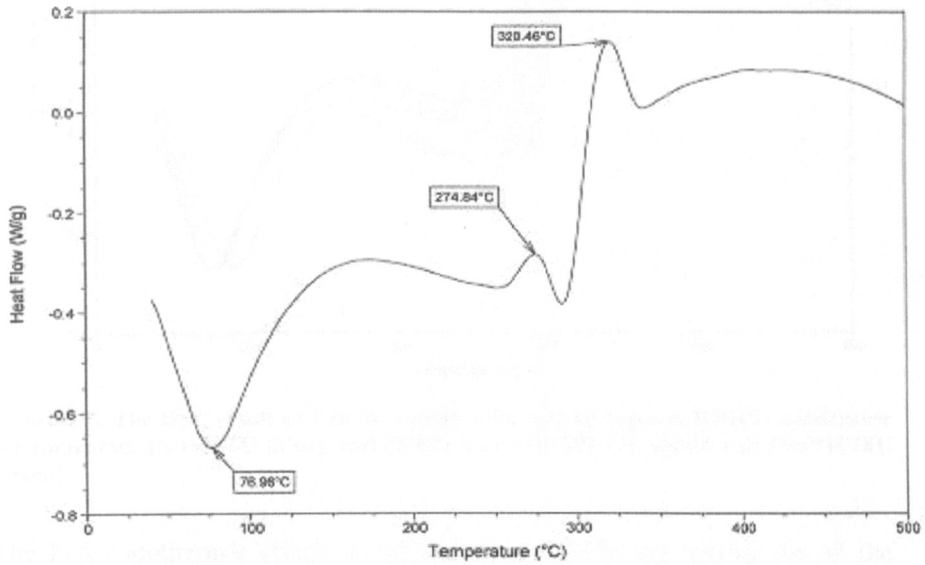

Figure4.34. The DSC result from the 1S/1PH/18U treated cotton fabric.

Table4.17. The DSC results of the fabric treated with S/PH/U condensates.

The type of S/PH/U condensate were applied to the fabric	Endothermic Centred Temperature °C	1st Exothermic Temperature °C	2nd Exothermic Temperature °C
1S/1PH/6U	91	251	294
1S/1PH/8U	78	246	296
1S/1PH/10U	81	264	304
1S/1PH/14U	81	269	313
1S/1PH/18U	77	275	320

An overlapping of DSC curves for all treated fabrics are shown in Figure 4.35.

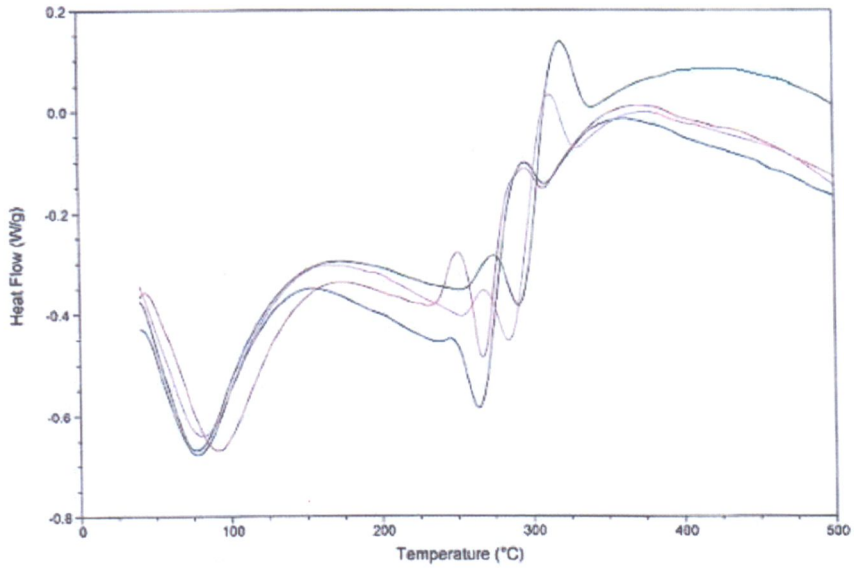

Figure4.35. The DSC result of fabrics treated with various types of S/PH/U condensate are compared, 1S/1PH/6U [blue], 1S/1PH/8U [red], 1S/1PH/14U [pink] and 1S/1PH/18U [green].

The first endothermic effects at approximately 100˚C are similar for all the treated fabrics. By increasing the amount of urea in the urea condensates, the first exothermic effect appears at 251˚C for the 1S/1PH/6U treated fabric and increases to higher temperature (274 ˚C) for the 1S/1PH/18U treated fabric. In various types of flame retardant fabrics, the thermal degradation process occurs by a dramatic increase in heat in a narrow temperature range, after that a second exothermic effect is observed. The fabric treated with higher concentration of urea in the pre-condensate (1S/1PH/18U) decomposed at higher temperature. In fact the high concentration of urea in the condensate can produce a polymer with a longer chain length and therefore more thermally-stable polymer will be formed between the hydroxyl groups of cellulose structure.

However a sufficient amount of phosphorous acid is required to produce the flame retardant properties on cotton fabric and the fabric treated with the 1S/1PH/20U condensate did not pass the flame test.

The thermal analysis of 1S/1PH/10U condensate treated fabric and commercial fabrics treated with Proban and Pyrovatex are compared in Figure 4.36.

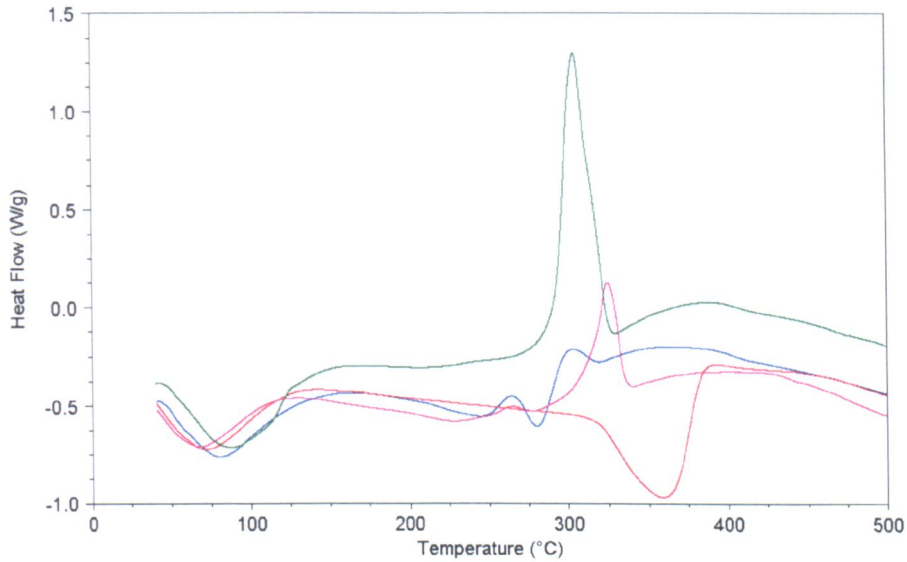

Figure4.36. The DSC result of untreated cotton fabric [red] and commercial fabric treated with Proban [green], Pyrovatex [pink] and also the sample treated with 1S/1PH/10U condensate [blue].

A significant difference between the thermal decomposition of the urea condensate and the other commercial flame retardant fabrics can be seen. Fabrics treated with Proban and Pyrovatex show a very sharp exotherm at about 300°C, but at this stage of decomposition for the treated fabric with the S/1PH/10U condensate only a small exotherm is indicated. In comparison with untreated cotton fabric this exothermic effect can also confirm the flame retardancy of the treated fabric.

To study the effect of phosphorous acid on the thermal behavior of treated fabric with urea condensates, the two DSC curves for cotton fabric treated with two urea condensates the1S/1PH/10U and 1S/2PH/10U are compared in Figure 4.37. It is very interesting to see that, by increasing the concentration of phosphorous acid in the urea condensates, it is possible to improve the exothermic effect on DSC thermal decomposition. In fact the potential to produce different urea condensates with various FR effects can be claimed.

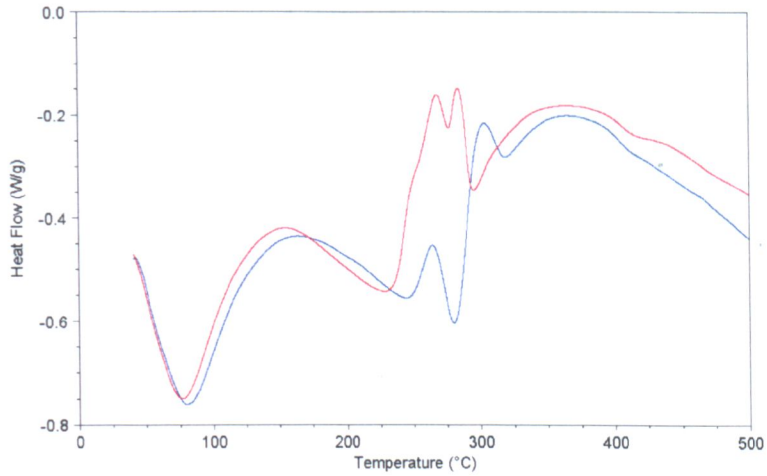

Figure4.37. DSC result of cotton fabric treated with 1S/1PH/10U condensate [blue] and treated with 1S/2PH/10U [red].

In Figure 4.38 the DSC result of fabric treated with 1S/2PH/10U is shown. There are two sharp exothermic effects, centred at 269˚C and 285˚C, which indicates that there are two products produced during thermal treatment on the fabric. The production of phosphoric acid at this temperature can be indicated from the literature [1], this is the main point to protect the fabric from further decomposition and introduce the flame retardancy properties.

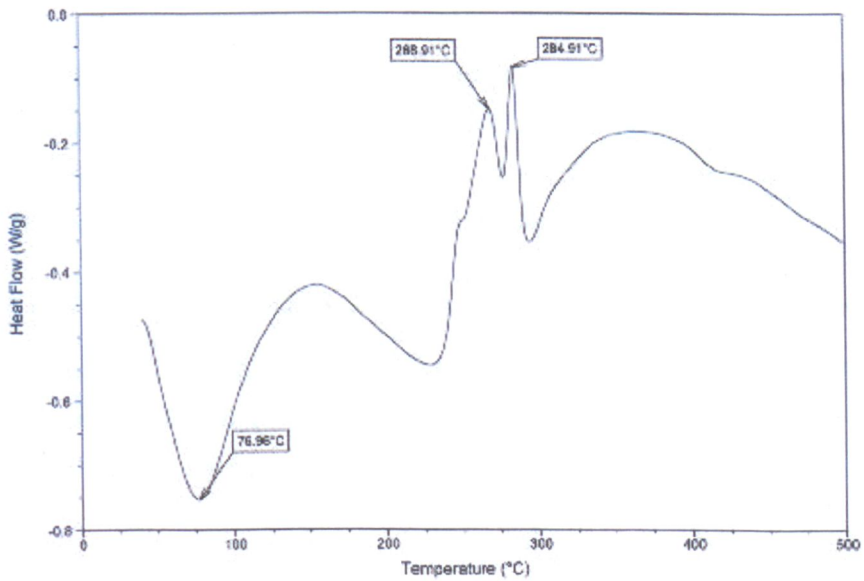

Figure4.38. DSC result of cotton fabric treated with 1S/2PH/10U.

4.7.3. TGA analysis of treated cotton fabric with S/PH/U condensates

The TGA results of untreated cotton fabric and treated with two different types of urea condensate 1S/1PH/10U and 1S/2PH/1U are compared in Figure 4.39.

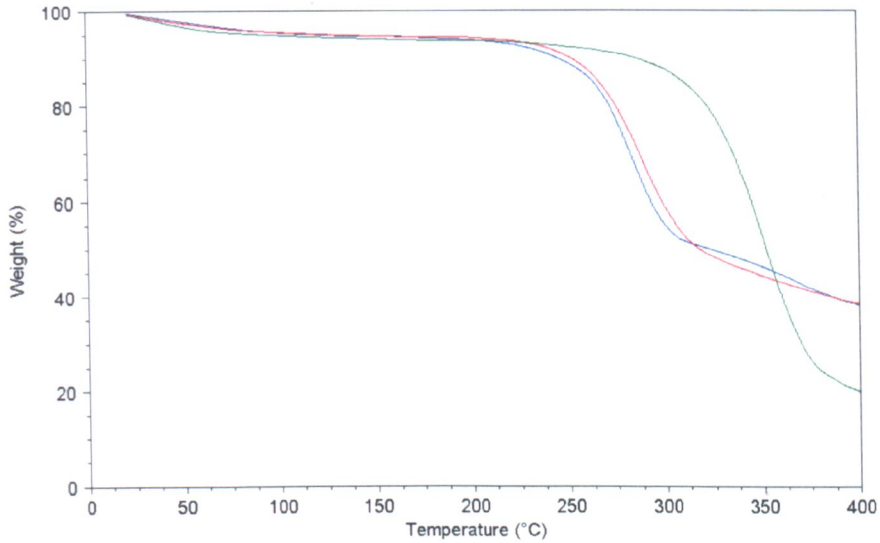

Figure4.39. The TGA results of untreated cotton fabric [green], the cotton fabric treated with 1S/1PH/10U condensate [red] and treated with 1S/2PH/10U condensate [blue].

A complete shift in the TGA results between the two treated samples and the untreated cotton fabric can provide further information regarding the cellulose dehydration during the thermal decomposition. In fact some volatile materials removed during the heating and these evaporations have an effect on the rate of weight loss of the treated samples. Following the dehydration more char formation with the new structure on treated samples expected to see after burning the samples. Therefore a significant effect of new flame retardant with the ability to produce more char formation can be confirmed,

4.7.4. Thermal decomposition of starch treated with 1S/2PH/10U condensate

To study the flame retardancy behavior of starch reacted with the 1S/2PH/10U condensate, DSC and TG analysis was carried out on the untreated and treated starch. The DSC results are shown in Figure 4.40.

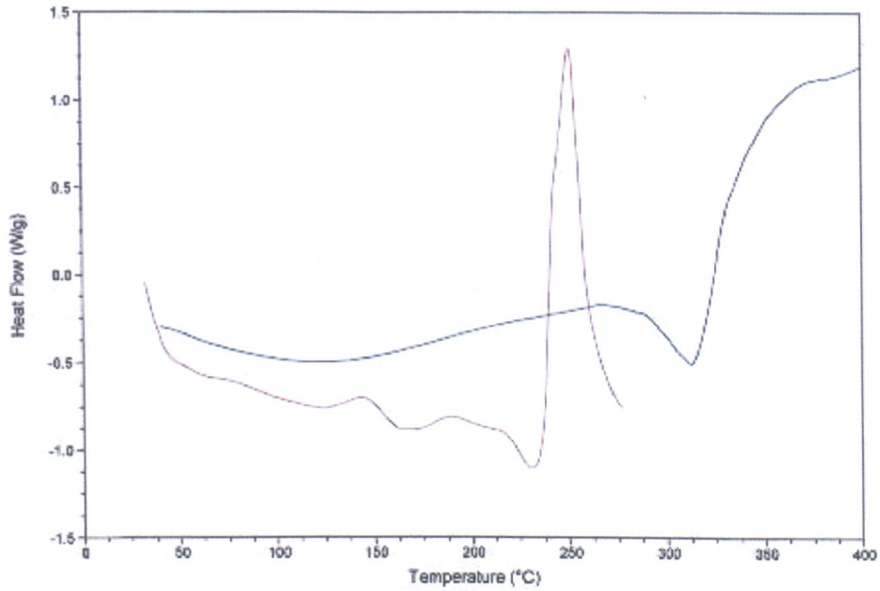

Figure4.40. DSC results of untreated starch [blue] and starch treated with 1S/2PH/10U [red].

The thermal decomposition of starch is completely different when compared to cellulose fabric, Figure 4.32. A similarity in chemical structure has no effect on its thermal behavior. The 80% amylopectin with branch chain structure in starch confirms the high availability of hydroxyl groups in its chemical structure. From the DSC results, it is possible to indicate that at high temperature, by liberating some water from the reaction between intermolecular and intra molecular hydrogen bonding of glucoside units, a new chemical structure will be formed which starts to decompose after 300˚C, with an exothermic curve appearing at a higher temperature.

In the case of starch treated with the urea condensate product, the reaction between starch and urea condensate products can be confirmed with the different thermal decomposition behavior. A very sharp exothermic peak at about 255˚C is a good evidence to confirm the presence of a new chemical structure similar to the urea 1S/2PH/10U treated cotton fabric (Figure 4.39) possibly indicative of the flame retardant properties of treated starch.

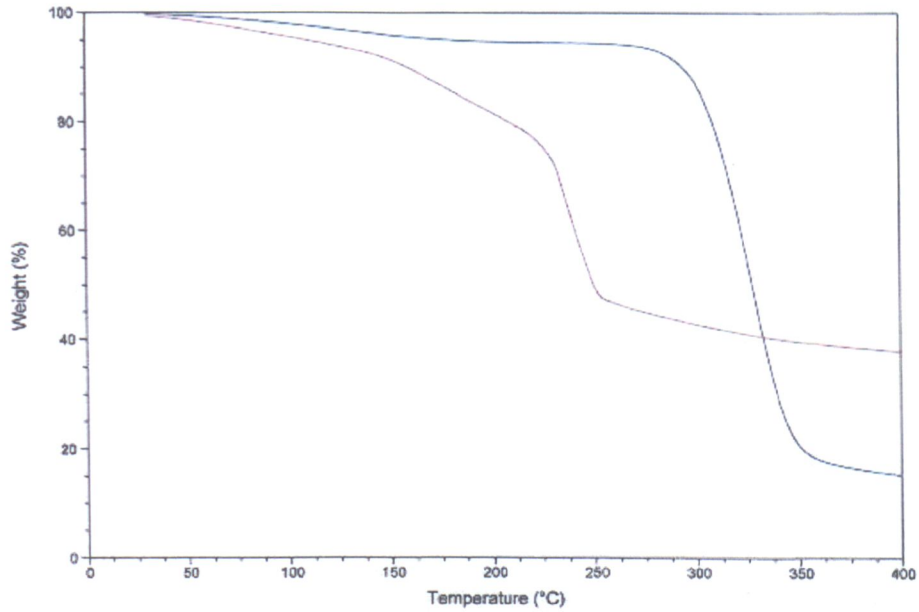

Figure4.41. The TGA results of untreated starch [blue] and treated starch with urea condensate products [red].

The thermo-gravimetric analysis (TGA) can complete the information in this regard. In Figure 4.41 the thermal degradation of untreated starch begins at approximately 300°C with a very sharp weigh loss within a small temperature range (50°C). The thermal analysis of the urea condensate treated starch is completely different, the weigh loss starts at lower temperature which gradually changes until 230°C (while the degradation of the new chemical structure on starch, with the urea condensate products, shows an exothermic effect in the DSC curve), after that a new structure which is more stable to heat is produced. Therefore no significant weigh loss has been observed above this temperature and the production of flame retardant starch can be claimed with high char formation.

4.7.5. Thermal degradation of polyvinyl alcohol treated with S/PH/U condensate

The DSC thermal analysis results for untreated polyvinyl alcohol film and film treated with the 1S/1PH/10U condensate are shown in Figure 4.42.

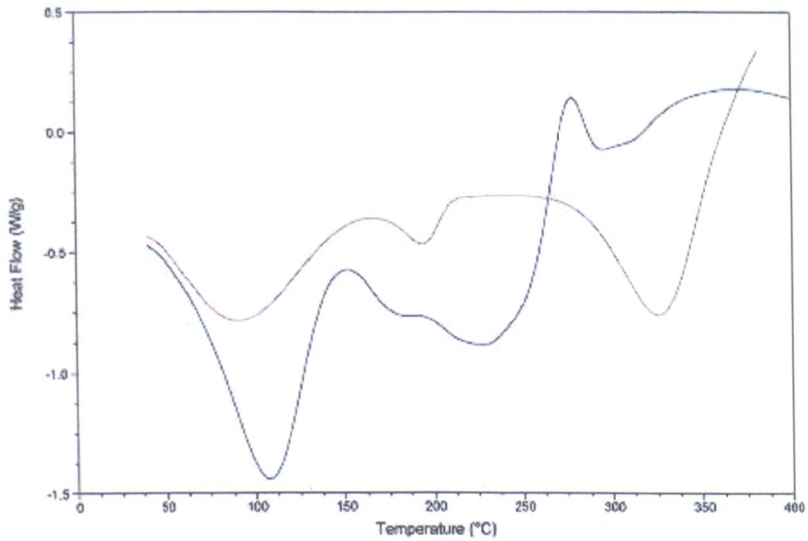

Figure4.42. DSC results of polyvinyl alcohol film heated to 165˚C for 4 minutes [red] and treated polyvinyl alcohol with 1S/1PH/10U condensate [blue].

In Figure 4.42 DSC result for untreated polyvinyl alcohol shows three endothermic effects. From the literature these two thermal transitions can be explained due to the increased molecular chain mobility resulting from inter and intra molecular hydrogen bonds between the hydroxyl groups of polyvinyl alcohol [2]. The third endothermic effect is attributed to the polymer decomposition which is clear from the TGA results in Figure 4.43. The weight loss for the polymer commences after 100˚C gradually until 300˚C, a dramatic change can be seen after 300˚C, representing the thermal degradation of the polyvinyl alcohol.

In polyvinyl alcohol treated with the urea condensate this thermal degradation performs differently. The polymeric structure of polyvinyl alcohol with hydroxyl groups and a large amount of crystalline regions in its physical structure, confirmed the low availability of hydroxyl groups to undergo a similar reaction as starch. The small exothermic effect can verify the flame retardant properties of the polyvinyl alcohol film treated with the urea condensate. However in the TGA results, shown in Figure 4.43, an obvious thermal shift explains the dehydration process which occurred on polyvinyl alcohol treated sample and therefore char formation with double bonds structure after burning process would be expected.

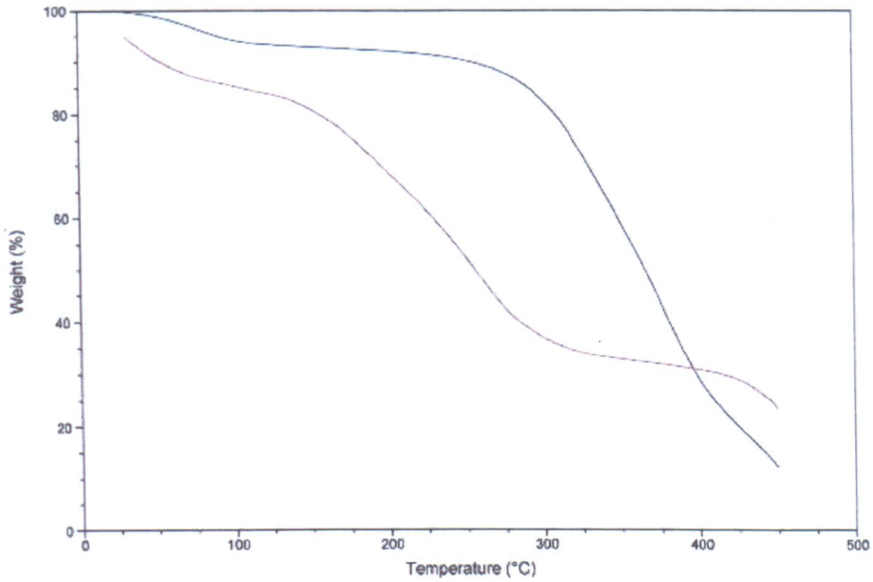

Figure4.43. The TG results for polyvinyl alcohol [blue] and treated polyvinyl alcohol with 1S/2PH/10U condensate [red].

4.8. FT-IR analysis of treated fabrics

To simplify the interpretation of the FT-IR spectra of the treated fabrics, it is necessary to describe the spectrum of the original cellulosic fabric by frequency region division.

Figure 4.44 shows the FT-IR spectrum of mercerized untreated cotton fabric and Figure 4.45 shows its Raman spectrum.

Assignments of the FT-IR and Raman bands observed for cellulose and its derivatives are given in Table 4.18.

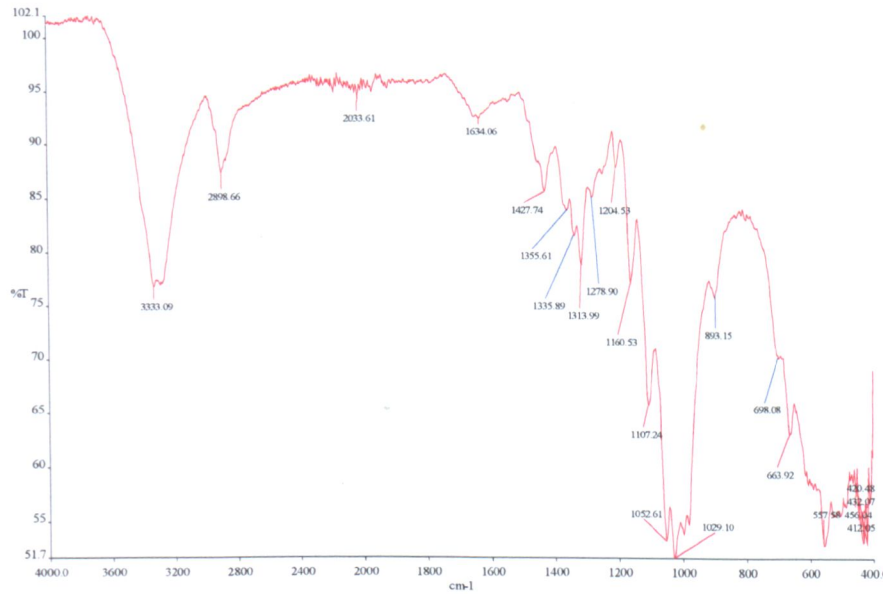

Figure4.44. The FT-IR spectrum of mercerized cotton fabric.

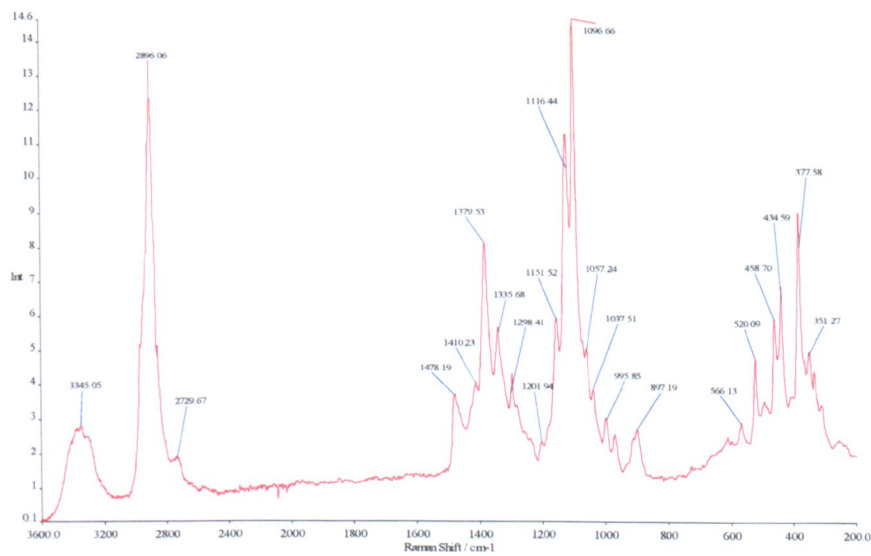

Figure4.45. The Raman spectrum of mercerized cotton fabric.

Table4.18. Characterization of cellulose functional groups bands in FT-IR and Raman spectra.

*Functional groups	Region cm^{-1}	IR		Raman		Comments
		Intensity	**Specific peaks cm^{-1}	Intensity	**Specific peaks cm^{-1}	
Cellulose	3575-3125	m	3335	w	3342	br. OH str
	1750-1725	s	-	w-m	-	C=O str, after oxidation
	1635-1600	m	1625	m	-	OH def vib
	1480-1435	w	1430	m	1474	CH_2 def vib, Intensity affected by degree of crystallinity
	~1375	w	-	m-w	1379	CH def vib
	~1340	w	1336	m-w	1338	OH def vib
	1320-1030	w	1313	m-w	1293	Numerous bands
			1236		1150	
			1206		1150	
	~830	w	815	w	-	CH_2 def vib
Primary alcohols	2990-2900	w-m	-	m-s	-	Asym CH_2 str
$-CH_2-OH$	2935-2840	w-m	2897	m-s	2896	Sym CH_2 str
(C-O stretching vibration,	1480-1410	w-m	1430	m	1474	CH_2 def vib
deformation)	1390-1280	w-m	1336	m-w	1379	CH_2 wagging –alcohol OH def vib may
					1338	obscure
	1300-1280	w-m	1313	m	1293	CH_2 twisting vib, may be obscured by OH def vib
	1090-1000	s	1029	s-m	1089	CCO str, characteristic band
					1036	
	900-800	m	815	s	899	CCO sr
	960-800	w-m	-	m	966	CH_2 twisting vib
	710-570	w-m	691	w	-	Br, OH out-of-plane def vib
	555-395	w-m	519	m-w	519	C-O def vib

*Functional groups	Region cm^{-1}	IR		Raman		Comments
		Intensity	**Specific peaks cm^{-1}	Intensity	**Specific peaks cm^{-1}	
Hydrogen-bonded O-H (intermolecular)	3550-3230	m-s	3335	w	3342	Usually broad but may be sharp, frequency is concentration dependent
Hydrogen-bonded O-H (intramolecular)	3590-3400	v	-	w	-	Usually sharp, frequency is concentration independent
Secondary alcohols	1400-1330	w	1336	m-w	1338 1379	CH wagging vib
CH-OH	1350-1290	w	1336	m	1338	CH def vib
	1150-1075	s	1108	m-s	1117 1089 1150	C-O str, often shows multiple bands due to coupling
	900-800	m	-	s,p	899	CCO str
	660-600	m-br	-	w	-	OH out-of-plane def vib
	500-440	w	481	m-w	457	CO in-plane def vib
	390-330	m	-	w	343 376	CO out-of-plane def vib
Cyclic ethers (six-membered ring)	1110-1090	S	1108	M	1089 1117	Asym COC str
	820-805	m	815	s	-	Sym COC str
Primary alcohols (O-H deformation vibration)	1440-1260	m-s	1314 1336	m-w	1338 1379	In-plane O-H def vib, br
Secondary alcohols	1430-1370	m-s	1430	m-w	1379	In-plane O-H def vib, coupling with CH wagging vib, br

*These Functional groups and their identified frequency regions are indicated in reference [3].

**These specific peaks are determined from the main FT-IR and Raman spectra of cotton fabric.

The 4000 – 2000 Cm^{-1} region

This region of the cellulose spectrum contains the main stretching vibration frequencies of the groups OH, CH, CH_2 as well as NH group on the modified fabric.

Regarding, the hydroxyl group field, definite information about hydrogen bonding in cellulose and its derivatives can be obtained by explaining the accuracy of substitution of the hydroxyl group.

It must also be considered that hydrogen bonds may affect the conformational characteristic of the cellulose macromolecule and its individual rings by unstable conformation. Thus, a change in the hydrogen bonds structure may be important criteria in the conformational conversion of cellulose and its derivatives.

In the original cotton fabric and the treated fabric, all the hydroxyl groups are involved in inter- or intra-molecular hydrogen bonding.

A frequency range of hydrogen bonds between hydroxyl groups is 2500 cm^{-1} – 3580 cm^{-1}, ranging from very weak to very strong bonds. In mercerized cotton fabric, the OH groups combine to form hydrogen bonds the stretching vibration has strong bands at 3484 cm^{-1} and 3447 cm^{-1} region representing the intra-molecular hydrogen bonds. Another band at 3350 cm^{-1} can be attributed to inter-molecular hydrogen bonds.

It must be considered that, hydrogen bonds in carbohydrates and similar compounds are independent, so that a change in one type of hydrogen bond may lead to a change in the nature of the other hydrogen bonds also [4].

In fact, within the 3200 – 3600 cm^{-1} region, the changes in intensity and frequency of the main maximum of the OH group band, can be used to investigate special features in the reactions of esterification and hydrolysis.

The analysis of highly substituted cellulose ester and ethers has shown that the maxima of the main hydroxyl group bands are located within the fairly narrow frequency range of 3470 – 3520 cm^{-1}[5].

In the highly substituted cellulose ester spectra, the relevant small variation in frequency of the hydroxyl group band with the nature of the esterifying group gives sufficient support that the vibration is mainly due to intermolecular hydrogen bonding [4].

The 2000-1500 cm^{-1} region

This region contains the frequencies corresponding to the stretching vibrations of the double bonds: N=O, C=O, C = C.

The cellulose carbamate group is also reported in this region. The kinetics of oxidation, nitration and esterification can change the band at this particular region. Any new carbonyl groups in the modified cellulose could be expected to appear at this region.

The 1500 – 1200 cm^{-1} region

In this region there are a number of relatively sharp absorption bands, which are very sensitive to chemical and structural transformation of the cellulose. Absorption bands of CH_2OH, associated with deformation vibration appear at this region 1450-1200cm^{-1} in the cellulose spectrum. The band at 1430 cm^{-1} is attributed to internal deformation vibration of the CH_2 group; the intensity of this band can give definite information about processes involving the CH_2OH group at the sixth position carbon atom. The other bands in this region 1336, 1314 cm^{-1} are also probably due to the CH_2OH group at other carbon positions. In fact it may be accepted that the intensity of these bands is determined by the primary hydroxyl groups of various rotational isomers.

The weak bands at 1236 cm^{-1} can probably be attributed to external deformation vibration of CH_2 groups.

The absorption increase at the region 1280-1190 cm^{-1}, is characteristic of cellulose containing a carboxyl group [5].

The 1200 – 950 cm^{-1} region

In this region some broad absorption bands are observed. The strong interaction of the vibration of individual groups and bonds, whose frequencies are located in this spectra range make some difficulty in the interpretation of the spectrum. However in Table 4.18 some particular bands relevant to C-O stretching vibration of secondary alcohols, in multiple bands due to coupling were indicated at this region. The cyclic ethers with six member ring also have a band at this specific region, relating to the asymmetric C-O-C stretching vibration. The characteristic bands due to the C-O stretching vibration and deformation of primary alcohols are seen in this region.

The 700 – 950 cm^{-1} region

Adsorption in the 700 – 950 cm^{-1} region is specific for many cellulose derivatives.

On changing from natural cellulose to hydrocellulose, the increased intensity of the band at 900cm^{-1} in FT-IR spectrum has been confirmed, due to the stretching and deformation vibration of CH_2. The new bands in the region 940-850 cm^{-1} are attributed to the CH_2OH group of dialcoholic cellulose in carbon position 2 and 3. In fact the spectrum in this region can reflect the conformational changes in cellulose derivatives and also related materials.

The 700-400 cm^{-1} region

According to the investigation of the cellulose derivative spectra, the reduction in intensity of the absorption and also the disappearance of the primary bands at this region, following the loss of hydrogen groups, is valuable evidence indicating the new chemical structure. In fact the wide range of various types of hydrogen bonds in cellulose, can explain the broad absorption bands that appear in the cellulose spectrum. The vibration frequency of the new functional groups introduced into the cellulose structure can be seen at this region.

4.8.1 Cotton fabric treated with urea solution

The spectra of untreated cotton fabric and urea treated fabric are compared in Figure 4.46.

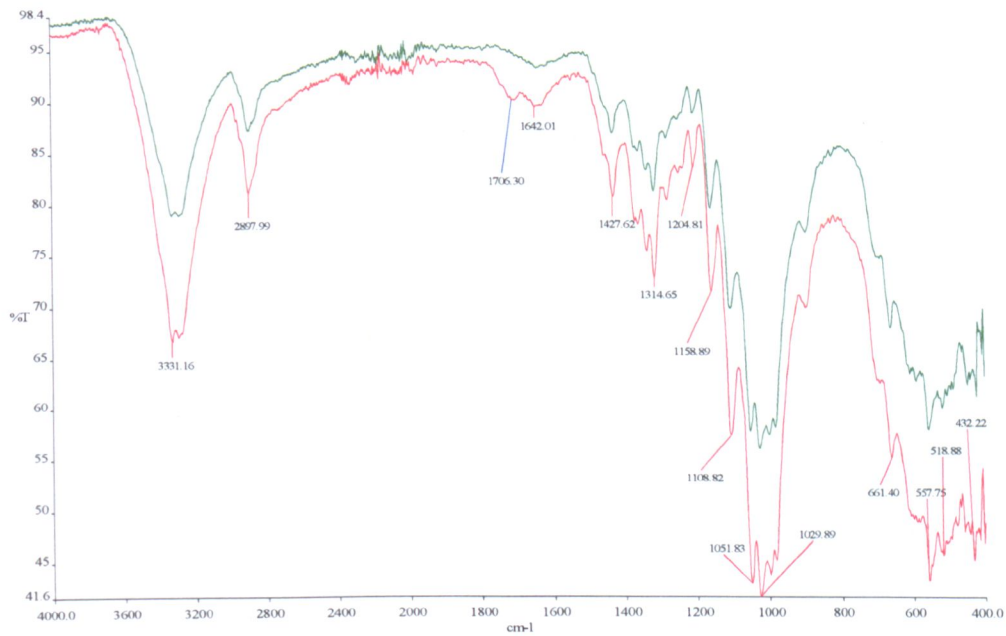

Figure4.46. The FT-IR spectra of untreated cotton fabric [green], and treated fabric with 500 g/l urea solution [red].

According to the knowledge provided in the previous section regarding the FT-IR analysis of cellulose fabric and its derivative, a brief interpretation of the spectrum of the urea treated cotton fabric is summarized in Table 4.19.

Table4.19. The interpretation of FT-IR spectrum of urea treated cotton fabric.

Specific peaks cm^{-1}	Vibrational mode of specific chemical bonds	Comment
3331 2898	Br OH str vib Sym CH_2 str	Due to the substitution of the new functional groups introduced to the hydroxyl groups of cellulose, the absorption intensity of these two bands increased
1706 1642	C=O stre of cellulose carbamate O-H def vibration	This broad band produced in urea treated fabric. The absorption intensity of this band is increased.
1428 1315	CH_2 def vib In-plane OH def vib	The vibrational mode of CH_2OH functional group in various carbon atoms in cellulose structure determined at this region. The intensity of these bands due to the new chemical bonds has changed.
1205 1159 1109 1052 1030	 C-O str of CH_2OH group C-O str of CH_2OH group	The C-O stretching of CH_2OH is indicated at this region, however the present of CCO stretching vibration is also seen at this region.
661 558 519 432	Br OH out-of-plane def vib C-O def vib C-O in-plane def vib	The secondary alcohol CH_2OH functional group of carbon atom 2, 3 are present at this region. However the presence of new band also can be determined, representing the new chemical structure for cellulose fabric.

4.8.2. Cotton fabric treated with ammonium sulphamate solution

The spectrum of treated fabric is given in Figure 4.47.

It can be seen from the FT-IR spectrum of the fabric treated with ammonium sulphamate solution that new chemical residues are present. Since on baking ammonia is removed and free sulphamic acid is then formed; this strong acid discoloured the fabric and decreased its strength both of which are undesirable.

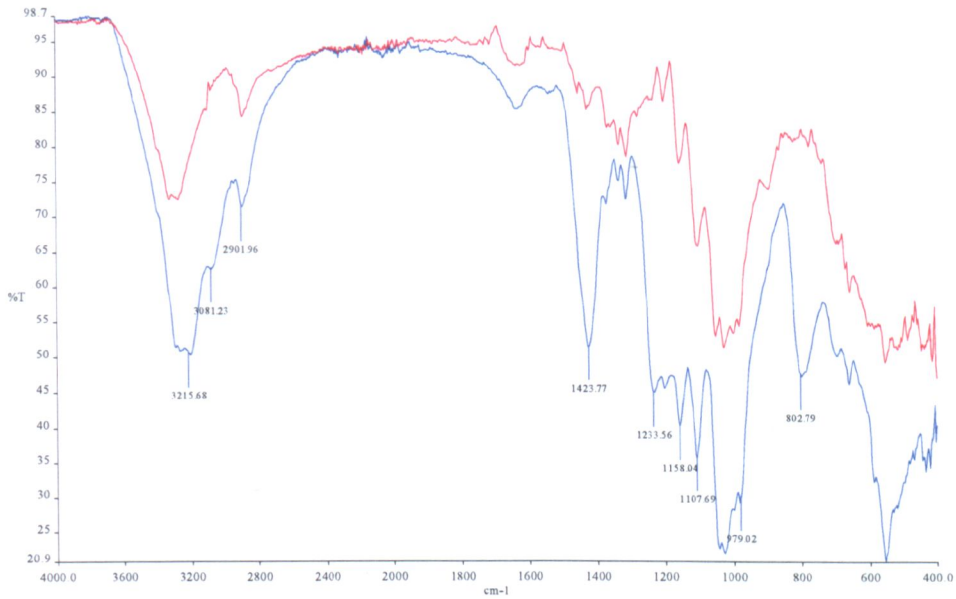

Figure4.47. The FT-IR spectra of untreated cotton fabric [red] and the fabric treated with ammonium sulphamate solution [blue].

The reactions which are to be expected between the cellulose and the sulphamic acid are indicated in Scheme 4.1.

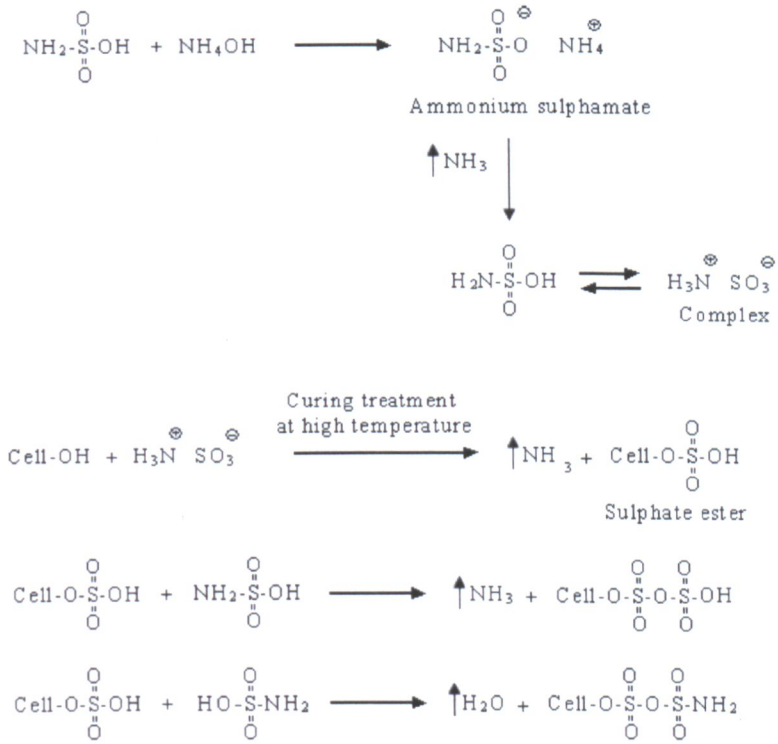

Scheme4.1. The possible chemical reactions occur between sulphamic acid and cellulose hydroxyl groups.

The 2nd derivative spectra of both fabrics for the specific frequency regions are explained in detail.

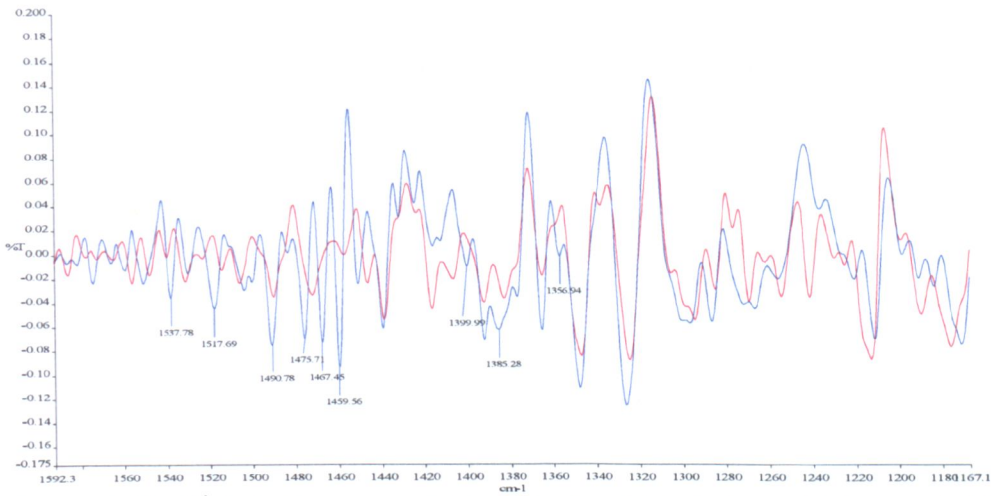

Figure4.48. The 2nd derivative spectra of untreated cotton fabric [red] and fabric treated with sulphamic acid [blue].

In Figure 4.48 the transformation on chemical structure of cellulose can be observed in the frequency region, 1500-1200 cm^{-1}. The deformation vibration plus C-O stretching vibration of the primary alcohol, or more familiar the hydroxyl group in position 6th carbon in the cellulose structure, can be determined in 1480-1435 cm^{-1} and 1480-1410 cm^{-1}[3]. In the 2nd derivative spectrum of the treated fabric with sulphamic acid, a few bands at 1460, 1467 cm^{-1} and 1476 cm^{-1} appear which can confirm the substitution on the hydroxyl functional groups.

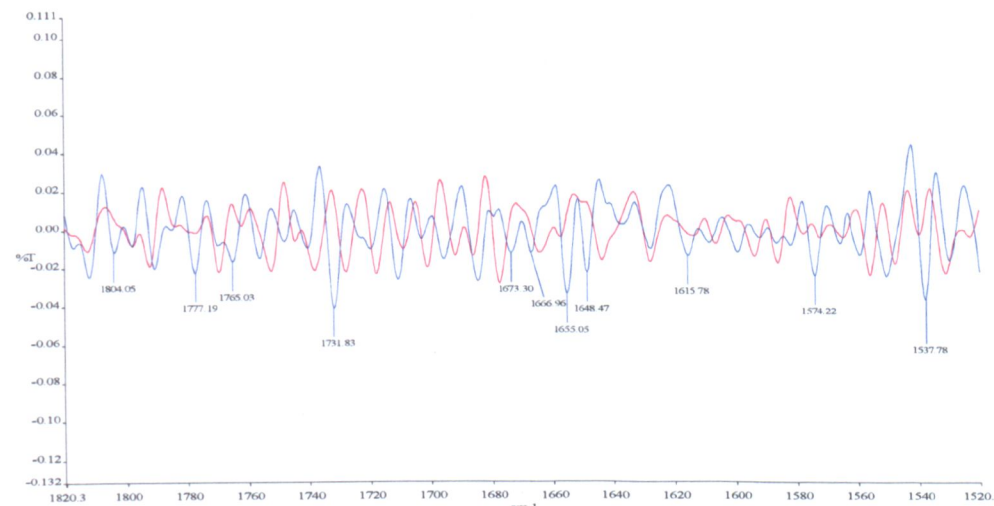

Figure4.49. The 2nd derivative spectra of untreated cotton fabric [red] and fabric treated with sulphamic acid [blue].

In Figure 4.49 the sulphonation of cellulose can be identified in this region. Some new bands appear at 1777, 1765, 1732 cm^{-1}, also the two bands at 1655 and 1648 cm^{-1} are attributed to this chemical reaction, and new sulphate ester which was formed by substitution at the hydroxyl groups. However the bands relevant to cellulose carbamate are also appeared at this region, see Table 4.19.

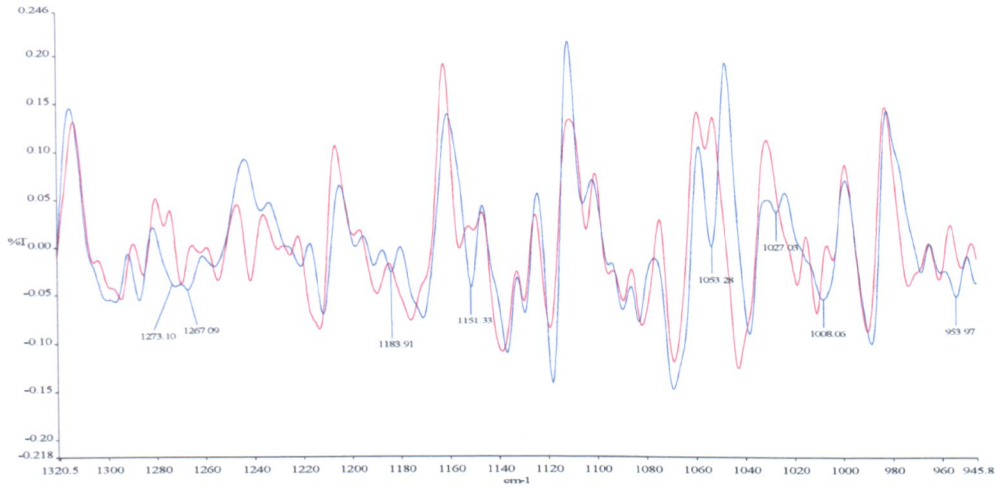

Figure4.50. The 2nd derivative spectra of untreated cotton fabric [red] and fabric treated with sulphamic acid [blue].

In Figure4.50 in the region, 1320-945 cm^{-1} the SO, SO_2 and also SO_4 stretching vibrations of various functional groups of sulphur compounds are indicated. Therefore it is simple to determine the possible functional groups present in the new modified cellulose. In the main FT-IR spectrum of fabric treated with sulphamic acid, the presence of $-SO_2NH_2$, $R-SO_2-OR$, $-SO_2-OH$ and also sulphate ion can be confirmed. The characteristic information relevant to each band is provided in Table 4.20.

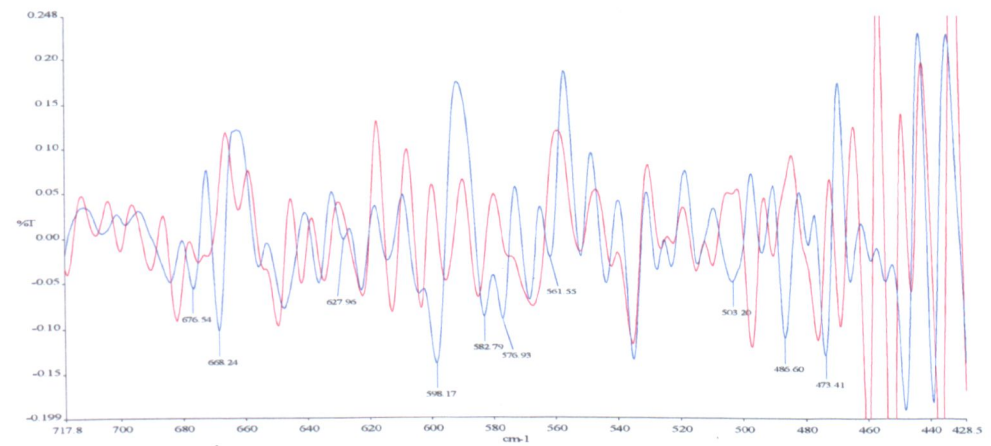

Figure4.51. The 2nd derivative spectra of untreated cotton fabric [red] and fabric treated with sulphamic acid [blue].

In Figure 4.51 the bands attributed to the NH_2 and SO_2 wagging vibration of the primary sulphonamides can be determined. However the two double bands at 583 cm^{-1} and 577 cm^{-1} due to the SO_2 deformation vibration of R-SO_2-OR group occur at this region. The presence of bands relevant to the SO_4 stretching vibration has to be considered at this frequency range.

In Table 4.20 the FT-IR characteristic information of fabric treated with sulphamic acid is indicated.

Table4.20. The interpreting of FT-IR spectrum of cotton fabric treated with sulphamic acid and ammonium hydroxide solution.

Specific bands cm^{-1}	comments
3288 3207	Asy and sym str vib of NH in primary sulphonamides The cellulose OH str vib
3081 2898	OH str vib of R-SO_2-OH
1635 1544	NH_2 def vib –SO_2NH_2
1427 1368	SO_2 str vib of O-SO_2-O
1336 1314	Asy SO_2 str vib of –SO_2NH_2
1233	SO_4 str vib
1203	Sym SO_2 str vib of R-SO_2-OH
1160	S-O str vib of R-SO_2-OH
1110 1029 982	SO_4 str vib
801	SO str vib of –SO_2-O-
696 661	NH_2 wagging vib of R-SO_2-OH and R-SO_2-OR
590	SO_4 str and SO_2 def vib of –SO_2 NH_2
435 421	SO_2 twisting vib of –SO_2NH_2

4.8.3. FT-IR analysis of the fabric treated with S/U condensate

A study of the FT-IR spectrum from the fabric treated with sulphamic acid/urea condensate indicates that the reactions shown in Scheme 4.2 are possible. At a curing temperature, above 140°C, the formation of cellulose carbamate by reaction with isocyanic acid from urea, and also cellulose esterification can be predicted. The liberation of CO_2 during the heat treatment is another point which needs to be investigated further using FT-IR analysis.

Cell-OH can react with various adducts formed from isocyanic acid and sulphamic acid according to the following steps:

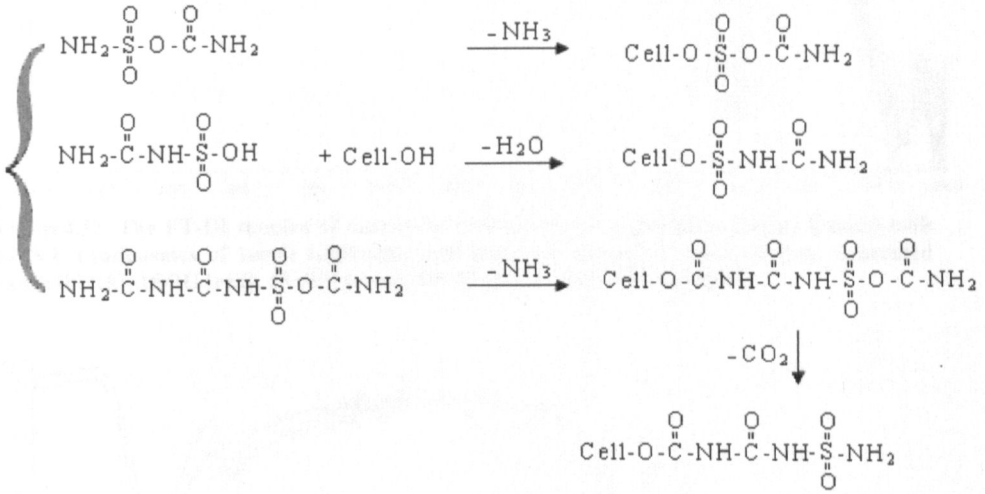

Scheme4.2. Possible reactions occur between S/U condensate and cellulose hydroxyl groups.

The spectra from the fabrics treated with various sulphamic acid urea condensates are shown in Figure 4.52. One mole of sulphamic acid is reacted with various molar ratios of urea, 2, 3, 4 or moles. By increasing the amount of urea in the pre-urea condensate, the intensity of the bands in specific regions decreases. These frequency regions can provide further information regarding the reactions which may occur. The absorption intensity of the bands relevant to sulphur compounds are also reduced

The spectra of the untreated and treated cotton fabrics with 1S/4U are shown in Figure 4.53. Due to significant differences in particular regions a new substitution on the cellulose hydroxyl groups can be confirmed. To determine the structure of the new groupings attached to cellulose at high temperature, a study of the second derivative spectra is required.

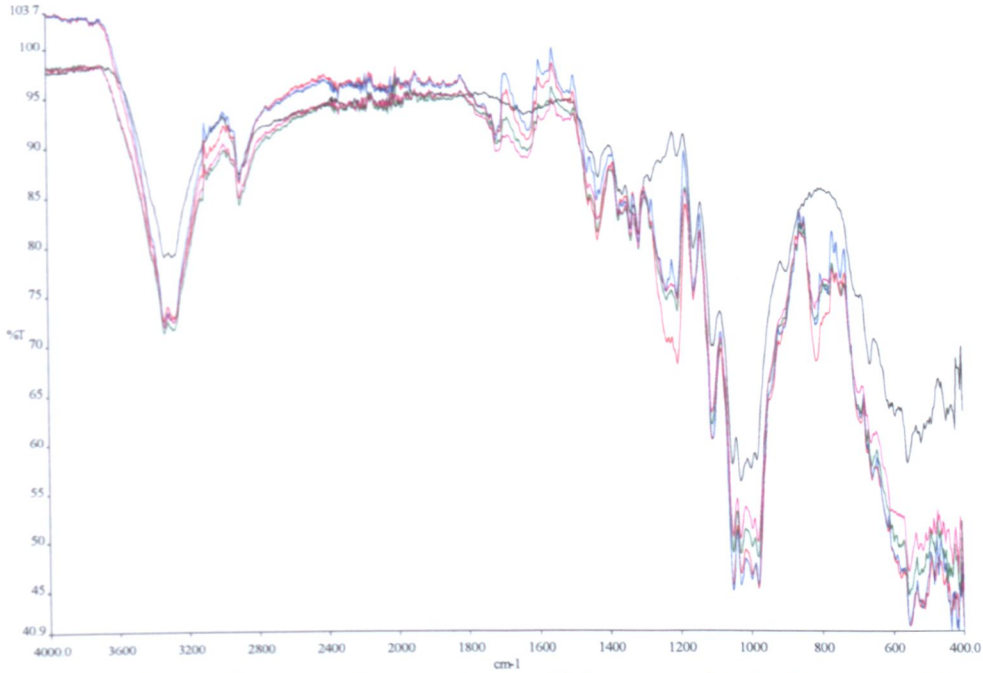

Figure4.52. The FT-IR spectra of untreated cotton fabric compared to fabrics treated with the S/U condensates of 1mole sulphamic acid and various molar ratios of urea, untreated fabric [black], 1S/2U [red], 1S/3U [green], 1S/4U [blue] and 1S/5U [purple].

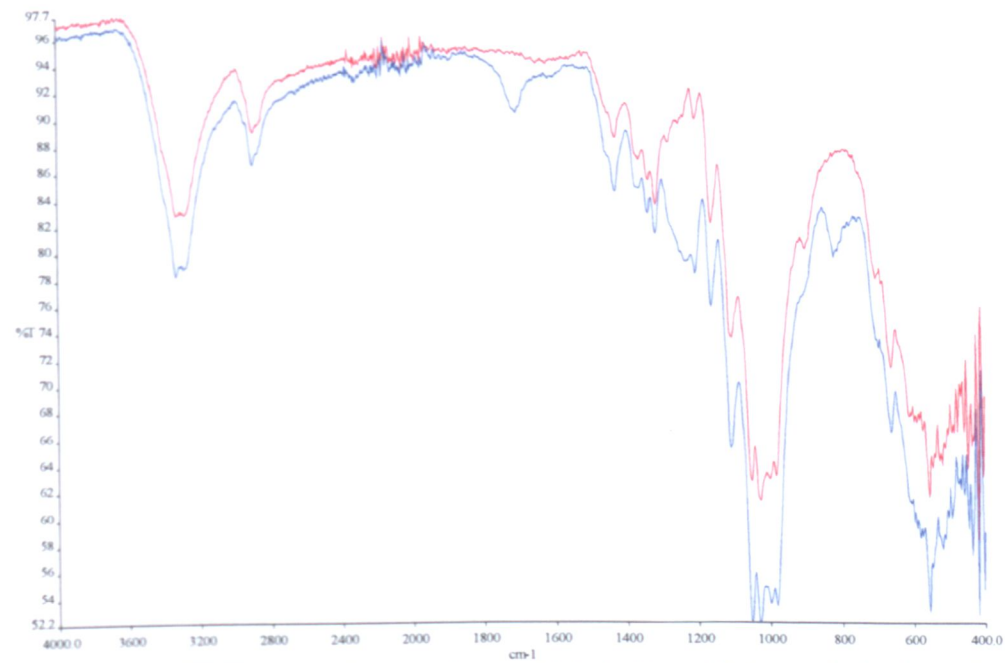

Figure4.53. The FT-IR spectra of untreated cotton fabric [red] and fabric treated with the 1S/4U condensate [blue]. Both fabrics were oven dried for 24 hours at 110°C.

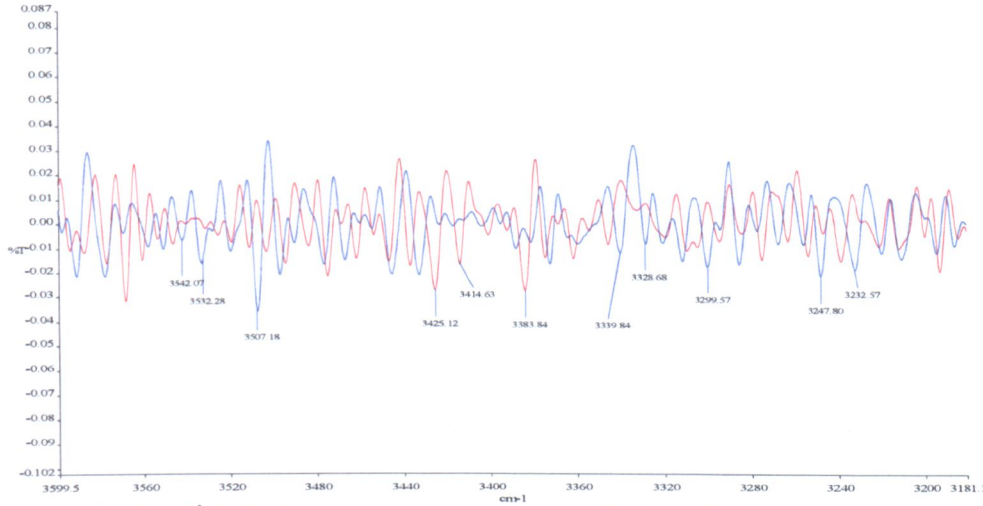

Figure4.54. The 2nd derivative spectra of untreated cotton fabric [red] and fabric treated with 1S/4U condensate [blue].

In Figure 4.54, in the region 3600-3100 cm^{-1} the bands representing the OH stretching vibration of cellulose appear; however by treating the fabric with the urea condensate, the presence of bands relevant to the primary amide and secondary amide may also be expected. In chapter 3, the possible formation of cyanuric acid and melamine at high temperature was described. The analysis of a highly substituted cellulose ester and ethers has shown that the maxima of the main hydroxyl group bands are located within a fairly narrow frequency region of 3470-3520 cm^{-1}[5].

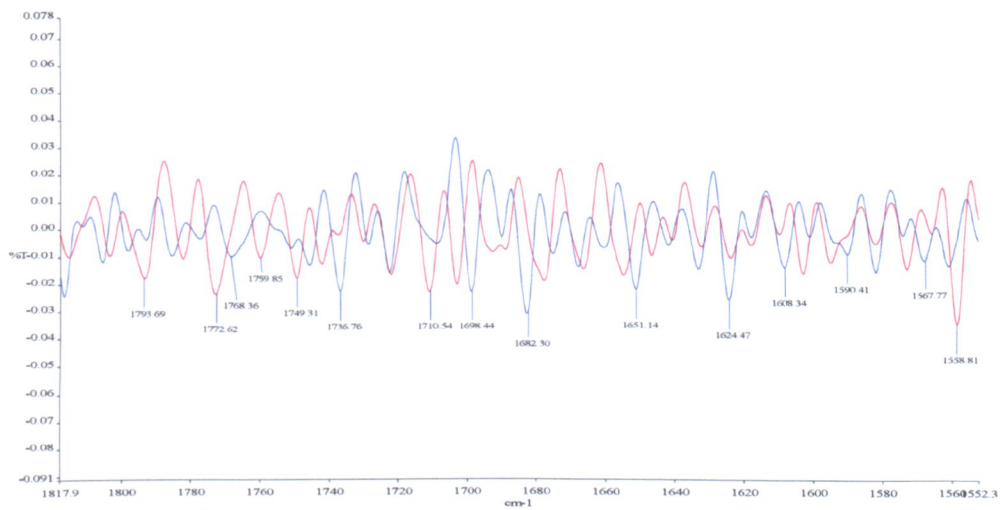

Figure4.55. The 2nd derivative spectra of untreated cotton fabric [red] and fabric treated with 1S/4U condensate [blue].

The cellulose modification can be determined in this particular region, 1800-1560 cm^{-1} in Figure 4.55. Following cellulose esterification, oxidation can change the bands in

this frequency range this difference can be seen in the main FT-IR spectrum of the treated fabric with 1S/4U condensate solution respectively.

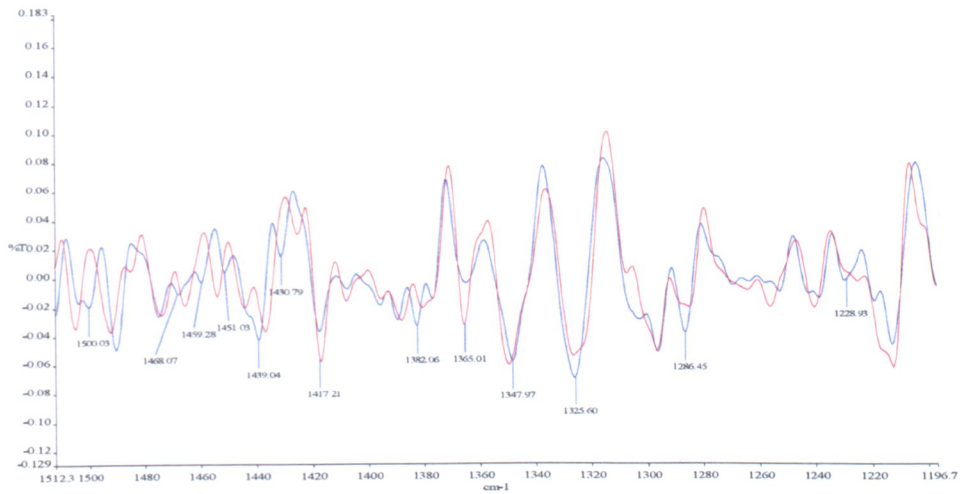

Figure4.56. The 2nd derivative spectra of untreated cotton fabric [red] and fabric treated with 1S/4U condensate [blue].

In Figure 4.56, the transformation of the cellulose chemical structure can be studied in the frequency region, 1500-1200 cm^{-1}. The bands relevant to the CH_2OH deformation vibration in cellulose appear in this specific frequency region. However the band representing the S=O asymmetric stretching vibration of sulphonamide $–SO_2$-NH- can also be found in this range.

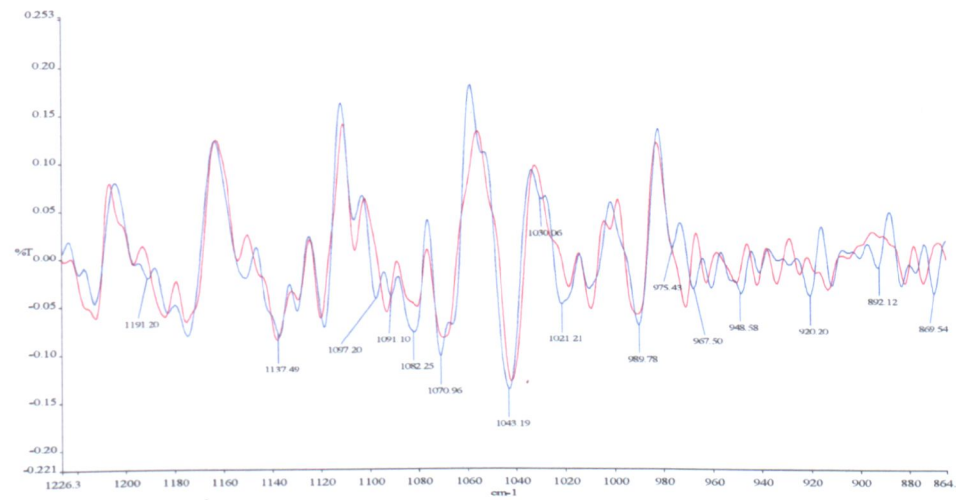

Figure 4.57.The 2nd derivative spectra of untreated cotton fabric [red] and fabric treated with 1S/4U condensate [blue].

The band attributed to the asymmetric and symmetric stretching vibration of S=O in the sulphonamide compounds can be identified in Figure 4.57. The C-O stretching

vibrations of the primary and the secondary alcohols in cellulose are also confirmed in the region, 1220-960 cm^{-1}.

In Figure 4.58 a significant difference in this frequency region, 840-540 cm^{-1}, can provide the required information regarding the cellulose modification.

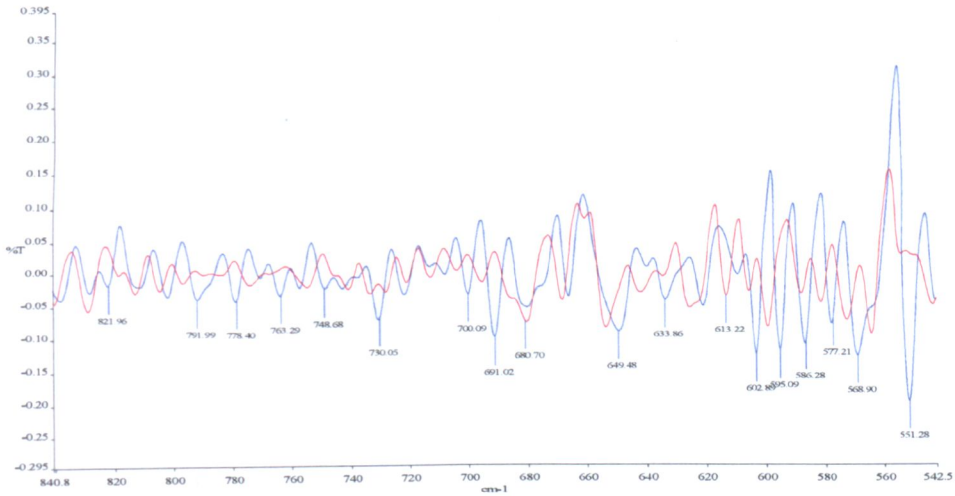

Figure4.58. The 2nd derivative spectra of untreated cotton fabric [red] and fabric treated with 1S/4U condensate [blue].

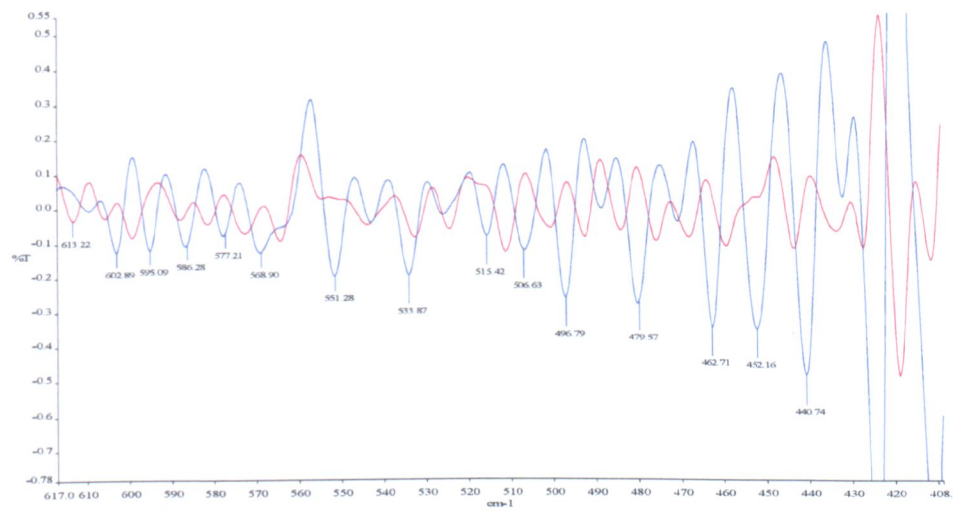

Figure4.59. The 2nd derivative spectra of untreated cotton fabric [red] and fabric treated with 1S/4U condensate [blue].

A study of the 2nd derivatives spectra of both untreated and treated cotton fabrics gave further information relevant to the cellulose modification with this new compound. The determination of each specific band present in the 2nd derivative spectrum, particularly with this expected complex structure, is a complicated process. Therefore

only the specific region with the new functional groups attached to the cellulose can be identified. A list of functional groups which have been observed is given in Table 4.21 more information relevant to each group has been indicated in chapter 2.

Table4.21. The list of functional groups which have been identified in the 2nd derivative spectrum of fabric treated with 1S/4U condensate.

Functional groups	Region cm^{-1}	Comments
ureas	1680-1635	C=O str, primary ureas, i.e. with NH_2 group
	3440-3200	NH stre
	1605-1515	amide II band
	1360-1300	asym N-C-N str
	1190-1140	sym N-C-N str
-$NHCONH_2$	3440-3400	asym NH_2 str
	3360-3320	NH str
	3240-3200	sym NH_2 str
	1605-1515	NH_2 def vib
	1360-1300	asym N-C-N str
	1190-1140	sym N-C-N str
	620-530	NH_2 def vib
-NHCONH-	3360-3320	NH str
	1585-1515	NH def vib
	1360-1300	asym N-C-N str
	1190-1140	sym N-C-N str
Primary amides	1420-1400	C-N str, known as amide III band
	~1150	NH_2 in plane rocking vib, not always seen
	750-600	Br, NH_2 def vib
	600-550	N-C=O def vib
	500-450	C-C=O def vib
Sym- triazines	3300-3100	C-H str
	1580-1520	ring str, doublet
	1450-1350	ring str, at least one band
	1000-980	ring str
	860-775	out-of-plane bending vib, at least one ban
Hydroxyl substituted triazines	1775-1675	C=O str vibration of keto
	795-750	iso form
Cyclic ureas (five membered ring) (in solid phase) (in solution)	1680-1635 1735-1685	keton groups in ring increase frequency
Melamines	3500-3100	NH_2 str
	1680-1640	NH_2 def
	1600-1500	Ring str
	1450-1350	sh, number of bands
	825-800	}Only one of the two is present
	795-750	

In Table 4.22 the possible linkages between the cellulose hydroxyl groups and the sulphamic acid urea condensate are indicated. The specific bands highlighted in the Table have been identified from the 2nd derivative FT-IR spectrum studies of the treated fabric.

Table 4.22.The possible functional groups linked with cellulose hydroxyl groups, all the specific bands are identified from the 2nd derivative spectrum of fabric treated with 1S/4U condensate.

*Functional Groups	Region cm^{-1}	**Specific Peak cm^{-1}	Intensity	Comments
RO-CO-NHR	1740-1730 1250-1210	1737 1229	s s	C=O str C-N str
N-Mono-substituted sulphonamides – SO_2NH- (hydrogen bonded or solid phase)	3335-3205 1420-1370 1360-1300 1190-1130 975-835 700-600 600-520 555-445 480-400 ~350 ~280	3300 1431 1326 - 949 649 569 463 452 - -	s m s s w-m w,br w-m w-m	N-H str, one band only NH def vib Asym SO_2 str Sym SO_2 str N-S str NH def vib SO_2 def vib SO_2 wagging vib SO_2 twisting vib SO_2 rocking vib CNS def vib
Covalent sulphonates, R-SO_2-OR	1420-1330 1235-1145 1020-850 830-690 700-600 610-500	- 1229 1191 792 691 569	s s s m w m-w	Asym SO_2 str Sym SO_2 str SO asym str SO sym str S-C str SO_2 def vib, usually two bands
Alkyl sulphonates, RO-SO_2-R	1360-1350	Figure 5.11	m-s	
Alkyl sulphonic acids (anhydrous), RSO_2-OH	3000-2800 2500-2300 1355-1340 1200-1100 1165-1150 1080-1040 910-890 700-600	- - 1348 1191 - 1071 892 634	s w-m s s s w s w	Br, O-H str Br, O-H str Asym SO_2 str Sym SO_2 str Br, S-O str S-O str S-C str
SO_4^-	1200-1140 1130-1080 1065-955 680-580 530-405	1191 1097 1021 602 497	m-s m-s s m-s m-s	 Br, with shoulders, SO4 str Sh, not always present Several bands

* These functional groups and their specific identified frequency regions are indicated in reference [3].

** These specific peaks are determined from the 2nd derivative spectra of 1S/4U condensate.

The possible chemical structures of the cellulose treated with the S/U condensate are shown in Scheme 4.3.

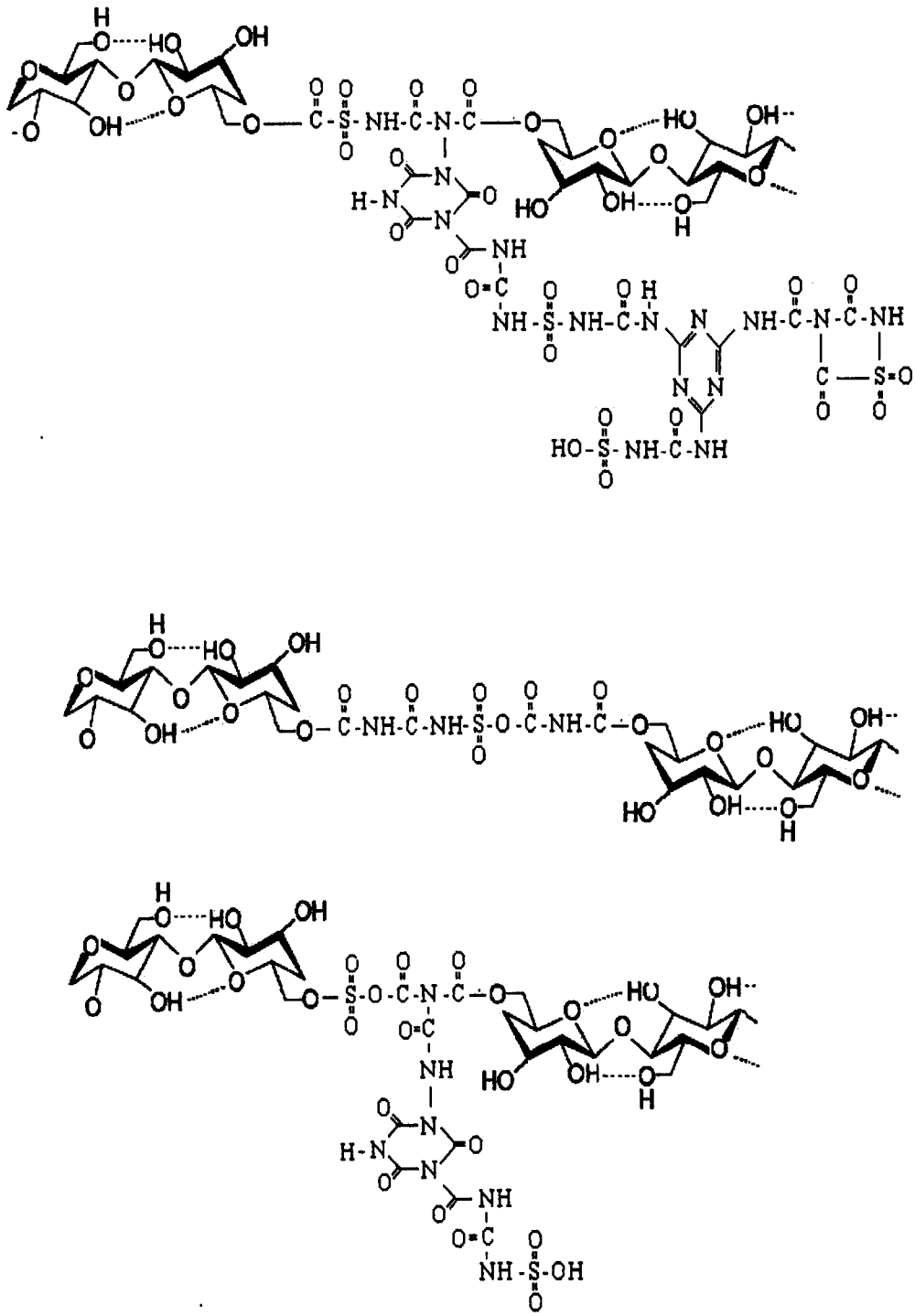

Scheme4.3. The possible chemical structure of the cellulose treated with S/U condensate.

4.8.4. Fabric Treated with phosphorous acid urea condensate

The cotton fabric was treated with various phosphorous acid/urea condensates containing one mole of phosphorous acid and 2, 3, 4 or 5 moles of urea. The FT-IR spectra of the treated fabrics are compared in Figure 4.60. No significant difference was observed; all the treated fabrics exhibited good flame retardancy performance.

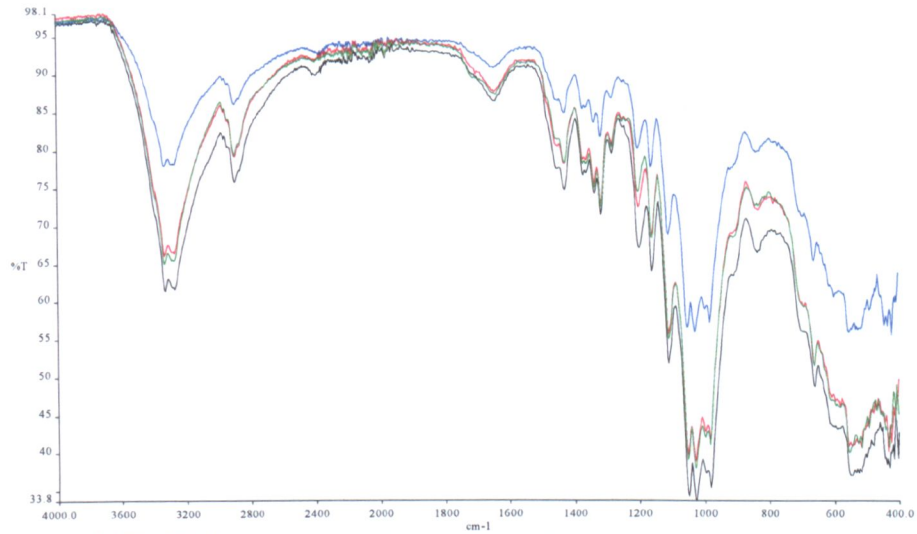

Figure4.60. The FTIR spectra of the fabric treated with prepared urea condensates; one mole of phosphorous acid : x mole urea - 1:2 [black], 1:3 [blue], 1:4 [red] and 1:5 [green].

The FT-IR analysis was carried out on one fabric sample, treated with the 1PH/3U condensate solution and compared against the FT-IR of untreated cotton. The FT-IR spectra of untreated cotton fabric and the 1PH/3U treated sample are shown in Figure 4.61.

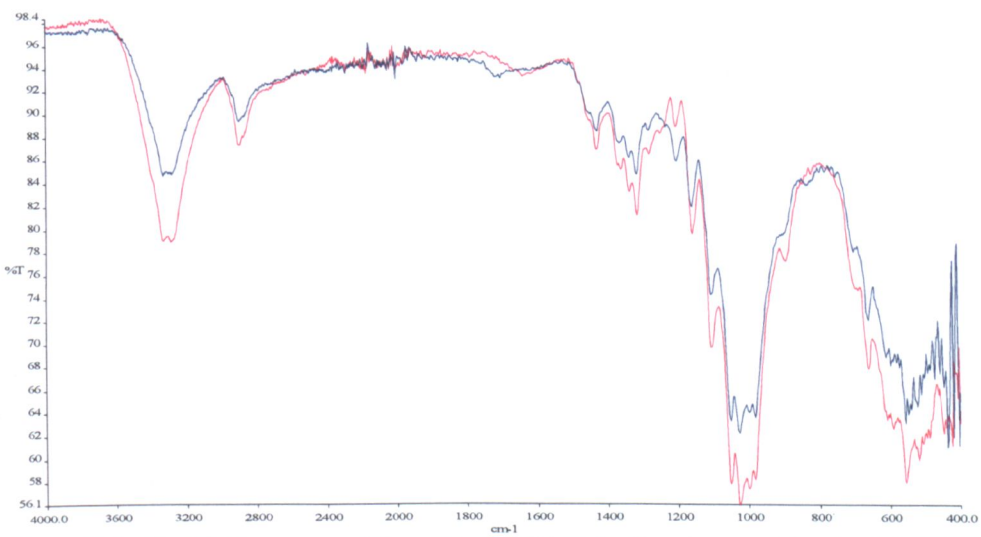

Figure4.61. The FT-IR spectra of the untreated fabric [red] and treated fabric with 1PH/3U condensate [blue].

The possible reactions between the cellulose hydroxyl groups and the urea condensate are illustrated in Scheme 4.4.

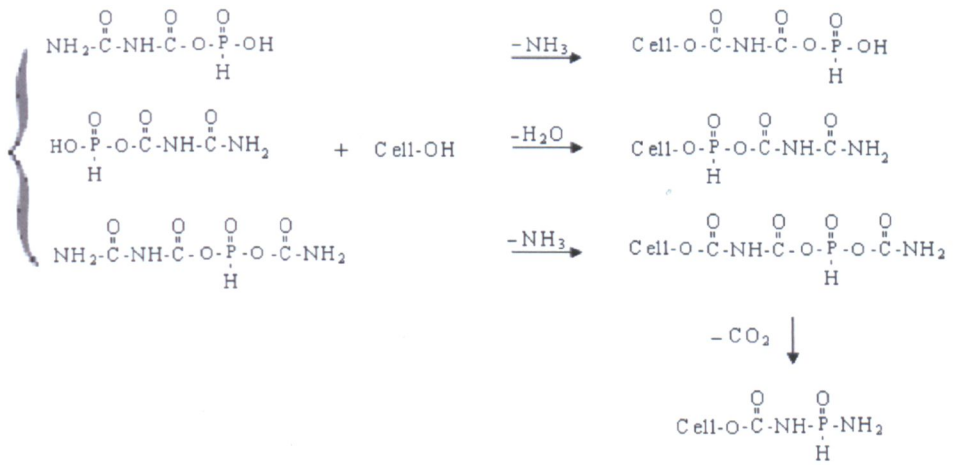

Scheme4.4. The possible reactions that may occur between the cellulose hydroxyl groups and the PH/U condensate.

A study of the 2nd derivative spectra can facilitate the interpretation of the absorption bands on the modified cellulosic fabric.

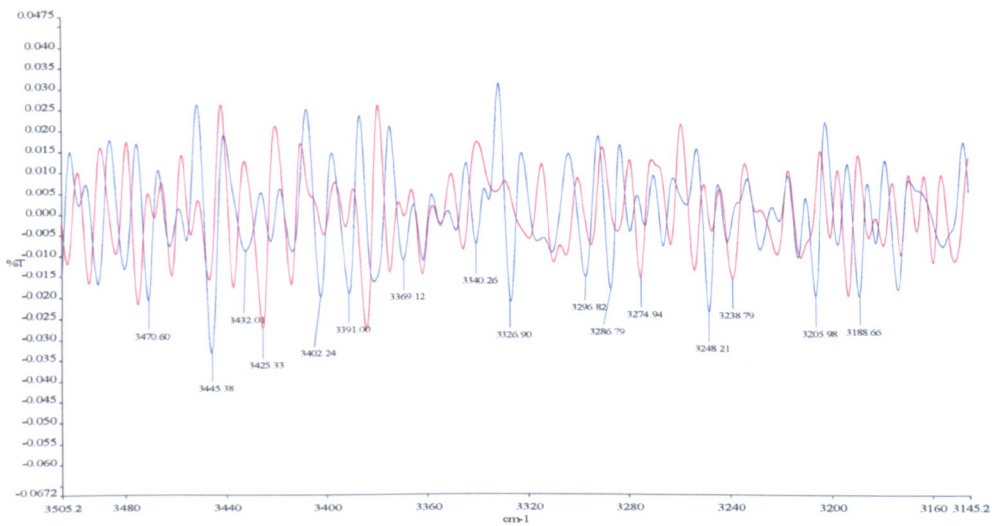

Figure4.62. The 2nd derivative spectra of untreated cotton fabric [red] and fabric treated with 1PH/3U condensate solution [blue].

In Figure 4.62 the OH stretching vibration of inter-molecular interaction (3550-3230 cm^{-1}) and intra-molecular interaction (3590-3400 cm^{-1}) of the cellulose hydroxyl groups are indicated. In the urea condensate product, the presence of the bands assigned for NH stretching vibration related to the P-NHR have been confirmed

(3200-2900 cm^{-1}), and for P-NH_2 these bands appear in the 3330-3100 cm^{-1} region. The absorption bands attributed to the NH and NH_2 stretching vibration of the urea group are assigned in this region (3440-3200 cm^{-1}). The free NH_2 anti symmetric and symmetric bonds for the solid phase alkyl amides measured in wider spectral ranges, the bands at 3475-3350 cm^{-1} and 3385-3180 cm^{-1} regions respectively relate to this group [3].

In the 2nd derivative spectrum of the fabric treated with the urea condensate solution, in Figure 4.62 the intensity absorption reduction of some bands can be seen due to the new substitution which occurs on the cellulose hydroxyl groups. At high temperature of curing process on cotton fabric, the aliphatic structure of the urea condensate (water soluble) can change to a cyclic structure; a combination of cyanuric acid, melamine and cyclic urea may be expected. The CH stretching vibration of the symmetric triazine (3300-3100 cm^{-1}) and NH_2 stretching vibration of melamines (3500-3100 cm^{-1}) are verified in this frequency region.

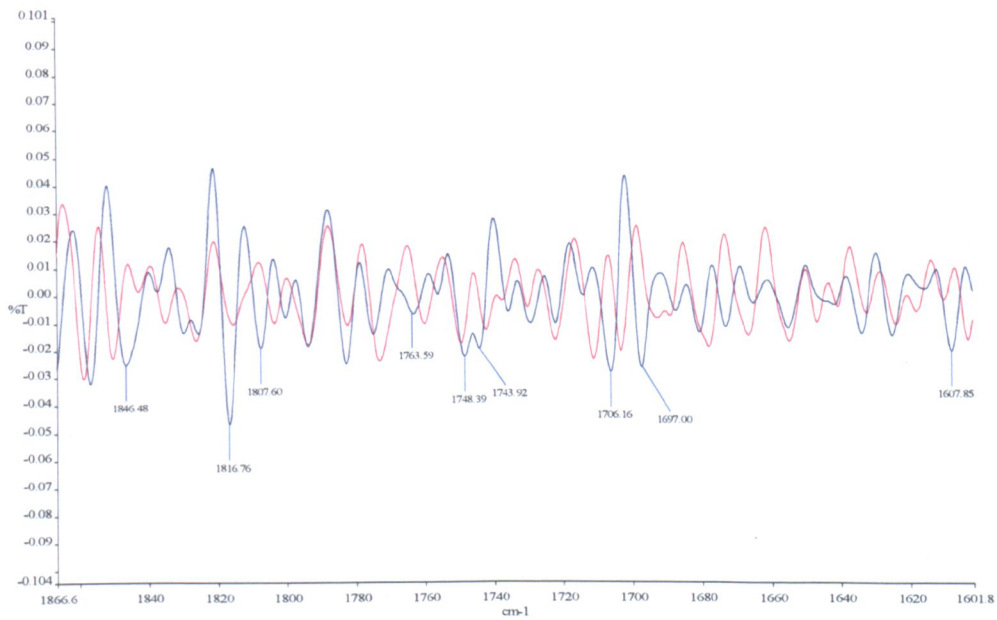

Figure4.63. The 2nd derivative spectra of the untreated cotton fabric [red] and treated fabric with 1PH/3U [blue].

In Figure 4.63 the C=O stretching vibrations of various types of compounds are indicated. The cellulose modification can be confirmed since the introduction of cellulose carbamate into the cellulose structure of the treated fabric is indicated. This functional group Cell-O-CO-NH- has specific bands in a narrow region 1740-1730

cm^{-1} due to the C=O stretching vibration which can be identified in the 2nd derivative spectrum.

Bands from triazine and melamine residues (ring stretching vibrations) can also be found in this region. Cyclic urea also shows a band at 1680-1635 cm^{-1} and 1735-1685 cm^{-1}.

The symmetric deformation vibrations of the water molecule correspond to a band in the region 1650 cm^{-1} and this band can be used for checking the extent of drying of cellulose.

Phosphorous acid/urea condensate treated fabric also gives bands due to the urea linkage, -CO-NH-CO-. The other C=O stretching vibration bands are characterized in Table 4.23.

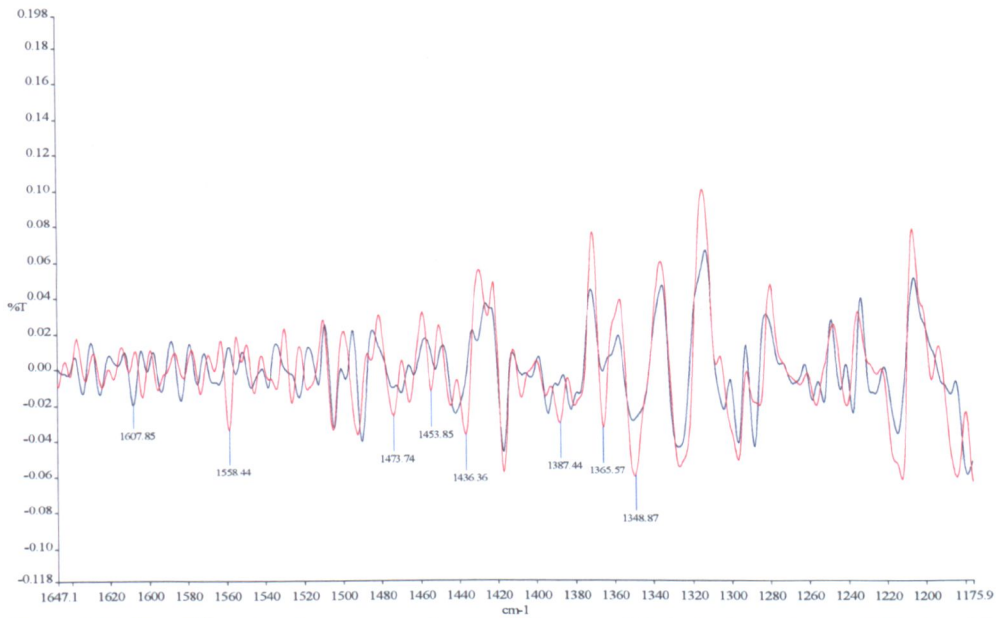

Figure4.64. The 2nd derivative spectra of untreated cotton fabric [red] and treated fabric with 1PH/3U [blue].

Bands relevant to the un-associated P = O group are apparent in Figure 4.64; these normally lie in the region 1250 – 1300 cm^{-1}.

In the cellulose FT-IR spectrum the CH_2 deformation vibration can be characterized in the narrow region, 1480-1430 cm^{-1}; the absorbance reduction in this region is clear in Figure 4.64. The CH_2 deformation vibration of P-CH_2 functional groups is assigned in 1440-1405 cm^{-1}, the new bands can be identified in the treated fabric spectrum.

The modified celluloses also show absorption bands in the 950-700 cm^{-1} frequency region. A significant difference between the 2nd derivative spectra of the two fabrics, untreated and PH/U condensate treated can be observed in Figure 4.64. In fact the bands relevant to the C-OH groups in cellulose at carbon positions 2 and 3 are indicated in 940-850 cm^{-1}; new bands due to these functional groups can be identified in the 2nd derivative spectrum of the phosphorous acid/urea condensate cotton fabric.

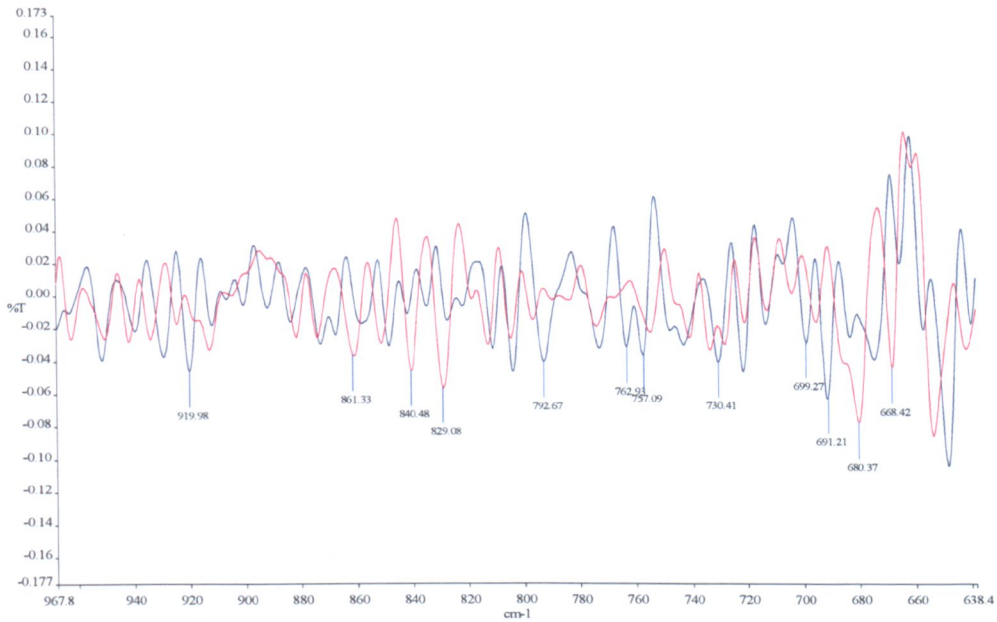

Figure4.65. The 2nd derivative spectra of untreated cotton fabric [red] and 1PH/3U treated fabric [blue].

Bands attributed to the ring stretching vibrations of triazines (860-775 cm^{-1}) and melamine (825-750 cm^{-1}) is demonstrated in Figure 4.65. The keto group assigned band from the tautomer of hydroxyl- triazines can be assigned at 795-750 cm^{-1}.

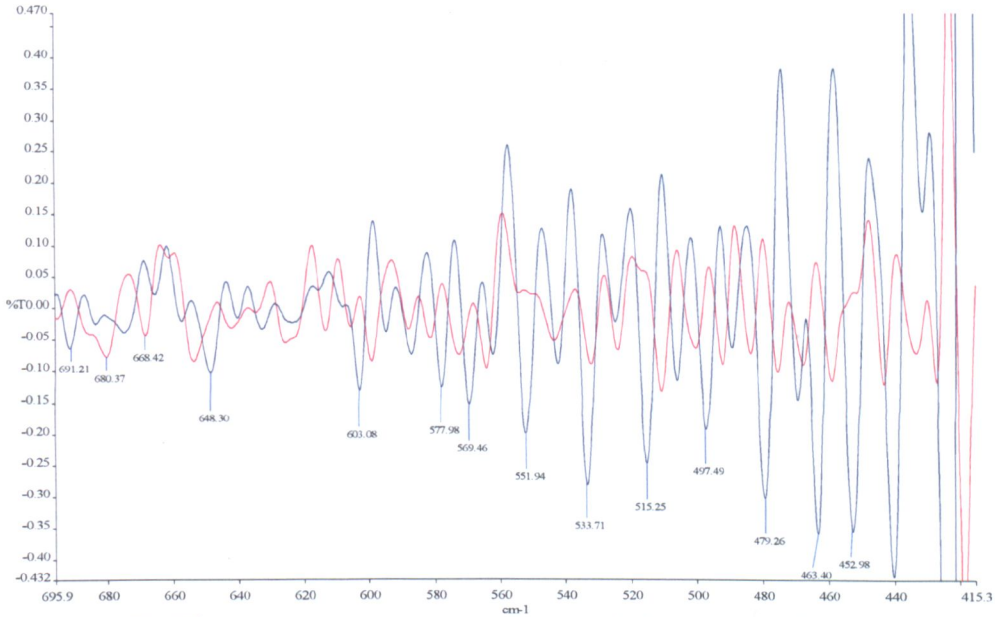

Figure4.66. The 2nd derivative spectra of untreated cotton fabric [red] and 1PH/3U treated fabric [blue].

1PH/3U treated fabric shows specific bands in the region 400-700 cm^{-1} indicating the presence of ester groups; the broad diffuse absorption in this region of the treated cellulose spectrum can be attributed to changes in hydrogen bond vibrations. In fact a reduction in absorbance of individual bands in this region can be attributed to the esterification reaction, Figure 4.66. Table 4.23characterizes the specific bands which appear in the 2nd derivative spectra.

Table4.23. The possible functional groups linkage with cellulose hydroxyl groups in reaction with 1PH/3U condensate.

Functional groups*	Region cm^{-1}	Intensity	**Specific Peak cm^{-1}	Comments
P-NH_2	3330-3100 1600-1535 1110-920 840-660	m m m-s m-s	- 1580 929-951	NH_2 str NH_2 def vib P-N-C asym str NH_2 wagging vib
P-NH	3200-2900 1145-1075 1110-930	m w-m m-s	- 1097 976	NH str C-N str P-N-C asym str
RPO_3^{2-}	1125-970 1000-960	s m	1056 990	asym PO_3^{2-} str sym PO_3^{2-} str
P=O (unassociated) (associated)	 1350-1175 1250-1150	 vs vs	 ~1290-1305 ~1180	 P=O str P=O str
P-O-R	1050-970	vs	1031	asym P-O-C str
P-H	2500-2225 1150-965	m w-m	- 1080-1087	P-H str P-H def vib
P-C	795-650	m-s	~665	P-C str
P-CH_2-	1440-1405 780-760	m s	~1430 ~770	CH_2 def vib P-C str
(RO)(HO)HP=O	1215-1200	vs	~1213	P=O str
R(OH)HP=O	1175-1135	vs	1161	P=O str
R-O-CO-NHR	1740-1730 1250-1210	s s	1744-1748 ~1230-1240	C=O str C-N str
Primary urethanes H_2N-CO-O	3450-3400 3240-3200	m m	3471 ~3235	NH_2 asym str NH_2 sym str
Secondary urethanes -HN-CO-O Associated Unassociated	 3340-3250 3410-3390	 m m	 3327 3391-3402	 N-H str vib N-H str vib

*These Functional groups and their specific identified frequency regions are indicated in reference [3].
**These specific peaks are determined from the 2nd derivative FT-IR spectra of fabric treated with PH/U condensate.

Table4.23. The possible functional groups linkage with cellulose hydroxyl groups in reaction with 1PH/3U condensate.

Functional groups*	Region cm^{-1}	Intensity	Specific Peak** cm^{-1}	Comments
Alkyl urethanes				
>NCO-O-	1740-1680	s	1706	C=O str
NH_2-CO-OR	1695-1680	s	1697	C=Ostr
(Free) Primary amides	3540-3480	m-s	-	asym N-H str
Associated	3420-3380	m-s	3391-3402	asym N-H str
	3375-3320	m-s	3327-3340	asym N-H str
	3205-3155	m-s	3189-3206	sym N-H str
	1670-1650	s	~1668	C=O str
	1650-1620	w-m	1608	N-H def vib, C-N str
	1420-1400	m	-	C-N str
	1150	w	1153	NH_2 in-plane
	750-600	m	691-699	rocking vib
	600-550	m-s	569-578	NH_2 def vib
	500-400	m-s	Several bands	N-C=O def vib
				C-C=O def vib
(Free) Secondary amides	3460-3420	m-s	3445	doublet if cis-trans isomerism present,
trans form	3370-3270	m	3287	N-H str
cis form	3180-3140	m	3155	N-H str
trans form	3100-3070	w	3086	N-H str
	1680-1630	s	~1640	N-H str
trans form	1570-1515	s	~1520	C=O str
trans form	1305-1200	w-m	~1290-1237	N-H def vib, C-N str
	770-620	m	730-648	
cis form	1450-1440	m	~1440-1450	out-of-plane N-H
	1350-1310	w-m	~1348	def vib
	~800	m-s	~804	
amides containing -CO-NH-CO- diacylamines	1790-1720	s	1748-1744	doublet

*These Functional groups and their specific identified frequency regions are indicated in reference [3].
**These specific peaks are determined from the 2nd derivative FT-IR spectra of fabric treated with PH/U condensate.

4.8.5. Further investigation of FT-IR analysis of fabric treated with urea condensate, S/U and PH/U

A Comparison of the treated fabric with 1S/3U and 1PH/3U and untreated cotton fabric can provide further information regarding the chemical reactions which are involved in the urea condensate solution fabric treatment.

In Figure 4.67 the FT-IR spectra of all three fabrics are shown. To determine the differences precisely, the 2nd derivative spectra of specific frequency regions are provided.

Figure4.67. The FT-IR spectra of untreated cotton fabric [red], the fabric treated with 1S/3U [blue] and the fabric treated with 1PH/3U [green].

In this study, the two prepared urea condensate solutions containing the same amount of urea were selected, 1S/3U and 1PH/3U. Therefore the bands relevant to the urea products such as triazine, cyanuric acid and melamine appear at the same frequency regions and can be identified easily.

The FT-IR spectrum of the fabric treated with sulphamic acid urea condensate with some very strong new bands has been analysed in more detail.

In Figure 4.68 the new bands at 3096, 3073 cm^{-1} and 3050 cm^{-1} are attributed to the O-H stretching vibration of R-SO_2-OH functional group.

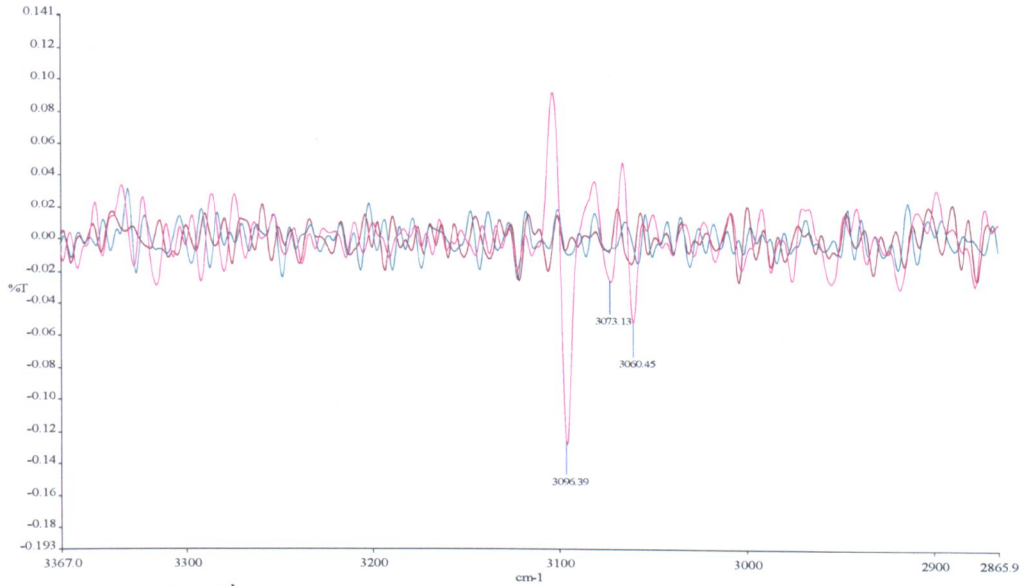

Figure4.68. The 2nd derivative spectra of untreated cotton fabric [brown], fabric treated with 1S/3U [pink] and fabric treated with 1PH/3U [aqua].

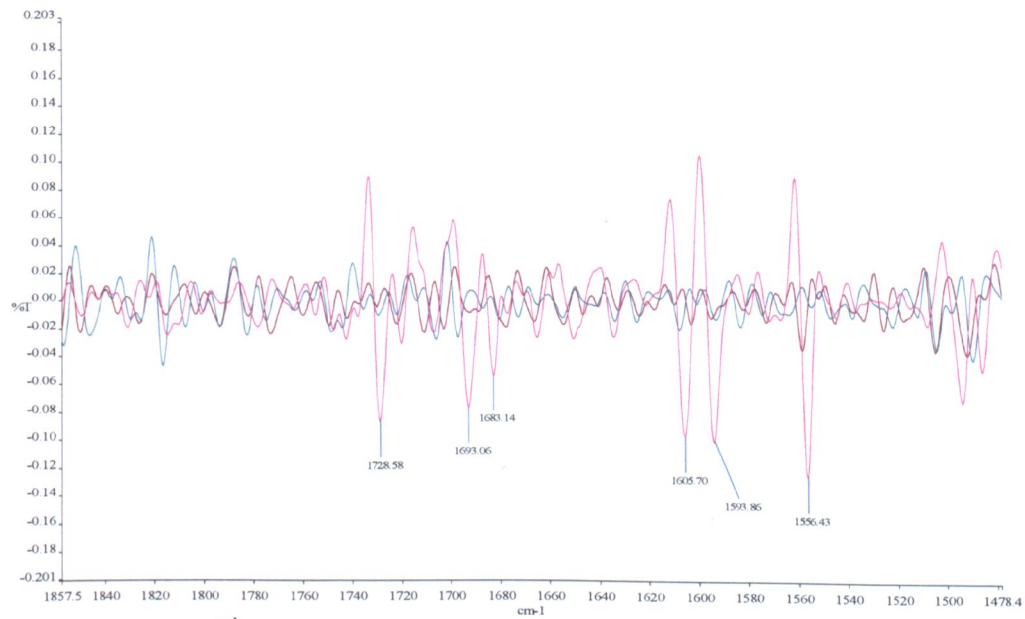

Figure4.69. The 2nd derivative spectra of untreated cotton fabric [brown], fabric treated with 1S/3U [pink] and fabric treated with 1PH/3U [aqua].

It has been indicated in section 4.8.3 that the hydroxyl groups on cellulose can react with the S/U condensate solution and the production of cellulose carbamate or a urethane linkage on the cellulose structure has been confirmed. In Figure 4.69 the

bands assigned to the C=O stretching vibration of urethane appear clearly; these specific bands for R-O-CO-NHR are found at 1729 cm^{-1} and for NH_2-CO-OR at 1693 $cm^{-1}$and 1683 cm^{-1}. In the solid phase, the C=O stretching vibration of secondary urethanes are identified in this region,1600-1500 cm^{-1}, therefore the three bands at 1606, 1594 cm^{-1} and 1556 $cm^{-1}$are probably defined due to this functional group. The ring stretching vibrations of melamine and sym triazine are also indicated in this region.

Increasing the amount of urea in the urea condensate, results in a reduction of absorption intensity of all these bands.

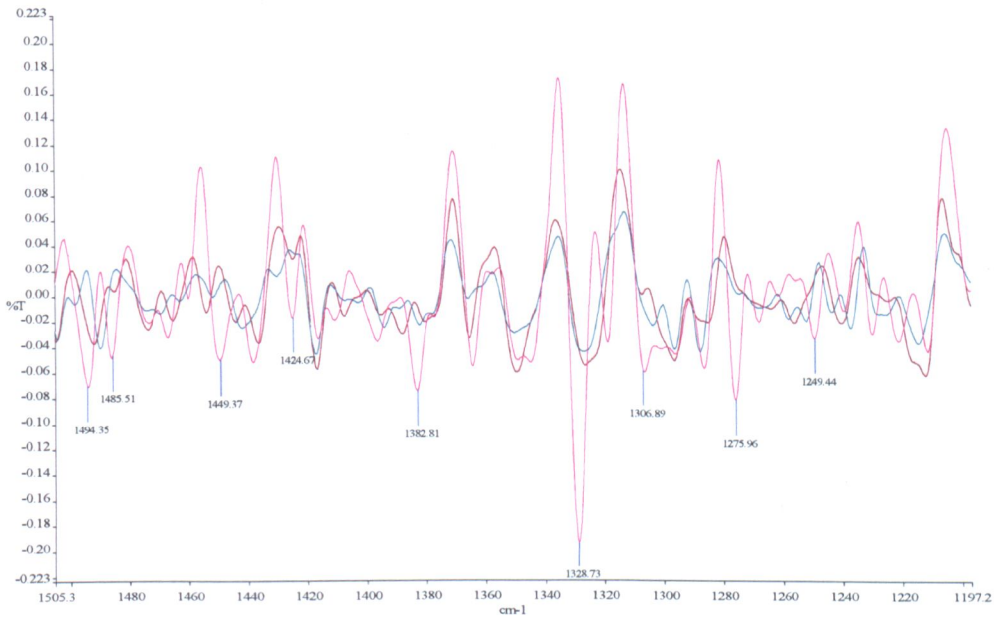

Figure4.70. The 2nd derivative spectra of untreated cotton fabric [brown], fabric treated with 1S/3U [pink] and fabric treated with 1PH/3U [aqua].

In Figure 4.70 the cellulose CH_2 deformation vibrations are indicated in this region. The new sulphur functional groups substituted on the cellulose hydroxyl groups can be identified by the new strong bands which appear in the 2nd derivative FT-IR spectrum of fabric treated with S/U condensate. The bands at 1494, 1486, 1449 cm^{-1} and 1425 cm^{-1} represent these functional groups on the modified cellulose. The CH deformation vibration of cellulose has a characteristic band at 1383 cm^{-1} which is very clear in Figure 4.70. The two bands at 1329 cm^{-1} and 1307 cm^{-1} are assigned to the asymmetric SO_2 stretching vibrations of $-SO_2$-NH- which are identified in the 1360-1300 cm^{-1} frequency region [3].

In the reaction between cellulose and the S/U condensate solution at high temperature, after removal of ammonia gas which evolves during the reaction, the possible formation of -C-N=SO_2 should be considered. In the literature [3], the thionylamines functional group can be verified with specific bands in 1300-1230 cm^{-1} due to the -N=S=O asymmetric stretching vibration and in 1180-1110 cm^{-1} to the symmetric stretching vibration. Therefore these two bands at 1276 and 1250 cm^{-1} can confirm the presence of this functional group.

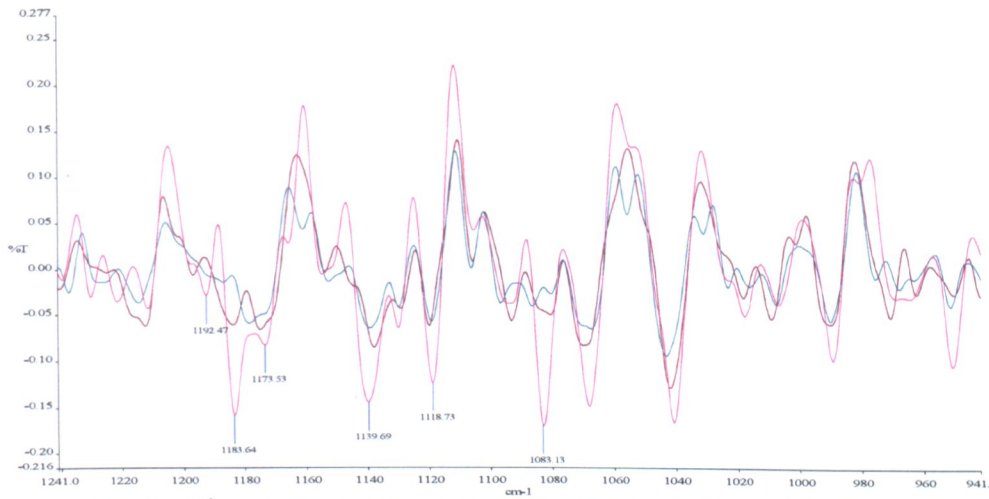

Figure4.71. The 2nd derivative spectra of untreated cotton fabric [brown], fabric treated with 1S/3U [pink] and fabric treated with 1PH/3U [aqua].

In Figure 4.71 the bands relevant to the SO_2, SO stretching vibrations are indicated in this region. The bands at 1192, 1184 cm^{-1} and 1174 cm^{-1} are attributed to the symmetric SO_2 stretching vibration of R-SO_2-OR, and the bands at 1140 cm^{-1} and 1119 cm^{-1} are due to the SO_4 stretching.

In Figure 4.72 the bands at 951, 870, 858 cm^{-1} and 845 cm^{-1} are attributed to the SO asymmetric vibration of R-SO_2-OR; however, the S-O symmetric stretching vibration appears at 800, 791, 767, 754 cm^{-1} and 732 cm^{-1}.

The N-S stretching vibrations of –SO_2NH- are also indicated in this frequency region.

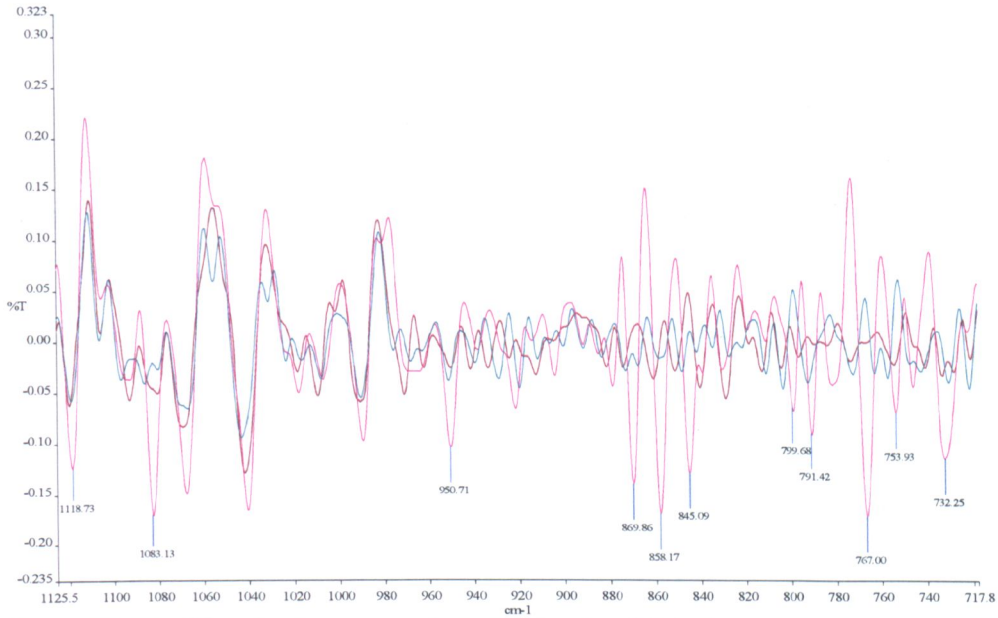

Figure4.72. The 2nd derivative spectra of untreated cotton fabric [brown], fabric treated with 1S/3U [pink] and fabric treated with 1PH/3U [aqua].

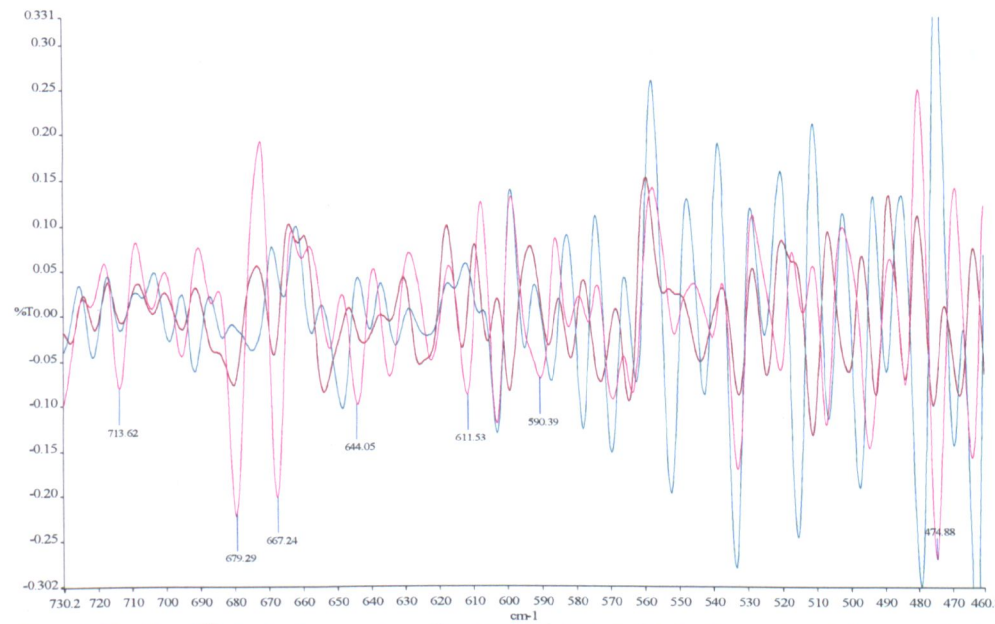

Figure4.73. The 2nd derivative spectra of untreated cotton fabric [brown], fabric treated with 1S/3U [pink] and fabric treated with 1PH/3U [aqua].

4.8.6. FT-IR analysis of fabrics treated with different types of S/PH/U condensate

The FT-IR spectra of fabrics treated with various urea condensates are shown in Figure 4.74. The urea condensates prepared by mixing one mole sulphamic acid, one mole phosphorous acid and various moles of urea 10, 12, 14, 16, 18 and 20, heated to high temperature (3.2.5). Aqueous solutions of these products were applied to cotton fabric 4.1.7.

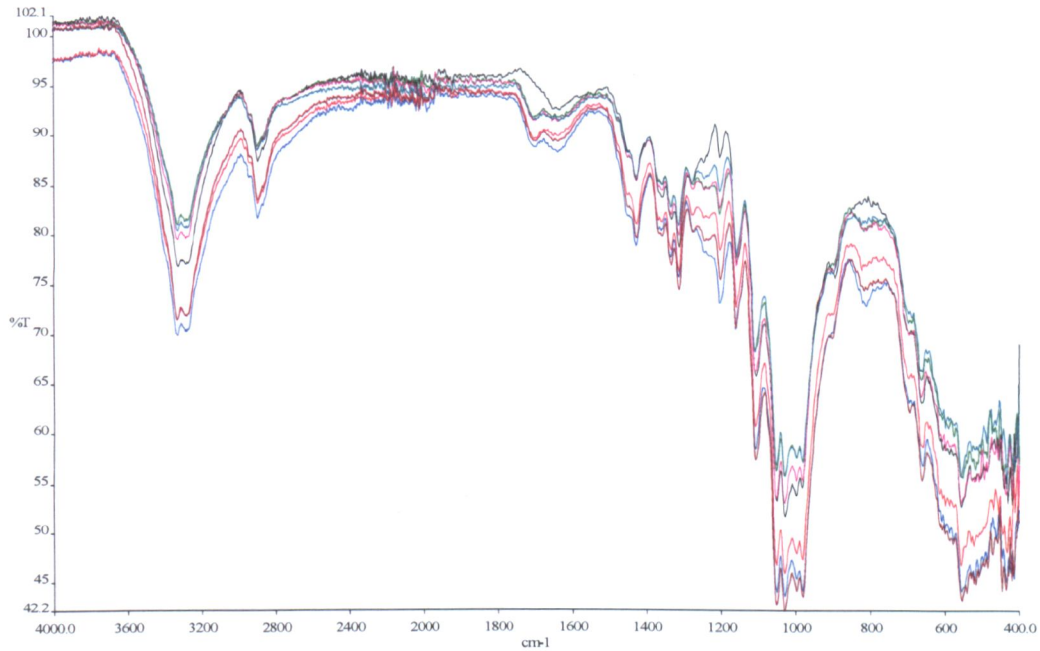

Figure4.74. FT-IR spectra of untreated cotton fabric [black] and urea condensate treated fabrics 1mole of sulphamic acid, 1mole phosphorous acid and various molar ratios of urea, 8[blue], 10 [red], 12 [green], 14 [pink], 16 [dark green], 18 [brown] and 20 moles [aqua].

In Figure 4.74 by increasing the amount of urea in the condensate, reductions in band absorbance intensity can be seen in particular regions. Nevertheless sufficient phosphorus and sulphur remained bonded to the cellulose to impart good flame retardancy; only the 1S/1PH/20U treated fabric failed the test. A comparison between the FT-IR spectra of this fabric (1S/1PH/20U) and the fabric treated with urea solution alone, confirmed the presence of more bonded urea derivatives, no other significant differences were observed, Figure 4.46.

4.8.7 FT-IR analysis of the treated fabric with 1S/1PH/10U condensate

FT-IR spectra of untreated cotton fabric and 1S/1PH/10U treated fabric are shown in Figure 4.75. A new substitution pattern on cellulose hydroxyl groups can be determined from the modified cellulose spectrum. To study in more detail, the second

derivative spectra for both fabrics were produced. The predicted chemical reactions involved in this high temperature treatment are indicated in Scheme 4.5.

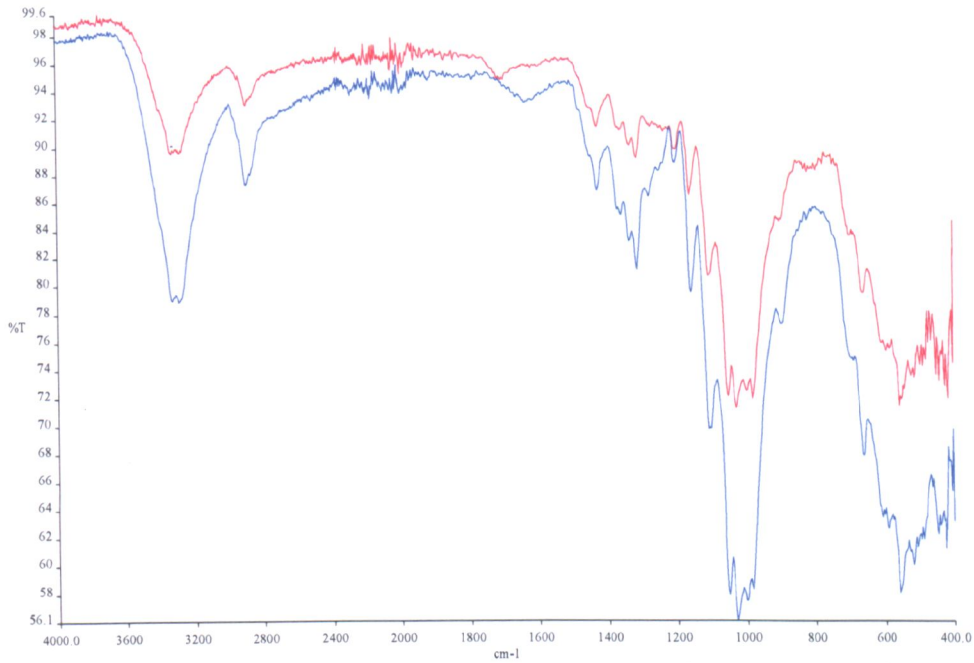

Figure4.75. FT-IR spectra of untreated cotton fabric [red] and the 1S/1PH/10U treated fabric [blue], both fabrics were oven dried for 24 hours at 110°C.

A possible mechanism for the production of a complicated polymer structure on cellulose after curing at 165°C, by liberating CO_2, NH_3 and also water, is shown in Scheme 4.6.

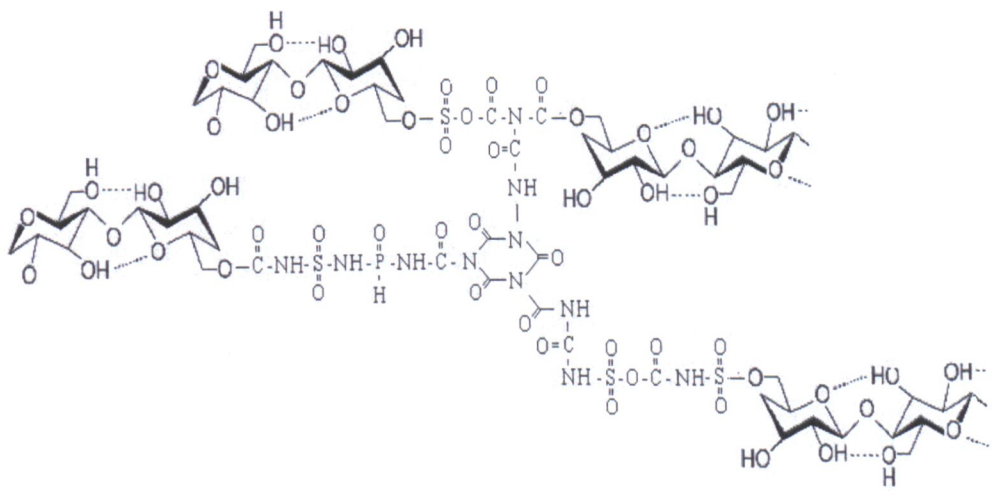

Scheme4.6. A possible new chemical structure formed on cellulose hydroxyl groups after reaction with the 1S/1PH/10U condensate.

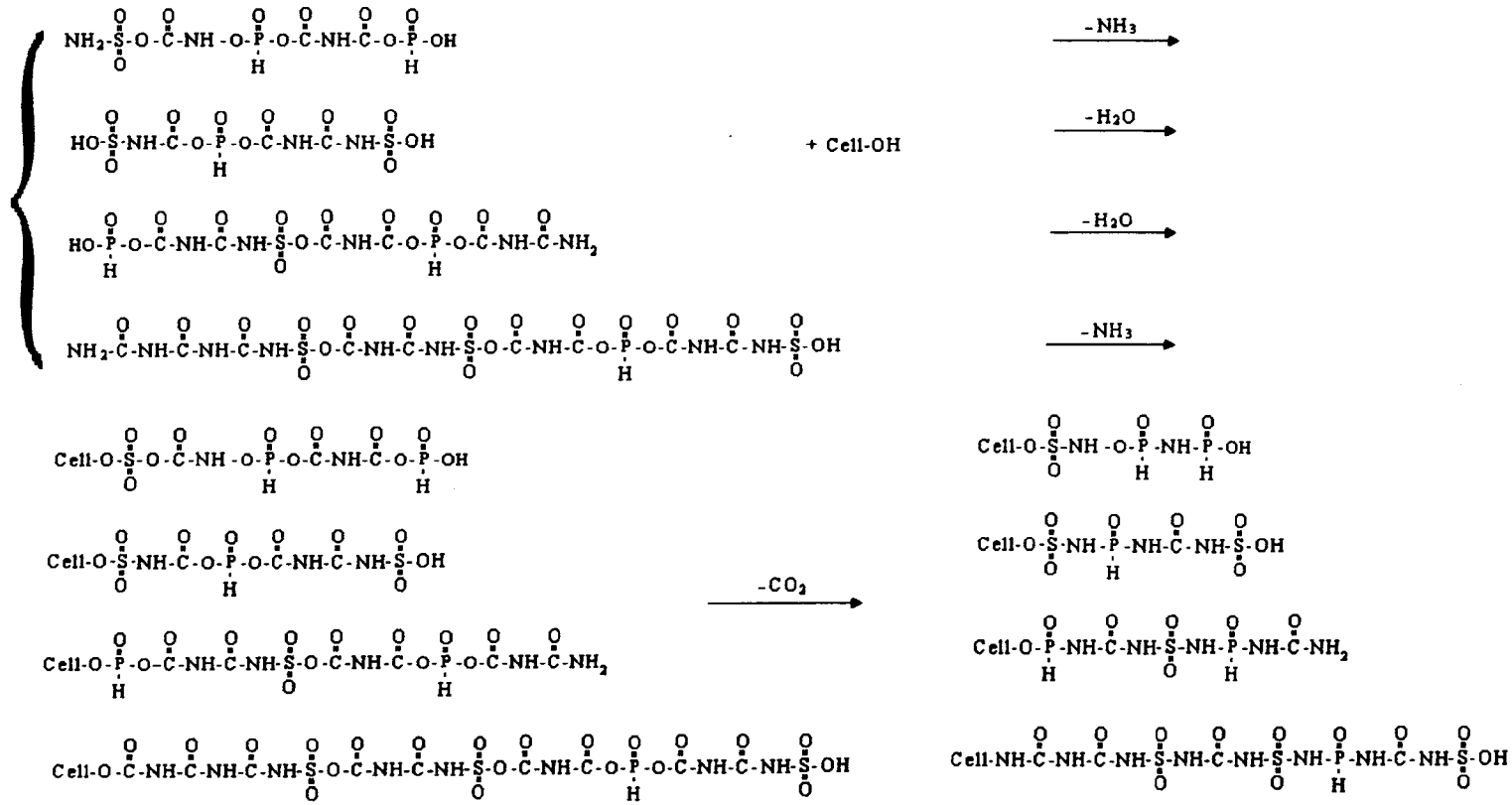

Scheme4.5. Possible reactions between 1S/1PH/10U condensate and cellulose hydroxyl groups.

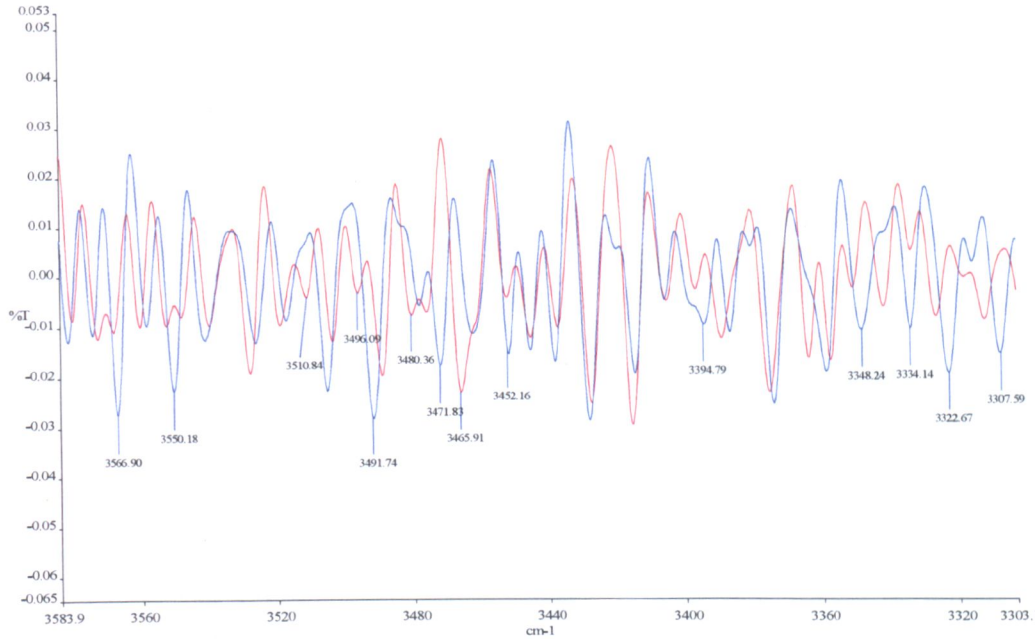

Figure4.76. The 2nd derivative spectra of untreated cotton fabric [red] and the 1S/1PH/10U treated fabric [blue].

In Figure 4.76, in the 2nd derivative spectrum, the absence of bands at 3496, 3480 cm^{-1} and 3466 cm^{-1} on the new modified cellulose are attributed to the new intra-molecular hydrogen bonding which occurred on the fabric at high temperature. The presence of few bands at 3348, 3334, 3323 and 3307 cm^{-1} and the disappearance of the cellulose relevant bands in this specific frequency region supports the same point.

Both primary and secondary amides exhibit a number of bands due to different hydrogen bonding states. The bands relevant to the N-H stretching and the asymmetric stretching of NH_2 residues in ureas are indicted in this region. However the N-H stretching vibration of primary sulphonamide $-SO_2NH_2$ can also be verified. The possible formation of triazine, cyanuric acid and melamine at high temperature on the modified cellulose should be considered. The NH_2 stretching vibration of melamine is indicated at this frequency region, 3500-3100 cm^{-1}.

In the modified cellulose spectrum (Figure 4.75) the new bands representing the NH stretching vibration of P-NHR cannot be identified easily. The asymmetric CH_2 stretching vibration of the cellulose primary alcohol appears in the 2990-2900 cm^{-1} region, The absorption intensity reduction and disappearance of bands at 2974, 2963, 2953 cm^{-1} and 2990 cm^{-1} confirm the new substitution apparent on the cellulose primary hydroxyl groups in carbon position six.

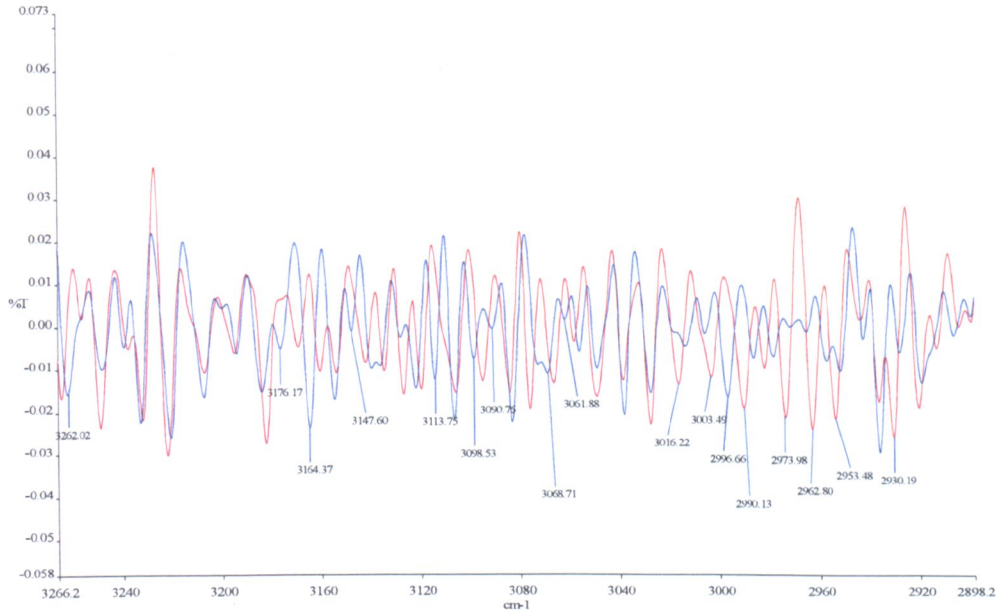

Figure4.77. The 2nd derivative spectra of untreated cotton fabric [red] and the 1S/1PH/10U treated fabric [blue].

New bands at 3099, 3091 cm^{-1} and 3069 cm^{-1} in the modified cellulose are attributed to the OH stretching vibration of R-SO_2-OH, and could be identified in the spectrum of 1S/4U condensate treated fabric.

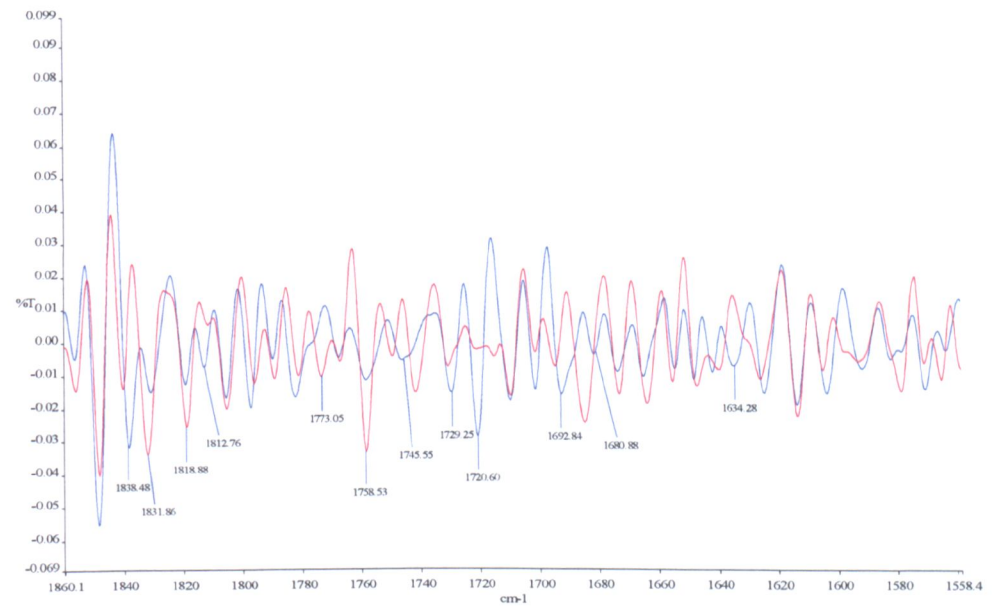

Figure4.78. The 2nd derivative spectra of untreated cotton fabric [red] and the 1S/1PH/10U treated fabric [blue].

In Figure 4.78 in the 2nd derivative spectrum of the modified cellulose the band at 1634 cm^{-1} and the other neighboring bands close to it are attributed to the N-H

deformation and C-N stretching vibration of primary amides. The C=O stretching vibration of amides containing-CO-NH-CO- has a double bands at 1720-1760 cm^{-1}, and in the case of ring amide, a large separation will be observed [3]. The band at 1721 cm^{-1} and a wide band at 1746 cm^{-1} can be assigned due to this mode of action regarding this functional group. The C=O stretching vibration of the primary and secondary amides can be found easily at their particular frequency region indicated in literature; 1670-1650 cm^{-1} for primary amide, and 1680-1630 cm^{-1} for secondary amides [3]. The production of cellulose carbamate can be confirmed by the presence of a new band at 1740-1730 cm^{-1} [3], the band at 1729cm^{-1} represents this functional group on modified cellulose. The absorption intensity reduction of cellulose relevant bands on the modified fabric is acceptable evidence for the new substitution pattern on the cellulose hydroxyl groups.

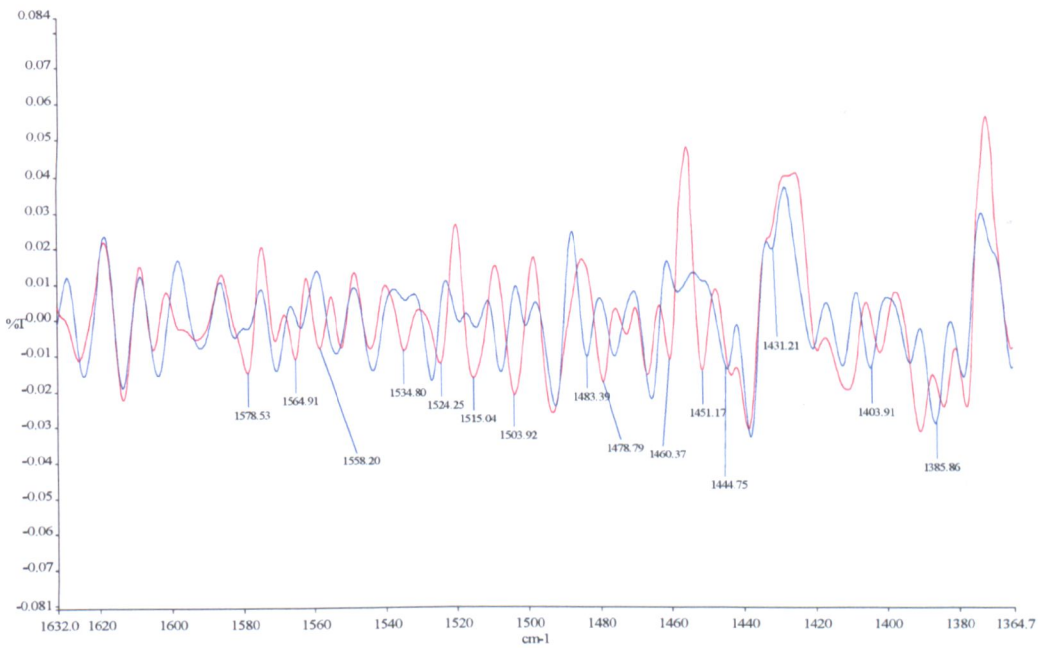

Figure4.79. The 2nd derivative spectra of untreated cotton fabric [red] and the 1S/1PH/10U treated fabric [blue].

In Figure 4.79 in the frequency region, 1530-1000 cm^{-1}, bands relevant to the CH deformation and wagging vibration of secondary alcohols of cellulose are indicated. In-plane OH deformation vibration of primary alcohols has bands in this region, however the coupling of this mode with CH wagging vibration for the secondary alcohol are determined in the narrow frequency region 1430-1370 cm^{-1}. The new bands in 1440-1405 cm^{-1} in the spectrum of the modified cellulose are attributed to the CH_2 deformation vibration of P-CH_2 group. A broad band at 1580 cm^{-1}

(approximately) in a treated fabric is attributed to the P-NH_2 functional groups which appear at the same frequency in a fabric treated with 1PH/3U condensate.

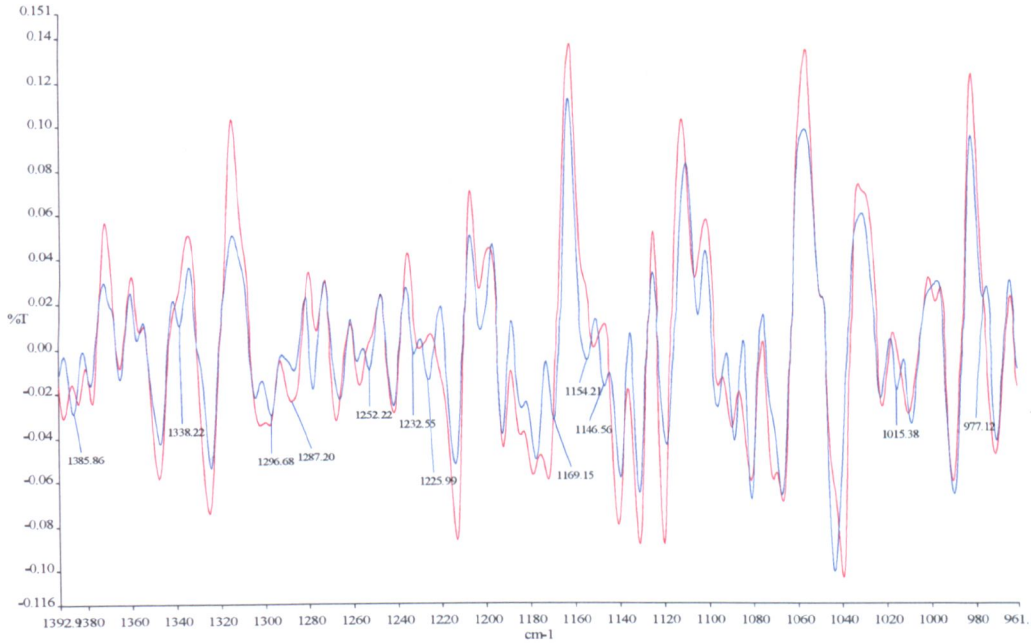

Figure4.80. The 2nd derivative spectra of untreated cotton fabric [red] and the 1S/1PH/10U treated fabric [blue].

In Figure 4.80 the band at 1338 cm^{-1} is attributed to the SO_2 stretching vibration of –SO_2NH- which is identified in the 1360-1300 cm^{-1} region. A characteristic band at 1386 cm^{-1} represents the CH deformation vibration of cellulose; this band does not appear in the two other treated fabrics with S/U and PH/U. In fact a secondary amide in cis form has a specific band in this region. The band at 1169 cm^{-1} and the other bands close to it has changed the cellulose bands in modified cotton fabric; there are defined SO and SO_2 stretching vibrations for the R-SO_2-OR new functional group. The three bands at 1154, 1147 cm^{-1} and 1169 cm^{-1} are determined as due to the P=O and S=O stretching vibrations of the R(OH)HP=O (1175-1135 cm^{-1}) and sulphondiamides (1145-1140 cm^{-1}), the presence of these bands in the other modified fabric has been confirmed.

For aliphatic compounds, the asymmetric stretching vibration of the P-O-C group gives a very strong band normally found in the region, 1050-970 cm^{-1}; the presence of the band at 1015 cm^{-1} are attributed to this mode of vibration. The band representing the P=O group is strong in the region 1350-1150 cm^{-1}. The frequency of the P=O stretching vibration is almost independent of the type of compounds in which the

group is present and also the size of the substituents. However the number of electronegative substituents bonded to it directly has an effect. The P=O band may sometimes appears as a doublet, the separation is either small or for some triaryl phosphate are at 50 cm^{-1}. Fermi resonance and rotational isomers often can split into doublet bands [6]. A doublet band at 1252 cm^{-1} on modified cellulose is attributed to the P=O stretching vibration. The presence of this band at the exact frequency in the 2nd derivative spectrum of the 1PH/3U treated fabric is precise verification. The new bands at 1233 cm^{-1} and 1226 cm^{-1} are attributed to the same mode of vibration in the modified cellulose.

The new functional group, R-(HO)HP=O on cellulose can be identified in a narrow frequency region 1175-1135 cm^{-1} due to the P=O stretching vibration,. The two bands at 1154 cm^{-1} and 1147 cm^{-1} represent this mode of vibration.

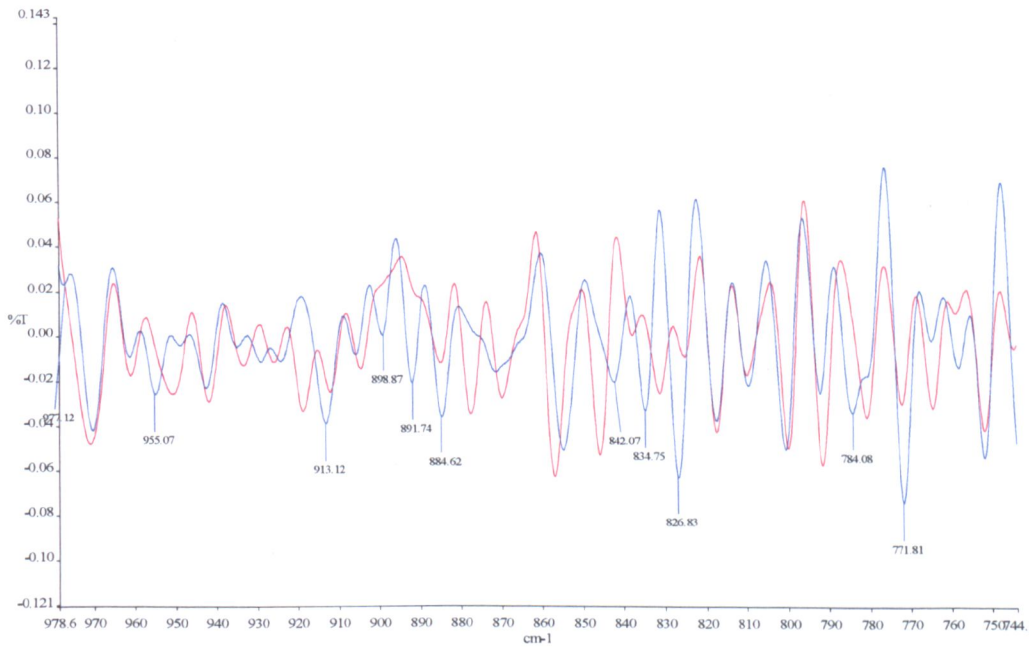

Figure4.81. The 2nd derivative spectra of untreated cotton fabric [red] and the 1S/1PH/10U treated fabric [blue].

In Figure 4.81 the new bands in the region 940-850 cm^{-1} are attributed to the CH_2OH group of cellulose in position 2 and 3 [4]. The bands at 899, 892 cm^{-1} and 885 cm^{-1} are identified regarding these functional groups. In the fabrics treated with the PH/U condensate these bands appear exactly the same, but in the other fabric treated with S/U condensate, an intensity reduction was observed.

In fact the absorbance reduction of cellulose bands at this frequency region can reflect the conformational changes which occur in the modified cellulose.

The NH_2 wagging vibrations of P-NH_2 are indicated in the 840-660 cm^{-1} frequency region, therefore several bands at 842 cm^{-1} are attributed to this mode of vibration. The absorption intensity of these bands in the 2nd derivative spectrum of treated fabric with 1PH/3U is reduced. The two bands at 835 cm^{-1} and 8276 cm^{-1} are assigned to the asymmetric P-O-S stretching vibration, which are identified only on the fabric treated with the 1S/1PH/10U condensate.

Two bands at 784 cm^{-1} and 772 cm^{-1} in the modified secondary spectrum represent the P-O-C stretching vibration however in a specific region 780-760 cm^{-1}, P-C stretching of P-CH_2 occurred.

In Figure 4.82 the absorption intensity reduction of the bands in the cellulose fabric spectrum can provide further information relevant to cellulose modification. The C-O deformation vibrations of primary alcohol in the cellulose structure are defined in the 555-395 cm^{-1} frequency region. A comparison between the 2nd derivative spectra of three modified cotton fabrics treated with 1S/4U, 1PH/3U and 1S/1PH/10U, gives accurate information regarding each band in this region.

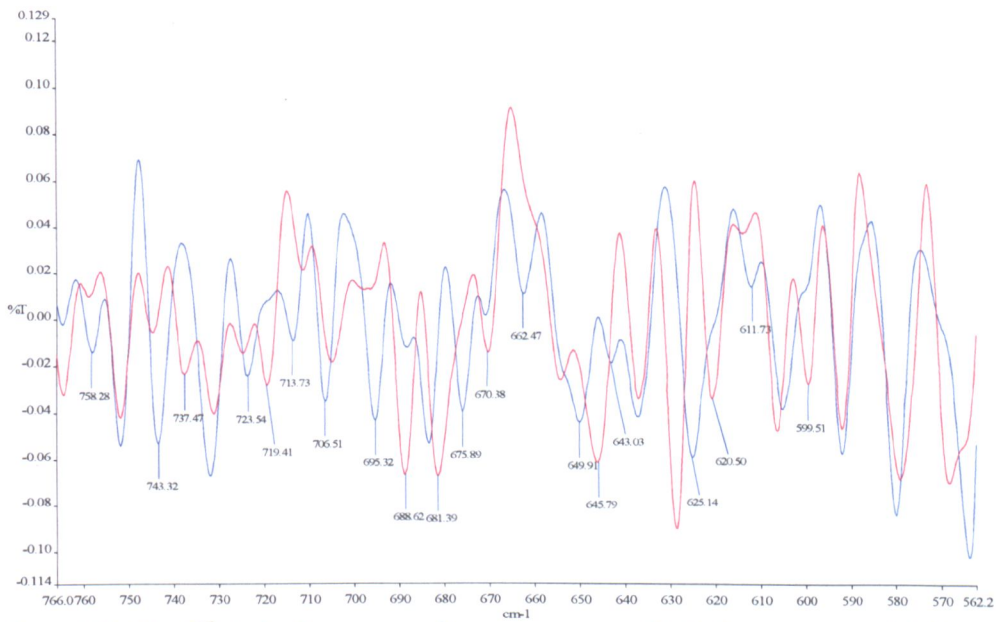

Figure4.82. The 2nd derivative spectra of untreated cotton fabric [red] and the 1S/1PH/10U treated fabric [blue]

In Figure 4.82 the NH_2 deformation vibrations of primary amides are indicated in this region, 750-600 cm^{-1}, the absorption intensity increases on 1S/1PH/10U modified

fabric can be explained due to the greater amount of urea applied to the pre-condensate.

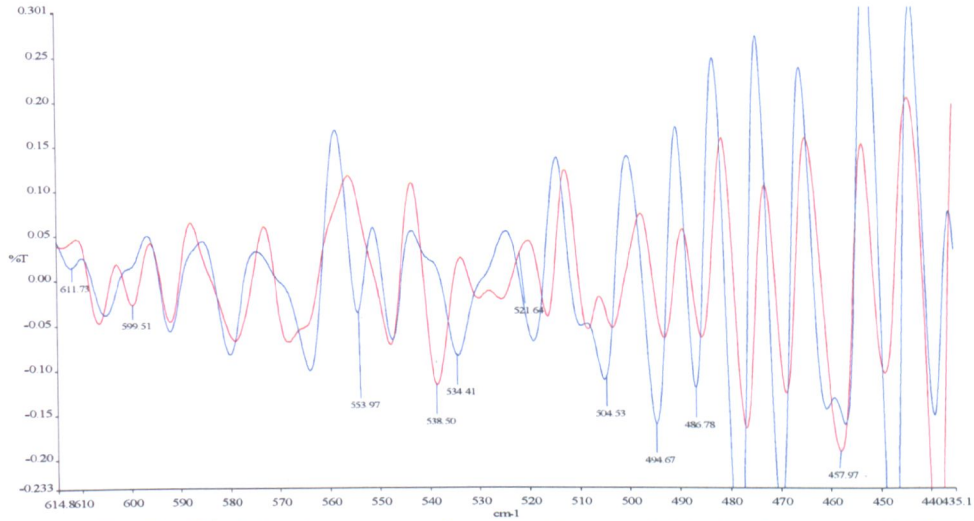

Figure4.83. The 2nd derivative spectra of untreated cotton fabric [red] and the 1S/1PH/10U treated fabric [blue].

The N-C=O deformation vibrations of primary amides are determined in 600-550 cm^{-1} frequency region. In the 2nd derivative spectra of modified fabrics in Figure 4.83 new bands in this region can be identified due to the vibration mode of this functional group. The absorption intensity increase for a number of bands in 500-440 cm^{-1} confirms the new substitution pattern on cellulose hydroxyl groups. In fabrics treated with 1PH/3U and 1S/3Uthe same intensity changes have been observed.

4.8.8 FT-IR analysis of the 1S/2PH/10U treated fabric

The FT-IR spectra of cotton fabric treated with the 1S/1PH/10U and 1S/2PH/10U condensates are compared in Figure 4.84, no significant differences are observed.

Therefore a study of second derivative spectra is required (see figure 4.85, 4.86 and 4.87). The FT-IR investigation on the product of 1S/2PH/10U condensate gave further information regarding the main chemical structure which expected to form during urea condensate preparation. All these new functional groups in 1S/2PH/10U have to be investigated in the fabric treated with this product.

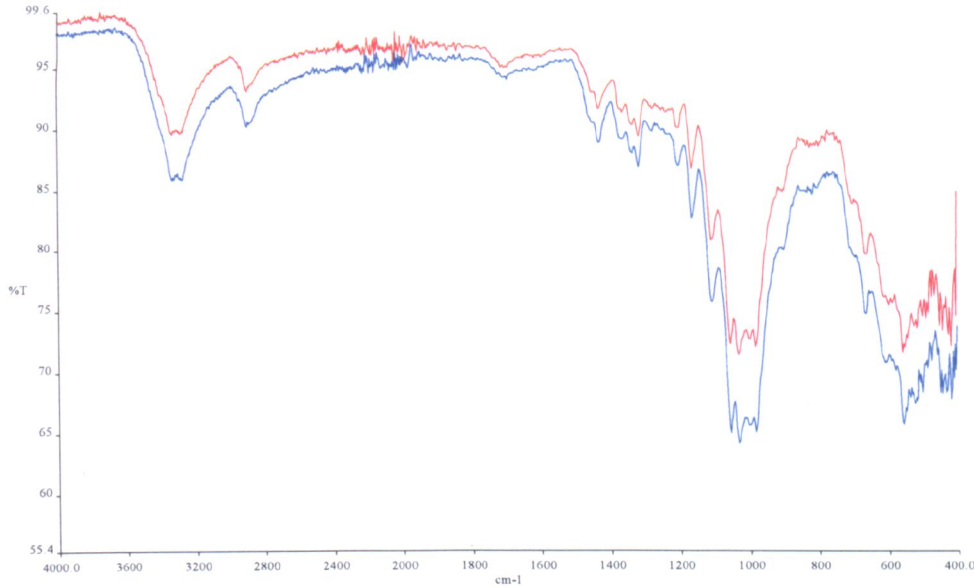

Figure4.84. The FT-IR spectra of treated fabric with the 1S/1PH/10U condensate [red] and 1S/2PH/10U condensate [blue].

According to the information provided in Table 4.24, the relevant specific bands can be identified from the second derivative spectrum of fabric treated with the S/2PH/10U condensate.

Table4.24. Identification of some peaks from the 2nd derivative spectrum of fabric treated with 1S/2PH/10U condensate.

*Functional Groups	Region cm^{-1}	Specific Peak cm^{-1}	Intensity	Comments
P-S-C	1050-970 565-550 490-440	1000 574 462	 m m	Observed for aliphatic compound
P-S-P	550-400 495-460	510 470	m m	
Phosphonic anhydrides RO)P-O-P(RO)R O O	1270-1250 930-915	1258 918 925 933	Vs s	P=O str Br, asym P-O-P
P-O-P	1025-870	876 867	s	Usually broad, asym str often found in region 945-925cm^{-1} (a weak band also near 700cm^{-1})

*These Functional groups and their specific identified frequency regions are indicated in reference [3].

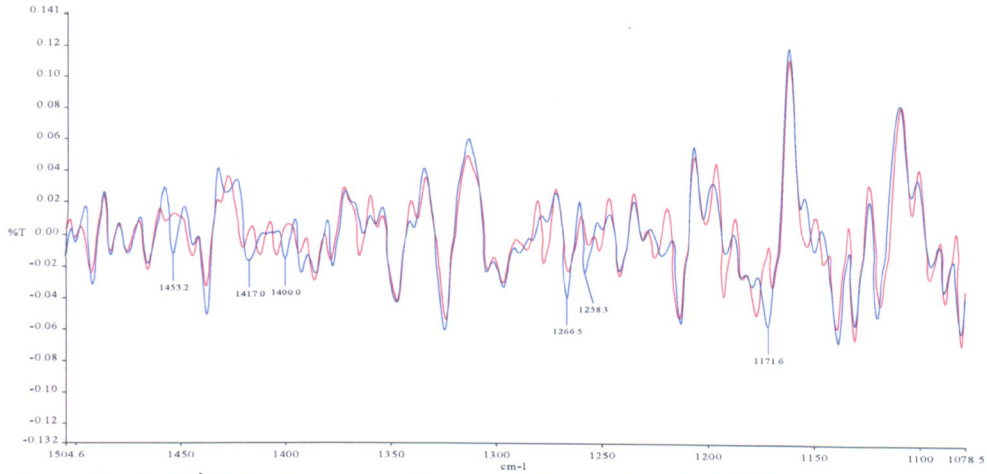

Figure4.85. The 2nd derivative spectra of treated fabric with the 1S/1PH/10U condensate [red] and 1S/2PH/10U condensate [blue].

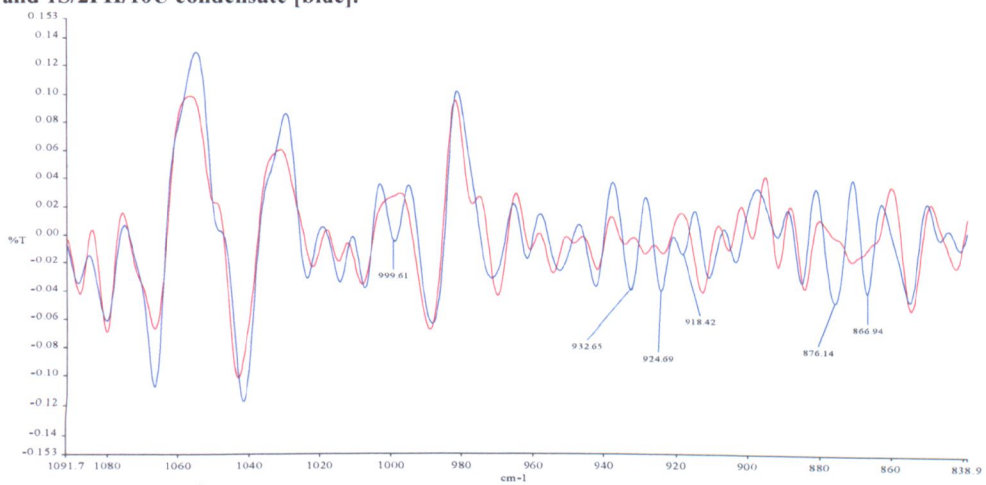

Figure4.86. The 2nd derivative spectra of treated fabric with the 1S/1PH/10U condensate [red] and 1S/2PH/10U condensate [blue].

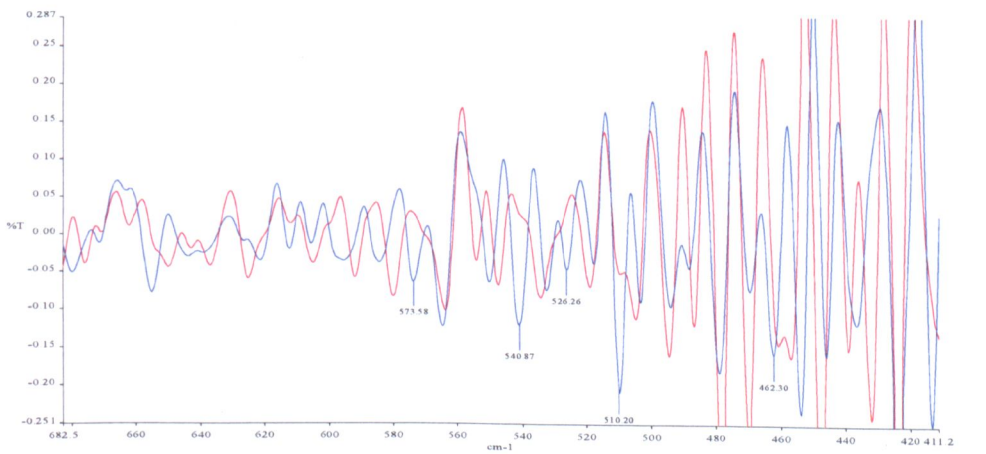

Figure4.87. The 2nd derivative spectra of treated fabric with the 1S/1PH/10U condensate [red] and 1S/2PH/10U condensate [blue].

4.9. FT-IR analysis of urea condensate treated starch

Starch is a polymer of glucose containing alpha-1,4-glucosidic linkages with a relatively small amount of alpha-1,6-glucosidic linkages. Starch contains 22-25% amylose, a linear chain-linked glucose molecule, and 75-80% amylopectin a highly branched chains of glucose units, Figure 4.88. When a suspension of starch in water is heated above a critical temperature, a gel is produced on cooling.

Further investigation regarding the reactions which occurs between the hydroxyl groups and the urea condensate is required.

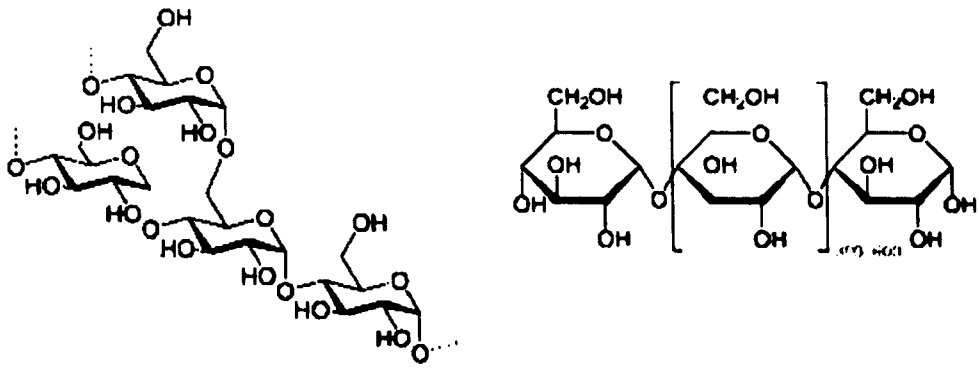

Amylopectin Amylose

Figure4.88. Starch chemical structure [7].

Figure 4.89 shows the FT-IR spectra of starch in powder form, a cured film of gelatinized[1] starch alone and starch reacted with 1S/2PH/10U condensate. A significant difference between the FT-IR spectrum of starch in powder form and the cured film of gelatinized starch has been described in the literature [8,9]. In fact by heating the starch in water the starch glucosidic linkage breaks coupled with increased hydrogen bonding between starch hydroxyl groups and water. The flame retardancy properties of the urea condensate modified starch, was confirmed by DSC thermal analysis, section 4.7.3.

On comparing the FT-IR spectra of treated starch and treated cellulose, a considerable difference was observed for the starch, which can be attributed to the more available hydroxyl groups in starch

1. A suspension of starch in water heated to produce a viscose solution.

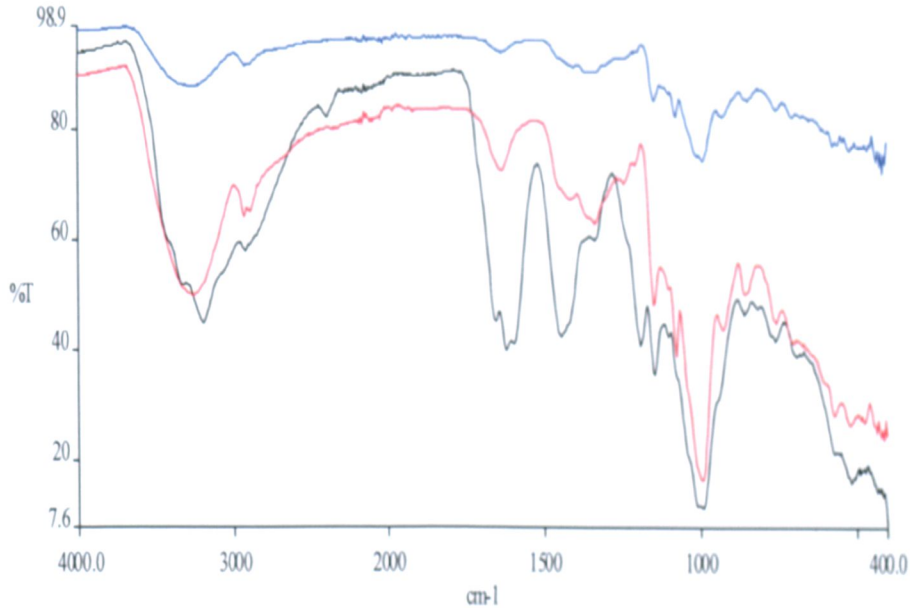

Figure4.89. The FT-IR spectra of starch in powder form [red], gelatinized starch heated at 165°C for 4 minutes alone [blue] and starch mixed with 1S/2PH/10U condensate, gelatinized and cured at 165°C for 4 minutes [black].

Figure 4.90 shows the FT-IR spectrum of gelatinized starch alone, and Figure 4.91 shows the spectrum of the urea condensate treated starch. The FT-IR analysis for both spectra is provided in Tables 4.25 and 4.26. However the Raman spectrum analysis can complete this investigation. In Figure 4.92 the Raman spectrum of a cured film of gelatinized mixture of urea condensate (1S/2PH/10U) treated starch is shown.

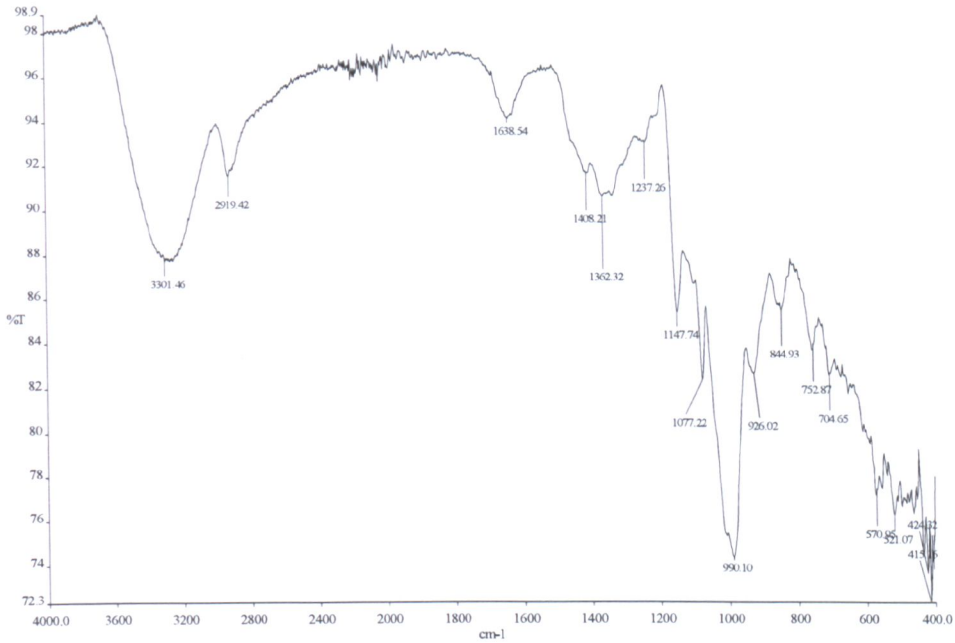

Figure4.90. FT-IR spectrum of gelatinized starch heated to 165°C for 4 minutes.

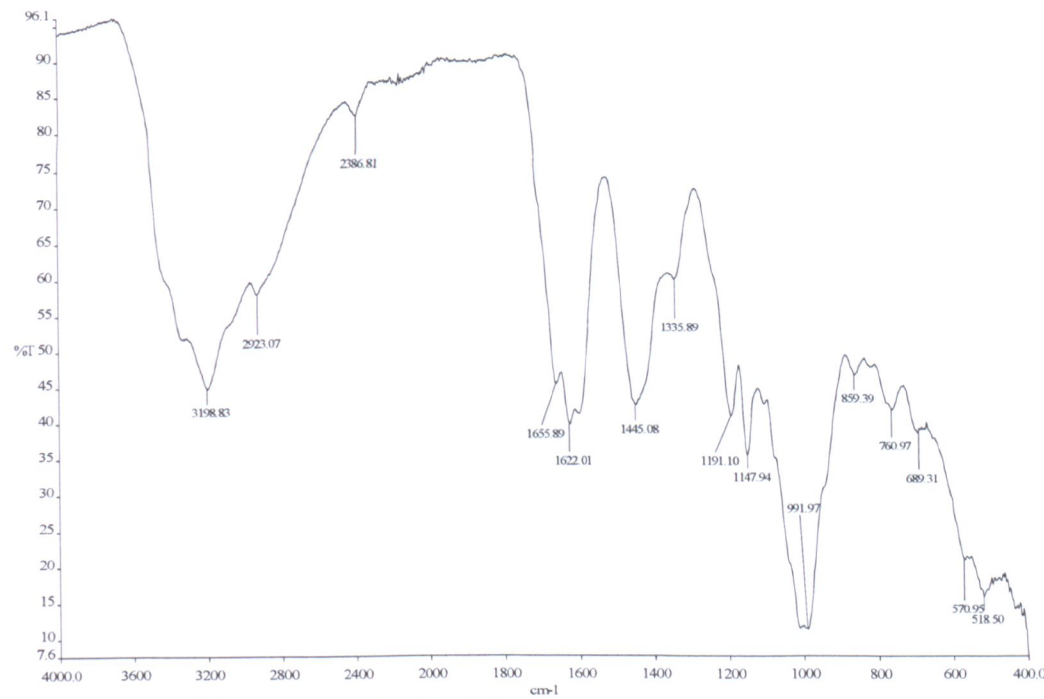

Figure4.91. The FT-IR spectrum of 1S/2PH/10U condensate treated starch, heated to make a gel and cured as a film at 165°C for 4 minutes.

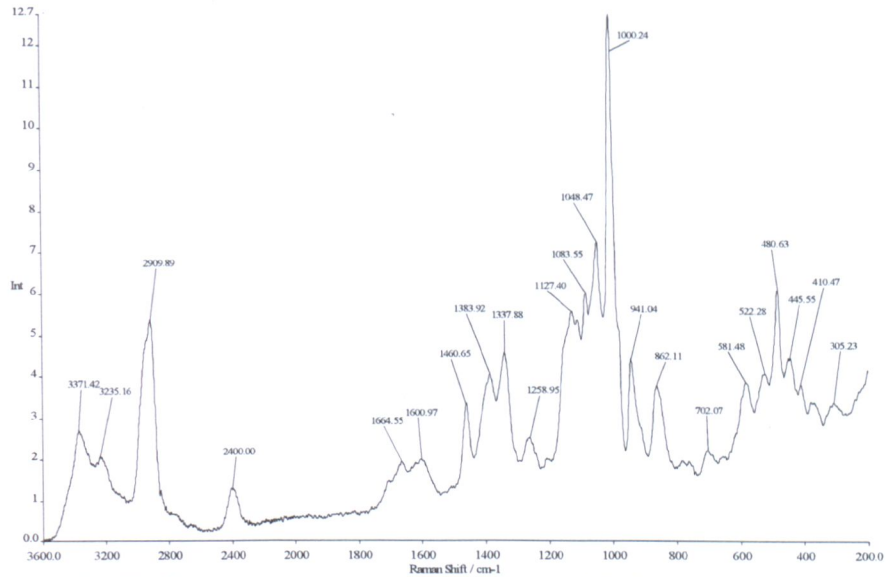

Figure4.92. The Raman spectrum of starch treated with 1S/2PH/10U condensate.

Table4.25. Characterization of starch functional groups bands in FT-IR spectrum.

Specific peaks cm^{-1}	Comments
3301	OH str vib of hydroxyl group
2919	Asym CH_2 str of primary alcohols $-CH_2OH$
1639	OH def vib
1408	In plane OH def vib of primary alcohols
1362	CH def vib of starch
1237	CH str vib of CH_2OH group
1148	C-O str vib of secondary alcohols
1077	Asym C-O-C srt vib saturated aliphatic ethers
990	CCO str characteristic band of primary alcohols
926	CH_2 twisting vib of primary alcohols
845	CCO str vib of primary alcohols
753 705	{ OH out-of-plane def of alcohols
571	OH out-of-plane def vib

Table4.26. FT-IR and Raman Spectra interpretation of starch treated with the 1S/2PH/10U condensate.

Specific peaks cm^{-1}		Comments
FT-IR	Raman	
-	3372	Asym NH_2 Str vib of primary amide
3199	3235	NH str vib of secondary amide
2923	2910	Asym CH_2 str vib of primary alcohol
2387	2400	P-H str vib of phosphorus compound
1656	1665	C=O str vib of primary urea
1622	1601	NH_2 def vib of primary urea
14455	1461	C-N str vib of amide III
	1384	Asym str vib of N-C-N, of urea linkage
1336	1338	Sym str vib of N-C-N of urea linkage -NH-CO-NH, -NH-CO-NH_2
1191	-	Asym PO_3^{2-} str
1148	1127	
	1000	
992	941	Ring str vib of sym-triazines and melamine
859	862	
761	702	C=O vib of hydroxyl-substituted triazines
689	-	NH_2 def vib of primary amides
571	581	N-C=O def vib of primary amide
518	522	NH_2 def vib of –NH CONH-, urea linkage
-	481	C-C=O def vib of primary amide
-	446	SO_2 wagging vib
-	410	SO_2 twisting vib
-	305	Aliphatic ester containing the –CH_2CO-O- group

4.10. The effect of urea condensate on polyvinyl alcohol

Polyvinyl alcohol with a repeat unit of -CH_2CH (OH)- is a water-soluble synthetic polymer with excellent film forming, emulsifying and adhesive properties.

This polymer is non-toxic, resistant to oil, grease and some solvents. The high oxygen and aroma barrier properties, with high tensile strength and flexibility make this polymer specific to industrial application. Water can act as a plasticiser with this polymer and reduce its tensile strength however its elongation and tear strength are improved. PVA has a melting point of 230°C and for the fully hydrolysed and partially hydrolysed grades it is reduced to 180 and 190°C respectively. Its thermal decomposition occurs above 200°C since it can undergo pyrolysis at high temperatures [2].

In coating industries, polyvinyl alcohol is an additive applied to a variety of materials; wood, fabric, carpet. Therefore to determine the possibility of producing a flame retardant polyvinyl alcohol, the treatment of this polymer with urea condensate product was carried out in this research. The thermal reactions between them were provided by heating a mixture of polyvinyl alcohol solution and urea condensate

product at high temperature. The chemical reactions which are involved between the hydroxyl groups of the polymer and the urea condensate product can be studied using FT-IR analysis of the treated polyvinyl alcohol as a model.

The flame retardancy performance of treated polyvinyl alcohol has been confirmed by DSC thermal decomposition process, in section 4.7.5.

The FT-IR spectra of polyvinyl alcohol heated to 165°C, and a mixture of polyvinyl alcohol with 1S/2PH/10U condensate heated to 165°C are shown in Figure 4.93.

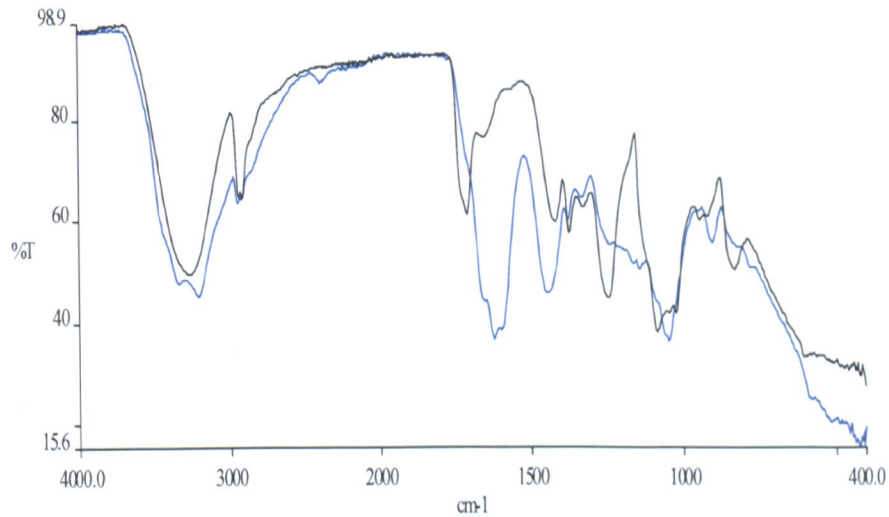

Figure4.93. The FT-IR spectra of polyvinyl alcohol heated at 165°C for 4 minutes [black] and polyvinyl alcohol solution mixed with 1S/2PH/10U condensate and heated for 4 minutes at 165°C [blue].

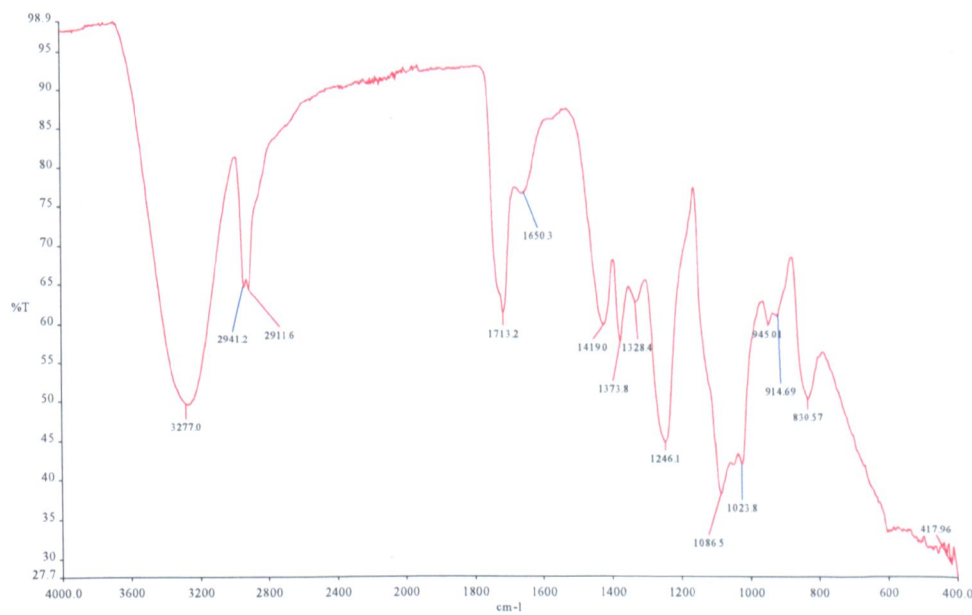

Figure4.94. The FT-IR spectrum of untreated polyvinyl alcohol.

The FT-IR spectrum of untreated polyvinyl alcohol is shown in figure 4.94. In figures 4.95 and 4.96 the FT-IR and also Raman spectra of polyvinyl alcohol treated with 1S/2PH/10U are shown.

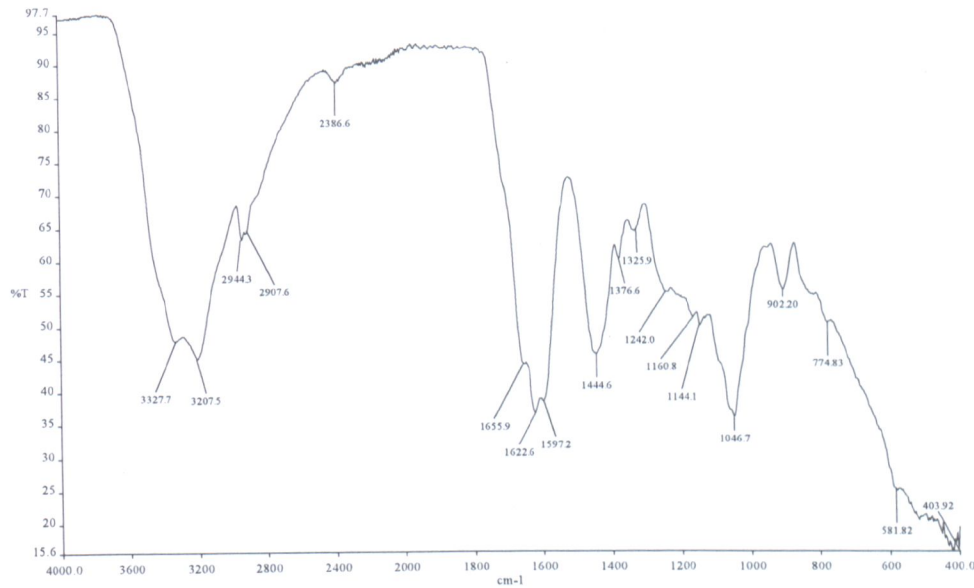

Figure4.95. The FT-IR spectrum of polyvinyl alcohol treated with the 1S/2PH/10U condensate.

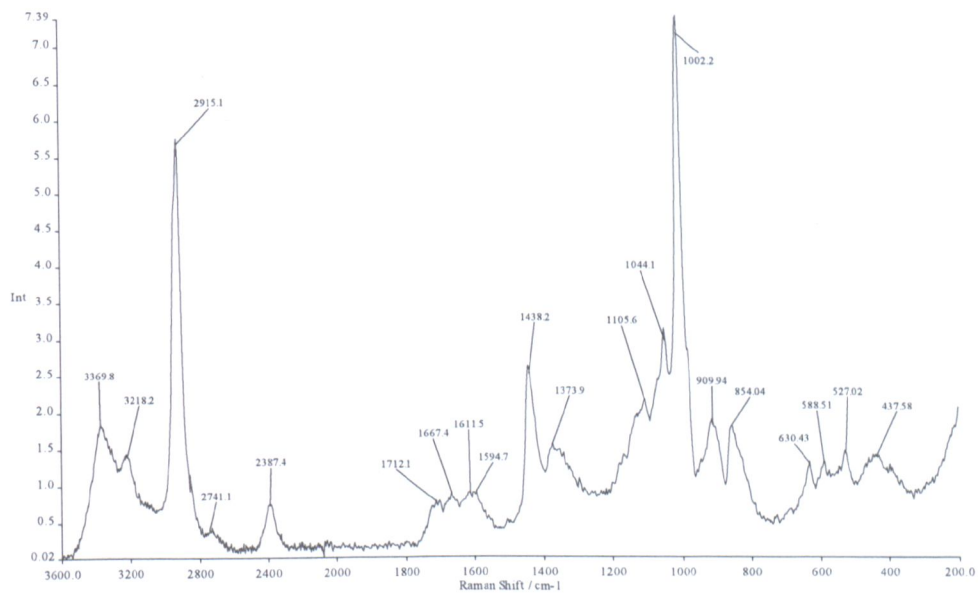

Figure 4.96. The Raman spectrum of polyvinyl alcohol treated with the 1S/2PH/10U.

The interpreting of FT-IR and Raman spectra for both untreated polyvinyl alcohol and treated with the urea condensate 1S/2PH/10U is provided in Tables 4.27.

Table 4.27.The FT-IR and Raman spectra interpretation of untreated polyvinyl alcohol and the treated with the 1S/2PH/10U condensate.

Untreated polyvinyl alcohol		Polyvinyl alcohol treated with 1S/2PH/10U		
Specific peaks cm^{-1}	Comment	Specific peaks cm^{-1}		Comments
		Raman	FT-IR	
3277	OH str vib of hydroxyl group	3370 3218	3328 3207	Asym NH_2 Str vib of primary amide NH str vib of secondary amide
2941	Asym CH_2 str of primary alcohols – CH_2OH	2915	2944 2908	Asym CH_2 str vib of primary alcohol
2912		2741 2387	- 2387	NH str vib of P-NH phosphorus compound P-H and OH str vib of phosphorus compound
1713	OH def vib	1667	1656	C=O str vib of primary urea
1650		1611 1596	1623 1597	NH_2 def vib of primary urea
1419	In plane OH def vib of primary alcohols	1438	1445	C-N str vib of amide III
1374	CH def vib of polyvinyl alcohol	1374	1377	Asym str vib of N-C-N, of urea linkage
1328		-	1326	Sym str vib of N-C-N of urea linkage P-O str vib of P=O un-assiciated
1246	CH str vib of CH_2OH group	1106	1242 1161 1144	P-N str vib Sym N-C-N str urea linkage and P-O str vib of P=O associated Sym N-C-N str vib of urea linkage
1086	CCO str of primary alcohol	1044	1047	P-H def vib P-O str vib of P-OH
1024		1002	-	P-S-C str vib -P-O-C asym str vib SO asym str of covalent sulphonates
945	CH2 Twisting vib	910	902	Ring str vib of sym-triazines and melamine asym PO_3^{2-} str
915				
831		854 630 589 527	- 775 582 -	Ring str vib of sym-triazines and melamine NH_2 def vib of primary amides N-C=O def vib of primary amide and SO_2 def vib of sulphonamide NH_2 def vib of –NH CONH-, urea linkage

Conclusions:

The urea condensate products were applied to cotton, starch and polyvinyl alcohol. Important findings:

The urea only treated fabric is not flame retardant, but the presence of cellulose carbamate was confirmed from the FT-IR analysis of the urea-treated cotton.

The treated S/U condensate fabrics are partially flame retardant and self-extinguishing.

The PH/U condensates give the desired flame retardancy on cotton fabric providing one mole phosphorous acid and more than 10 moles of urea are used; in the case of PA/U condensates, the maximum 10 moles of urea to one mole phosphoric acid can provide the required flame retardancy to cotton fabric. Elemental analysis of the washed fabric showed the P:N ratio was 1.75: 1; the P:N ratio of the condensate reactants was 20:1 but due to loss of ammonia in condensation the P:N ratio dropped.

Comparing the burning results of the treated samples, the fabric finished with 1PA/12U produced a char length of 8.5 cm whereas the 1PH/10U condensate treated fabric gave a 3.8 cm char length.

The sulphamic acid/phosphorus acid/urea condensate, containing the higher amount of phosphorous acid, 1S/2PH/10U, gave a very small char length of 2.5 cm, while with the 1S/1PH/10U a char length 4.5 cm was reported.

Durability of the FR effect to 13x washing cycles was excellent.

From the elemental analysis, the phosphorus remaining in the fabric after alkaline washing process was 1.5% which is less than the amount of phosphorus measured on commercial Proban treated fabric (2.8%). To produce the desired flame retardancy the amount of sulphur needs to be considered, 0.5% is very low. The amount of nitrogen is also very low, compared with the original applied in the urea condensation products. It is very clear that most of the nitrogen is removed as ammonia from the product during condensate preparation and also in baking the urea condensates on the fabric. In conventional elemental analysis, only 1% nitrogen remained on the sample treated with 1S/1PH/10U (washed in alkaline condition for 20 minutes at boil temperature).

The DSC and TGA results on treated samples confirmed the activity of the flame retardant on cotton, starch and polyvinyl alcohol. Exothermic transition on thermal analysis of the treated samples can provide further information regarding

the presence of new compounds on the fabric which can retard the pyrolysis process. In fact the obvious curve shifts seen in TGA analysis, are valuable evidence regarding the dehydration of cellulose and char formation. Therefore it is reasonable to say that the flame retardant compound changed the course of the burning process with exotherms showing new pyrolysis products responsible for extra char formation.

Fabric treated with higher concentration of urea in the urea condensate can decompose at higher temperature; this effect can be explained as due to formation of a high molecular polymer on the fabric which requires more thermal energy for decomposition.

FT-IR analysis shows the formation of a cyclic urea in combination with the presence of triazines such as cyanuric acids and melamines cross-linked with urethane linkage.

References –Chapter 4

1. Kurlya, W.C. and Papa, A.J., "Flame Retardancy of Polymeric Materials", Vol. 5, Publisher: Mercel Dekker Inc, 1978.

2. Chinnasamy, T.V., "Thermal Properties of Polyvinyl Alcohol", Thermochimica Acta, 11983, 60, 3, 383-387.

3. Socrates, G., "Infrared and Raman Characteristic Group Frequencies", Publisher: John Wiley and Sons, Ltd, 2001.

4. Zhbankov, R.G, and Firsov, D.K., "Structural Physico-Chemistry of Cellulose Macromolecules. Vibrational Spectra and Structure of Cellulose", Journal of Molecular Structure, 2002, 614, 117-125.

5. Zhbankov, R.G., "Infrared Spectra of Cellulose and its Derivatives", Publisher: New York, Consultants Bureau, 1966.

6. Nyquist, R.A. and Muelder, W.W., "An Infrared Study of Organophosphorus Compounds-1, Rotational Isomers and Assignments", Spectrochimica Acta, 1966, 22, 9, 1563-1569.

7. Wikipedia Encyclopedia, Starch, Online, [Accessed 20/9/2009], Available from: http://en.wikipedia.org/wiki/starch

8. Durrani, M. and Donald, A.M., "Compositional Mapping of Mixed Gel Using FT-IR Microscopy", Carbohydrate Polymer, 1995, 28, 4, 297-303.

9. Dolmatova, L. and Ruckebusch, C., "Identification and Modified Starches Using Infrared Spectroscopy and Artificial Neural Network Processing", Applied Spectroscopy, 1998, 52, 3, 329-338

Chapter 5 - Conclusions

This thesis describes the successful development of new flame retardant systems based on urea condensates formed by heating urea with phosphoric acid, phosphorous acid, sulphamic acid and mixtures thereof; as flame retardant agents these condensates show great potential in numerous industries. In the design of the effective flame retardants, the environmental safety (especially zero formaldehyde content), the availability and low cost of the initial materials, simplicity of production, wash-durable flame retardancy and end use properties, all have to be considered. These products were applied to various materials without introducing new techniques or equipment. The new products gave little adverse effect on ground colour (shade change of dyeing or prints and no discoloration of white grounds), no handle change, minimal changes in tensile strength, tear/burst strength and abrasion resistance. The elimination of formaldehyde from the condensate preparation chemistry is very important as current commercial FR systems use this unpleasant chemical.

Urea in the form of a solid compound containing nitrogen has been used as a non-durable flame retardant agent for many years. Numerous patents use solid urea, condensed urea phosphates, urea borates and other derivatives as flame retardant agents.

The current research, concentrated upon the preparation of the urea condensates which were water soluble and which can be applied easily to textile materials.

The production of isocyanic acid and ammonia during the thermal decomposition of urea at high temperature (above its melting point) was confirmed [1]. In combination of sulphamic acid, phosphorous acid or phosphoric acid and urea, heated in an open vessel to high temperature, the exothermic reactions between isocyanic acid and these compounds occurred readily. The water soluble urea condensates were produced at a temperature between 125-140°C.

An exothermic reaction occurred at a short temperature range which required careful control. Following the observations during the reactions of the various types of urea condensate (section 3.2) and the DSC results (section 3.4) it is quite feasible to indicate the most controllable process; in order of exotherm controllability:

1S/1PH/10U > 1S/2PH/10U > 1S/1PA/10U> 1PH/U (various moles of urea) > 1S/U (various moles of urea) >1PA/U (various moles of urea)

When the concentration of urea was increased, the urea condensates changed to hard crystals which were difficult to dissolve in cold water. Higher amounts of phosphorus in the urea condensate can reduce the exotherm temperature between the initial materials, and in contrast, higher amounts of urea lead to higher exotherm temperatures. Therefore a variety of products were produced depending upon the types and the amounts of the initial materials.

From the NMR and FT-IR analysis results, the condensates contained aliphatic polyamide chain structures, with a high density of urea linkages; these were water soluble products.

At high temperature, above 150°C, water insoluble products were produced. Since these reactions were exothermic it was necessary to use an open vessel; thus allowing all liberated gases to be removed from the reaction vessel. The application of these compounds to textiles was carried out using aqueous pad liquor techniques and curing at high temperature (165°C), to facilitate cross-linking of the polymer structure between the cellulose fibre and the water insoluble product formed on the surface of fabric.

The thermal decomposition of urea also leads to the formation of water insoluble products above 160°C; a combination of cyclic urea, cyanuric acid, triazine and also melamine residues were found as the main products at this reaction temperature [1].

All the urea condensates used in this research were applied to cotton fabric by padding and curing.

The fabrics treated with S/U condensate exhibit partial flame retardancy (self extinguishing) while the rest of the urea condensate treated fabrics passed the flame test.

The maximum urea required to pass the desirable flame retardancy test on cotton fabric has been investigated. SEM analysis of phosphorus and sulphur elemental distribution on the surface and cross section of the flame retardant fabric showed excellent evenness. The presence of a polymer coating on the surface of the fabric was verified by SEM before and after the washing process.

The thermal analysis of the treated fabrics with the urea condensates was compared with that of the commercially treated fabrics (Proban and Pyrovatex); there were significant differences in the thermal decomposition of these latter fabrics compared to the urea condensate fabrics. In the DSC results for the 1S/1PH/10U condensate treated fabric a

very small exothermic effect before complete decomposition of cellulose can be attributed due to the low level of phosphorus in the urea condensate. By increasing the amount of phosphorous, this exothermic effect was moved to a higher temperature with a higher enthalpy. However the higher amount of urea also had an effect on the flame retardancy behaviour and higher temperature decomposition was indicated.

FT-IR and also NMR analysis gave sufficient evidence in this regard, indicating the formation of urethane linkages and also cellulose carbamate. The formation of cyclic urea, triazine, cyanuric acid was also indicated. In the 2nd derivative FT-IR study of all treated fabrics, some characteristic bands appear in all the spectra at the same frequency. In fact the reproducibility of these treatments and similarity in chemical structure of the products and treated fabrics was confirmed with these analyses.

Treatment of starch and polyvinyl alcohol with the urea condensates was carried out and their flame retardant properties have been reported (DSC thermal analysis).

Future work

The industrial-scale introduction of this new urea-condensate system will require further development and trialling work.

The reaction of the highly reactive isocyanic acid at 130°C in a mixture with the other materials containing nucleophilic groups can provide a powerful technique for scientist to produce a variety of products.

The possible analysis of the gases which are evolved during the reaction could afford more information regarding the chemical reactions which are involved in these processes.

At an industrial scale the production of these urea condensates can be undertaken by using a specific wide diameter reaction vessel, equipped with a stirrer; facilitate to remove all the liberated gases quickly from the reaction. A temperature control device can control the production process however a cooling jacket system is also necessary. A powerful gas transfer compressor can deliver all the gases produced during the reaction and by using a membrane gas separation unit it is possible to collect all the produced gases and recycle them for further applications.

The characterization of these new novel treatments on cotton fabric can be studied further to find the effect of these finishing materials on the physical properties of fabric, such as

strength, abrasion resistance, crease recovery angle and also moisture absorption. The co-operation of these new urea condensates with the other chemical materials used as a finishing treatment needs to be investigated, such as a water repellency finishing with flourochemical compounds. There is a potential to do both treatment in one liquor bath treatment and one curing process to provide flame retardancy, water and oil repellency effects in a simple process. It is also valuable to mention that both phosphorus and sulphur elements can improve the antibacterial finishing effect on cotton fabric which is required to be investigated with all the details. However the sulphonation of cellulose by S/U condensate system determined this modification can improve the ion metallic absorption on cotton fabric to produce the desirable antibacterial finishing.
This new system produces various types of finishing materials water-soluble and water-insoluble, which can be categorized in different industries application.

Water-soluble products:
These types of urea condensate which are produced at low temperature can be reacts into the water solution to various types of materials with hydroxyl groups on their chemical structures. In curing section over 165°C, these products can change to water-insoluble products, the polymeric network with cyclic structure. Through this work the application of these products on starch and polyvinyl alcohol has also been investigated. These two compounds are well known in textile coating industries as thickeners and adhesives. The positive chemical reactions between them have been confirmed while the flame retardancy performance properties on the treated samples are indicated. Therefore the interaction of these urea condensates products and the other two coating additive compounds needs to be studied further. These novel products can be introduced to the fabric coating, carpet back coating and paper making industries.
The flame retardant treatment of the cotton/polyester (80/20) fabric with the commercial FR agents used on cotton substrate is only successful in the Proban process [2], and unmodified process with a higher polyester blend are usually unsatisfactory. In fact all the available FR agents in the market can react only on cellulosic part of the fabric and because of that, the main fabric is still burn and melt. The urea condensate products suggested in this work can produce the FR effect in two different ways, first the reaction

with cellulose hydroxyl groups has been confirmed precisely, and secondly these compounds can produce a urea linkage and urethane formation polymer complex between the hydroxyl groups of fabric. The whole chemical structures of the fabric are involved with these materials and a new cross-linking structure is formed on the surface of fabric. This purpose with this new novel system needs to study further.

Water-insoluble products

In the case of application of these water-insoluble urea condensate products, several patents close to these products have been published in recent years [3-8], but their initial materials were used in their condensate is different. At high temperature preparation of urea condensate, the production of an aryl-aryl and alkyl-aryl urea and urethane linkage complex has been confirmed and the present of molecular weight until 900, for a single fragment was determined using mass spectroscopy analysis. These products are in solid form and white in colour. It is possible to apply them in various types of polymerisation as filler to produce FR properties. In fibre technology, it is possible to use these compounds as a flame retardant finishing in a molten polymer in melt spinning process. The smaller size of urea condensate crystal can facilitate the homogeneity of the treatment. However the white colour of these products has no effect on the appearance of the fibre. In the production of acrylic fibre in wet spinning process, it is possible to dissolve these products in DMSO and mix then with the spinning dope to produce FR acrylic fibre.

In the case of viscose spinning solution with similar structure to cotton fabric, it is not possible to react these products to the solution in the water-soluble form. Regarding all the information provided, after the reaction between cellulose and urea condensate the complex structure with cyclic urea would be possibly formed in hydroxyl groups of cellulose, therefore it may have an effect on spinning process, and make a difficulty to produce a fibre. In all the research works in the field of viscose flame retardant fibres, they recommended phosphorus products in the solid particles, and there are no difficulties to do the spinning process with these materials. In addition, these urea condensates in water-insoluble structure can be applied to the viscose solution to produce the FR fibre.

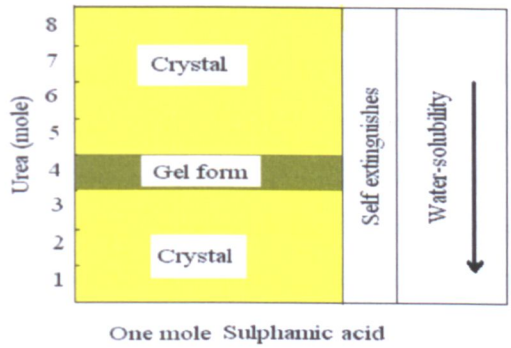

Figure5.1. The characteristic information for urea condensate products produced from one mole sulphamic acid and different moles of urea.

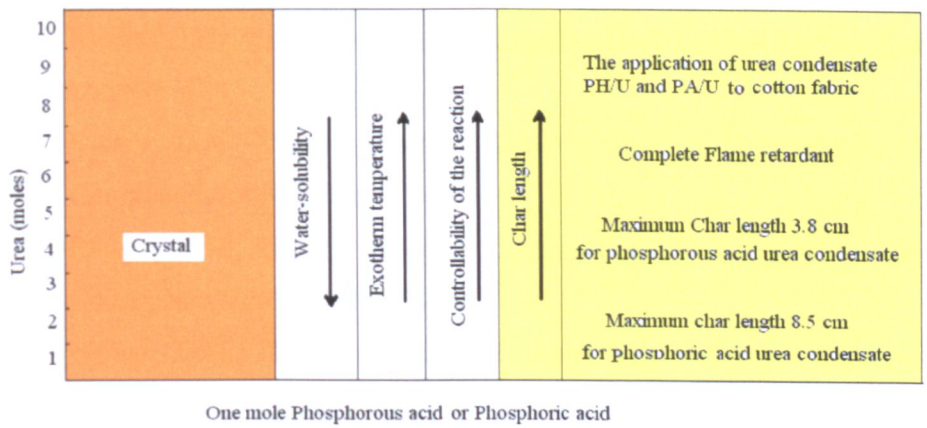

Figure5.2. The characteristic information for urea condensate products produced from one mole phoaphorous acid or one mole phosphoric acid and different moles of urea.

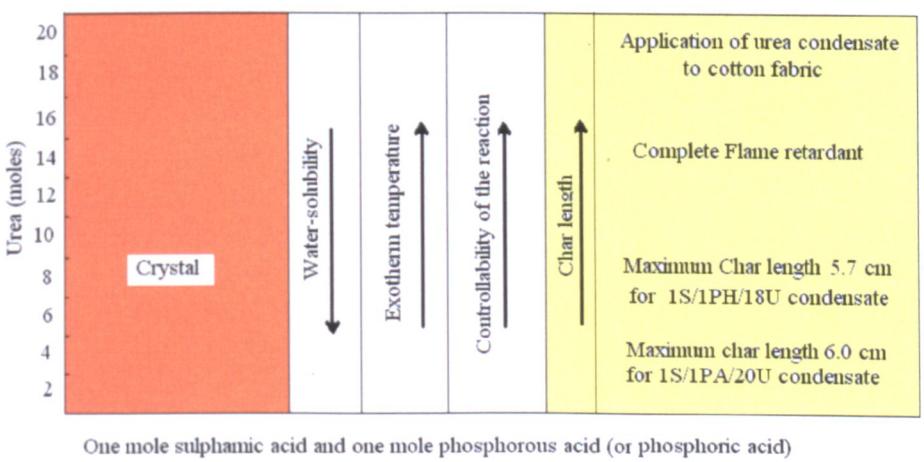

Figure5.3. The characteristic information for urea condensate products produced from one mole sulphamic acid / one mole phosphorous acid (or one mole phosphoric acid) and different moles of urea.

References – Chapter 5

1. Schaber, P.M., Colson, J. and Higgins, S., "Thermal Decomposition (Pyrolysis) of Urea in an Open Reaction Vessel", Thermochimica Acta, 2004, 424, 131-142.
2. Weil, E.D. and Levchik, S.V., "Flame Retardants in Commercial Use or Development for Textiles", Journal of Fire Sciences, 2008, 26, 243.
3. Rohringer, P., "Fire-Retardant, Intumescent Composition and its Use for the Flame-proofing of Substrates, and as a Fire-Extinguishing Agent Comprising an Ammonium Salt, a Water-Soluble Nitrogen Compound as a Blowing Agent Dextrin", 1983, USP4382884.
4. Blount, D.H., "Urea Condensate Salt of Sulphur Oxyacid for Fire Control", 2002, USP6464903.
5. Blount, D.H., "Flame retardant Compositions Utilizing Amino Condensation Compounds", 1998, USP5854309.
6. Blount, D.H., "Flame retardant Compositions Utilizing Amino Condensation Compounds",2001, USP6258298.
7. Blount, D.H., "Flame retardant Compositions Utilizing Amino Condensation Compounds",2001, USP6348526.
8. Blount, D.H., "Organic Phosphorus-Phosphorus Oxyacid Compounds", 2002, USP6492444.